HYPOXIA-MEDIATED TUMOUR MICROENVIRONMENT IN HORMONE RECEPTOR-NEGATIVE BREAST CANCER

WARAPAN NUMPRASIT

MD

Submitted in fulfilment of the requirements for the degree of PhD

School of Cancer Sciences

College of Medical, Veterinary and Life Sciences

University of Glasgow

May 2025

The work presented in this thesis was performed by the author except where acknowledged. This thesis has not been submitted for a degree or diploma at this or any other institution.

Warapan Numprasit
May 2025

Summary

Breast cancer is the most common malignancy in women, causing approximately 670,000 deaths annually worldwide. Prognostic and predictive markers largely rely on the expression of oestrogen receptor (ER), progesterone receptor (PR), and human epidermal growth factor receptor-2 (HER-2). ER/PR-negative subtypes represent a more aggressive form of the disease, with a higher likelihood of relapse compared to ER/PR-positive cases.

Hypoxia is a hallmark of solid tumours, driving cancer aggressiveness and treatment resistance. It is preferentially associated with ER/PR-negative breast cancer. Carbonic anhydrase IX (CAIX) is a well-established hypoxic marker linked to poor survival outcomes in breast cancer, particularly in ER/PR-negative cases. Currently, a CAIX-targeted inhibitor is under investigation in a phase I clinical trial for advanced solid tumours. This study aimed to explore the CAIX-associated gene signature and identify novel hypoxia-related therapeutic targets in breast cancer.

Bulk RNA sequencing (Tempo-Seq) analysis was conducted on 131 ER/PR-negative breast cancer samples with available CAIX immunohistochemistry (IHC) data from the Glasgow Breast Cancer Cohort. Differential gene expression analysis comparing high versus low CAIX expression identified four significantly upregulated genes: *NDRG1, CA9, VEGFA,* and *PPFIA4*. Gene Set Enrichment Analysis (GSEA) revealed that hypoxia and glycolysis were the top two enriched pathways. Additionally, protein-protein interaction analysis using the STRING tool showed moderate interactions between the identified genes with the exception of PPFIA4.

The expression of NDRG1, CA9, VEGFA, and PPFIA4 was validated at both the mRNA and protein levels in vitro using MDA-MB-231, SKBR-3, and MCF-7 breast cancer cell lines. Under hypoxic conditions (1% O_2), all four genes exhibited increased mRNA expression. At the protein level, CAIX and NDRG1 were upregulated in hypoxia, thus NDRG1 warranted further investigation.

Immunohistochemistry analysis of NDRG1 was performed on tissue microarrays (TMA) from the full Glasgow Breast Cancer Cohort. High cytoplasmic NDRG1 expression correlated with significantly poorer overall survival (OS) and cancer-specific survival (CSS). However, when stratified by ER/PR status, NDRG1 expression did not significantly impact survival outcomes. Several limitations should be noted: TMAs might not fully represent whole tumour sections, and there is no standardised cutoff for high versus low NDRG1 expression, which may introduce bias. Additionally, the lack of an independent validation cohort highlights the need for further studies.

To explore the functional role of NDRG1 under hypoxic conditions, it was hypothesised that NDRG1 contributes to aerobic glycolysis, similar to CAIX, as suggested by GSEA. Metabolic assessments were performed using Seahorse assays to measure the extracellular acidification rate (ECAR) and oxygen consumption rate (OCR). Additionally, lactate and ATP assays were conducted to validate the Seahorse findings. Silencing NDRG1 led to decreased lactate production (a glycolysis byproduct) in MDA-MB-231 and MCF-7 cells. However, its impact on ECAR varied: no effect was observed in MDA-MB-231 cells, while ECAR increased in MCF-7 cells. Silencing NDRG1 increased OCR and ATP production in MCF-7 cells but had no effect in MDA-MB-231 cells. These findings suggest that NDRG1 plays a role in glycolytic pathways under hypoxic conditions, but its function may vary depending on the molecular background of the different breast cancer subtypes. Further studies are needed to investigate alternative metabolic pathways, such as fatty acid oxidation and glutamine metabolism, which may be mediated by NDRG1 under hypoxic conditions, particularly in MDA-MB-231 cells.

This study identified *NDRG1, CA9, VEGFA,* and *PPFIA4* as differentially expressed genes associated with CAIX-driven hypoxia in breast cancer. NDRG1 emerged as a potential hypoxic biomarker, as high expression correlated with worse OS and CSS in the Glasgow Breast Cancer Cohort. Additionally, NDRG1 was upregulated in hypoxia and played a role in aerobic glycolysis. Silencing NDRG1 alleviated glycolysis by reducing lactate production and enhanced mitochondrial respiration by increasing OCR. Further studies are warranted to explore the mechanistic role of NDRG1 in hypoxia-driven metabolism and to validate these findings in independent breast cancer cohorts.

Graphical abstract

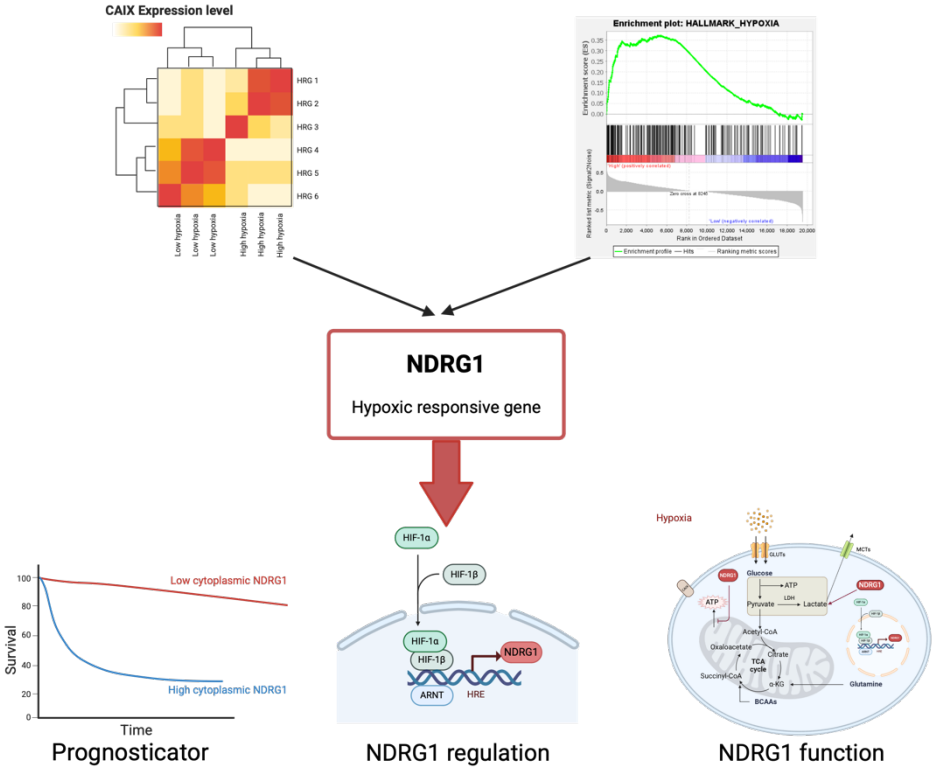

Publication and presentations

Publication relating to this thesis

Warapan Numprasit, Supaporn Yangngam, Jaturawitt Prasopsiri, Jean A. Quinn, Joanne Edwards and Chanitra Thuwajit.,2023. Carbonic anhydrase IX-related tumoral hypoxia predicts worse prognosis in breast cancer: A systematic review and meta-analysis. Frontier in Medicine.

In preparation - Warapan Numprasit, Jean A Quinn, Chanitra Thuwajit and Joanne Edwards. The prognostic role of N-Myc Downstream Regulated 1 (NDRG1) in breast cancer: Systematic review and meta-analysis

In preparation - Warapan Numprasit, Guan-Yu Lian, Jean A Quinn, Sarawut Jitrapakdee, Chanitra Thuwajit and Joanne Edwards. NDRG1 Links Hypoxia-Associated Aggressiveness to Metabolic Plasticity in Breast Cancer

Poster presentations

CAIX and related genes predict poor survival outcomes in hormonal receptor-negative breast cancer. W. Numprasit, J.A. Quinn, Suad Shamis, W Ronney, E Mallon, C Thuwajit, J Edwards. 14th European Breast Cancer Conference 2024 – Milan, Italy

Hypoxia-regulated NDRG1 predicted breast cancer survival. Warapan Numprasit, Jean A Quinn, Chanitra Thuwajit and Joanne Edwards. 19th St.Gallen International Breast Cancer Conference 2025 – Vienna, Austria

Table of Contents

List of Tables

List of Figures

Acknowledgement

I would like to express my deepest gratitude to Prof. Chanitra Thuwajit, Prof. Joanne Edwards, and Dr. Jean Quinn for giving me the incredible opportunity to explore breast cancer from different perspectives. Your guidance and support have been invaluable throughout my journey. A special thanks to Miss Tussanee, a scientist in the pharmacological department at Siriraj Hospital, for being the first to teach me how to work with hypoxia. I truly appreciate her patience in mentoring a surgeon who was new to scientific experiments.

I am also grateful to all the members of the Edwards Lab for their warm welcome and unwavering support. Your willingness to help, even when my work was somewhat outside your field, meant a lot to me. Aula, thank you for your kindness, your sweet treats that helped relieve my stress, and your thoughtful suggestions. Amna, I am beyond grateful for everything you have done for me. Most importantly, Guanyu, I cannot express how much I appreciate your presence. I cannot imagine how I would have managed without you. I owe you so much—I admire your logic, keen insights, and patience with me.

Eric, you were a key figure in helping me navigate the challenges of Seahorse experiments. I will never forget it for the rest of my life. Prof. Sarawut, thank you for your valuable advice on metabolism—it was incredibly helpful.

I am also deeply thankful to my colleagues at Siriraj Hospital, who have always supported me and lifted me up during difficult times.

Finally, I dedicate everything I have accomplished to my family. The small morning conversations with you were my first achievement of each day, and your unwavering support kept me going, even in the toughest moments. I would not have made it to the end without you.

Author's Declaration

I declare that all the work presented in this thesis is entirely my own unless otherwise stated below. This study was conducted by me at the Wolfson Wohl Cancer Research Centre, School of Cancer Sciences, College of Medical, Veterinary, and Life Sciences, University of Glasgow, between January 2023 and December 2024, under the supervision of Professor Joanne Edwards, Dr. Jean A. Quinn, Professor Chanitra Thuwajit, and Professor Sarawut Jitrapakdee.

The clinicopathological parameters, including age, histological grade, tumour size, nodal status, molecular subtypes, and treatment, were retrieved with authorization from Professor Joanne Edwards. Immunostaining for CAIX was performed by Dr. Suad A.K. Shamis. Tissue microarrays and slides were provided by Dr. Hannah Morgan, Research Technician, Glasgow Tissue Research Facility, School of Cancer Sciences, University of Glasgow.

Inter-observer reproducibility for NDRG1 immunohistochemistry was assessed with the assistance of Dr. Jean A. Quinn and Dr. Kathryn Pennel at the Wolfson Wohl Cancer Research Centre, University of Glasgow.

Definitions/Abbreviations

AIs = Aromatase inhibitors

AJCC = American Joint Committee on Cancer

AHR = Aryl hydrocarbon receptor

ALND = Axillary lymph node dissection

AKT1 = AKT Serine/Threonine Kinase 1

AP-1 = Activator protein-1

ATM = Ataxia Telangiectasia Mutated

BCA = Bicinchoninic acid

BCSS = Breast cancer-specific survival

BCS = Breast-conserving surgery

BMI = Body mass index

BRCA = BReast CAncer gene

CAIX = Carbonic anhydrase 9

CCND1 = Cyclin D1

CCNE = Cyclin E1

CDH1 = Cadherin 1

CHEK2 = Checkpoint kinase 2 gene

CI = Confidence interval

CSCs = Cancer stem cells

CSS = Cancer-specific survival

DCIS = Ductal carcinoma in situ

DEGs = Differentially expressed genes

DFS = Disease-free survival

DFRI = Distant recurrence-free interval

ECAR = Extracellular acidification rate

Egr-1 = Early growth response 1

eIF3 = Eukaryotic initiation factor 3

ER = Oestrogen receptor

ERE = Oestrogen response element

EFS = Event-free survival

ETC = Electron transport chain

FA = Fatty acid

FCCP = Carbonyl cyanide-4 (trifluoromethoxy) phenylhydrazone

FDA = the Food and Drug Administration

FFPE = Formalin-fixed paraffin-embedded tissue

FOXM1 = Forkhead Box M1

GATA3 = GATA Binding Protein 3

GLUT-1 = Glucose transporter-1

GSEA = Gene set enrichment analysis

GSK-3β = Glycogen synthase kinase-3

HCA = Heterocyclic amine

HER-2 = Human epidermal growth factor receptor-2

HIF = Hypoxia-inducible factor

HK-2 = Hexokinase-2

HR = Hazard ratio

HRE = Hypoxia response element

IBC = Inflammatory breast cancer

ICB = Immune checkpoint blockade

ICCC = Intraclass correlation coefficient

IGF-2 = Insulin-like growth factor-2

IHC = Immunohistochemistry

IMN = Internal mammary node

is = In situ

ISH = In situ hybridization

ITCs = Isolated tumour cells

LAR = Luminal androgen receptor

LDHA = Lactate dehydrogenase

LOX = Lysyl oxidase

LDH-5 = Lactate dehydrogenase isoenzyme-5

LDLR = Low-density lipoprotein receptor

MAP3K1 = Mitogen-Activated Protein Kinase Kinase Kinase 1

mTORC1 = The mammalian target of rapamycin complex 1

mi = Microinvasion

MYC = MYC Proto-Oncogene

NF1 = Neurofibromatosis type 1

Nur77 = The orphan nuclear receptor

OCR = Oxygen consumption rate

OFS = Ovarian function suppression

OPN = Osteopontin

OS = Overall survival

PALB2 = Partner And Localizer Of BRCA2

PCA = Principal component analysis

pCR = Pathological complete response

PD-1 = Programmed death-1

PD-L1 = Programmed death-ligand 1

PDK-1 = Pyruvate dehydrogenase kinase-1

PET = Positron emission tomography

PHD = Prolyl hydroxylase

PI3K = Phosphoinositide 3-kinase

PPFIA4 = Protein Tyrosine Phosphatase, Receptor Type, F Polypeptide (PTPRF), Interacting Protein Alpha 4

PR = Progesterone receptor

PTEN = Phosphatase and tensin homologue deleted on chromosome 10

RB1 = Retinoblastoma 1

RCT = Randomised control trial

RFS = Recurrence-free survival

RRS = recurrence risk scores

RT = Radiation therapy

SC = Scramble control

SERM = Selective oestrogen receptor modulators

SGK1 = Serum and glucocorticoid-regulated kinase 1

SLNB = Sentinel lymph node biopsy

SPECT = Single-photon emission CT

STK = Serine/threonine kinase

STR = Short tandem repeat

TBX2 = T-box 2

TCA = Tricarboxylic acid cycle

TCGA = The Cancer Genome Atlas

TGFβ = Transforming growth factor β

TSGs = Tumour suppressor genes

TMA = Tissue microarrays

TNBC = Triple-negative breast cancer

UTR = Untranslated region

VEGFA = Vascular endothelial growth factor receptor

VHL = Von Hipple Lindau

WB = Western blot

WISP1 = WNT1inducible signalling pathway protein 1

WST = Water-soluble tetrazolium salt

Chapter 1: Introduction

1.1 Breast cancer epidemiology and prognosis

Breast cancer is the most frequently diagnosed cancer in women across the world (1, 2). In the UK, 1 in 7 women will develop breast cancer in their lifetime and there were approximately 11500 deaths annually between 2017-2019 (3). Although most patients are diagnosed at an early stage, in part due to breast screening (mammography) programs, breast cancer remains a leading cause of cancer-related mortality (4). Factors associated with poor survival outcomes include age at diagnosis, race, sex, inherited penetrance, staging, breast cancer subtypes, treatment response and modifiable causes such as smoking, alcohol consumption and obesity. Each of these factors is discussed in detail below.

1.1.1 Age at diagnosis

The median age for breast cancer diagnosis is 62 years, however, breast cancer occurring in younger or extremely elderly women has a worse prognosis (4). Breast cancer in patients under 30 years old (HR 1.20; 95%CI: 1.02-1.42, p=0.032) or over 80 years old (HR 2.71; 95%CI: 2.55-2.89, p<0.001) has a significantly shorter breast cancer-specific survival (BCSS) when compared to patients diagnosis at age 50-59 years (5). Younger breast cancer patients usually have more aggressive disease and may carry a germline mutation (6) and tend to live longer hence are more likely to be at risk of recurrence (7). Elderly breast cancer patients tend to have comorbidities and a decline in functional status leading to less tolerance of treatment toxicity (8). Older patients may present at a later stage due to delayed diagnosis as a result of the absence of breast cancer screening in older age groups or other medical conditions (9).

1.1.2 Ethnicity/race

Certain populations carry a specific familial genetic mutation. For example, 2-2.5% of the Ashkenazi Jewish population have a *BRCA1* (BReast CAncer gene 1) or *BRCA 2* mutation that increases the lifetime risk of breast and ovarian cancer (10). In the USA, black women are more often diagnosed with the triple-negative

subtype (81%), which is an aggressive form of breast cancer, and have a higher mortality risk (40%) than non-Hispanic white women (4, 11).

1.1.3 Sex

Although most breast cancer occurs in women, approximately 1% of breast cancers are detected in men (12). They usually present at a later stage and have a poorer prognosis than women (13). The BRCA mutation, accounts for 16 % of male breast cancers thus affected individuals should be counselled for genetic testing (14).

1.1.4 Inherited breast cancer

Ten to fifteen per cent of breast cancer are the result of genetic abnormalities (15). BRCA 1 and 2 are the most common hereditary breast cancer mutants predisposing carriers to early-onset breast and ovarian cancer (15, 16). *BRCA 1* mutations are more commonly associated with triple-negative breast cancer, while *BRCA 2* results in hormone-sensitive breast cancer (17). *BRCA 1* and *2* germline mutations are among the high penetrance genes with a 41-90% lifetime breast cancer risk (18). Although the overall prognosis of BRCA carrier breast cancer patients is similar to non-carriers, the recurrence rate, whether ipsilateral or contralateral, is higher (19, 20). Other high-risk genes include *TP53* (lifetime risk 54%) and *PTEN* (lifetime risk 25-80%). Additionally, moderate penetrance genes, for example, *PALB2, CDH1, STK* and *NF1,* confer an intermediate breast cancer risk of approximately 30-58% (21).

1.1.5 Breast cancer staging

Anatomical TNM staging is the most widely accepted prognosticator. Tumour size (T), nodal metastasis (N) and evidence of distant metastasis (M) are the parameters used to stage most cancers. Localised disease usually has a superior survival outcome to disease that has extended to regional lymph nodes or distant organs. According to the anatomical staging of breast cancer, 5-year overall survival (OS) in stage 0 DCIS is 97.2%, stage I 96.5%, stage II 91.0%, stage III 72.5% and stage IV 40.3%, (22).

1.1.6 Breast cancer subtypes

The prognosis of breast cancer was traditionally based on tumour size, nodal status and the evidence of distant metastasis, with more advanced stages correlating with poorer survival outcomes (23). Histological features are also important prognostic indicators. While approximately 60-75% of breast cancers are classified as invasive carcinoma of no special type (NST), certain histological variants are associated with more favourable outcomes, such as tubular carcinoma and invasive cribiform carcinoma. Conversely, some special types, like squamous cell metaplastic carcinoma and high-grade spindle cell carcinoma, are typically linked to a poorer prognosis (24). Since advances in molecular oncology have identified key biomarkers, including oestrogen receptor (ER), progesterone receptor (PR), and human epidermal growth factor receptor-2 (HER-2), that not only provide prognostic information but also predict treatment response (25).

Current clinical practice generally relies on the classification of breast cancer into five intrinsic subtypes based on surrogate histology and immunohistochemical (IHC) markers, including ER, PR, HER2, and Ki-67 (**Table 1.1**) (26). When integrated with TNM staging, molecular subtypes serve as essential adjuncts in predicting survival outcomes and informing treatment response.

Table 1.1-The intrinsic molecular subtypes of breast cancer stratified by IHC classification

Breast cancer subtypes	ER	PR	HER-2	Ki-67
Luminal A-like	+	+	-	Low
Luminal B-like				
Luminal B/HER-2-	+	+	-	High
Luminal B/HER-2+	+	+	+	
HER-2 enriched	-	-	+	
Triple negative	-	-	-	

In terms of survival, ER/PR positive and HER-2 negative have the best prognosis (4-year OS 92.5%), followed by ER/PR positive and HER-2 positive (4-

year OS 90.3%), ER/PR negative and HER-2 positive (4-year OS 82.7%) and ER/PR negative and HER-2 negative (TNBC) (4-year OS 77%), (27).

ER-positive breast cancers have a better survival than ER-negative, with 15-year breast cancer-specific survival rates 77% in ER-positive compared to 70% in the ER-negative group (adjusted HR = 0.69; 95% CI 0.56-0.85; p = 0.0006) (28). Within ER-positive disease, PR positivity further refines prognosis, with ER+/PR+ patients exhibiting approximately a 20-25% lower risk of recurrence and death compared to ER+/PR- patients (29).

HER-2 overexpression is associated with aggressive tumour behaviour and worse prognosis (30). However, the introduction of HER-2 targeted therapies since 1998, such as trastuzumab, has dramatically improved outcomes. In the pivotal trial by Romond et al., adding trastuzumab to chemotherapy reduced the risk of recurrence by 52% and mortality by 33% at 3 years (31). Similarly, adjuvant trastuzumab was shown to improve 5-year disease-free survival (DFS) by approximately 7-10% compared to chemotherapy alone (32). Moreover, ER and PR status predict responsiveness to endocrine treatment, with tamoxifen and AIs reducing recurrence risk by about 40-50% in hormone receptor-positive disease (33, 34). Collectively, these biomarkers have become essential not only for prognostication but also for tailoring personalised treatment strategies, substantially improving clinical outcomes in breast cancer.

Proliferative marker Ki-67 is a nuclear protein expressed during the active phases of the cell cycle (G1, S, G2, and M phases) (35). Elevated Ki-67 expression is related to aggressive tumour features and poorer prognosis in breast cancer (36). The St. Gallen International Expert Consensus recommends measuring Ki-67, particularly in ER+/HER-2-negative breast cancer, where a Ki-67 index above 20% is used to distinguish the more aggressive luminal B subtype from luminal A (37). However, the clinical utility of Ki-67 is limited by several pre-analytical and analytical challenges that affect its reproducibility and accuracy. Pre-analytical variables, such as tissue types, fixation protocols, and cold ischemic time, may significantly impact Ki-67 immunoreactivity, often leading to decreased staining intensity and underestimation of proliferation indices. Furthermore, immunohistochemistry staining and scoring methods lack standardisation, resulting in considerable intra-and inter-observer variability (38). The absence of

accepted standard cut-points further complicates the interpretation of Ki-67 levels, limiting their widespread adoption in clinical practice in some regions. Therefore, despite its prognostic and predictive potential, standardisation efforts remain crucial for Ki-67 to be reliably integrated into routine breast cancer management.

1.1.7 Treatment response

In addition to adjuvant treatment, neoadjuvant treatment can be a surrogate marker of survival outcomes based on the degree of responsiveness (39). Triple-negative breast cancer (TNBC) and HER-2 overexpression subtypes are the most common subtypes that benefit from systemic neoadjuvant treatment. A meta-analysis of TNBC patients who received neoadjuvant chemotherapy treatment revealed that they have a lower risk of disease progression of 76% and lower cancer-related death of 81% if they achieve pathological complete response (pCR) (40). The addition of the immune checkpoint inhibitor pembrolizumab to neoadjuvant chemotherapy has further increased pCR and event-free survival (EFS) in stage II and III TNBC (41). Similarly, HER2-overexpression subtypes also benefit from neoadjuvant HER2-targeted therapy. Combining trastuzumab, a HER2 monoclonal antibody, with neoadjuvant chemotherapy resulted in an increased pCR rate compared to neoadjuvant chemotherapy alone (43% vs 23%, p=0.002) as well as improved 5-year EFS (HR 0.64; 95%CI: 0.44-0.93, p=0.016) (42). Dual HER2 targeted therapy with trastuzumab and pertuzumab enhances pCR rates compared to trastuzumab plus chemotherapy (45.8% vs 24%). This survival benefit was confirmed by its superior 5-year breast cancer-specific survival (BCSS) compared to single targeted therapy (95% vs 98%, HR 0.58; 95%CI:0.36–0.95) (43, 44). However, for patients who do not achieve pCR, the 5-year EFS and OS dropped significantly, to 57% and 47% for TNBC, and 63% and 76% for HER2 subtypes, respectively (45).

1.1.8 Smoking and alcohol consumption

These poor lifestyle choices exacerbate breast cancer survival outcomes (46). Breast cancer patients who continue to smoke after diagnosis have an increase in all-cause mortality of up to 59% compared to non-smokers and tend to

have poorer breast cancer-specific mortality particularly if they are followed up for longer than 10 years (47). This may be due to a higher risk of secondary cancer and other chronic diseases related to smoking such as cardiovascular and respiratory diseases. The higher the use of alcohol the higher the risk of breast cancer and alcohol intake may increase the risk of recurrence after breast cancer diagnosis although results are inconsistent across studies (48). Drinking alcohol >6g/d increases the risk of breast cancer recurrence and specific breast cancer mortality compared to non-drinkers (HR=1.35; 95%CI: 1-1.83 and HR=1.51; 95%CI: 1-2.29), respectively) (49). However, there is no obvious effect on OS from alcohol use (50).

1.1.9 Dietary and obesity

Research suggests that certain foods may increase the risk of breast cancer. Recent meta-analyses and systematic reviews have reported that consuming red and processed meats, saturated fats, and high-carbohydrate diets is associated with a higher likelihood of breast cancer (51). When red and processed meats are cooked at high temperatures, they form heterocyclic amines (HCAs), which are carcinogenic and mutagenic compounds. HCAs can damage DNA by forming DNA adducts, leading to replication errors and mutations (52, 53). A meta-analysis of 13 studies found that a high intake of red meat (RR = 1.06; 95% CI: 0.99 and 1.14) and processed meat (RR = 1.09; 95% CI: 1.03 and 1.16) was linked to a higher risk of breast cancer compared to low intake (54).

Similarly, a high intake of sugar and carbohydrates is linked to an increased risk of breast cancer. One meta-analysis found that a high glycaemic index diet was associated with a higher risk of breast cancer (RR = 1.04; 95% CI: 1.00 and 1.07), particularly in postmenopausal women (RR = 1.06; 95% CI: 1.02 and 1.10) (55). High consumption of saturated fat has also been associated with an increased incidence of breast cancer, particularly in ER+ subtypes (RR = 1.12; 95% CI: 1.03 and 1.21; p = 0.006) (56).

Overall, the combined effects of poor dietary habits, a sedentary lifestyle, and inadequate physical activity can contribute to excessive weight gain or even obesity. Obesity not only increases the incidence of breast cancer but also raises mortality rates after diagnosis (57). Women with a high BMI or obesity have more

fatty tissue, which is a key source of oestrogen production, particularly in postmenopausal women (58). This can lead to prolonged exposure to the pro-tumorigenic effects of oestrogen, especially in oestrogen-receptor-positive (ER+) breast cancer.

In addition to hormonal effects, fatty tissue can be converted into fatty acids (FAs). The metabolism of these fatty acids produces ceramides and diacylglycerols (DAGs), which can disrupt cellular function by promoting cell cycle arrest, mitochondrial dysfunction, and apoptosis (59, 60). Additionally, cancer cells can use fatty acids as an energy source, as building blocks and as mediators of oncogenic signalling (61). As a result, postmenopausal women with obesity may face a higher risk of breast cancer progression (62). Additionally, breast cancer patients with a body mass index (BMI) >30 kg/m^2 tend to have poorer OS and DFS, regardless of cancer subtype (63).

1.1.10 Deprivation

Women in deprived areas have a lower risk of developing breast cancer but experience higher mortality rates compared to those in wealthier areas (64). This may be due to women in affluent areas having more risk factors, such as nulliparity, advanced maternal age, and greater use of hormone replacement therapy. However, they may also have better access to screening mammograms, leading to earlier detection (65). A systematic review conducted across Europe found that women from deprived areas are less likely to attend mammogram screenings and face greater barriers to accessing healthcare services (66).

1.2 Breast cancer pathogenesis and staging

Many factors drive normal breast tissue to become cancerous. Over 70% of breast cancer patients are ER-positive therefore oestrogen, particularly, 17-β oestradiol and its receptors are crucial in the initiation of cancer (67, 68). Oestrogen receptors have two forms ERα and ERβ which are nuclear transcription factors. ER-α is dominant in carcinogenesis and can activate the transcription of multiple targeted genes by binding to oestrogen response elements (ERE) leading to increased cell proliferation, progression and genetic mutation (69, 70). The

role of progesterone-driven breast cancer is controversial however a high ratio of PR-A/PR-B has been found in aggressive breast malignancy (71, 72). Androgen and prolactin may contribute to breast carcinogenesis, but the mechanisms remain unclear (73, 74).

Gain of function mutated oncogenes result in uncontrolled cell division, proliferation and survival (75). Twenty per cent of breast cancer patients have amplification/overexpression of HER2 the proto-oncogene that ERBB2 codes for (76). Dimerisation of HER2 with the HER family (HER1, HER3 and HER4) activates downstream signalling pathways that promote tumorigenesis, for example, PI3K/AKT (77, 78). The *MYC* oncogene is commonly mutated in breast cancer resulting in escalation of cell cycle progression, apoptosis and cell dedifferentiation (79). Other established oncogenes such as *CCND1, CCNE1, PIK3CA* and *AKT1* contribute to accelerate tumorigenesis (80).

Loss of function of tumour suppressor genes (TSG) can result in unrestricted cell proliferation, impaired cell adhesion and disrupted DNA damage control (81). Mutations in these genes can be either germline or somatic. *TP53* is the most commonly mutated TSG in many cancers, including breast cancer (82). Normal functions of p53 include cell cycle regulation, apoptosis, senescence and DNA repair. Loss of p53 function results in DNA instability, evading apoptosis and metastasis (83). *BRCA1* and *BRCA2* are TSGs, mutations are autosomal dominant and are strongly associated with breast and ovarian cancer in affected families. Both genes are involved in precisely repairing double-stranded DNA breaks thus abnormal DNA repair due to BRCA mutation can lead to genomic instability and carcinogenesis (84). Other established TSGs are *PALB2, CHEK2, ATM, PTEN, RB1* and *CDH1*, most of which are related to cell cycle regulation and cell adhesion (80).

Epigenetic dysregulation also promotes breast cancer development. Alterations in DNA methylation, histone acetylation and miRNA regulation of oncogenes or TSGs can contribute to the conversion of normal cells to tumour cells (85).

Breast carcinogenesis is a complex mechanism that involves many factors that influence one another. In addition to oncogenes and TSGs, the tumour

microenvironment, cancer stem cells (CSCs) and cell immunity also play a significant role in cancer initiation (86, 87).

1.2.1 Breast cancer staging

Staging is important in describing the extent of disease. TNM staging is classified using tumour size (T), nodal status (N) and evidence of metastasis (M), as staging increases, the disease becomes more aggressive. **Table 1.2** provides a brief definition of the clinical and pathological features of tumour size, nodal status, and metastatic evidence, and **Table 1.3** summarises the anatomical staging.

Table 1.2-The definition of tumour size, nodal status and evidence of metastasis regarding AJCC 8th edition criteria

Components	Clinical TNM	Pathological TNM	Descriptions	
Tumour size (T)				
Tis	cTis	pTis	Ductal carcinoma in situ or pure nipple Paget disease	
T1				
T1mi	cT1mi	pT1mi	≤1 mm	
T1a	cT1a	pT1a	>1 mm but ≤5 mm	
T1b	cT1b	pT1b	>5 mm but ≤10 mm	
T1c	cT1c	pT1c	>10 mm but ≤20 mm	
T2	cT2	pT2	>20 mm but ≤50 mm	
T3	cT3	pT3	>50 mm	
T4	cT4a	pT4a	Extension to the chest wall	
	cT4b	pT4b	Skin ulceration, satellite nodules or oedema (including peau d'orange) not meeting inflammatory carcinoma criteria	
	cT4c	pT4c	Both T4a and T4b	
	cT4d	pT4d	Inflammatory breast cancer	
Nodal status (N)			Clinical (c)	Pathological (p)
N0	cN0	pN0/pN0(i+)	No nodal metastasis	No nodal metastasis or ITCs only
N1	cN1	pN1/pN1(mi)	Movable axillary lymph node **or** micrometastasis	Micrometastasis, 1–3 axillary nodes, or IMN micro/macro metastasis detected by SLNB
N2	cN2	pN2	Clinically fixed or matted axillary nodes	4–9 axillary nodes metastasis or IMN metastasis by imaging without axillary involvement
N3	cN3	pN3	Metastasis to Ipsilateral infraclavicular, supraclavicular, or both IMN and axillary node	≥ 10 axillary nodes or metastasis to infraclavicular, supraclavicular, or IMN with axillary involvement
Metastasis (M)			Clinical (c)	Pathological (p)
M0	cM0	pM0	No clinical or radiographic evidence of metastasis	
M0(i+)	cM0(i+)		No clinical or radiographic evidence of distant metastasis; only microscopic or molecular deposits ≤ 0.2 mm	
M1	cM1	pM1	Distant metastases detected clinically or via radiography	Histologically confirmed distant metastasis or or non-regional nodal metastasis > 0.2 mm

Abbreviation: IMN = internal mammary node, is = *in situ*, i+/ITCs = isolated tumour cells, mi = microinvasion, SLNB = sentinel lymph node biopsy

Table 1.3-AJCC 8th edition breast cancer staging based on TNM status

Stage	T	N	M
0	Tis	N0	M0
IA	T1	N0	M0
IB	T0-1	N1mi	M0
IIA	T0-1	N1	M0
	T2	N0	M0
IIB	T2	N1	M0
	T3	N0	M0
IIIA	T0-2	N2	M0
	T3	N1-2	M0
IIIB	T4	N0-2	M0
IIIC	Any T	N3	M0
IV	Any T	Any N	M1

TNM staging is a prognostic indicator and is used to identify the treatment regimens for patients at each stage (22).

1.3 Breast cancer treatment

Treatment of breast cancer consists of locoregional and systemic treatment. Breast surgery and radiation are the mainstay for locoregional control while systemic therapy whether hormonal, chemotherapy or targeted therapy is based on the intrinsic subtypes and staging.

1.3.1 Locoregional management

1.3.1.1 Breast cancer surgery

Breast and axillary surgery are the two main surgical options that are curative, particularly in non-metastatic settings.

Breast surgery

Breast-conserving surgery (BCS), a limited breast resection, has become the standard of care, offering equivalent oncological outcomes to mastectomy in patients without contraindications(88). The long-term follow-up with a median of 20 years confirmed that BCS has a non-inferior mortality rate compared to mastectomy (26.1% vs 24.3%, p=0.8),(89). However, radical surgery, such as

modified radical mastectomy, remains necessary for certain aggressive breast cancer histologies, such as inflammatory breast cancer (IBC)(90). The role of breast surgery in advanced-stage breast cancer remains controversial. However, recent randomised controlled trials suggest a potential benefit in selected cases, particularly in oligometastatic or ER-positive subtype, where surgery possibly extends life expectancy(91). Therefore, surgical treatment should be tailored on a case-by-case basis.

Axillary surgery

Axillary lymph node dissection (ALND) has been replaced by sentinel lymph node biopsy (SLNB) in early-stage breast cancer (90, 92). In low tumour burden disease, ALND is not superior to SLNB which only removes a few nodes.

The ACOSOG Z0011 clinical trial revealed in T1-2 disease with 1-2 metastatic sentinel nodes, SLNB is not inferior compared to ALND in terms of 10-year DFS; 80.2% in SLNB and 78.2% in ALND (HR 0.85; 95% CI: 0.62-1.17; P = 0.32)(93). In breast cancer patients with biopsy-proven lymph node metastases before treatment who convert to node-negative status after preoperative systemic therapy, SLNB combined with targeted axillary dissection (TAD), which selectively removes previously positive nodes, has shown a significantly lower false negative rate (1.4%) compared to SLN alone (10.1%) (95% CI: 0.03-7.3; p= 0.03) (94). Kuemmel et al. validated that TAD resulted in no inferior axillary recurrence and invasive disease-free survival (IDFS) at 3 years (1.8% recurrence rate and 82.4% IDFS) compared to TAD with ALND (1.4% recurrence rate and 91.2% IDFS), with no statistically significant difference (p=0.56 recurrence rate and HR 0.83; 95% CI: 0.34-2.05; p=0.69 IDFS) (95).

The benefit of axillary surgery in elderly breast cancer patients, particularly in ER-positive tumours, is limited. Several RCTs and prospective studies have concluded that omitting axillary surgery is safe in low-risk elderly patients (tumour size ≤2 cm and no suspicious axillary lymph node metastasis), with no inferior survival outcomes (96). Thus, de-escalating axillary surgery has currently been accepted without inferior survival and recurrence outcomes in the era of advanced systemic therapy and radiation techniques.

ALND is currently reserved for patients with extensive disease, for example, IBC, clinical matted lymph nodes, and persistent palpable lymph nodes after pre-operative systemic therapy (90).

1.3.1.2 Radiation therapy (RT)

RT is indicated in patients who have undergone BCS, have nodal metastasis or are stage II-III BC (97). Breast-conserving surgery requires additional RT for optimal locoregional control. The NSABP B-06 clinical trial reported that the rate of recurrence is higher in BCS alone (39.2%) than BCS with whole breast irradiation (WBI) (14.3%) ($p < 0.001$) after 20-year follow-up (98). Nodal radiation is beneficial in patients with nodal metastasis and can replace ALND in selected cases. In patients with 1-2 metastatic nodes who have undergone BCS with SLNB, ALND is avoidable if patients have planned WBI following the ACOSOG Z0011 protocol (93). In mastectomy patients with 1-2 positive SLNB, axillary radiation is preferred over ALND, as there was no significant difference in axillary recurrence at 10-year follow-up between axillary RT (1.82%) and ALND (0.93%) (HR 1.71; 95% CI: 0.67-4.39)(99). Recent advancements have allowed for reduced radiation field exposure in low-risk patients by partial breast irradiation (PBI) instead of whole breast irradiation or by lowering radiation dose and treatment cycles without compromising survival outcomes (100, 101).

While low-risk early breast cancer patients are good candidates for de-escalated radiation therapy, standard-dose radiation remains crucial for locally advanced breast cancer patients (tumour size >5 cm or N2-3 disease) to improve locoregional control (102, 103).

1.3.2 Systemic treatment

1.3.2.1 Chemotherapy

Systemic chemotherapy is recommended for high-risk luminal subtypes, non-luminal breast cancer, and locally advanced and metastatic breast cancer (104). Anthracycline-, taxane- and platinum-based regimens form the backbone of chemotherapeutics in breast cancer (90, 105). The dosage and treatment cycles are determined by tumour burden and patient performance status.

Anthracyclines, such as doxorubicin and epirubicin, exert their anticancer effect by inhibiting topoisomerase II, an essential enzyme responsible for preventing double-strand DNA breaks (106). This inhibition disrupts DNA repair, leading to DNA damage and apoptosis. In addition, anthracyclines intercalate into DNA, destabilising chromatin by extracting histones, further impairing DNA function (107). They also generate free radicals and induce mitochondrial damage, exacerbating cellular stress and promoting cancer cell death (108).

Taxane, including paclitaxel and docetaxel, act by stabilising microtubules, which are crucial for mitotic spindle formation during cell division (109). By preventing microtubule depolymerisation, taxane blocks cell cycle progression at the G2/M phase, leading to mitotic arrest and apoptosis.

Platinum-based chemotherapeutics, such as carboplatin, induce cytotoxicity by forming cross-linkage, which prevents DNA replication and transcription (110). This disruption ultimately triggers cell cycle arrest and programmed cell death, particularly in rapidly dividing cancer cells.

With the discovery of more targeted therapies and predictive biomarkers, systemic treatment has become increasingly personalized. Multigene assays, such as Oncotype DX and MammaPrint, help tailor chemotherapy decisions, reducing unnecessary toxicity while maintaining survival outcomes (111).

1.3.2.2 Hormonal therapy

Oestrogen receptor-positive breast cancer patients benefit from anti-hormonal treatment. There are 2 main classes of endocrine treatment: selective oestrogen receptor modulators (SERM) and aromatase inhibitors (AIs) (112). Tamoxifen, a SERM, prevents oestrogen from binding to ER in cancer cells, thereby reducing recurrence. It is effective in both pre- and post-menopausal women (113). In contrast, AIs, comprising anastrozole, letrozole and exemestane, inhibit the conversion of androstenedione and testosterone into oestrone and oestradiol, respectively, in peripheral tissue such as the liver, breast, muscle, and adipose tissue. These inhibitors are effective only in post-menopausal women, as they lack ovarian oestrogen production (114).

The efficacy of both drug classes has been demonstrated in large-population RCTs. A 5-year tamoxifen regimen reduces the annual breast cancer recurrence rate by 50% and mortality by approximately 30%. After 15 years of follow-up, patients who received tamoxifen had a significantly lower recurrence rate (33.2% vs 45%, $p < 0.00001$) and breast cancer mortality rate (25.6% vs 34.8%, $p < 0.00001$) compared to the non-tamoxifen group(113).

ER-positive post-menopausal women, particularly those at medium to high risk, benefit more from AIs than tamoxifen. A large meta-analysis of 35,000 patients found that a 5-year AI regimen led to a greater reduction in recurrence (19.1% vs. 22.7%, $p < 0.00001$) and breast cancer mortality (12.1% vs. 14.2%, $p = 0.009$) at 10-year follow-up (115). However, while AIs are more effective than tamoxifen, their unfavourable side effects, such as osteoporosis and joint pain, must be considered, especially for patients with pre-existing conditions or those who develop these issues during treatment (116). Selecting the optimal endocrine therapy for ER-positive postmenopausal breast cancer should involve balancing the risk of recurrence against potential side effects.

Premenopausal women with breast cancer benefit from ovarian function suppression (OFS) in combination with either exemestane or tamoxifen. The combined analysis of the SOFT and TEXT trials, with 13 years follow-up, demonstrated that OFS with exemestane was superior to OFS with tamoxifen in terms of disease-free survival (DFS) (HR 0.79; 95% CI: 0.70-0.90; $p < 0.001$) and disease-free relapse interval (DFRI) (HR 0.83; 95% CI: 0.70-0.98; $p = 0.03$). However, overall survival (OS) was similar between the two groups (HR 0.93; 95% CI: 0.78-1.11; $p = 0.03$) (117). High-risk patients, particularly those under 35 years old, with tumours larger than 2 cm and histological grade 3, were found to benefit most from the combination of OFS and exemestane (117). These characteristics indicate more aggressive tumour behaviour, leading to poorer prognosis and greater risk of recurrence. In these patients, OFS and exemestane showed improved overall survival (OS) compared to other treatment combinations, highlighting its effectiveness in reducing recurrence risk for this subgroup. The role of OFS in premenopausal patients is crucial, as it effectively lowers ovarian oestrogen production, which can fuel the growth of ER-positive tumours (118). This, combined with exemestane's mechanism of action as an aromatase inhibitor,

provides a more comprehensive suppression of oestrogen and offers a more effective treatment option for high-risk premenopausal women.

1.3.2.3 Targeted therapy

Advancements in targeted therapies have emerged with a deeper understanding of molecular mechanisms and predictive biomarkers that influence tumour response and prognosis. Following the discovery of HER-2 overamplification in breast cancer in 1987, the first monoclonal antibody targeting HER-2 protein was developed (119). In 1998, the humanised monoclonal antibody trastuzumab was approved for the treatment of metastatic breast cancer and was later adopted as a standard of care for early-stage, non-metastatic disease as it significantly improved survival outcomes in these patients (120, 121). The discovery of anti-HER2 monoclonal antibodies prompted extensive research into additional HER-2-targeted therapies aimed at inhibiting the HER-2 signalling pathway through different mechanisms. Among these were small-molecule tyrosine kinase inhibitors such as lapatinib, which was approved in 2007 and functions by reversibly inhibiting both HER-1 and HER-2 (122). Antibody drug conjugates, such as T-DM1 (trastuzumab emtansine), emerged as a promising class introduced in 2013, combining the specificity of trastuzumab with the cytotoxicity of a chemotherapeutic agent(123). Furthermore, the combination of HER-2 targeted antibodies gained clinical significance with the approval of pertuzumab in 2012, which, when used in conjunction with trastuzumab, enhances HER-2 blockade by preventing receptor dimerisation (124, 125, 126, 127). Collectively, these advancements have significantly expanded the therapeutic landscape for HER-2 positive breast cancer and improved clinical outcomes across various stages of the disease.

Cyclin-dependent kinase 4 and 6 (CDK4/6) inhibitors—palbociclib, ribociclib, and abemaciclib—have revolutionised the treatment of ER-positive, HER2-negative luminal breast cancer by targeting cell cycle progression, with approval beginning in 2015 (128). These inhibitors prevent the phosphorylation of retinoblastoma protein (Rb), thereby halting the transition from the G1 to S phase and leading to cell cycle arrest (129). CDK4/6 inhibitors are now a standard treatment option in both early-stage and advanced hormone receptor-positive

breast cancer, often combined with endocrine therapy (e.g., aromatase inhibitors or fulvestrant) to improve progression-free and overall survival (130, 131, 132).

Another major advancement in targeted therapy is the use of poly (ADP-ribose) polymerase (PARP) inhibitors, such as olaparib and talazoparib, in patients with BRCA1/2-mutated breast cancer. Both drugs were approved by the Food and Drug Administration (FDA) in 2018 for the treatment of germline BRCA-mutated, HER-2 negative metastatic breast cancer (133). These inhibitors exploit synthetic lethality by blocking the repair of double-stranded DNA breaks, leading to genomic instability and cancer cell death (134).

1.3.2.4 Immunotherapy

Immunotherapy has been underinvestigated in breast cancer for two decades; however, only Immune checkpoint blockade (ICB) has gained prominence as a targeted therapeutic strategy in breast cancer treatment in recent years, particularly since the FDA approval of atezolizumab in 2019 for TNBC (135). As TNBC is highly aggressive and has limited targeted therapy options, immune checkpoint inhibitors targeting the programmed death-1 (PD-1) and programmed death-ligand 1 (PD-L1) pathways have been developed to enhance antitumor immunity. These inhibitors work by preventing immune evasion, allowing cytotoxic T cells to recognise and attack tumour cells more effectively (91).

Pembrolizumab, a PD-1 inhibitor, has been widely used in the treatment of locally advanced and metastatic TNBC. Clinical trials have demonstrated that pembrolizumab, in combination with chemotherapy, significantly prolongs progression-free survival (PFS) by up to 7 months compared to chemotherapy alone (136). It is currently approved as a neoadjuvant therapy for early-stage TNBC, where it has been shown to improve pathological complete response (pCR) rates (136, 137). In the KEYNOTE-522 trial, 64.8% of patients receiving pembrolizumab achieved pCR compared to 51.2% in the placebo group, highlighting its role in improving treatment outcomes before surgery (136). Another immune checkpoint inhibitor, atezolizumab, a PD-L1 inhibitor, has also been studied in TNBC. It has shown improved pCR rates in stage II-III TNBC patients, particularly in the PD-L1-positive subgroup (137). Atezolizumab, in

combination with nab-paclitaxel, was the first immunotherapy to receive FDA approval for metastatic TNBC with PD-L1 expression (135).

The role of immune checkpoint blockade has been explored in other breast cancer subtypes, including high-risk luminal and HER2-overexpressing breast cancers. Clinical trials are ongoing to investigate the potential of ICB in these subtypes, particularly in combination with targeted therapies, chemotherapy, and endocrine therapy (138, 139, 140, 141). In HER2-positive breast cancer, combining ICB with HER2-directed agents such as trastuzumab is being investigated to enhance immune activation (138, 139). Similarly, in high-risk ER-positive breast cancer, the interplay between hormone signalling and immune modulation is being studied to optimise treatment strategies (140, 141). As research advances, ICB is expected to play an increasingly significant role in personalised breast cancer treatment, particularly in patients with high-risk features and immune-responsive tumours (140, 141).

1.4 Breast cancer subtypes

Before the 21st century, prognosis and predictive factors for breast cancer relied on tumour size, nodal status, histologic grade and the expression of ER/PR using immunohistochemistry (23). However, this approach was significantly refined after Perou et al. identified 4 subtypes classified by gene expression; basal-like, Erb-B2 overexpression, normal-breast-like and luminal breast cancer (142). These subtypes were distinguished by unique molecular signatures, with basal-like tumours often exhibiting high expression of cytokeratin and lacking hormone receptor expression, while luminal A tumours are typically ER-positive, HER2-negative, and exhibit a slower growth pattern. This was validated by Sørlie et al. who reported at least 5 distinct subclasses using cDNA microarrays: two luminal/ER epithelial gene expression (luminal A and B) and three non-luminal gene expression (normal-breast-like, ERBB2+ and basal-like) (143). These molecular subtypes have significant clinical implications. Basal-like tumours, which are more aggressive, tend to have a worse prognosis, with shorter overall survival (OS) and relapse-free survival (RFS) compared to luminal subtypes. In contrast, luminal A tumours are typically more responsive to endocrine therapies and are associated with a more favourable prognosis (143). These findings helped

establish the heterogeneity of breast cancer with distinct biological behaviours across subtypes (144, 145, 146).

Molecular profiling has been used since 2007 to predict treatment response and prognosis, leading to the development of genomic tests such as Oncotype DX and MammaPrint (147). These tests assess the expression of multiple genes to predict the likelihood of recurrence and chemotherapy benefit. However, genomic testing remains limited to specialized centres, often due to cost or availability. Thus, current clinical practice generally relies on the classification of breast cancer into five intrinsic subtypes based on surrogate histology and immunohistochemical (IHC) markers, including ER, PR, HER2, and Ki-67 (26). While IHC-based classification remains widespread, it lacks the precision and depth provided by genomic profiling, highlighting the need for broader access to molecular testing in clinical settings.

1.4.1 Luminal A

Luminal A breast cancer is defined as ER-positive, high PR, HER-2 negative, low Ki-67 and low-risk molecular signature if available (37). This subtype accounts for about 60-70 % of all breast cancers and generally has a good prognosis due to its lower proliferation rate and high expression of ER-signalling proteins (148). *PIK3CA* is the most significantly mutated gene in luminal A (45%) followed by *MAP3K1* (14%), *GATA3* (14%) and *TP53* (12%). In addition, luminal A tumours exhibit high expression of *RB1* and cyclin D 1 amplification (149).

Luminal A responds well to anti-hormonal treatment, such as, tamoxifen and AIs,however, it tends to be less responsive to chemotherapy compared to other subtypes. The DBCG77B trial investigated the benefit of chemotherapy in high-risk premenopausal women. In the subgroup of luminal A patients (n=165), defined by ER>1%, PR>20%, HER2 negative and Ki-67 <14%, chemotherapy with cyclophosphamide-based regimens did not show any improvement in DFS (HR 1.06;95%CI: 0.53-2.14) and OS (HR 1.00;95%CI: 0.55-1.82) compared to no chemotherapy with a 10-year follow-up (150). The Stockholm Tamoxifen (STO-3) RCT trial, with long-term follow-up demonstrated that luminal A patients who received tamoxifen had a significantly longer distant relapse-free interval at 25-years compared to untreated patients. Specifically, patients who received

tamoxifen had a 25-year DRFI of 87%, compared to 70% for untreated patients (log-rank P < 0.001), even after tamoxifen was discontinued after 15 years (151).

1.4.2 Luminal B

1.4.2.1 Luminal B/HER-2 negative

Luminal B/HER-2 negative breast cancer is defined as ER or PR positive, HER-2 negative, high Ki-67 and high-risk molecular signature if available (37). *PIK3CA* (29%) and *TP53* (29%) are the most mutated genes followed by *GATA3* (15%), *MML3* (6%), *CDH* (5%) and *MAP3K1* (5%) (149). Compared to luminal A, the luminal B subtype is more aggressive, often associated with larger tumour size, higher nodal metastasis and higher histologic grade (152). A recent study by Yang et al. reported that the survival outcomes for luminal B/HER2 negative are worse than those for luminal A (153). This highlights the more aggressive clinical behaviour of luminal B, suggesting that more intensive treatment strategies may be necessary for optimal patient outcomes.

The treatment regimens for luminal B typically include endocrine treatment, which is the mainstay treatment. In high-risk cases, chemotherapy may be considered. Gene expression testing, for example, the 21-gene breast cancer recurrence score (Oncotype Dx®), is commonly used to predict which patients will benefit from chemotherapy (90, 154). The test categorises ER-positive/HER2-negative breast cancer patients into 3 recurrence risk scores (RRS): low, intermediate or high risk. An RRS≥26 indicates a higher likelihood of chemotherapy benefit, regardless of menopausal status (155). Patients in this category are generally considered to have a high risk of recurrence and are more likely to benefit from chemotherapy in addition to endocrine therapy (156).

1.4.2.2 Luminal B/HER-2 positive

Luminal B/HER-2 positive or triple positive breast cancer is defined as ER and or PR positive and HER-2 positive and accounts for 10% of all breast cancers (157). The genomic landscape of luminal B/HER2-positive breast cancer shares gene expression characteristics with both luminal and HER2-enriched classifications (158). The HER2 overexpression plays a key role in

endocrine treatment failure, primarily by activating signalling pathways such as the mitogen-activated protein kinase (MAPK) and phosphatidylinositol 3-kinase (PI3K)/mTOR pathways, which are involved in cell growth and survival (159). Additionally, ER can independently activate growth signalling pathways, further contributing to tumour progression and treatment resistance (160). This combination of factors generally results in a poor prognosis for patients with Luminal B/HER2-positive breast cancer.

Patients with this subtype can benefit from a combination of anti-HER2 antibody therapy (such as trastuzumab or pertuzumab) and endocrine treatment (such as tamoxifen or aromatase inhibitors), which can improve survival outcomes (88).

1.4.3 HER-2 enriched

The HER-2 overexpression subtype is defined as ER negative, PR negative and HER-2 positive. The latter is confirmed by IHC 3+ or IHC 2+ with HER-2 gene amplification, as assessed by in situ hybridisation (ISH) (161). This subtype accounts for 15-20% of all breast cancer patients (148). The HER2 receptor is one of the 4 epidermal growth factor receptor (EGFR) family members (162). Dimerisation of HER-2 with other EGFRs induces oncogenic PI3K/mTOR and MAPK signalling pathways that result in cancer cell proliferation and invasion (163).

In HER2 overexpression breast cancer, *HER2*/*ERBB2* amplification is central, occurring in about 80% of cases. Mutations in the *TP53* gene are found in approximately 72% of cases, and *PIK3CA* mutation in39% (149).

Targeted anti-HER2 antibodies are critical in treating HER2-overexpressing breast cancer. Trastuzumab, pertuzumab, neratinib and T-DM1 are recommended for adjuvant treatment. For metastatic disease, additional targeted HER2 therapies, for example, lapatinib and tucatinib, further improve patient outcomes (164). Trastuzumab has become a cornerstone in the treatment of HER2-positive breast cancer at all stages (165). A recent meta-analysis showed that trastuzumab reduced the absolute 10-year recurrence rate by 9% and mortality by 6.4% in patients with early-stage HER2-positive breast cancer (166). High-risk HER2-

positive patients had improved survival outcomes if they achieved pCR following neoadjuvant anti-HER2 therapy (127, 167). For metastatic HER2-positive breast cancer, anti-HER2 treatments have also been shown to improve both progression-free survival (PFS) and overall survival, highlighting their ongoing efficacy in advanced disease (168).

1.4.4 Triple-negative

Triple-negative breast cancer (TNBC) is characterised by the absence of ER, PR, and HER2 expression. This subtype comprises approximately 10-15% of all breast cancers and is associated with poor prognosis, early recurrence, and high metastatic potential (169). The Cancer Genome Atlas Network identified that 75% of TNBC patients have basal-like genetic expression profiles, which align closely with basal epithelial cells of the breast. *TP53* is the most common mutation (84%), followed by *PIK3CA* (9%) (149). Alterations in *ATM*, *BRCA1/2, cyclin E* amplification and *RB1* loss are also common in TNBC. At the transcriptional level, TNBC frequently exhibits hyperactivation of key oncogenic transcription factors, including *FOXM1*, *MYC* and *HIF-1a /ARNT*, which drive proliferation, metabolic reprogramming and therapy resistance (149). Molecular subtyping has further categorised TNBC into basal-like, immunomodulatory, mesenchymal, and luminal androgen receptor (LAR) subtypes, each with distinct biology and therapeutic vulnerabilities (170). Epigenetic modifications, such as DNA methylation and histone modifications, also contribute to TNBC heterogeneity and aggressiveness (171).

The lack of hormone receptors and HER2 amplification means that targeted therapies used in other breast cancer subtypes are ineffective, making chemotherapy the backbone of treatment. However, emerging targeted therapies have improved outcomes for specific subgroups. Immune checkpoint inhibitors such as pembrolizumab are approved for PD-L1-positive TNBC (136, 137), while PARP inhibitors (olaparib and talazoparib) are effective in germline BRCA-mutated TNBC (41, 172, 173). Antibody-drug conjugates (ADCs), such as sacituzumab and govitecan, have shown efficacy in metastatic TNBC (174) and AKT inhibitors are being explored for tumours with PI3K/AKT pathway alterations (175). Additionally, androgen receptor inhibitors may be beneficial in

the LAR subtype (176). Future research is focused on combination strategies, liquid biopsy monitoring, and novel immunotherapeutic approaches to further refine treatment options (177, 178).

1.5 Hypoxic tumour microenvironment in breast cancer

Hypoxia is a pivotal hallmark of the tumour microenvironment (TME), occurring when rapid tumour proliferation outpaces its blood supply, leading to oxygen deprivation (179). In breast cancer, the median partial pressure of oxygen (PO_2) is 10 mm Hg (~1% O_2), while in normal breast tissue it is 65 mm Hg (180). Intra-tumoural hypoxia is observed across all breast cancer subtypes but is particularly higher in TNBC. Ye et al. analysed RNA sequencing data from breast cancer cell lines and found 42 hypoxia signature genes and upregulation of 22 pathways after inducing hypoxic conditions with 1% oxygen. Notably, hypoxic gene expression was higher in the basal-like subtype (181).

Hypoxia-inducible factor 1 alpha (HIF-1α) is a master transcription factor activated under low-oxygen conditions (182). In normoxia, HIF-1α is degraded through multiple steps. Initially, HIF-1α is hydroxylated by prolyl hydroxylase (PHD) before binding to Von Hipple Lindau protein (pVHL) and this complex is the target of ubiquitination by E3 ubiquitin ligase leading to complete proteasomal degradation (183). However, under hypoxic conditions, HIF-1α is stabilised and, subsequently, activates multiple transcriptional targets, for example, vascular endothelial growth factor (VEGF), insulin-like growth factor-2 (IGF-2) and glycolytic enzymes, resulting in increased tumour proliferation, angiogenesis, and metabolic adaptation (184, 185). The mechanism of HIF-1α regulation is summarised in **Figure 1.1**.

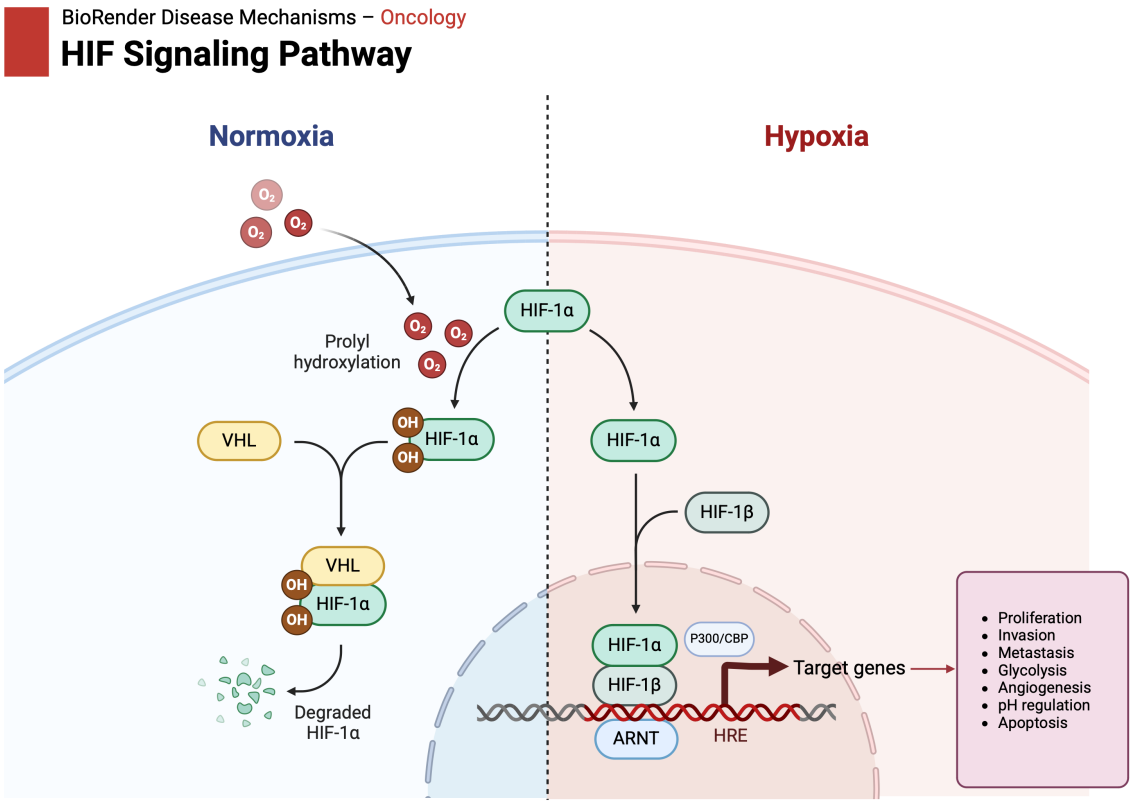

Figure 1.1-Schematic depicts HIF-1α regulation and target genes of HIF-1α (Created with BioRender.com)

Tumour hypoxia is of interest as it has been associated with tumour invasion, progression, and therapeutic resistance (186). A number of clinical studies have shown that hypoxia is related to poor oncological outcomes and its potential as a druggable target is currently being explored (187).

While tumoural hypoxia holds potential as a therapeutic target, its accurate measurement remains a subject of debate. Measurement of hypoxic is complex and depends on the method used and spatial relationship between tumour cells and blood vessels. Ideally, an optimal measurement technique should be precise, non-invasive, and capable of identifying suitable candidates for targeted interventions. Currently, hypoxia assessment methods fall into two categories: direct (A) and indirect (B-C), as detailed below.

A. **Direct assessment of tumour oxygenation**

The direct measurement of tumour oxygen levels (pO_2) involves assessing oxygen pressure within the tumour microenvironment. One traditional approach is the use of polarographic oxygen electrodes, which are inserted directly into the tumour to generate a histogram of oxygen pressure distribution (188, 189). While this method provides precise pO_2 readings, it is invasive, requires technical expertise, and cannot differentiate between hypoxic regions and necrotic tissue, limiting its clinical application (190).

To overcome these limitations, alternative non-invasive and minimally invasive techniques have been developed, including immunohistochemistry of hypoxic markers in tissue samples and imaging techniques tracking specific hypoxic markers (191). Although these techniques provide valuable insights into tumour hypoxia, challenges remain regarding accuracy, resolution, and standardisation.

B. **Endogenous markers of hypoxia**

Oxygen deprivation in cancer cells activates specific pathways resulting in the expression of the hypoxic-responsive protein, many of which are associated with tumour progression and poor patient survival. Several endogenous hypoxia markers have been studied; however, each has its limitations.

a) Hypoxia-inducible factor -1 alpha (HIF-1α)

HIF-1α is a critical regulatory transcription factor under hypoxic conditions. However, it has a short half-life of 5-10 minutes after re-oxygenation (192), making its detection challenging. Additionally, HIF-1α can be upregulated or stabilised even in normoxia by alternative signalling pathways, for example, PI3K/AKT/mTOR pathways, mutation in pVHL and PTEN, or dysfunction of PHD (193). Despite these complexities, HIF-1α expression has been linked to poor survival outcomes in multiple cancers, including oral cavity, breast, and colon cancers (194, 195, 196).

b) Carbonic anhydrase 9 (CAIX)

CAIX is a transmembrane enzyme that converts carbon dioxide (CO_2) into H^+ and HCO^-_3, contributing to an acidic tumour microenvironment (197). CAIX expression is exclusively regulated by HIF-1α, as its hypoxia-responsive

element (HRE) is located in the promotor of CAIX gene (198). CAIX is predominantly expressed in cancer cells, with little or no expression in normal tissues (198). Additionally, CAIX has a longer half-life of 2-3 days, allowing detection even after re-oxygenation (199). Many studies have reported a strong correlation between CAIX expression and poor survival outcomes in cervical cancer (200), head and neck cancer (201), non-small cell lung cancer (202), and breast cancer (203, 204).

c) Glucose transporter-1 (GLUT-1)

GLUT-1 is one of eight glucose transporters that are upregulated in conditions of oxygen deficiency. The alteration of glucose metabolism in hypoxia results in increased glycolysis and thus requires more glucose uptake which could be in response to GLUT-1 overexpression(205). Clinical studies have shown that high GLUT-1 expression is associated with a worse prognosis in several cancer types (206).

d) Other hypoxia-responsive genes

Additional hypoxia markers include osteopontin (OPN), VEGF, lysyl oxidase (LOX) and lactate dehydrogenase isoenzyme-5 (LDH-5). While these markers have been identified as hypoxia-responsive genes, their clinical relevance remains inconsistent (207). The presence of hypoxia markers such as VEGF and OPN in blood samples has been investigated for potential biomarker use, but their clinical implications remain unclear (208, 209).

C. Hypoxia imaging

Localisation of the hypoxic area by imaging is an emerging modality that may help improve treatment outcomes. The most commonly used modalities include Single-Photon Emission Computed Tomography (SPECT) and Positron Emission Tomography (PET), both of which utilise nitroimidazole-based hypoxia tracers (210). PET is generally more sensitive than SPECT in detecting hypoxia. Dynamic contrast-enhanced MRI can detect the region of hypoxia by determining perfusion and proliferation gradients (211). Other imaging approaches include Blood Oxygen Level-Dependent (BOLD) MRI, which leverages deoxyhaemoglobin levels to differentiate vascularised from non-vascularised tissues, resulting in low

T2 signals in hypoxic areas on T2-weighted images (212). Metabolite-detected MRI is an alternative option that measures hypoxia-induced metabolic byproducts, for example, lactate accumulation (213). Optical contrast imaging combined with ultrasound offers high sensitivity for assessing blood flow and vessel direction, relying on the contrast gradients between internal and external vessels (214).

Several hypoxia-specific radiotracers have been developed for 18F-FDG PET, MRI, and other radiosensitive techniques. These include mizonidazole (1-(alpha-methoxymethyl ethanol)-2-nitroimidazole) (215), pimonidazole (1-(2-nitro-1-imidazolyl)-3-N-piperidino-2-propanol) (216), and EF5 (a nitroimidazole compound) (217). In addition, PET with 150-labeled water, contrast-enhanced CT, and Doppler ultrasound can provide indirect assessment of tumour oxygenation by measuring blood flow (207).

Despite the potential of these imaging techniques, none have been fully integrated into routine clinical practice for breast cancer due to limitations in sensitivity, resolution, and standardisation. However, endogenous hypoxia markers remain promising non-invasive alternatives, with growing evidence supporting their role as surrogate biomarkers for prognosis and treatment response.

1.5.1 The effect of hypoxia on angiogenesis and metabolism in cancer cells

1.5.1.1 Hypoxia-associated angiogenesis

Hypoxia-inducible factor- 1α (HIF-1α) facilitates tumour proliferation by promoting angiogenesis. Under hypoxic conditions, HIF-1α activates the transcription of vascular endothelial growth factor (VEGF) or VEGF-A and its receptor (VEGFR-1) and nitric oxide synthase (NOS) (218). VEGF and VEGFR-1 are involved in the vascular formation process by increasing vascular permeability and inducing endothelial cell proliferation, migration and assembly (219). NOS is an enzyme that produces nitric oxide (NO), which subsequently induces vasodilation and stimulates endothelial cell proliferation and migration while inhibiting endothelial cell apoptosis (220). HIF-1α also regulates angiogenesis through PI3K/AKT signalling pathways. Fibroblast growth factors (FGFs) couple with

receptor tyrosine kinase to activate PI3K/AKT and MEK1/ERK downstream signalling, consequently increasing HIF-1α and VEGF expression (221). HIF-2α also facilitates vasculogenesis as does HIF-1α, however, there is a non-overlapping function for both HIFs (222). HIF-1α decreases interleukin-8 (IL-8) by upregulating Mxi-1 and downregulating nrf2 and c-Myc while HIF-2α reverses this (223).

1.5.1.2 Hypoxia-associated alteration of cancer lipid metabolism

Tumour cells always encounter some degree of hypoxia and nutrient deprivation. Although hypoxia activates angiogenesis to promote tumour proliferation, neo-vessels are structurally abnormal and functionally inefficient compared to normal vasculature (224). Thus, tumours continue to face metabolic stress, including limited oxygen and nutrient supply. One of the key metabolic pathways affected by these conditions is lipid metabolism, which plays a vital role in cell membrane formation, energy storage, and intracellular signalling (225). Unlike normal cells that primarily acquire fatty acids (FAs) through dietary intake, cancer cells rely heavily on de novo fatty acid synthesis to sustain their rapid proliferation (226, 227).

Acetyl-CoA is a major source for FA synthesis (228). In normal tissue, acetyl-CoA is primarily derived from pyruvate oxidation in the TCA cycle. However, under hypoxic conditions, cancer cells adapt by utilising alternative carbon sources such as glutamate and acetate, which are converted into acetyl-CoA (229). Acetyl-CoA carboxylase converts Acetyl-CoA to Malonyl-CoA which is then converted with Acetyl-CoA by fatty acid synthase (FASN) to generate palmitate; the first substrate for FAs synthesis (61, 230). Although de novo FA synthesis is the main source of FAs in cancer cells, FAs can be taken up via the low-density lipoprotein receptor (LDLR), FA transport proteins (FATPs) or FA translocase (FAT) combined with FA binding proteins (FABPs) (229, 231).

One potential regulator of lipid metabolism in hypoxia is the N-myc downstream-regulated gene 1 (NDRG1), which is directly activated by HIF-1α (232). A few studies have explored the role of NDRG1 in lipid metabolism, and research in breast cancer cell lines has shown that silencing NDRG1 leads to increased lipid droplet accumulation while also reducing cell viability and proliferation. Conversely, overexpression of NDRG1 was found to limit lipid

droplet formation, particularly under nutrient-deprived conditions, suggesting its role in modulating lipid storage and utilisation in tumours (233). A study investigated the effects of lovastatin in breast cancer found that it increased PTEN regulated Akt signalling pathways, leading to the upregulation of NDRG1 protein in the MDA-MB-231 cell line (234). However, the precise mechanisms by which NDRG1 regulates cancer lipid metabolism remain unclear, highlighting the need for further research to establish its clinical significance.

1.5.1.3 Hypoxia-associated alteration of cancer glucose metabolism

Metabolic activity of cancer cells differs significantly from that of normal cells, as they often shift their primary energy production from mitochondrial oxidative phosphorylation to glycolysis, even in the presence of sufficient oxygen—a phenomenon known as the Warburg effect (235, 236). This shift enables cancer cells to produce ATP more rapidly, though less efficiently, through glycolysis. As a result, cancer cells require an increased uptake of glucose to sustain their high energy demands and to support the production of metabolic intermediates needed for rapid cell growth and proliferation (237). Under hypoxic conditions, HIF-1α stimulates the transcription of enzymes required for glycolysis, such as glycolysis regulator phosphoglycerate mutase (PGAM1), lactate dehydrogenase A (LDHA), lactate dehydrogenase C (LDHC) and lactate dehydrogenase-5 (LDH-5) (179). Conversely, HIF-1α inhibits enzymes that facilitate pyruvate entry into the tricarboxylic acid (TCA) cycle. HIF-1α and HIF-2α also enhance LDHA expression at the transcription level (238). This results in an increase in lactate and protons (H^+).

The hypoxic TME shifts the metabolism of cancer cells toward aerobic glycolysis and glutaminolysis resulting in less energy production and promoting tumour acidity (239). Lactate, proton and carbon dioxide (CO_2) are the main end products of cancer cell metabolism and need to be eradicated from the intracellular space because of the acidic toxicity (239). Monocarboxylate transporter (MCT), sodium-hydrogen exchanger (NHE) and transmembrane diffusion are the main methods by which they are exported into the extracellular space. Accumulation of acid extracellularly causes extracellular acidosis along with HCO_3^-, a product of CO_2 hydration by CAIX, which is imported into the cells

to maintain intracellular alkalosis (**Figure 1.2**). This supports cancer cell proliferation, progression and metastasis (240).

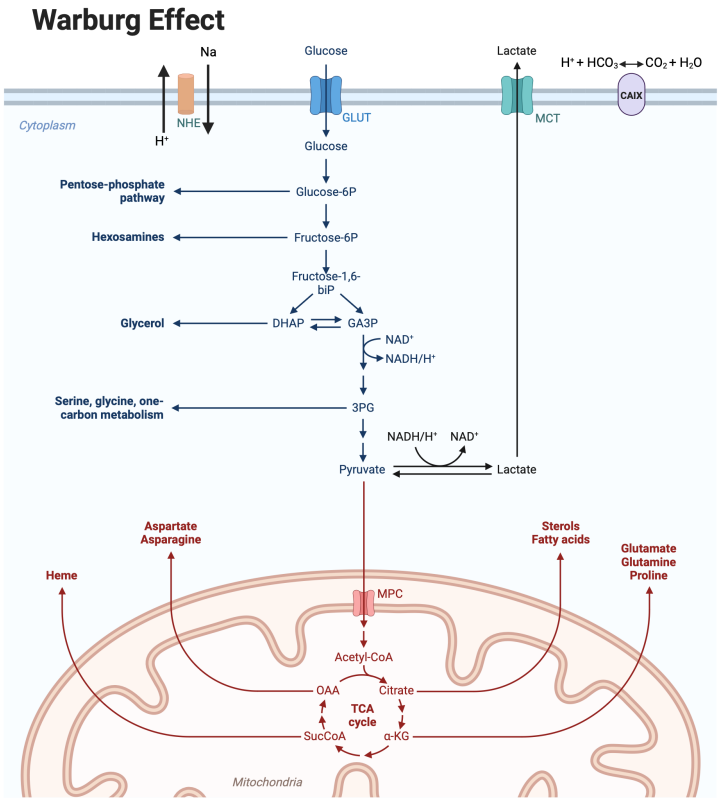

Figure 1.2-Alteration of metabolism in cancer cells is mediated by hypoxia (Created with BioRender.com)

1.6 Carbonic anhydrase 9 (CAIX)

Carbonic anhydrase 9 (CAIX), a 54/58 kDa homodimer protein, functions as a pH regulator by catalysing extracellular CO_2 to react with H_2O to generate HCO_3^- and H^+ (241, 242, 243). CAIX is a transmembrane enzyme, one of the zinc metalloenzyme family, and is activated by HIF-1α (244). The *CA9* gene activates CAIX transcription when HIF-1α binds to the hypoxia response element (HRE) at the promotor (245). The other less important CAIX regulatory pathways are phosphatidylinositol 3-kinase (PI-3K) and the extracellular signal-regulated (ERK) signalling (198). The PI3K oncogenic pathway can directly activate HIF-1α expression promoting CAIX activity. In cancer cell-specific types, PI3K activates AP-1 expression and subsequently binds to PR2, one of the regulatory elements in

the promoter (246, 247). ERK also stimulates AP-1 activity and stimulates SP1/SP3 transcription factor binding to PR1 or HRE (247, 248).

Hypoxia is a hostile condition which occurs in many cancers, however, measuring the degree of hypoxia is quite difficult and has long been debated. HIF-1α expression has been shown to correlate with poor prognosis in many cancers, including breast (249). The estimation of HIF-1α is challenging as it is labile; half-life < 10 minutes and rapidly disappears after reoxygenation (250). Therefore, identifying alternative hypoxic markers is required. CAIX expression is also an endogenous marker of hypoxic as its expression is dependent on HIF-1α activity. Unlike HIF-1α, CAIX protein is more stable, with half-life over 24 hours, making it a valuable indicator of hypoxia and poor prognosis (251). Carbonic anhydrase IX optimises tumoural pH and co-operates with other pathways in facilitating cancer cell survival. Evidence suggests that CAIX expression is associated with poor disease-free and overall survival in breast cancer regardless of subtypes (204). This may be due to CAIX mediating cellular functions and escalating other tumour escape mechanisms.

1.6.1 CAIX-mediated metabolic change

Carbonic anhydrase IX (CAIX) plays a crucial role in cancer metabolism by regulating pH homeostasis, thereby supporting tumour cell survival under hypoxic and other stress conditions (252). CAIX coordinates membrane transporters and membrane diffusion to maintain an optimal intracellular pH, while acidifying the extracellular environment, which promotes glycolysis (253). This pH regulation supports glycolytic metabolism by preventing intracellular acidosis and facilitating proton (H^+) extrusion in cooperation with monocarboxylate transporters (MCTs), which transport lactate and protons out of the cell (254).

CAIX also contributes to mitochondrial adaptations in response to hypoxia. While glycolysis is often the dominant metabolic pathway in tumours, CAIX helps optimise conditions that allow cancer cells to shift between glycolysis and oxidative metabolism as needed. A recent study induced mitochondrial DNA mutations, leading to disrupted OXPHOS. These conditions resulted in HIF-1α instability and downregulation of its target gene CAIX (255). Its expression is

tightly regulated by HIF-1α, a transcription factor that governs metabolic reprogramming in hypoxic tumours. Inhibiting CAIX function has been shown to reduce glycolytic enzyme expression and lower intracellular pH by suppressing lactate dehydrogenase (LDH) activity, thereby disrupting the metabolic balance of cancer cells (256).

Beyond its role in glycolysis, the extracellular acidity partially created by CAIX activation may influence lipid metabolism, as tumour acidity has been linked to increased lipogenesis and lipid droplet formation, processes that support cancer cell survival under metabolic stress (257). Additionally, CAIX is involved in glutamine metabolism, as it helps sustain glutaminolysis—a key pathway for producing metabolic intermediates necessary for biosynthesis and energy generation in hypoxia (258). CAIX interacts with solute carrier family 1 member 5 (SLC1A5), a glutamine transporter, to maintain redox homeostasis. Inhibition of CAIX using SLC-0111 induced glutamine uptake, which eventually increased glutathione levels. This, in turn, accelerated lipid peroxidation, resulting in increased ferroptosis in the SUM159PT cell line (258).

Glycolysis has been linked to CAIX expression through NADPH metabolism. Specifically, C-terminal binding proteins (CtBPs), which act as coregulators of NADPH production, have been reported to stimulate CAIX expression, highlighting the interplay between glycolysis, redox balance, and pH regulation in cancer cells (256, 259). These findings emphasize the multifaceted role of CAIX in metabolic adaptation, making it a promising target for therapeutic intervention in cancer.

1.6.2 CAIX and immune cell function

Tumour acidity impairs immune cell function, thus antitumour immune function, as well as related cytotoxic cytokines/chemokines, are depleted. Cytotoxic T cells decrease secretion of interleukin-2 (IL-2), interferon-gamma (IFNγ) and tumour necrosis factor-alpha (TNFα) through lactic acid induction or low pH (260, 261). Dendritic and NK cells are also depleted under acidic conditions. In contrast to tumour immunity, populations of M2 macrophages, myeloid-derived suppressor cells and regulatory T cells are increased (262). Inhibiting CAIX results in glycolytic reduction and an increase in extracellular pH in melanoma and basal breast cancer cell lines (263). The killing activity of T-cells

was improved when CAIX was inhibited by increasing activity of Th1. The TCGA-BRCA dataset provided additional information on CAIX and immune cell function, CA 9 gene upregulation decreases the expression of the antitumour immune response by CD3E, CD8A and CD4 (263). However, the direct mechanism by which CAIX mediates immune checkpoint blockades, for example, PD-1 and PD-L1, is uncleared and needs further elucidation.

1.6.3 CAIX and epithelial-mesenchymal transition (EMT)

Tumoural hypoxia can activate the EMT process through HIF-1α. The promotor of the EMT transcription factors TWIST, ZEB1, Slug and Snail contains the hypoxia response element (HRE) that can bind HIF-1α and activate transcriptional activity (264, 265, 266, 267). HIF-1α expression can crosstalk with EMT signalling pathways TGF-ß, Wnt/ß and hedgehog (268). Acidosis and hypoxia can lead to EMT activation as evidenced by decreased E-cadherin, increased vimentin, and upregulation of transcriptional factors TWIST1-2 and Zeb2 (269, 270). As CAIX is a transmembrane protein it can interact with cell-adhesion molecules such as ß-catenin, and E-cadherin, resulting in tumour progression. CAIX protein preferentially binds to ß-catenin causing disruption of ß-catenin/E-cadherin/catenin-p120 complex (244, 271). CAIX also interacts with integrins and MMP14 forming invadopodia resulting in cell invasion and migration (272).

1.7 NDRG1 function and hypoxia

1.7.1 N-myc downstream-regulated gene family

The N-myc downstream-regulated gene (NDRG) family comprises 4 members; NDRG1-4, which have 53-65% conserved amino acid homology (273). They are part of the α/ß hydrolase superfamily but lack a hydrolytic catalytic function (274). In humans, *NDRG1, NDRG 2, NDRG 3* and *NDRG 4* are located on chromosomes 8q24.3, 14q11.2, 20q11.21–11.23, and 16q21–q22.1, respectively (275) (**Figure 1.3**). NDRG1 is 43 kDa and composed of 394 amino acids with three amino acid tandem repeat sequences (GTRSRHTSE) (276). NDRG1 expression is predominantly cytoplasmic and nuclear (277).

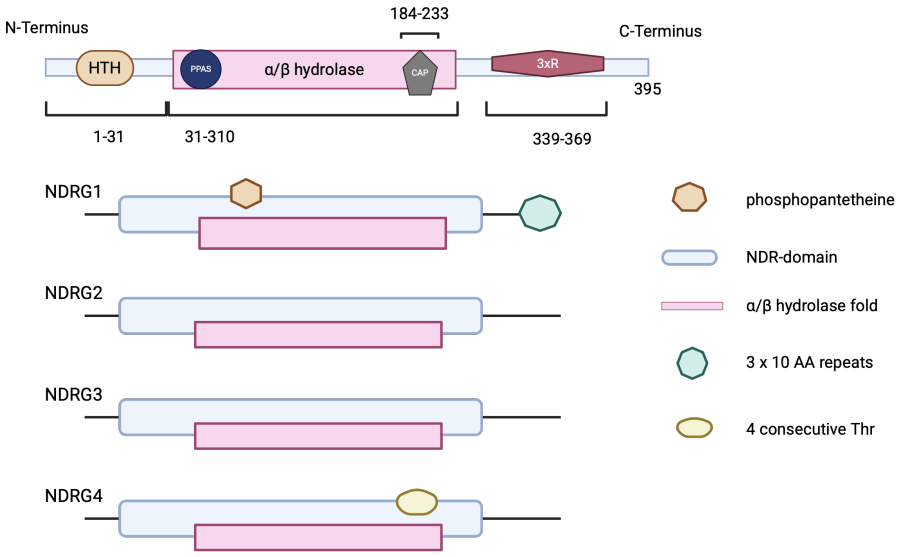

Figure 1.3-NDRG family protein sequence structure (Created with BioRender.com)

1.7.2 Regulation of NDRG1

NDRG1 is a stress-responsive gene and stressors such as hypoxia, DNA damage, cell differentiation and increased intracellular Ca^{2+} can induce NDRG1 upregulation (278). Hypoxia mediates NDRG1 expression through HIF-1α. A genetic knock-out mouse model was used to show that NDRG1 expression was present in HIF-$1\alpha^{+/+}$ while no NDRG1 was detected in HIF-$1\alpha^{-/-}$ fibroblasts (232, 279, 280). Wang et al. identified an HRE that HIF-1α can bind to in the NDRG1 promotor region at -405 to -1202 by ChiP assay in A 549 lung cancer cell line (281).

Hypoxia can induce another transcription factor in addition to HIF-1α : aryl hydrocarbon (AHR). AHR binds at −412 and −388 of the *NDRG1* promoter in hypoxia (282). An increase in intracellular Ca^{2+} as a result of hypoxia can activate activator protein-1 (AP-1), specifically c-Fos/c-Jun dimer, leading to NDRG1 expression (279). Hypoxia-mimicking conditions, such as iron depletion, or exposure to nickel, or cobalt compounds, also induce NDRG1 expression. Iron is necessary for cell proliferation and an insufficient amount inhibits cell cycle progression from G1 to S phase (283). Iron is also a cofactor for prolyl hydroxylase (PH) which is required for HIF-1α degradation (284). Decreased iron levels stabilise HIF-1α resulting in activation of HIF-1α responsive genes. Iron depletion can also

induce NDRG1 expression by downregulating eukaryotic initiation factor 3 (eIF3); a translation initiation factor and stress granule key component (285). Nickel and cobalt generate reactive oxygen species (ROS) and may trigger the hypoxic signalling pathway. Culturing the A549 cell line in the presence of nickel or cobalt induced HIF-1α and activation of HIF-1α dependent transcription gene Cap43 (286).

DNA damage also induces NDRG1 expression through activation by the tumour suppressor p53. Stein et al. reported that NDRG1 expression was rapidly upregulated in p53-expressing colorectal cancer cell lines, HCT116 p53+/+ and DLD-1-p53, but was absent in HCT116 p53−/− and DLD-1 cells. They identified a p53 binding site located 406 base pairs upstream of the NDRG1 promoter, confirming a direct regulatory link between p53 and NDRG1 expression (287). Phosphatase and tensin homologue deleted on chromosome 10 (PTEN); a tumour suppressor gene, can enhance NDRG1 expression through an Akt-dependent pathway (288). Bandyopadhyay et al. transfected prostate (ALVA, PC3) and breast cancer (MDA-468, BT-549) cell lines, which lacked PTEN, with either an empty pcDNA3 vector or a pcDNA3/PTEN plasmid. Western blot analysis showed increased NDRG1 protein expression in the pcDNA3/PTEN-transfected cells. PTEN regulates NDRG1 expression through Akt signalling, as inhibition of Akt in PC3 cells (which have high phosphorylated Akt and no PTEN) resulted in increased NDRG1 expression. This suggests that NDRG1 is regulated through the PTEN-Akt pathway (288). Another report from Zhang et al. found that the induction of early growth response 1 (Egr-1) transcription factor under hypoxic conditions increased NDRG1 expression. They identified an Egr-1/Sp1 binding site in the promoter region of NDRG1, which likely facilitates this regulation (289).

c-Myc and N-Myc suppress NDRG1 expression by acting as transcriptional repressors that bind to the NDRG1 promoter. In a study using Hela cells, the relative luciferase activity assay of human *NDRG1* promoter showed that knockdown of c-Myc increased the activity of the pGL3-*NDRG1* (− 1307/+ 254) reporter gene and this effect was completely reversed with thymidine kinase core promotor *NDRG1* (− 33/+ 165) (290).

These findings highlight the complex regulation of NDRG1 by various stress factors, including hypoxia, DNA damage, and changes in intracellular signalling,

as well as tumour suppressors like P53 and PTEN. Conversely, NDRG1 expression can be suppressed by c-Myc and N-Myc.

1.7.3 NDRG1 functions in breast cancer

The functions of NDRG1 are diverse depending on cellular types and context. In breast cancer, NDRG1 can function as both a tumour promotor and a tumour suppressor.

1.7.3.1 NDRG1 and tumour growth

NDRG1 plays a complex role in tumour proliferation and growth, with evidence supporting both oncogenic and tumour-suppressive functions. NDRG1 overexpression increased proliferation of MCF-7 and MDA-MB-231 cell lines by reducing the WNT1 inducible signalling pathway protein 1 (WISP1)/WNT axis (291). It is also a target of the aryl hydrocarbon receptor (AHR), which has been linked to enhanced proliferation of the MCF-7 cell line (282). Knockdown of NDRG1 reduced the proliferation of breast cancer cell lines, including MCF-7, SK-BR-3, MDA-MB-231 and HCC 1569 (233, 292).

NDRG1 has also been shown to have tumour-suppressive properties. The transcription factor T-box 2 (TBX2), which promotes cancer cell proliferation, recruits early growth response 1 (EGR1) to the NDRG1 promotor, leading to its transcriptional repression and increased proliferation. However, this effect was reversed when NDGR1 was overexpressed, suggesting its anti-proliferative role in certain contexts (293).

1.7.3.2 NDRG1 and tumour migration and invasion

NDRG1 plays a crucial role in regulating cancer cell migration and invasion, although its effects appear to be context dependent. Several studies suggest that NDRG1 functions primarily as a migration suppressor. Li et al. reported silencing NDRG1 significantly increased the migratory activity of MCF-7 cell lines after incubating under hypoxic conditions (0.5% O_2 for 48 hours) (282). Additionally, hypoxia-induced NDRG1 expression showed a reduction in NDRG1 expression after reoxygenation and increased migration in the MCF-7 cell line, while

overexpression of NDRG1 during reoxygenation blocked this migration effect, further supporting its role in migration inhibition (294). Similarly, NDRG1 expression was found to reduce migration in MDA-MB-231 cells (295).

Tian et al. demonstrated that serum and glucocorticoid-regulated kinase 1 (SGK1) partially mediates migration and invasion through NDRG1. The study found that inhibiting SGK1 reduced cell migration in NDRG1-depleted cells, but had no effect when NDRG1 was overexpressed (296). This suggests that SGK1 requires NDRG1 to promote migration, but under conditions where NDRG1 is abundant, it may exert a dominant anti-migratory effect. These findings indicate that while NDRG1 generally suppresses migration, its interactions with other pathways, such as SGK1 signalling, may modulate its role in a cell-type and condition-specific manner.

1.7.3.3 NDRG1 and EMT

The role of NDRG1 in epithelial-mesenchymal transition (EMT) appears to be context-dependent and may vary across different cell lines. López-Tejada et al. studied the role of transforming growth factor ß (TGFß) in TNBC cell lines. They reported that silencing NDRG1 alone did not affect the expression of EMT markers unless cells were stimulated with TGFß (297). Under these conditions, NDRG1 inhibition resulted in suppressed expression of key EMT markers, including Twist, Snail, Slug, and Vimentin.

In contrast, an earlier study by Liu et al. using a different cell line, MCF-7, found that NDRG1 acts as an EMT suppressor by inhibiting Wnt-mediated EMT signalling. They reported that NDRG1 interacts with low-density lipoprotein receptor-related protein 6 (LRP6) to block Wnt signalling, leading to increased E-cadherin expression, a hallmark of epithelial characteristics (298).

These findings suggest that NDRG1 may exert different effects on EMT depending on the cell type and the dominant signalling pathways involved. While in TNBC models, NDRG1 depletion reduced EMT markers under TGFß stimulation, in luminal MCF-7 cells, NDRG1 appeared to suppress EMT via the Wnt pathway (291, 297). Further research is needed to clarify how NDRG1 integrates different signalling pathways to regulate EMT across various breast cancer subtypes.

1.7.3.4 NDRG1 and metastasis

NDRG1 plays a complex role in metastasis through distinct mechanisms across different breast cancer subtypes. A study using a breast cancer brain metastatic model; JIMT1 and MDA-MB-231, found that NDRG1 knockdown suppressed intravascular arrest, the first step in brain metastasis (299). In addition, higher NDRG1 expression was observed in the MDA-IBC-3.2 cell line, an aggressive brain metastatic model, compared to the less aggressive MDA-IBC-3.1 model. The NDRG1 level was higher in brain metastasis compared to primary breast cancer, suggesting a role in metastatic progression (300).

NDRG1 not only has a role in the regulation of aggressive breast cancer, but it also has a role in luminal breast cancer. Unlike in more aggressive breast cancer subtypes, the progesterone receptor ratio can predict the metastatic potential in luminal tumours. A higher PRA/PRB ratio is correlated with increased lung and axillary lymph node metastasis, whereas tumours with a higher PRB/PRA have elevated levels of NDRG1 (301).

These findings indicate that NDRG1 may contribute to metastasis through multiple, context-dependent mechanisms. Its expression varies across aggressive and less aggressive breast cancer subtypes, suggesting that it may facilitate tumour progression through different molecular pathways. Given its diverse roles in metastasis, NDRG1 represents a potential therapeutic target across various breast cancer subtypes.

Hypoxia plays a crucial role in driving the aggressiveness of breast cancer, both directly through HIF-1α and indirectly via other hypoxia-associated factors. Carbonic anhydrase IX (CAIX) has been identified as a promising biomarker for predicting survival outcomes and as a potential therapeutic target, particularly in aggressive breast cancer subtypes. Although the functions of CAIX are well-documented, the molecular mechanisms underlying its regulation and interactions with other hypoxia-associated proteins are not fully understood.

In this thesis, NDRG1, a protein upregulated under stress conditions, including hypoxia, was identified and co-expressed with CAIX in aggressive breast cancer models. NDRG1 is involved in a range of cancer-related processes, but its

role remains controversial. It appears to function differently depending on the cellular context, particularly in hypoxic environments. Some studies suggest NDRG1 promotes tumour progression, while others point to its role as a tumour suppressor. Therefore, further research is needed to clarify how NDRG1 works in concert with CAIX and whether it contributes to the aggressive phenotype of breast cancer under hypoxic conditions. This investigation could open new avenues for understanding breast cancer aggressiveness and inform future therapeutic strategies.

1.8 Hypothesis and aims

We hypothesise that CAIX is a poor prognostic marker in breast cancer, and by understanding the underlying biology associated with increased expression of CAIX in ER-negative breast cancer novel therapeutic markers associated with hypoxia in breast cancer will be identified.

Therefore, the aims of this thesis are:

a) To identify gene signatures associated with high CAIX expression in hormone-negative breast cancer.
b) To identify signalling pathways associated with high CAIX expression.
c) To investigate the prognostic value of CAIX-associated genes and proteins.
d) To investigate the regulation of CAIX-associated genes in in vitro.
e) To investigate the functions of CAIX-associated genes in in vitro.

Chapter 2 : Materials and Methods

2.1 The Glasgow breast cancer cohort

This study received ethical approval from the Research Ethics Committee of the North Glasgow University Hospital NHS Trust (NHS GG&C rec no 16WS0207). The cohort is composed of 850 invasive breast cancer patients identified retrospectively from a review of patients attending Glasgow hospitals (Glasgow Royal Infirmary, Southern General, Victoria and Stobhill Hospital) between 1995 and 1998). Clinicopathological features, including age, histologic types, histological grade, tumour size, nodal status, lymphovascular invasion, ER status, PR status, HER-2 status, Ki-67, type of surgery, adjuvant treatment and follow up status were retrieved. The date and cause of death were recorded until 31st of May 2013 and defined as the censor date. Patients with incomplete follow-up data, unidentified molecular subtypes and inadequate tissue samples for TMA processing were excluded from the study. This study followed the Reporting Recommendations for Tumour Marker Prognostic studies (REMARK) criteria with one exception (**Figure 2.1** and **Table 2.1**). The sample size could not be predetermined because the study analysed existing samples with available clinicopathological data. However, approximately 100 events occurred for each endpoint, which should be sufficient for statistical analysis. The clinical endpoints in this study are cancer-specific survival (CSS), overall survival (OS) and recurrence-free survival (RFS). The definition of CSS is the duration between curative surgery and the date of death originating from breast cancer. The definition of OS is the duration from curative surgery to the date of death from any cause. The definition of RFS is the duration from curative surgery to the date of first documented recurrence of the disease.

Table 2.1-The REMARK checklist for NDRG1 biomarker

	Item to be reported	Page no.
INTRODUCTION		
1	State the marker examined, the study objectives, and any pre-specified.	116
MATERIALS AND METHODS		
Patients		
2	Describe the characteristics (e.g., disease stage or co-morbidities) of the study patients, including their source and inclusion and exclusion criteria.	118-119
3	Describe treatments received and how chosen (e.g., randomized or rule-based).	120
Specimen characteristics		
4	Describe type of biological material used (including control samples) and methods of preservation and storage.	44
Assay methods		
5	Specify the assay method used and provide (or reference) a detailed protocol, including specific reagents or kits used, quality control procedures, reproducibility assessments, quantitation methods, and scoring and reporting protocols. Specify whether and how assays were performed blinded to the study endpoint.	44-45
Study design		
6	State the method of case selection, including whether prospective or retrospective and whether stratification or matching (e.g., by stage of disease or age) was used. Specify the time period from which cases were taken, the end of the follow-up period, and the median follow-up time.	42
7	Precisely define all clinical endpoints examined.	42
8	List all candidate variables initially examined or considered for inclusion in models.	42
9	Give rationale for sample size; if the study was designed to detect a specified effect size, give the target power and effect size.	42
Statistical analysis methods		
10	Specify all statistical methods, including details of any variable selection procedures and other model-building issues, how model assumptions were verified, and how missing data were handled.	45
11	Clarify how marker values were handled in the analyses; if relevant, describe methods used for cut point determination.	121
RESULTS		
Data		
12	Describe the flow of patients through the study, including the number of patients included in each stage of the analysis (a diagram may be helpful) and reasons for dropout. Specifically, both overall and for each subgroup extensively examined report the numbers of patients and the number of events.	119
13	Report distributions of basic demographic characteristics (at least age and sex), standard (disease-specific) prognostic variables, and tumor marker, including numbers of missing values.	120
Analysis and presentation		
14	Show the relation of the marker to standard prognostic variables.	124-126
15	Present univariable analyses showing the relation between the marker and outcome, with the estimated effect (e.g., hazard ratio and survival probability). Preferably provide similar analyses for all other variables being analyzed. For the effect of a tumor marker on a time-to-event outcome, a Kaplan-Meier plot is recommended.	128-129
16	For key multivariable analyses, report estimated effects (e.g., hazard ratio) with confidence intervals for the marker and, at least for the final model, all other variables in the model.	128-129
17	Among reported results, provide estimated effects with confidence intervals from an analysis in which the marker and standard prognostic variables are included, regardless of their statistical significance.	128-129
18	If done, report results of further investigations, such as checking assumptions, sensitivity analyses, and internal validation.	NA
DISCUSSION		
19	Interpret the results in the context of the pre-specified hypotheses and other relevant studies; include a discussion of limitations of the study.	145-149
20	Discuss implications for future research and clinical value.	149

2.1.1 Tissue microarrays construction

A tissue microarray (TMA) was constructed from the formalin-fixed paraffin-embedded tissue (FFPE) from the identified patients. Tumour-rich areas were selected and marked by a breast pathologist (Dr Elizabeth Mallon). Three 0.6 mm^2 cores from different areas in each sample were punched and embedded into new paraffin array blocks. Cores of prostate, colon, lung, liver, heart, and kidney were included in TMA as controls. Sections were cut from the blocks at a thickness of 2.5 μm and floated onto glass microscope slides. TMA slides were baked at 60°C overnight and stored at 4°C until required.

2.1.2 Antibody validation

NDGR1 (Cell Signalling, D8G9 (XP)®) specificity was validated by protein expression on WB and staining cell pellet between 1% O_2 and normoxic conditions before the antibody was used to stain the Glasgow breast cancer cohort. A single band of NDRG1 in WB at 46 kDa and a difference in staining intensity of NDRG1 between normoxic and hypoxic MDA-MB-231 cell pellets would demonstrate antibody specificity. Other antibodies used had previously been validated in the lab.

2.1.3 Control tissue

Antibody optimisation was carried out using whole tissue sections and TMAs from breast cancer tissue not included in the Glasgow breast cancer cohort. Positive controls (normal colonic tissue) and negative controls (no primary antibody) were included

2.1.4 Immunohistochemistry (IHC)

The Glasgow breast cohort was stained for NDGR1 using an automated stainer (Leica BOND RX). Each step is detailed in **Table 2.2**.

Table 2.2–Immunohistochemistry protocol for NDRG1 staining using the Leica BOND RX automated staining system

Steps	Reagents	Times
Dewaxing	100% Alcohol	Pre-programmed Leica BOND
Antigen retrieval	BOND Epitope Retrieval ER2 solution	20 mins at 100°C
Peroxidase block	Refine Detection Kit Peroxidase Block	5 min
Wash step		
Primary antibody	NDRG1 (D8G9) (1:800) dilute in antibody diluent	30 min
Wash step		
Secondary detection	Refine detection kit polymer	
Visualisation	Refine detection kit mixed DAB	5 min
Wash step		
Counterstain	Refine detection kit haematoxylin	5 min
Wash step		

On completion, slides were removed from the machine and dehydrated in 70% ethanol for 2 minutes, 90% ethanol for 2 minutes, 100% ethanol for 2 minutes x 2 times and Xylene for 2 minutes x2 times. The Slides were mounted using DPX mountant (06522, Sigma-Aldrich, St Louis, USA).

2.1.5 Slide scanning and scoring

TMA slides were scanned and analysed using NZ connect 1.1.0 HAMAMATSU (Welwyn Garden City, Hertfordshire, UK). Scoring was performed at 20x objective magnification. The weighted histoscore method was used to determine protein expression at the membrane, cytoplasm, and nucleus. The values were produced using the following calculation - weighted histoscore = (% no staining x 0) +(%weak staining x 1) +(% moderate staining x 2) +(% high staining x 3). The scoring was evaluated blindly by 2 independent observers.

2.1.6 Statistical analysis

The interobserver score for NDRG1 IHC was determined using the ICCC and Bland-Altman plot. R studio including “survminer” was used to determine the cut-point. Kaplan Meier curves were plotted to evaluate the association between

groups and survival outcomes, including CSS, OS, and RFS. The Chi-squared test was used to determine associations with clinicopathological features. Significance was set to $p<0.05$. Cox regression analysis was performed with a stepwise backward elimination to identify a significant independent relationship with survival. All statistical analyses were 2-sided with significance at p-value <0.05. All statistical analysis was performed using the SPSS software version 29 (SPSS Inc., Chicago, IL, USA).

2.1.7 Initial analysis

This study was restricted to REMARK guidelines (**Figure 2.1**).

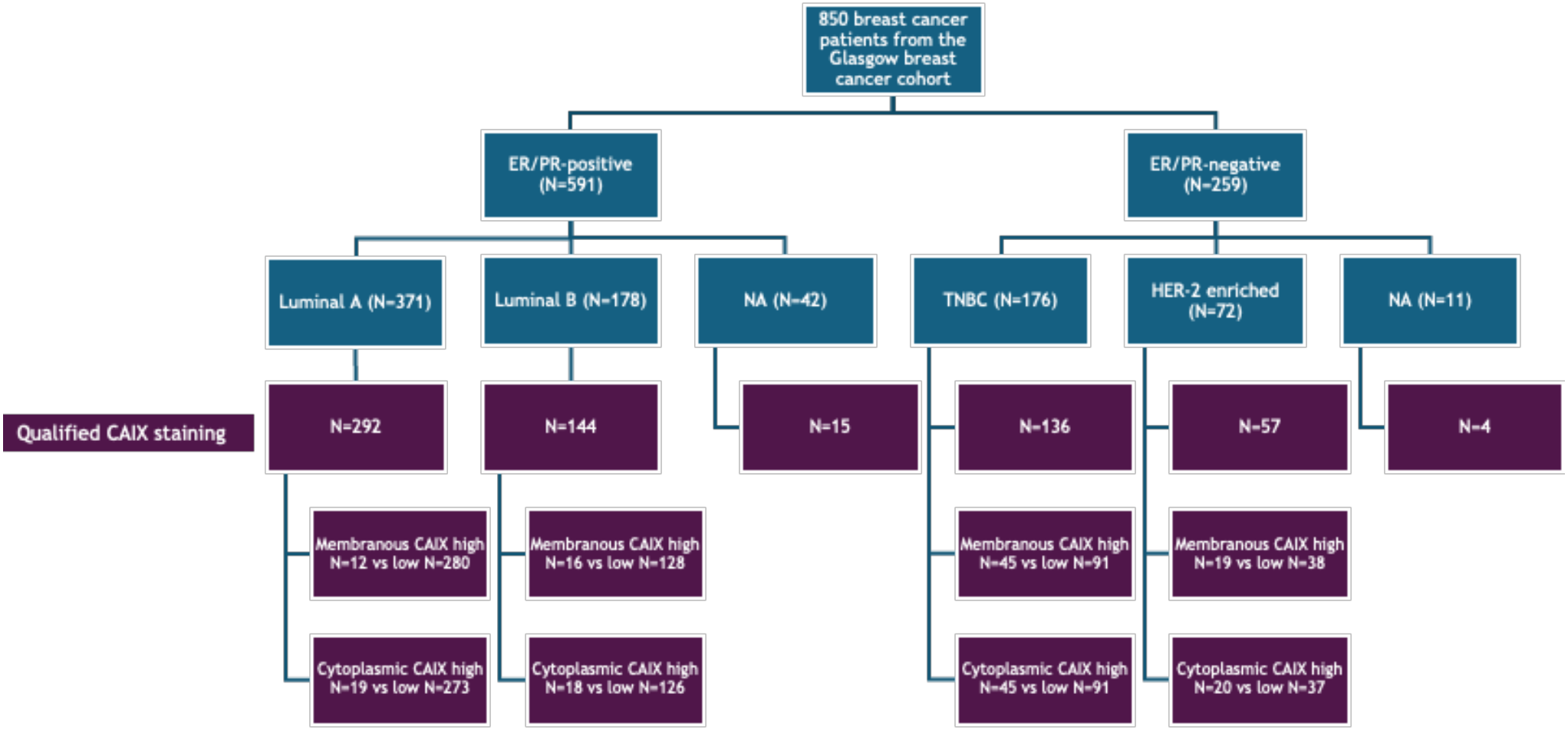

Figure 2. 1- REMARK diagram of patient distribution and enrolled for CAIX analysis

In the whole Glasgow breast cancer cohort, the median age of breast cancer patients was 58 years (range 23-93, IQR; 49-67). The median tumour size was 20 mm (range 1-100, IQR; 13-27), and 40.9% of breast cancer patients had nodal metastasis. The intrinsic molecular subtypes were determined by immunohistochemistry for ER, PR, HER-2, and Ki-67. Tumours were considered ER and PR positive if ≥1% of tumour cell nuclei showed immunohistochemical staining for the respective receptor.

I. Luminal A: ER and/or PR positive, HER-2 negative and Ki-67 ≤ 14%
II. Luminal B: ER and/or PR positive, and is divided into 2 subgroups
    a. Luminal B/HER-2 negative is ER or PR positive, HER-2 negative and Ki-67 > 14%
    b. Luminal B/HER-2 positive is ER or PR positive, HER-2 positive, and any Ki-67
III. Her-2 enriched: ER and PR negative and HER-2 overexpression
IV. Triple-negative (TNBC): all ER, PR and HER-2 are negative

Luminal A was the most diagnosed subtype in 371 patients (46.5%) followed by luminal B in 178 patients (22.3%), TNBC (ER-/PR-/HER-2-) in 176 patients (22.1%) and HER-2 overexpression in 73 patients (9.1%). The clinicopathological factors are summarised in **Table 2.3**. The median follow-up time for survival analysis was 12.53 years (range 0.08-15.25 years). The median overall survival was 150.37 months (range 1-183 months). 482 patients (56.70%) were alive, and 333 patients (31.60%) died at censored time points.

There were 259 cases diagnosed as ER and PR negative. They can be subdivided into ER/PR/HER-2 negative, 176 patients (68%), HER-2 overexpression, 72 patients (27.80%) and unknown HER-2 status, 11 patients (4.20%). The mean age was 56.04 (range 23-89, SD±12.60). The median tumour size was 20 mm. (1-89, IQR; 15-30). Most had tumour size less than 50 mm; 131 patients ≤ 20 mm and 117 patients 21-50 mm. Nodal involvement was found in 117 patients (45.20%) and usually not more than 3 nodes. One hundred and eighty-five cases (71.40%) had a poor histological grade. For surgical treatment, 166 patients (64.10%) underwent total mastectomy and axillary lymph node dissection in most ER-negative patients; 247 out of 259 patients (95.40%). For adjuvant treatment, chemotherapy was given to 159 patients (61.40%) and 133 patients (51.40%) were additionally treated

with radiation. One hundred and seventy cases (65.60%) had no recurrence but if recurrence occurred it usually presented at distant sites (56 cases (21.60%)) while local relapse was only observed in 24 patients (9.30%). 316 patients (52.50%) are still alive at the censored time points while 75 patients (29%) died from breast cancer. The clinicopathological details are summarised in **Table 2.3**. The median survival time was 147.00 months (range 6-180 months).

Table 2.3-Clinicopathological characteristics of the whole Glasgow breast cancer cohort and the ER/PR negative subgroup

Clinicopathological factors	All breast cancer subtypes 850 cases (%)	ER/PR negative 259 cases (%)
Age, yr median (range, IQR)	58 (23-93,49-67)	56.04 (23-89, 46-65)
≤50	248 (29.20)	93 (35.90)
>50	602 (70.80)	166 (64.10)
Nodal involvement		
No	490 (57.60)	141 (54.40)
Yes	348 (40.90)	117 (45.20)
NA	12 (1.40)	1 (0.40)
Tumour size, mm median(range, IQR)	20 (1-100, 13-27)	20 (1-89, 15-30)
≤ 20	496 (58.40)	131 (50.60)
>20-50	309 (36.40)	112 (43.20)
>50	44 (5.20)	15 (5.80)
NA	1 (0.10)	1 (0.40)
Histological types		
Ductal	736 (86.60)	243 (93.80)
Lobular	68 (8.00)	3 (1.20)
Other	46 (5.40)	13 (5.00)
Tumour grade		
I	161 (18.90)	9 (3.50)
II	382 (44.90)	63 (24.30)
III	305 (35.90)	185 (71.40)
NA	2 (0.20)	2 (0.80)
ER status		
Negative (<1%)	276 (32.50)	259 (100)
Positive (≥1%)	570 (67.10)	0 (0)
NA	4 (0.50)	0 (0)
PR status		
Negative (<1%)	448 (52.70)	259 (100)
Positive (≥1%)	396 (46.60)	0 (0)
NA	6 (0.70)	0 (0)
HER-2 status		
Negative	699 (82.20)	176 (68.00)
Positive	128 (15.10)	72 (27.80)
NA	23 (2.70)	11 (4.20)
Ki-67		
≤14%	567 (66.70)	167 (64.50)
>14%	228 (26.80)	72 (27.80)
NA	55 (6.50)	20 (7.70)
Breast cancer subtypes		
Luminal A	371 (43.60)	0 (0)
Luminal B	178 (20.90)	0 (0)
TNBC	176 (20.70)	176 (68.00)
HER-2 enriched	73 (8.60)	72 (27.80)
NA	52 (6.10)	11 (4.20)
Endocrine treatment		
No	141 (16.60)	102 (39.40)
Yes	560 (71.10)	83 (32.10)
NA	149 (17.60)	74 (28.60)
Adjuvant chemotherapy		
No	516 (60.70)	99 (38.20)
Yes	331 (38.90)	159 (61.40)
NA	3 (0.40)	1 (0.40)
Radiation therapy		
No	446 (52.50)	125 (48.30)
Yes	401 (47.20)	133 (51.40)
NA	3 (0.40)	1 (0.40)
Recurrence status		
No	648 (76.20)	170 (65.60)
Local	50 (5.90)	24 (9.30)
Distant	123 (14.50)	56 (21.60)
Both local and distant	8 (0.90)	4 (1.50)
NA	21 (2.50)	5 (1.93)
Status		
Alive	482 (56.70)	136 (52.50)
Breast cancer related death	174 (20.50)	75 (29.00)
Non breast cancer related death	179 (21.10)	44 (17.00)
NA	15 (1.80)	4 (1.50)

NA=not applicable

The traditional biological breast cancer prognostic markers were analysed to identify any correlation with survival by the Cox-regression model in the Glasgow Breast cancer cohort including age at diagnosis, tumour size, tumour grade, nodal metastasis status, lymphovascular invasion and molecular subtypes. The results showed that all markers mentioned above were significantly associated with CSS and OS except age only related to CSS (**Table 2.4**).

Table 2.4- The relationship of well-established breast cancer prognostic markers with CSS and OS in the whole Glasgow breast cancer cohort

Clinicopathological features	CSS		OS	
	HR (CI)	P	HR (CI)	P
Age, yr				
≤50 (N=240)	1			
>50 (N=580)	1.412(1.106-1.802)	0.005	0.949(0.689-1.307)	0.748
Tumour size, mm				
≤ 20 (N=485)	1		1	
>20-50 (N=306)	1.676(1.351-2.080)	<0.001	2.191(1.593-3.015)	<0.001
> 50 (N=43)	2.410(1.615-3.595)	<0.001	4.460(2.708-7.346)	<0.001
Tumour grade				
I (N=155)	1		1	
II (N=369)	1.213(0.896-1.642)	0.190	2.017(1.134-3.589)	0.013
III (N=294)	1.617(1.190-2.196)	0.002	3.949(2.251-6.982)	<0.01
Nodal involvement				
No (N=474)	1			
Yes (N=334)	2.095(1.696-2.587)	<0.001	3.246(2.370-4.447)	<0.001
Lymphovascular invasion				
No (N=351)	1			
Yes (N=146)	2.569(1.950-3.384)	<0.001	4.255(2.813-6.435)	<0.001
Breast cancer subtypes				
Luminal A (N=356)	1		1	
Luminal B (N=171)	1.566(1.198-2.047)	<0.001	2.293(1.533-3.429)	<0.001
HER-2 enriched (N=72)	1.986(1.405-2.808)	<0.001	3.054(1.867-4.995)	<0.001
TNBC (N=172)	1.406(1.067-1.854)	0.016	2.544(1.708-3.789)	<0.001

2.2 Systematic review methodology

Search strategy, inclusion and exclusion criteria

The search term included “prognosis”, “survival”, “CAIX” (carbonic anhydrase IX), and “breast cancer”. Boolean operators (AND/OR) and MeSH terms were applied where appropriate to enhance sensitivity. A systematic literature search was conducted in the electronic databases EMBASE, PubMed, Cochrane, and Scopus. The studies were included if they met all the following criteria (1) the patients were diagnosed with invasive breast cancer, (2) CAIX expression was determined by IHC, and (3) the study reported DFS or OS with HRs and 95%CI. The

studies were excluded if they (1) involved non-human subjects, (2) were published in a language other than English, and (3) could not be accessed in full text.

Study selection and data extraction

Two independent reviewers screened titles and abstracts, followed by full text review. Disagreements were resolved through discussion or a third reviewer. The PRISMA flow diagram for retrieving the study was demonstrated in Chapter 3.

Statistical analysis

Meta-analysis was performed using pooled HRs and their related 95% CIs to assess the relationship between CAIX expression by IHC and survival outcomes. The I^2 statistic was used to determine study heterogeneity, with values greater than 50% indicating high heterogeneity. The fixed-effects model was initially analysed, when heterogeneity was low; otherwise, a random-effects model was applied.

2.3 Gene expression analysis

This study aimed to classify differential gene expression between high and low expression of CAIX in the ER/PR-negative subgroup. TempO-Seq (BioClavis), a high throughput assay with many advantages was used to determine this. It requires minimal tissue without prior nucleic acid extraction or cDNA which might result in RNA loss. Up to 6144 samples can be processed at one time. TempO-Seq can analyse 22539 target genes with high sensitivity and specificity which is beneficial in the identification of novel gene correlations.

Genes with statistically significant changes in expression were identified based on the following criteria: a log2 fold change of ±1.0 and an adjusted p-value (padj) of <0.05. The final set of differentially expressed genes (DEGs) was determined using these thresholds. To identify the "top" DEGs, genes were ranked by their adjusted p-value (padj). Cluster analysis was then performed on the top

20 DEGs, grouping them into clusters based on similarities in their expression profiles.

The STRING database (version 10.0) was employed to analyse the DEGs in terms of their GO annotations and related biological pathways. A Protein-Protein Interaction (PPI) network was constructed and visualized using the STRING online database. The analysis applied the following criteria: a required interaction score > 0.4 (medium confidence), a false discovery rate (FDR) < 0.05, and a PPI enrichment p-value < 0.05. To further characterise the identified functional groups, pathway analysis was performed. These analyses helped identify DEGs associated with distinct biological functions, suggesting a common mechanism in tumours with high expression of CAIX.

One hundred and forty-seven samples of ER/PR negative breast cancer, from the Glasgow breast cancer cohort, were used for this analysis. Of those, 131 cases had complete data for CAIX expression. For cytoplasmic CAIX expression, 87 cases have low expression, and 44 cases have high expression. For membranous CAIX, 87 cases have low expression, and 44 cases have high expression.

A total of 14304 of 16382 genes were identified to categorise high and low CAIX expression. The genes with a statistically significant fold change were identified. A log2 fold change of 1 in both directions and an adjusted P value (padj) of <0.05 were considered to determine the final DEGs. “Top” genes were determined by ranking the padj. Cluster analysis was then used to group the top 10 DEGs into clusters using RStudio. The cluster analysis was able to group the top 10 DEGs based on the similarity in their expression profiles.

Statistical analysis for transcriptomic analysis

Data normalization was performed using DESeq2 in RStudio (RStudio, Boston, MA, USA). Principal Component Analysis (PCA) was used to explore the clustering of top genes between high and low CAIX expression groups. Box plots and volcano plots were generated in RStudio using ggplot to visualize differentially expressed genes. Gene Set Enrichment Analysis (GSEA) was conducted to identify significantly enriched pathways and associations with differentially expressed genes. Statistical significance was defined as padj < 0.05.

2.4 Cell lines and culture conditions

The MDA-MB-231 (ER-/PR-/HER2-) breast cancer cell line was purchased from the American Type Culture Collection (ATCC:70029549), the MCF-7 (ER+/HER2-) cell line was a gift from Tobias Ackerman and SK-BR3 (ER-/PR-/HER2+) cell line was a gift from Katie Hanna. All cell lines were authenticated for identity by STR profiling, ensuring that they are not misidentified or contaminated. The results are shown in the appendix. Although the receptor status of these cell lines is generally well-characterised in the literature, receptor expression can vary due to passage number. In this study, direct validation of receptor status was not performed at protein or mRNA level. Nonetheless, the use of STR-authenticated, maintained under standard culture conditions supports their validity as subtype-specific models. This limitation is acknowledged, and future studies may benefit from including functional confirmation of receptor status.

MDA-MB-231 and MCF-7 were grown in Dulbecco's modified Eagle's medium (DMEM(1x) + GlutaMAX^{TM}-l: 31966-021; Gibco; ThermoFisher Scientific, Paisley, UK) with 10% fetal bovine serum (FBS: F9665, Sigma-Aldrich, Gillingham, UK). SK-BR3 cells were cultured in McCoy'5A(1x) + GlutaMAX^{TM}-l medium (36600-021; Gibco; ThermoFisher Scientific, Paisley, UK) supplemented with 10% FBS. The cell lines were maintained in a humidified atmosphere at 37°C in 5% CO_2, 21% O_2, and 74% N_2 and checked for mycoplasma contamination every 3 months. In this study, MDA-MB 231 passages 4-8, MCF-7 passages 76-79 and SK-BR3 passages 17-23 were used in experiments.

2.5 Bringing up frozen cultures

Aliquots of cells were retrieved from liquid nitrogen storage, gently thawed in a 37°C water bath before being transferred to a 15 ml centrifuge tube with the appropriate growth medium. Tubes were centrifuged at 125 xg for 5 minutes. After removing the supernatant, the cells were resuspended in complete and transferred to culture flask.

2.6 Sub-culturing cells

The cells were regularly checked for morphology, growth, viability and microbial contamination using an inverted microscope. The medium was changed 2-3 times a week and cells sub-cultured when they reached 70-90% confluence. Cells were sub-cultured as follows (75 cm^2 flask). The medium was discarded and the monolayer washed with 10 ml of DPBS (14190-094; Gibco; ThermoFisher Scientific, Paisley, UK) . 1-2 ml of 0.25% trypsin-EDTA (1x) was added and the flask incubated at 37°C for 5 minutes. Once the cells had completely detached6-8 ml of complete medium were added. The cells were passaged at a ratio of 1:2 to 1:4 in 75 cm^2 flask with 15 ml fresh medium.

2.7 Cryopreservation

Stocks of the cell lines were stored in liquid nitrogen. Complete medium supplemented with 10% DMSO was prepared as the freezing medium. The cells were trypsinised and pelleted as outlined above. The freezing medium was added, and the cells resuspended at the desired concentration of $1x10^6$ to $2x10^6$ cells/ml. 1 ml of suspension was added to each cryopreservation vial and the lids closed. The vials were left at room temperature for 15 minutes before being placed in a pre-cooled freezing container. The container was then kept at -70°C for at least 24 hours before transferring to liquid nitrogen for storage.

2.8 Cell seeding densities for experiments

For western blot and qPCR, the cells were seeded $2.5\text{-}3x10^5$ cells in 2 ml of complete medium in a 6-well plate (Corning Inc, Costar®) 24 hours before the experiment. In normoxic and control conditions, the cells were incubated at 37°C in 5% CO_2, 21 O_2, and 74% N_2 for specific times. For hypoxic conditions, the cells were incubated at 1% O_2 and 94% N_2 in a cell culture incubator.

2.9 Western blot analysis

2.9.1 Sample preparation

The 6-well plate containing cells was removed from the incubator at designated time point. The medium was removed and the monolayer washed with 1 ml cold DPBS. After removing DPBS, 100 µl of radioimmunoprecipitation assay buffer (RIPA) with protease inhibitor was added to each well and sonicated for 15 minutes before scraping, then transferred to 1.5 ml Eppendorf microtubes and centrifuged at 18000 xg for 15 minutes at 4°C. The samples were then stored at -80°C until required. Samples were quantified using BCA and the desired volume and protein concentration required determined. This was mixed with 4xSDS and DTT then heated at 95°C for 5 minutes.

2.9.2 Protein concentration determination

Pierce™ BCA protein assay kit (Thermo Scientific®, 23225, 23227, A65453) was used to estimate protein concentration. In brief, this method is the calorimetric measurement of Cu^{+} which is the reduction of CU^{2+} to CU^{+} by alkaline medium protein. The cuprous ion (CU^{+}) forms a complex with BCA that shows a significant absorbance at 562 nm. Samples were diluted 10-fold in assay reagents before measurement. Absorbance was recorded using a TECAN® Multimode Microplate Reader. The absolute protein concentration was determined using a standard curve with six standard points (0, 250, 500, 1000, 1500, and 2000 µg/ml). Curvilinear regression was applied to interpolate sample concentrations based on the standard curve (**Figure 2.2**).

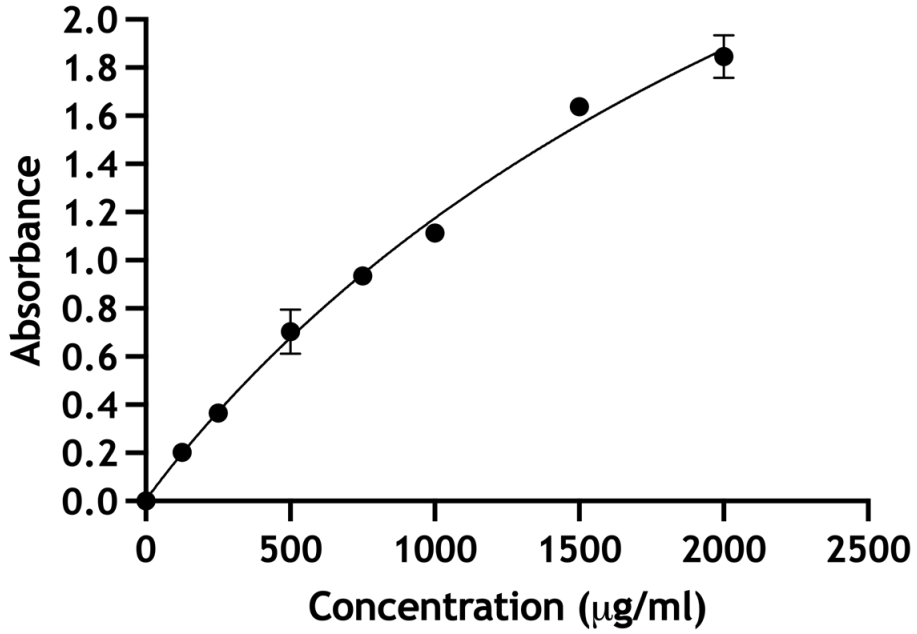

Figure 2. 2-The representative standard curve. The dots were six standard points. The line is a regression for the whole set of standard points.

The final protein concentration (x) was calculated using the regression equation (R^2 and y value) and then multiplied by 10 to obtain the actual sample concentration.

2.9.3 Western blot protocol

The lysates were loaded at 10 µg of total protein in each well of 10% SDS-PAGE gel together with a prestained protein ladder (#1610374, BIO-RADS). The samples were separated by gel electrophoresis at 120 mV and then electrotransfer was performed at 300 mA onto PVDF membrane. Protein transfer was confirmed using Ponceau red staining before washing three times with1xTBS-T for 5 minutes. The membranes were incubated with 5% milk-blocking buffer for 1 hour and then incubated over night with one of the primary antibodies at 4°C (HIF-1a rabbit monoclonal antibody (1:1000; HIF-1α (D1S7W) XP® Rabbit mAb #36169, Cell Signaling), CAIX mouse monoclonal antibody (1:2000, M75, Bioscience), NDRG1 rabbit monoclonal antibody (1:1000; 9485, Cell Signaling) and PPFIA4 rabbit polyclonal antibody (1:5000; HPA053419, Atlas antibodies)). beta-actin mouse monoclonal antibody was used as a loading control (1:10000; 8H10D10, Cell Signaling). After this incubation, the membranes were washed with 1xTBS-T for 5

minutes then incubated with either goat anti-rabbit or donkey anti-mouse IgG secondary antibodies (1:5000; 111-035-144 and 715-035-150, Jackson Immunoresearch) for 90 minutes then washed three times 1xTBS-T for 5 minutes. To visualise the protein bands, the membranes were incubated in Pierce ECL western blotting substrate (32109 or 32134; Thermo Fisher Scientific) for 5 minutes then imaged using the LI-COR odyssey FC imager system. Protein quantification was analysed with the ImageJ software. For different western blots, all measured protein concentrations on one blot were normalised to the concentration of paired protein in the same blot.

2.10 Quantitative real-time polymerase chain reaction (qPCR)

Total RNA was isolated from MB-231, SKBR3 and MCF-7 breast cancer cell lines using TRIzol® Reagent (Thermo Fisher Scientific #15596018). TRIzol-lysates were mixed with chloroform (Merck), followed by centrifugation at 12,000 xg for 15 min at 4 °C. RNA was extracted from the supernatants by incubating with isopropanol at -30°C overnight. The RNA pellet was washed with 70% ethanol and the concentration measured using the NanoDrop (ThermoFisher Scientific). Complementary DNA (cDNA) was synthesized from 1 µg RNA using MMLV Reverse Transcriptase (Thermo Fisher Scientific #28025013), following the manufacturer's protocol. The cDNA was diluted to a working concentration of 10 ng/µl with RNase-free water. Specific primer sets were designed, spanning exon/exon boundaries wherever possible. PowerTrack™ SYBR™ Green PCR Master Mix (Applied Biosystems #A46109) was used for qPCR reactions. The PCR conditions used were as follows: 95 °C for 10 min, followed by 45 repeat cycles of 95 °C for 10 s, then 60 °C for 45 s. A dissociation stage of 95 °C for 15 s, 50 °C for 10 s, and 95 °C for 15 s was added. The assay conditions were as follows: 95 °C for 10 min, followed by 45 repeat cycles of 95 °C for 15 s, and 60 °C for 1 min. Data generated from the qPCR reactions were analysed using the 2-ΔΔCt method. All samples were run in triplicate and experiments were repeated at least three times. The primer sequences used in this study are listed in **Table 2.5**.

Table 2.5-Primer sequence for qPCR

Gene name	Forward primer	Reverse primer
CA9	TTTGCCAGAGTTGACGAGGC	GCTCATAGGCACTGTTTTCTTCC
HIF1A	ATCCATGTGACCATGAGGAAATG	TCGGCTAGTTAGGGTACACTTC
NDRG1	CTCCTGCAAGAGTTTGATGTCC	TCATGCCGATGTCATGGTAGG
PPFIA4	GGAAGCCCTAAACCTGAAGCA	ACTGCGGGAGGTGAGCTTA
VEGFA	AGGGCAGAATCATCACGAAGT	AGGGTCTCGATTGGATGGCA
ANKRD30A	GCGTGGCAAGAGTAACATCTAA	AGAGACTCCGAGAATCACAAGA
ANKRD30B	CCTTCAGCGAACGGGTCTAC	CAGGTTGACGGGCTTCTTCC
CITED1	GCTGGCTAGTATGCACCTGC	CATTGGCTCGGTCCAACCC
ESR1	GAAAGGTGGGATACGAAAAGACC	GCTGTTCTTCTTAGAGCGTTTGA
SRARP	CTTGTCACCCCACCAATGAAG	GGTTTCCCCTTAGCCTCGG
Beta-actin	CATGTACGTTGCTATCCAGGC	CTCCTTAATGTCACGCACGAT

2.11 Cell proliferation

WST-1 assay (Sigma-Aldrich, 05015944001) was used to determine cell proliferation. WST-1 is cleaved to formazan by the succinate-tetrazolium reductase system, which belongs to the respiratory chain of the mitochondria, and is found only in the active metabolic cells (**Figure 2.3**).

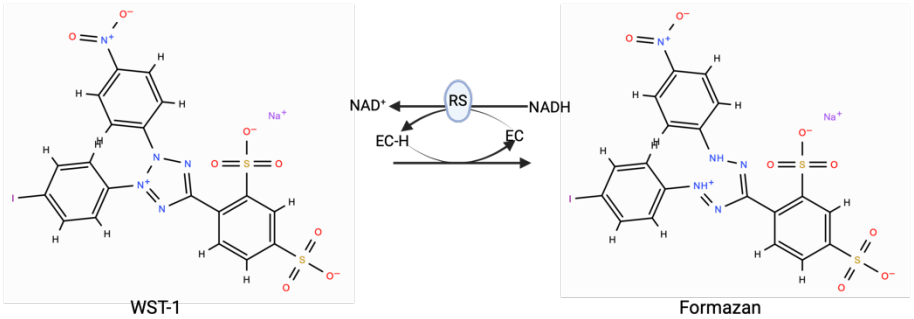

Figure 2.3-WST-1 reaction to detect viable cells (structure adapted from ChemSpider with modification)(302)

Cells were seeded in a 96-well plate with a final volume of 120 µl per well and treated according to the experimental conditions. On the required day, 12 µl of WST-1 reagent was added to each well. Following a 2-hour incubation, absorbance was measured using a microplate reader (Tecan Infinite® 200 PRO) at 420–490 nm, with background controls used as blanks. Scramble-treated cells served as the control group.

2.12 Silencing NDRG1 gene

Table 2.6-Materials used in silencing NDRG1

Silencer®select NDRG1	S20336	ThermoFisher scientific
RNAase free water	23111146	ThermoFisher scientific
Lipofectamine RNAiMAX	2533491	ThermoFisher scientific
Scramble	4390843	ThermoFisher scientific
Opti-MEM®I reduce serum medium	11058-021	Gibco

Table 2.7-Silencing NDRG1 protocol

Culture vessel	Volume of complete medium	Plated cells/well	Optimem medium	RNAi duplex amount (pmol)	Final RNAi duplex conc.	Lipofectamine
96-well	100 µL	10000	20 µl	0.6	5nM	0.2 µl
6-well	2.5 mL	200000	500 µl	15	5nM	5 µl

2.12.1 Methods

Silencing of NDRG1 was carried out in MDA-MB-231 and MCF-7 cells using reverse transfection with Lipofectamine™ RNAiMAX. Silencer® Select NDRG1 siRNA powder (5 nmol) was dissolved in 250 µl of RNase-free water to generate a 20 nM stock solution. The silencing materials and protocol are shown in **Tables 2.6** and **2.7**. A working concentration of 2 nM siRNA was prepared by diluting the stock solution with RNase-free water. For transfection, siRNA or scramble control were complexed with Lipofectamine® in Opti-MEM® I Reduced Serum Medium as per the protocol (**Table 2.7**). The siRNA-Lipofectamine complexes were incubated at room temperature for 10-15 minutes before being added to the labelled wells. The cells in complete medium in the required volume were added to each well. The plates were gently rocked to ensure even distribution of the transfection mix. Plates were then incubated for 24 hours at 37°C in a CO_2 incubator, after which they were transferred to a hypoxic incubator for an additional 48 hours. Following this hypoxic exposure, the cells were assessed for the knockdown effect.

2.13 The oxygen consumption rate (OCR) and extracellular acidification rates (ECAR) measurement

The OCR (oxygen consumption rate) and ECAR (extracellular acidification rate) were measured using the Agilent Seahorse XFe Analyser under both hypoxic (3% O_2) and normoxic conditions. The experimental workflow for hypoxic conditions is illustrated in **Figure 2.4**. Normoxic conditions followed the same protocol but without the oxygen level adjustments.

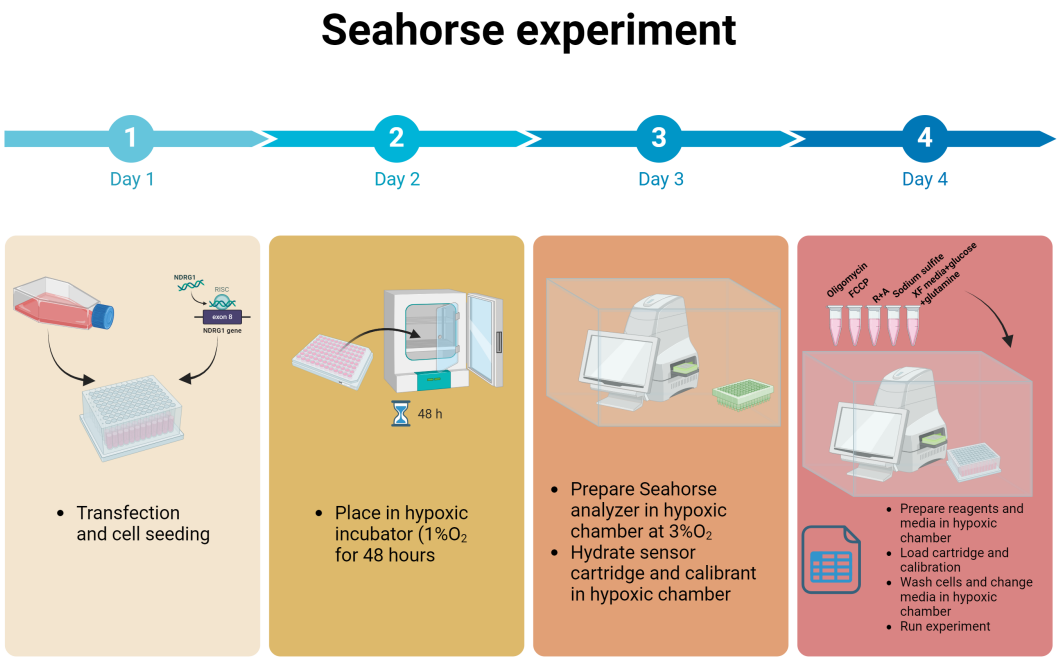

Figure 2.4-The workflow for the determination of OCR and ECAR by the XFe 96 seahorse analyser

The Seahorse XFe96 Analyser (Agilent) is designed to measure two key parameters in the culture media of live cells: oxygen consumption rate (OCR) and extracellular acidification rate (ECAR). OCR serves as an indicator of the cell's oxidative phosphorylation (OXPHOS) activity, while ECAR reflects their glycolytic activity. Three days before the assays, MDA-MB-231 and MCF-7 cells were seeded and silenced by transfection in Seahorse XF 96 cell culture microplates at 15000 cells/well with a final volume of120 µl and placed in a 20% O_2 incubator. After 24 hours, the plate was moved to the hypoxic incubator for 48 hours. The day before the assays, the Agilent Seahorse XF Analyser was set to 3% O_2 overnight. The sensor cartridge was hydrated with 200 µL of calibrant to the 96-well utility plate and 10

ml of calibrant in a 15 ml conical tube were incubated overnight in hypoxic chambers. On the day of the assay, 100 ml XF Assay medium was warmed to 37°C. Fresh 1M sodium sulfite (1.26 g sodium sulfite to 10 ml of XF calibrant) and fresh stock solution of Mito stress test/glycolysis Stress test were prepared and placed in the hypoxic chamber 1 hour before adding to the cartridge. The compounds were added to the sensor cartridge in order. To evaluate OCR, oligomycin (1.5 µM), CCCP (1 µM), rotenone (0.5 µM) and antimycin A (0.5 µM) were injected subsequently as illustrated in **Figure 2.5**. To measure ECAR, glucose (15 mM), oligomycin (1.5 µM) and 2-deoxy-glucose (2DG, 50 mM) were added subsequently (**Figure 2.6**). The Seahorse 96-well microplate was moved to the hypoxic chamber and the cells were washed with warm media twice with the final volume at 175 µl. The sensor cartridge was loaded on the XF Instrument for calibration, followed by the cell plate for cell readings. The data obtained were then analysed using the Seahorse desktop software Wave (Agilent). Scramble was used as control.

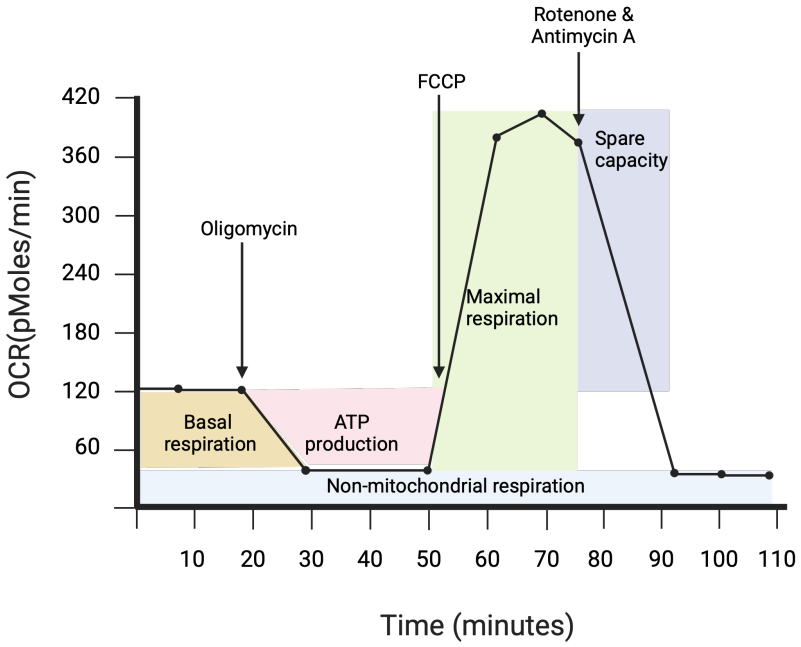

Figure 2.5-The oxygen consumption rate (OCR) of cells was measured using the Seahorse Mito Stress Test. During the assay, a series of compounds were sequentially injected to assess mitochondrial function. First, oligomycin was added to inhibit ATP synthase (complex V of the electron transport chain). Next, CCCP (a proton ionophore) was introduced to dissipate the proton gradient and disrupt the mitochondrial membrane potential. Finally, rotenone and antimycin A were injected to inhibit complex I and complex III, respectively.

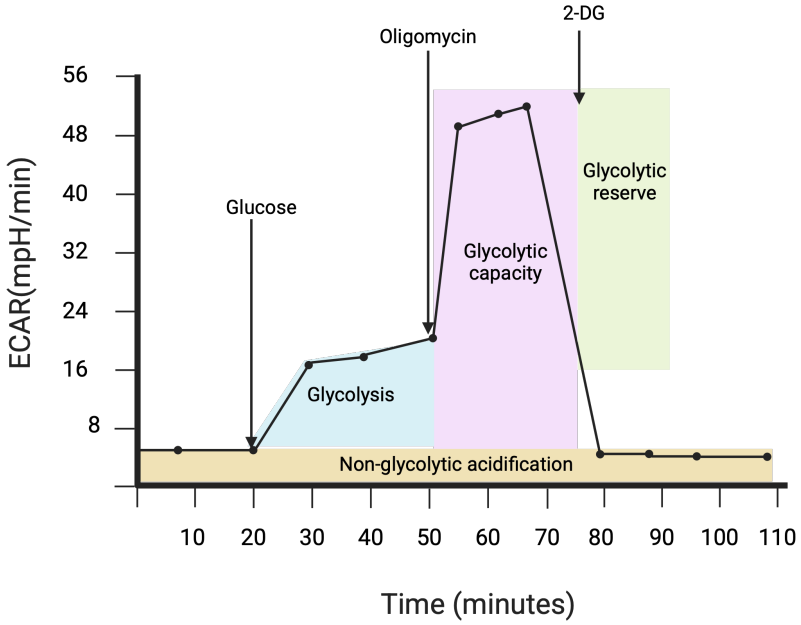

Figure 2.6-The extracellular acidification rate (ECAR) of cells was measured using the Seahorse Glycolysis Stress Test. A series of compounds were sequentially injected to evaluate glycolytic function. First, glucose was added to stimulate glycolysis. Next, oligomycin was injected to inhibit ATP synthase (complex V of the electron transport chain), thereby increasing the reliance on glycolysis for energy production. Finally, 2-deoxy-glucose (2-DG), a glucose analogue, was added to inhibit glycolysis by competitively binding to hexokinase, the enzyme that phosphorylates glucose in the first step of the glycolytic pathway.

2.14 ATP measurement

Intracellular ATP levels were measured using the Luminescent ATP Detection Assay Kit (ab113849, Abcam, Cambridgeshire, UK). MDA-MB-231 and MCF-7 cells (15000 cells per well) were seeded in 96-well plates. The cells were treated with or without siNDRG1 and incubated for 48 hours in either 20% oxygen (normoxia) or 1% oxygen (hypoxia). On the day of the assay, the plates were removed from the incubator. 50 µl of detergent was added to each well and the plate shaken for 5 minutes. 50 µl of substrate solution was then added, and the plate was shaken briefly before being kept in the dark for 10 minutes. Luminescence was then measured using a luminometer (Promega Corporation, Madison, USA, J5021). An ATP standard curve was used to quantify the

luminescence signals. Wells containing only culture media were included as negative controls.

2.15 Lactate measurement

Lactate concentration in conditioned media was measured using the Lactate-Glo™ Assay (Promega Corporation, Madison, USA, J5021). MDA-MB-231 and MCF-7 cells (15,000 cells per well) were seeded in 96-well plates and treated with or without siNDRG1. The cells were incubated for 48 hours in either 20% oxygen (normoxia) or 1% oxygen (hypoxia). After incubation, the cultured medium was collected and diluted 1:100 with Dulbecco's Phosphate-Buffered Saline (DPBS). A volume of 50 µl from each sample and a lactate control was transferred to a 96-well plate, followed by the addition of 50 µl of `lactate detection mixture. The plate was shaken for 60 seconds and incubated at room temperature for 60 minutes. Luminescence was recorded using a luminometer (GloMax®-Multi+ Detection System, Promega Corporation, Madison, USA, J5021). A lactate titration curve was used to quantify the luminescence signals. Wells containing only culture media were included as negative controls.

Statistical analysis for in vitro study analysis

Mean data between two groups were compared with a two-sided Student's *t*-test. Two-way ANOVA was used to compare multiple groups. The data were expressed as the mean ± standard error of the mean (SEM). $P < 0.05$ was set as the threshold of statistical significance

Chapter 3 : Identification of hypoxic-related genes based on CAIX expression

3.1 Introduction

Hypoxia plays a vital role in driving tumorigenesis in breast cancer. HIF-1α is a key regulator under hypoxic conditions and acts by activating the transcription of hypoxia-associated genes related to angiogenesis (VEGFA), metabolic alteration (for example, GLUT-1 and LDHA) as well as pH regulation (CAIX) (303). The resulting consequences of hypoxia in cancer are the promotion of optimal conditions for cancer proliferation, invasion, migration, metastasis and treatment resistance(304).

CAIX transcription always requires HIF-1α activation and is rarely seen in normal tissue except for gall bladder and stomach (199). The function of CAIX is to lower extracellular pH in response to a metabolic shift from oxidative phosphorylation to aerobic glycolysis (Warburg effect) under hypoxic conditions. CAIX also plays a role in promoting angiogenesis, EMT, and the invasion and spread of cancer(305).

The presence of CAIX was reported to be a more accurate prognostic marker than molecular subtypes alone. Ye et al. reported the hypoxia signature genes based on HIF-1 were preferentially expressed in TNBC (181), which reflects the suggestion that hypoxia drives the aggressive phenotypes of breast cancer. Although CAIX may be of importance, the clinical application of CAIX has not been utilised in cancer treatment. Therefore, additional biomarkers and a better understanding of cellular processes are urgently needed.

Previously, Dr. Suad A.K. Shamis reported that elevated CAIX expression, whether in the membrane or cytoplasm, correlated with higher tumour grade, ER-negative status, and absence of HER-2 overexpression in the Glasgow breast cancer cohort. Moreover, high CAIX levels have been linked to poorer CS and OS, suggesting that CAIX may contribute to tumour aggressiveness (306). Given the potential clinical relevance of CAIX and to strengthen the generalisability of our findings beyond a single cohort, a meta-analysis was performed to evaluate the association between CAIX expression and breast cancer survival outcomes across multiple studies.

In addition, this study aimed to further investigate the role of hypoxia in poor-prognosis subtypes (ER/PR negative subgroups) based on CAIX at the transcriptomic level. Differential gene expression analysis was conducted using TempO-Seq (bulk RNA transcriptomics) to compare tumour with high versus low CAIX expression. Gene set enrichment analysis (GSEA) identified enriched pathways. Finally, key differentially expressed genes were preliminarily validated for association with survival outcomes using TempO-Seq data and the public cBioPortal database.

3.2 CAIX expression and breast cancer prognosis: Meta-analysis

In brief, the search term, including prognosis, survival, CAIX, and breast cancer, was searched in the EMBASE, PubMed, Cochrane, and Scopus databases. The studies were included if (1) the patients were diagnosed with invasive breast cancer, (2) IHC determined CAIX expression, and (3) they reported DFS or OS with HRs and 95%CI. The studies were excluded if they were (1) on non-human subjects, (2) published in a non-English language, and (3) could not be accessed in full text. The PRISMA flow for retrieving the study was demonstrated in **Figure 3.1**.

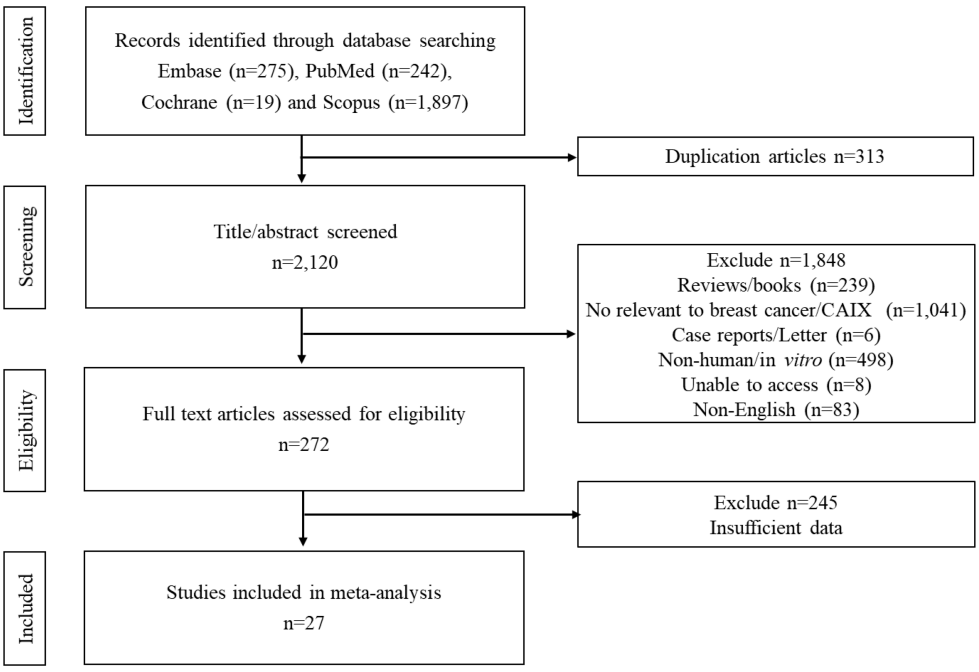

Figure 3.1-The PRISMA flow for retrieving studies of CAIX-related survival in breast cancer

A total of 2433 records were retrieved from four databases. After removing 313 duplicates, 2120 articles were screened for title and abstract. Of these, 272 underwent full-text review, and the 27 studies met the eligibility criteria for inclusion in the meta-analysis. Details of the enrolled studies are presented in **Table 3.1**.

The included reports were published from 2001 to 2022. Among them, 21 studies investigated breast cancer without specifying molecular subtypes, while 3 focus on TNBC, 2 on ER-positive subtypes and 1 on ER-negative subtype. One study by Shamis et al. separately reported outcomes for ER-positive cases across two distinct cohorts. Most studies (21 out of 27) assessed CAIX expression using a semi-quantitative scoring method based on staining intensity and percentage, where CAIX cut-off levels were inconsistent across all included studies. However, CAIX cut-off thresholds varied across studies. Eighteen studies reported only univariate analyses, while 9 included multivariate analyses to adjust for confounding variables.

Table 3.1-Characteristics of studies included in the meta-analysis of CAIX expression and breast cancer prognosis

References	Country	Mean age	BC subtypes (n)	Stage	Treatment (n)	IHC score method	CAIX cut-off level	CAIX high (%)	Ab clones	HR (95% CI) for DFS	p-value	HR (95% CI) for OS	p-value
Shamis et al. 2022(307)	UK	NA	ER+ (373)	I-III	CMT (110)	Weight H score	Log-rank statistics by R Studio	9	M75	UV = 1.81 (1.12–2.92)	0.018	NA	NA
										MV = 1.04 (0.46–2.35)	0.926		
		NA	ER+ (285)	I-III	CMT (71)			28		UV = 1.64 (1.14–2.37)	0.008		
										MV = 1.74 (1.08–2.82)	0.023		
Ong et al. 2022(203)	Singapore	55	TNBC (306)	NA	NA	I and P	≥1	39.3	NA	MV 2.77 (1.78-4.31)	<0.001	MV 2.48 (1.50-4.09)	<0.001
Li et al. 2020(308)	China	49	ER+ (55)	Recurrence	NA	I and P	NA	34.5	ab108351	UV 2.64 (1.28-5.44)	0.0086	NA	NA
Alves et al. 2019(309)	Brazil	49.6	Mixed BC (196)	IIb or III	CMT (196)	I and P	≥3	7.4	ab15086	UV 0.32 (0.19-0.55)	<0.00001	UV 0.33 (0.15-0.66)	<0.00001
Ozretic et al. 2017(310)	Croatia	60	TNBC (64)	NA	NA	I and P	>60	77	ab15086	NA	NA	UV 2.85 (0.36-22.25)	0.32
Jin et al. 2016(311)	South Korea	NA	TNBC (270)	I-II	NA	NA	≥10%	21.9	NA	UV 1.45 (0.77-2.67)	0.25	NA	NA
Chu et al. 2016(312)	China	55.34	Mixed (149)	I-IV	CMT	I and P	Strong intensity in ≥10% cells	15	NA	MV 5.758 (2.28-14.50)	<0.001	NA	NA
Samaka et al. 2016(313)	Egypt	48	Mixed (56)	I-IV	NA	I and P	>1%	91.1	ab107257	NA	NA	UV 2.09 (1.05-4.19)	0.0358
Aomatsu et al. 2014(314)	Japan	NA	Mixed (102)	IIA-IIIA	CMT (102)	I and P	Moderate to strong staining in >10% cells	46	M75	UV 4.52 (2.05-9.97)	0.0002	UV 3.31 (1.56-7.05)	0.0018
Deb et al. 2014(315)	Australia	NA	Male (276)	I-IV	NA	I and P	Strong intensity in ≥ 10% cells	8	NA	UV 2.2 (0.8-5.7)	0.11	NA	NA

References	Country	Mean age	BC subtypes (n)	Stage	Treatment (n)	IHC score method	CAIX cut-off level	CAIX high (%)	Ab clones	HR (95% CI) for DFS	p-value	HR (95% CI) for OS	p-value
Kim et al. 2014(316)	South Korea	52	Mixed metastasis (162)	IV	NA	I and P	≥2	19.8	NA	NA	NA	MV 1.69 (0.77-3.69)	0.189
Noh et al. 2014(317)	South Korea	NA	ER-AR+ (127)	I-III	NA	I and P	≥2	28.7	NA	MV 2.231 (0.670-7.426)	0.191	MV 15.89 (1.82-131.6)	0.01
Betof et al. 2012(318)	USA	48	Mixed (209)	I-III	CMT (209)	I and P	≥50	88	M75	UV 1.75 (0.92-3.31)	0.088	UV 2.73 (1.2-6.21)	0.0166
Kaya et al. 2012(319)	Turkey	46	Mixed (111)	I-III	NA	I	Any staining	55.8	H-120	UV 0.86 (0.54-1.36)	0.5253	UV 2.77 (1.58-4.85)	0.0004
Beketic-Oreskovic et al. 2011(320)	Croatia	61.5	Mixed (40)	I-III	NA	I and P	52.5	60	NA	UV 6.74 (2.27-20.03)	<0.001	UV 5.68 (2.11-15.31)	<0.001
										MV 4.14 (1.28-13.35)	0.018	MV 3.99 (1.38-11.59)	0.011
Lou et al. 2011(321)	Canada	NA	Mixed (3,630)	I-III	NA	I and P	Any staining	15.6	M75	UV 2.30 (1.91-277)	<0.00001	NA	NA
Pinheiro et al. 2011(322)	Portugal	NA	Mixed (122)	T1-3anyN	NA	I and P	≥3	18	ab15086	UV 2.24 (0.79-6.35)	0.1294	NA	NA
Jubb et al. 2010(323)	UK	57 (27-80)	Mixed (151)	I-III	CMT (63)	I and P	>10%	32	M75	CAIX score 1; UV 0.63 (0.29-1.41)	0.26	NA	NA
										CAIX score 2; UV 1.24 (0.49-3.13)	0.65		
										CAIX score 3; UV 1.83 (0.86-3.89)	0.12		
Tan et al. 2009(324)	UK	55	Mixed (407)	I-III	NA	I and P	≥10%	14	M75	UV 1.81 (1.14-2.86)	0.0119	UV 4.29 (2.61-7.04)	<0.00001
Crabb et al. 2008(325)	Canada	NA	Mixed (602)	II-III	NA	NA	NA	16.7	M75	MV 1.58 (1.12-2.22)	0.008	NA	NA
Kyndi et al. 2008(326)	Denmark	NA	Mixed (945)	II-III	NA	I and P	≥10%	16	M75	UV 1.29 (1.02-1.62)	<0.05	UV 1.3 (1.06-1.60)	<0.05

References	Country	Mean age	BC subtypes (n)	Stage	Treatment (n)	IHC score method	CAIX cut-off level	CAIX high (%)	Ab clones	HR (95% CI) for DFS	p-value	HR (95% CI) for OS	p-value
Hussain et al. 2007(327)	UK	62	Mixed (144)	I-II	NA	I and P	Weak or strong staining and focal or diffuse distribution	26	M75	NA	NA	UV 2.63 (1.21-5.70)	0.01
												MV 2.43 (1.07-5.53)	0.035
Trastour et al. 2007(328)	France	62	Mixed (132)	I-III	CMT/ET	I and P	>1%	29	M75	MV 2.0 (1.0-4.2)	0.05	NA	0.2
Brennan et al. 2006(329)	Ireland	NA	Mixed (400)	II	ET (199)	I	Any staining	11	M75	UV 1.62 (1.02-2.72)	0.041	UV 1.92 (1.09-3.38)	0.0239
Generali et al. 2006(330)	UK	NA	Mixed (166)	T2-4N0-1	CMT/ET (187)	I and P	Any staining	24.7	M75	UV 1.79 (0.84-3.89)	0.1315	UV 1.99 (0.79-5.02)	0.1443
Tomes et al. 2003(331)	Canada	NA	Mixed (53)	any T,N	NA	P	NA	NA	M75	NA	NA	UV 0.50 (0.30-0.85)	<0.0001
Chia et al. 2001(332)	Canada	59	Mixed (103)	I-III	CMT (27)/ ET (80)	I and P	≥1	48	M75	UV 2.38 (1.34-4.22)	0.0031	UV 2.61 (1.01-6.75)	0.05

Abbreviation: CMT = chemotherapy, ET = endocrine treatment, I = intensity, P = percentage, MV=multivariate analysis, NA = not applicable, UV = univariate analysis

3.2.1 High CAIX expression is associated with poor DFS

Twenty-two studies were included for DFS analysis that comprised 9157 breast cancer patients. The pooled HR was 1.70 (95% CI: 1.39-2.07), indicating a significant association between high CAIX and poorer DFS. while the heterogeneity was high (I^2 =83%), the overall effect remained highly significant (p<0.00001), suggesting that CAIX may serve as prognostic marker for aggressive disease (**Figure 3.2**).

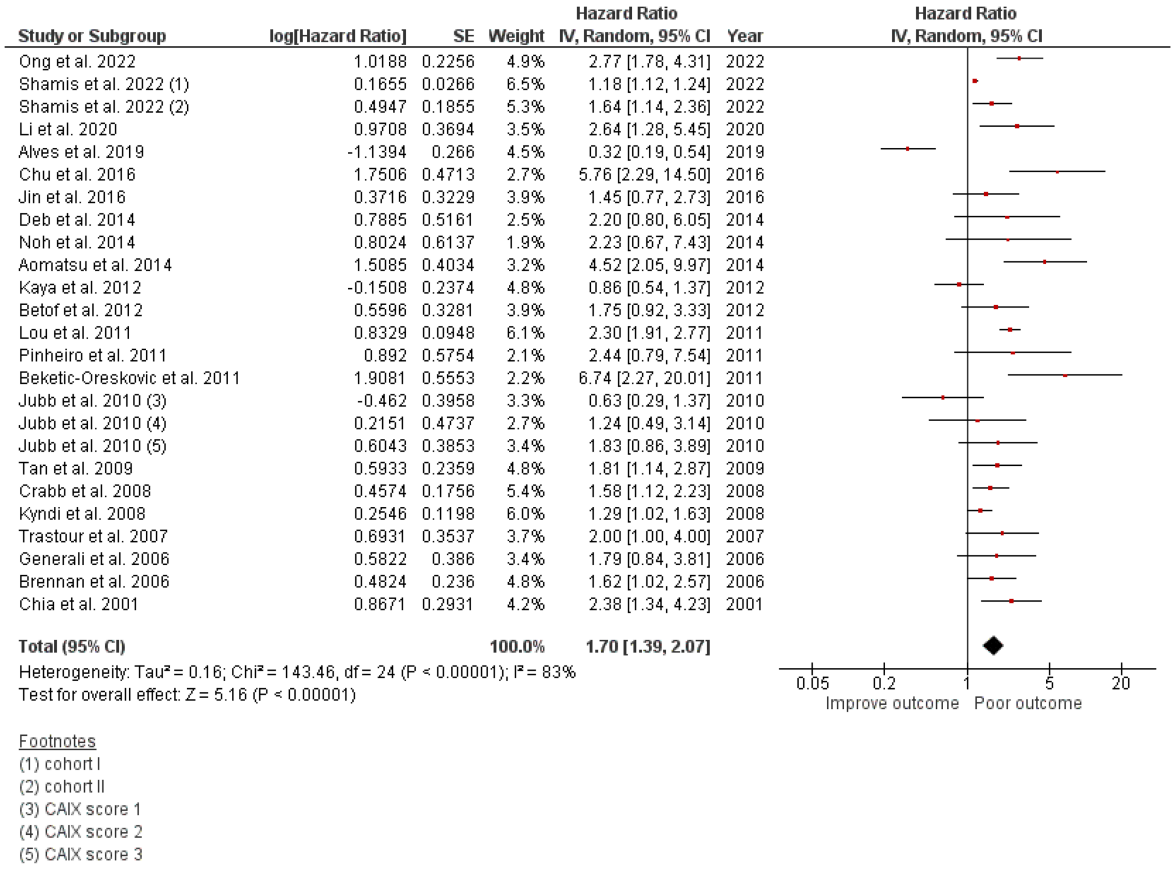

Figure 3.2- The forest plot of DFS in all breast cancer cases

3.2.2 High CAIX expression is associated with poor OS

A meta-analysis of 17 studies assessing the prognostic impact of CAIX expression in breast cancer revealed that elevated CAIX levels were significantly associated with worse OS (pooled HR= 2.05; 95%CI: 1.44-2.91; p < 0.0001). Despite the strong association, substantial heterogeneity was observed (I^2=80%), likely reflecting differences in cohort characteristics, CAIX scoring systems, and

detection methodologies. Nevertheless, these results support the hypothesis that CAIX may act as a marker of tumour aggressiveness in breast cancer (**Figure 3.3**).

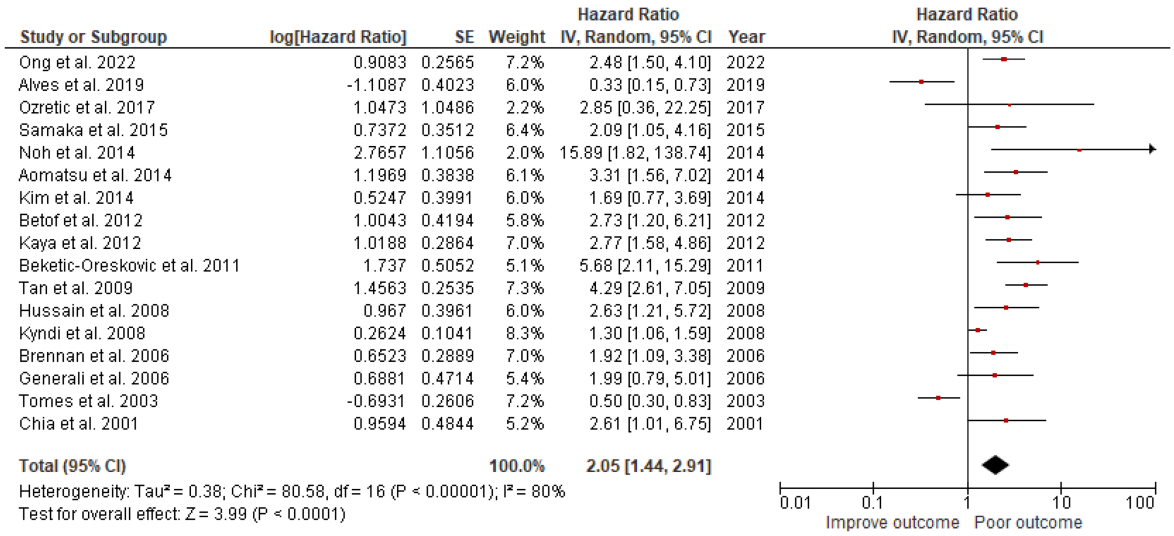

Figure 3.3- The forest plot of OS in all breast cancer cases

Subgroup meta-analysis was performed to further explore the prognostic relevance of CAIX expression in TNBC populations (**Figure 3.4**). In DFS subgroup analysis including 576 patients, elevated CAIX expression was associated with 2.09-fold increased risk of poor survival (95%CI: 1.11-3.92, p = 0.02), although moderate heterogeneity was observed (I^2 =63%). In OS subgroup analysis including 370 patients, high CAIX expression in TNBC demonstrated as even stronger association with adverse outcomes (HR = 2.50; 95%CI: 1.53-4.07, p = 0.0002) with no observed heterogeneity (I^2 = 0%). These findings support the hypothesis that CAIX may contribute to poor prognosis, particularly in molecularly aggressive breast cancer subtypes.

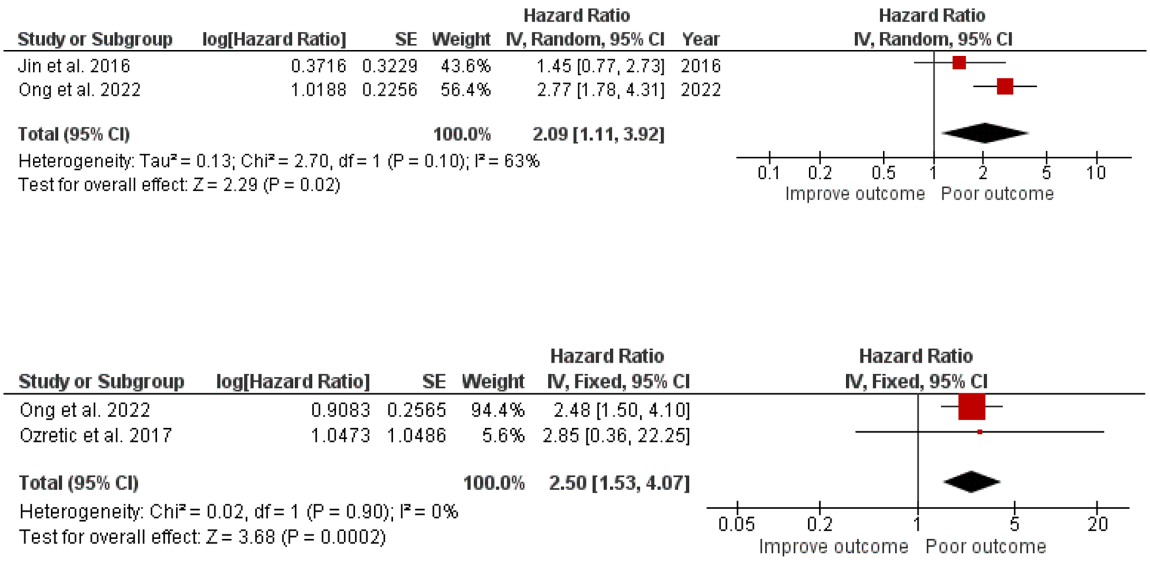

Figure 3.4- The forest plot of DFS and OS in TNBC subgroup

3.3 The association between CAIX expression and clinical outcomes in the ER/PR negative subgroup of the Glasgow breast cancer cohort

The meta-analysis showed that high CAIX expression was associated with significantly worse DFS and OS in TNBC. This suggests that CAIX may play a more central role in driving both early recurrence and long-term outcomes in TNBC, a subtype known for its aggressive clinical behaviours and lack of targeted therapies.

Prior to conducting transcriptomic analysis using FFPE samples from the Glasgow breast cancer cohort, the clinicopathological characteristics of ER-negative subgroup were reviewed. Although our primary interest was in TNBC, the number of TNBC cases available (n=136) was limited. Therefore, to ensure sufficient statistical power, the analysis was expanded to include all patients lacking both ER/PR expression including 197 patients, which encompassed an additional 61 cases. CAIX expression was scored in both the membrane and cytoplasm of tumour cells. The median weighted histoscore for membrane CAIX

was 5 (range 0-260) and cytoplasmic CAIX was 3.3 (range 0-217.5). The cut point for CAIX expression was re-determined by the R surminer as only ER/PR-negative cases were selected for downstream analysis. The newly calculated thresholds were 32.5 for membrane (previously 30) and 20 for cytoplasmic (previously 18). Notably, these slightly change did not lead to any patient classification changes. Membranous CAIX, was classified as low (≤32.5) in 133 cases and high (>32.5) in 64 cases (**Figure 3.5A**). Cytoplasmic CAIX was classified as low (≤ 20) in 133 cases and high (> 20) in 64 cases (**Figure 3.5B**). The correlation between CAIX and clinical outcomes was determined by the Chi-square test. The results showed no significant difference in clinicopathological features; patient age, tumour size, tumour grade, nodal involvement, and HER-2 status, between low and high membranous CAIX (**Table 3.2**). This was also similar when cytoplasmic CAIX was analysed (**Table 3.2**).

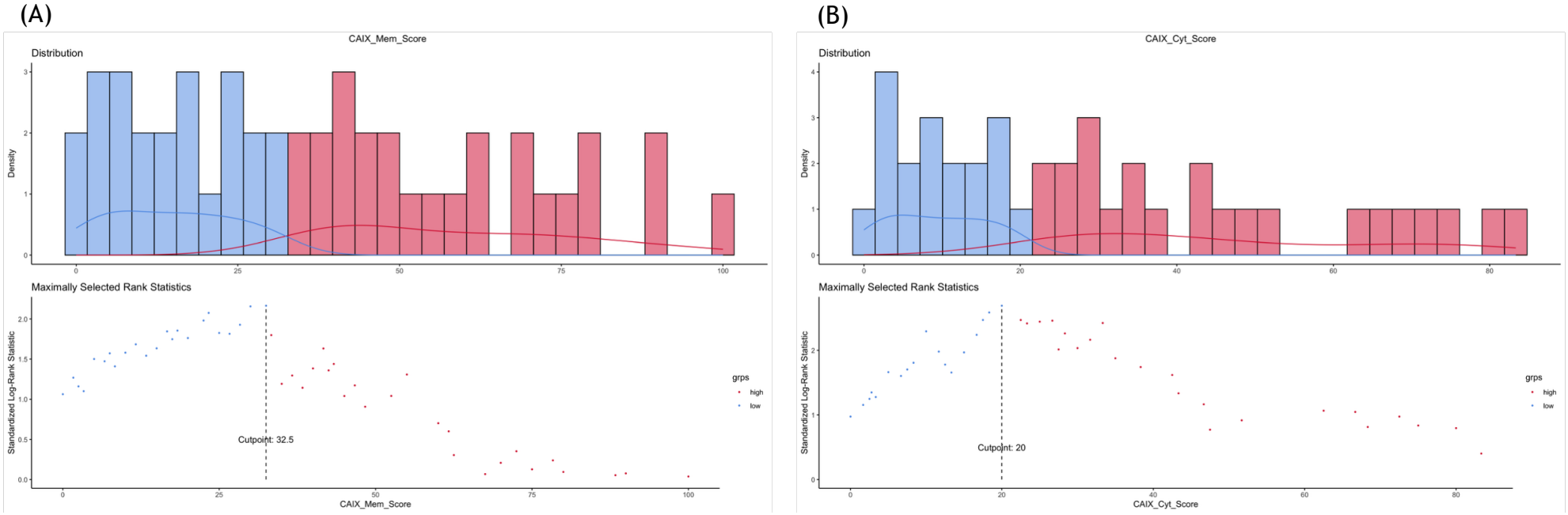

Figure 3.5-The CAIX cut point based on CSS was obtained by the R-survminer package (R version 4.2.3). (A) membrane CAIX expression and (B) cytoplasm CAIX expression

Table 3.2- The correlation between CAIX localisation and clinicopathological factors in the ER/PR negative subgroup

Clinicopathological factors	Membranous CAIX		p-value	Cytoplasmic CAIX		p-value
	Low (%)	High (%)		Low (%)	High (%)	
Age, yr (n=197) ≤50 >50	 49(36.80) 84(63.20)	 19(29.70) 45(70.30)	0.342	 49(36.80) 84(63.20)	 19(29.70) 45(70.30)	0.342
Tumour size, mm (n=197) ≤ 20 >20-50 >50	 71(53.40) 56(42.10) 6(4.50)	 29(45.30) 33(51.60) 2(3.10)	0.446	 73(54.90) 54(40.60) 6(4.50)	 27(42.20) 35(54.70) 2(3.10)	0.176
Tumour grade (n=195) I II III	 4 (3.00) 29 (22.00) 99 (75.00)	 0 (0) 13 (20.60) 50 (79.40)	0.359	 4 (3.00) 30(22.70) 98(74.20)	 0 (0) 12(19.00) 51(81.00)	0.297
Nodal involvement (n=197) No Yes	 66 (49.60) 67 (50.40)	 39 (60.90) 25 (39.10)	0.17	 67(50.40) 66(49.60)	 38(59.40) 26(40.60)	0.286
HER-2 status (n=193) Negative Positive	 91 (70.00) 39 (30.00)	 45 (71.40) 18 (28.60)	0.868	 92(70.80) 38(29.20)	 44(69.80) 19(30.20)	0.1

3.4 Identification of signature gene expression related to CAIX in ER/PR negative breast cancer

Identifying the gene expression patterns based on CAIX expression is necessary to understand the underlying biology, particularly in chronic hypoxic exposure. Transcriptomic analysis was performed by high throughput TempO-Seq (BioSpyder Inc) technology. A total of 147 ER/PR negative samples from the Glasgow breast cancer cohort were available for gene expression analysis. Of those, 131 cases had complete data for CAIX expression (**Figure 3.6**). For membranous CAIX, 87 cases were low, and 44 cases were high. For cytoplasmic CAIX expression, 87 cases were low, and 44 cases were high. A total of 14304 from 16382 genes were identified to categorise high and low membranous/cytoplasmic CAIX expression. Genes with a statistically significant fold change were identified. A log2 fold change of 1.0 in both directions and an adjusted P value (P adj) of <0.05 were used to determine the final DEGs.

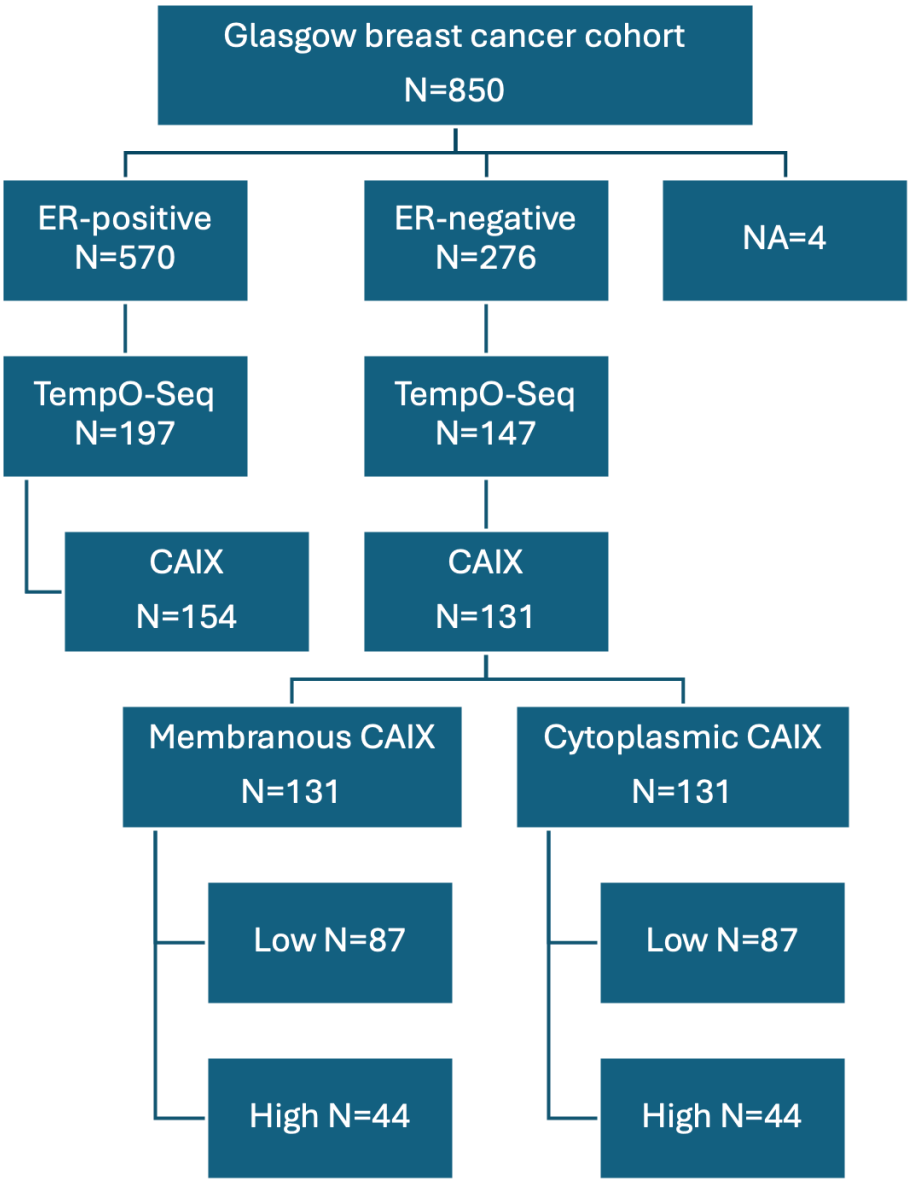

Figure 3.6 - Diagram to illustrate the workflow for retrieving transcriptomic data from ER-negative breast cancer patients with available CAIX IHC results.

3.4.1 Differentially expressed genes (DEGs) in ER/PR negative breast cancer with high versus low expression of CAIX

Principal component analysis (PCA) plots were generated using DESeq2 to determine whether samples in each group (high vs low membranous or cytoplasmic CAIX expression) clustered with each other or other groups. They both had PC1 = 13 and PC2 = 12, indicating that each component contributed nearly equally to the total variance in the data and these two principal components were equally significant in capturing the variance. Overall, the PCA results demonstrated that

the two groups of samples formed weak clusters with some overlap based on the expression of the top 20 DE genes. PC1 and PC2 components accounted for 25 % of the total variations around the PCs for the top 20 DEGs (**Figure 3.7**).

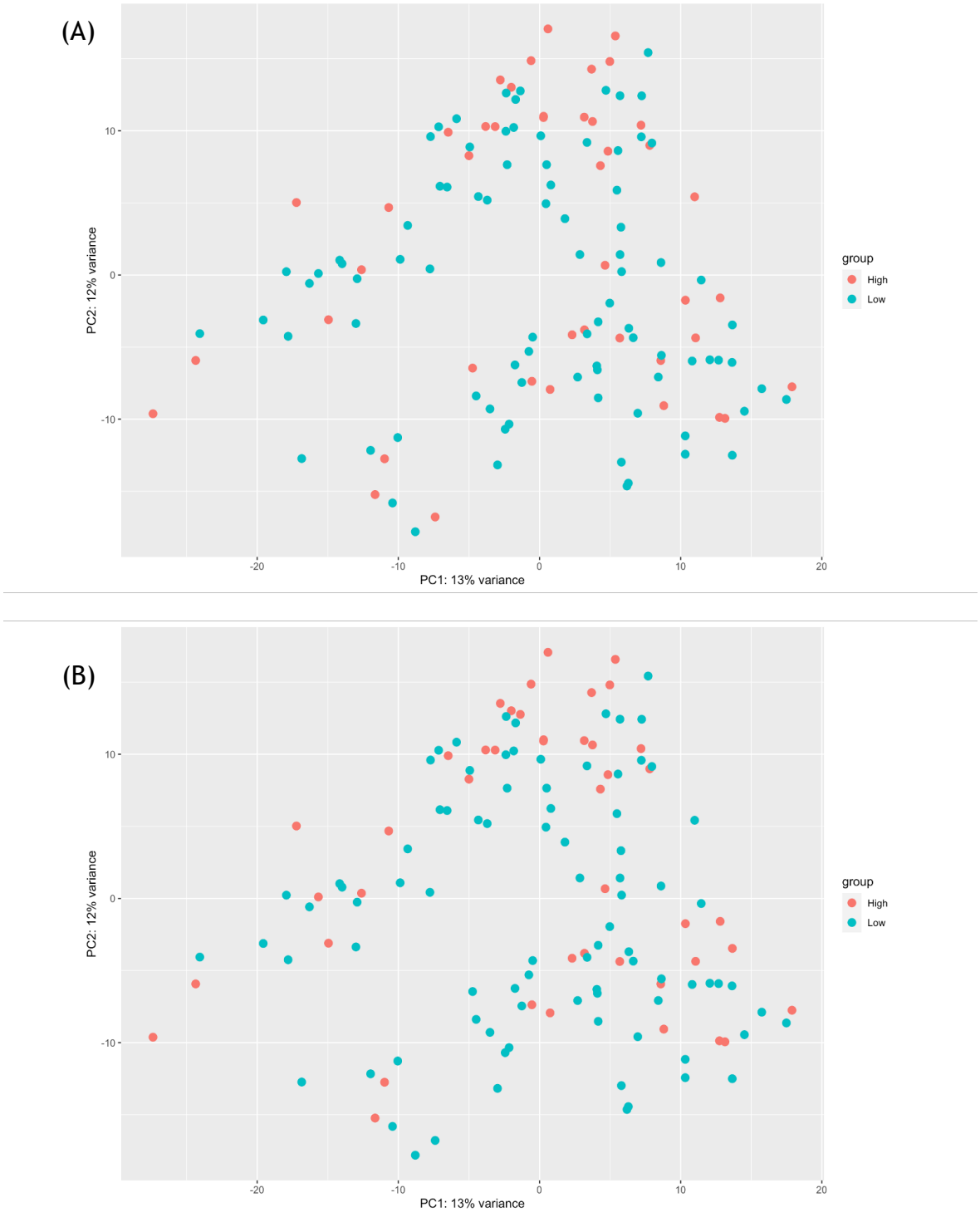

Figure 3.7 -PCA plots differential gene expression between high (Red) and low (Green) CAIX expression (A) membranous CAIX expression and (B) cytoplasmic CAIX expression

Differential gene expression between high and low membranous CAIX was processed by the DESeq2 package (version 1.4.4.0; R version 4.2.2; RStudio 2023.03.0+386). A total of 22539 genes were analysed and the top 20 DEGs between high and low expression of membranous/cytoplasmic CAIX were identified. For membrane CAIX expression, 22 DEGs had a significantly adjusted P value of 0.05 (**Figure 3.8A and Supplement Table 1**). For cytoplasmic CAIX expression, 26 significant DEGs were identified (**Figure 3.8B and Supplement Table 2**). All upregulated genes in both membrane and cytoplasm CAIX expression were identical and included *CA9*, *NDRG1*, *VEGFA* and *PPFIA4* while 14 downregulated genes overlapped between membrane and cytoplasmic CAIX expression (**Figure 3.9**).

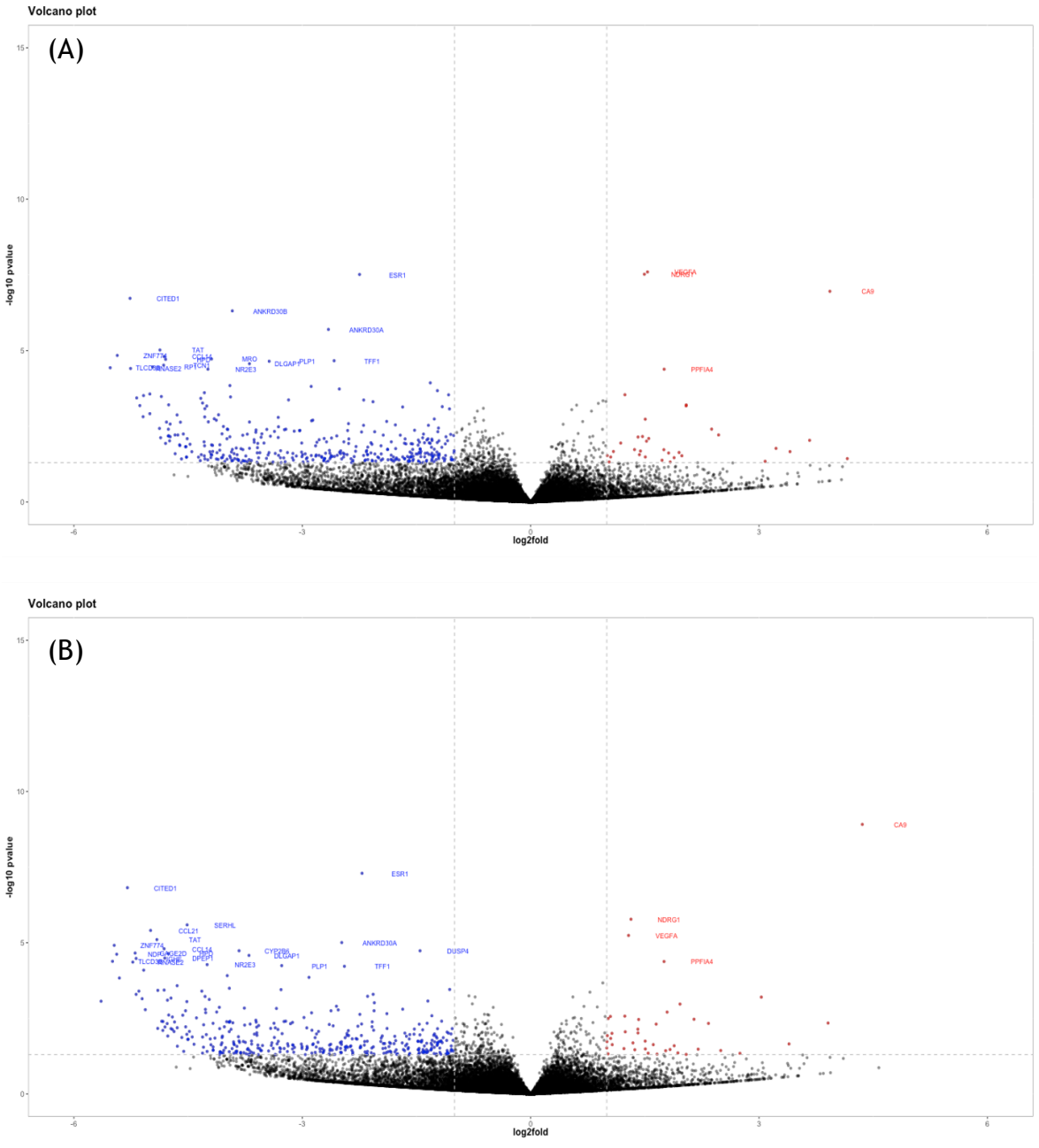

Figure 3.8 -Volcano plot representation of differential expression analysis of genes associated with CAIX expression. Red and blue points mark the genes with significantly increased or decreased expression respectively in high CAIX compared to low CAIX expression samples (P adj. < 0.05). The x-axis shows log2 fold-changes in expression and the y-axis shows the -log 10 of a gene being differentially expressed. (A) membranous CAIX expression (B) cytoplasmic CAIX expression

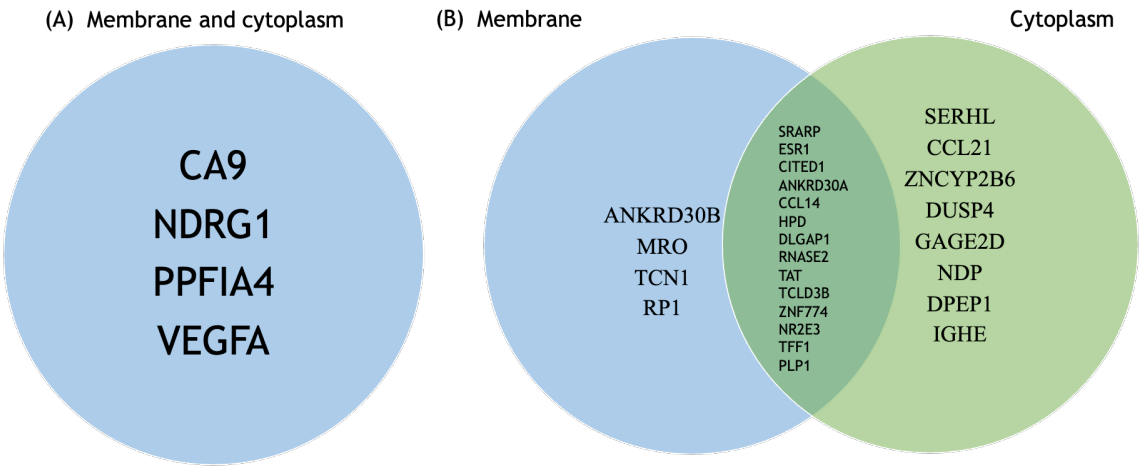

Figure 3.9 -Venn diagram summarising the overlap between differentially expressed genes from membranous and cytoplasmic CAIX expression. (A) upregulated genes (B) downregulated genes

Violin plots for significant genes with P adj. < 0.05 were constructed. The *CA9* gene was significantly upregulated in both high membranous and cytoplasmic CAIX expression (**Figure 3.10** and **3.11**).

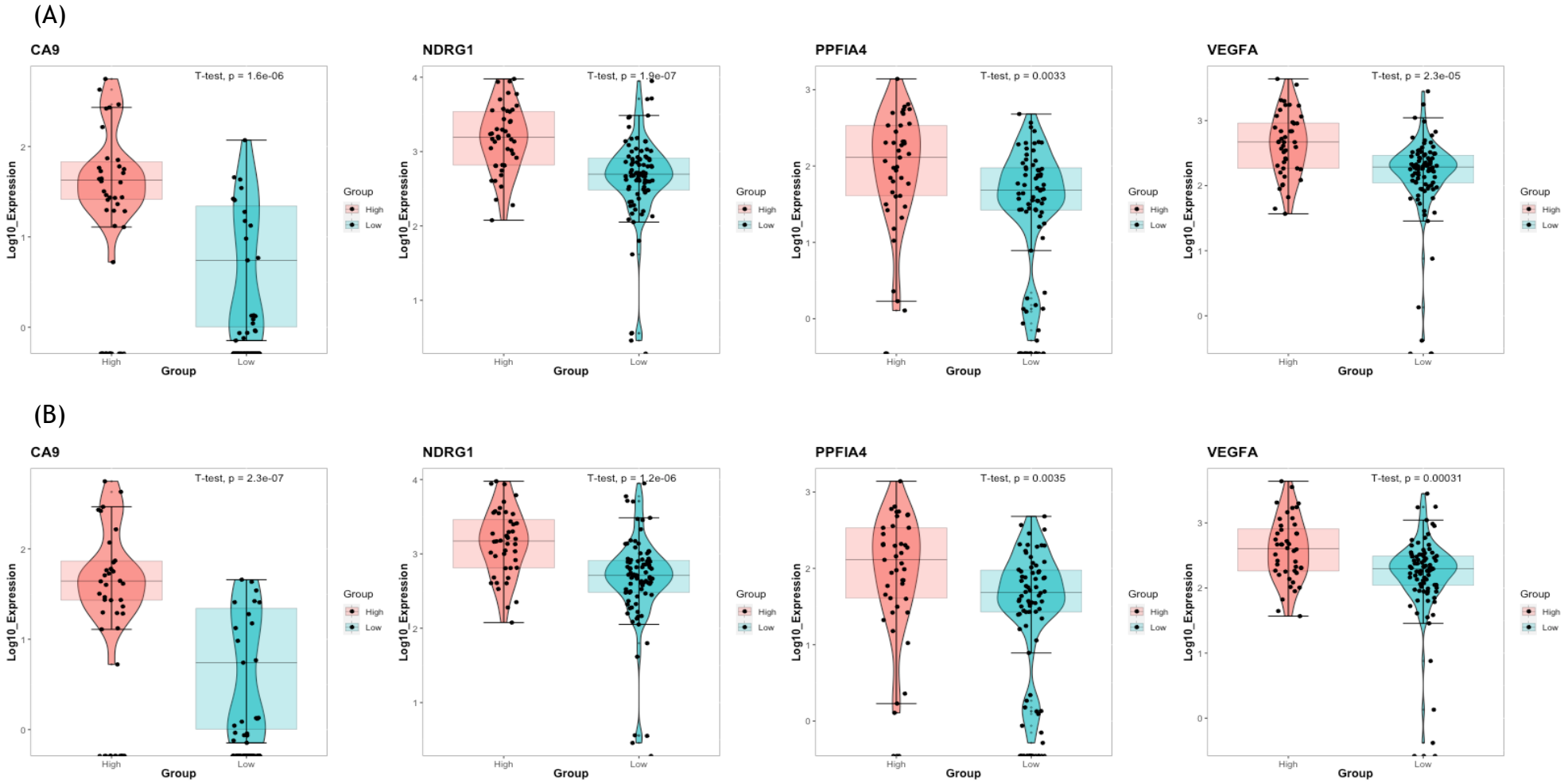

Figure 3.10 - Violin plots of upregulated significant P adj. DEGs for CAIX expression phenotypes (A) membrane (B) cytoplasm

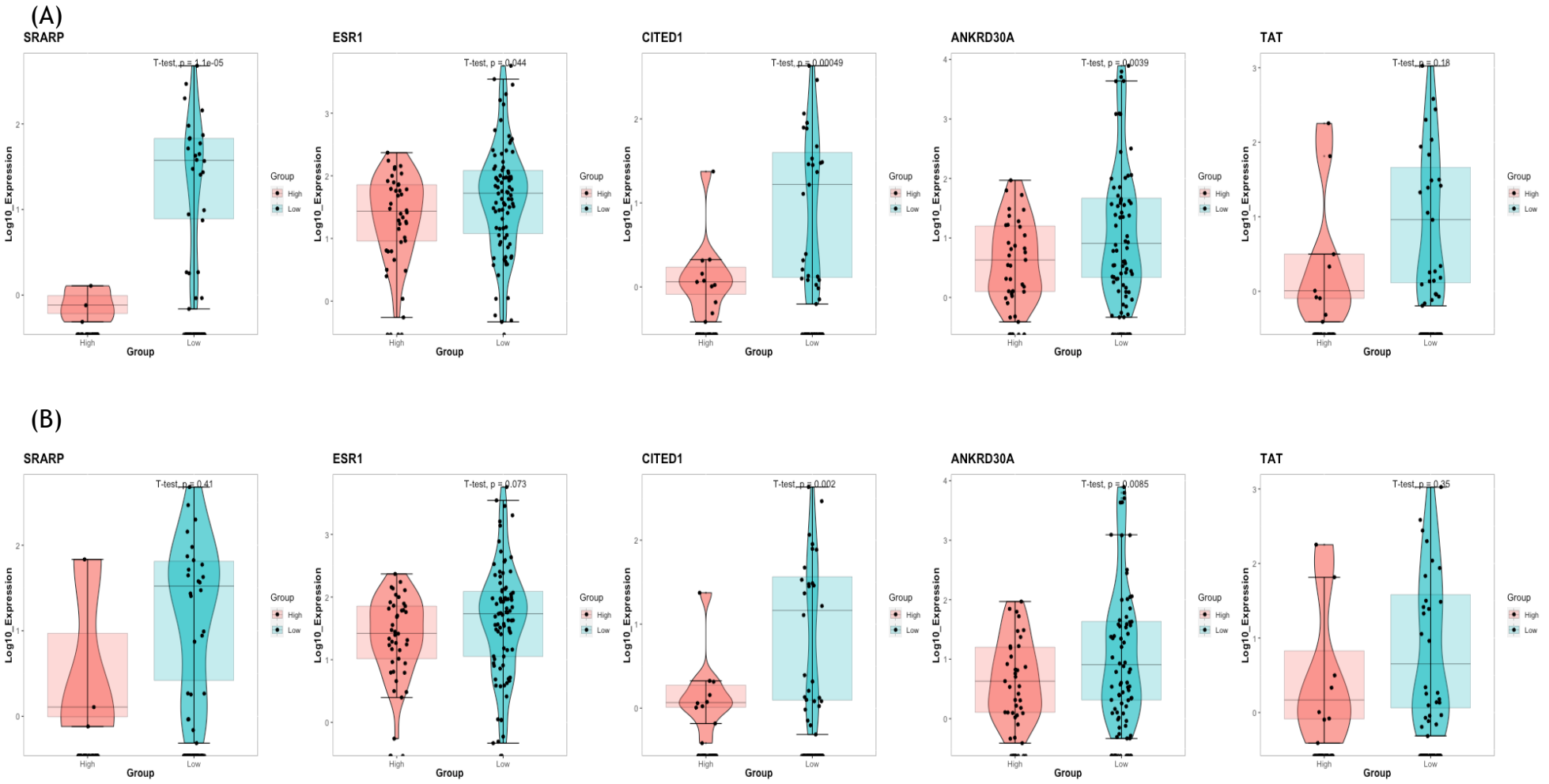

Figure 3.11 - Violin plots of downregulated significant P adj. DEGs for CAIX expression phenotypes (A) membrane (B) cytoplasm

3.4.2 Cluster analysis of ER/PR negative breast cancer with high versus low expression of CAIX

The heatmaps for DEGs with a significant adjusted P value for membranous and cytoplasmic CAIX expression were constructed. There were distinct differences in the gene expression between high and low CAIX expression, for both membrane and cytoplasmic (**Figure 3.12**).

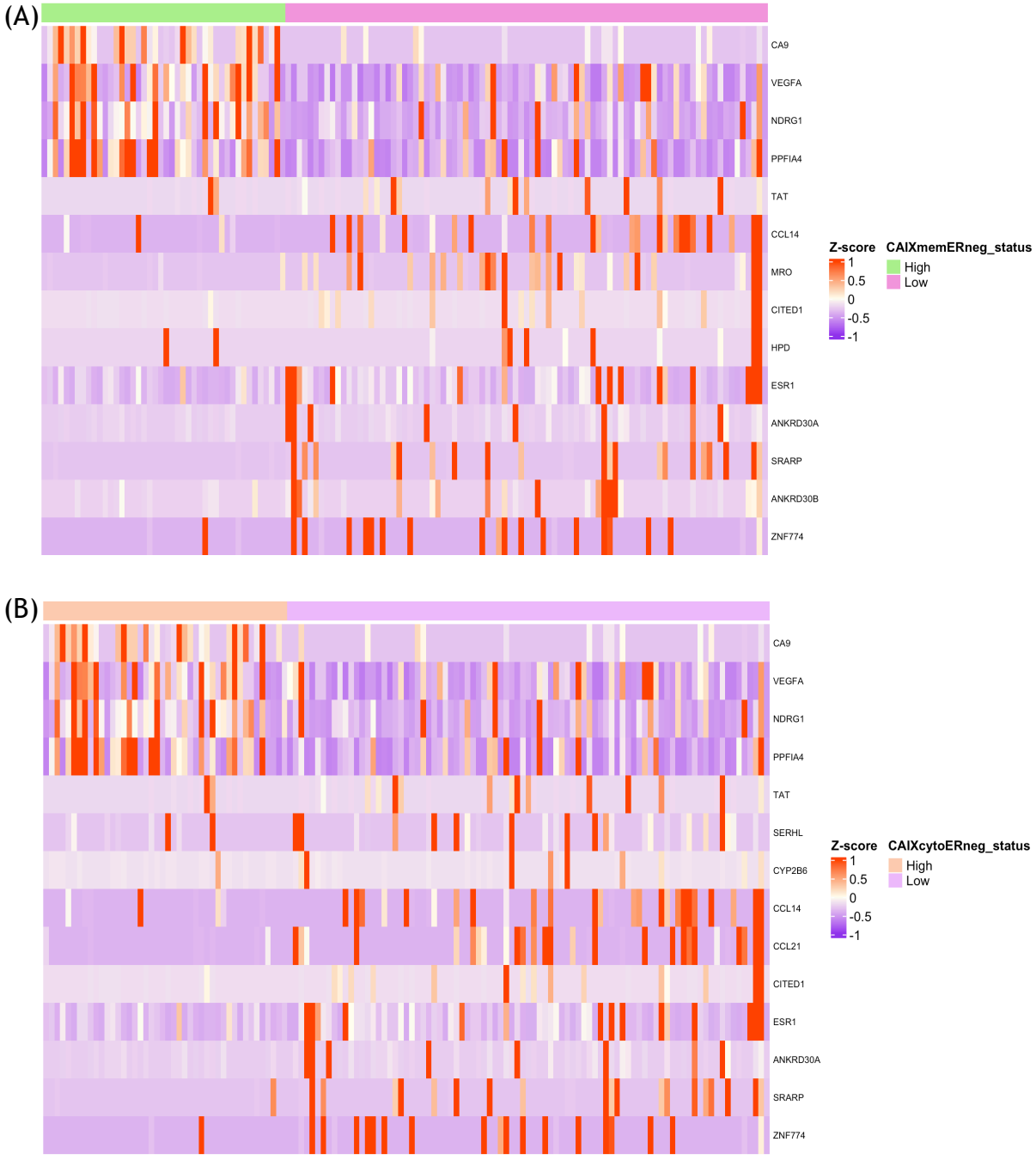

Figure 3.12-Heatmaps for significant P adj. DEGs for (A) membranous CAIX expression and (B) cytoplasmic CAIX expression

3.4.3 Dysregulated pathway analysis of ER/PR negative breast cancer based on CAIX expression

Gene set enrichment analysis (GSEA) determining h.all.v2023.1.Hs.symbols.gmt and chip platform Human_Gene_Symbol_with_Remapping_MSigDB.v2023.1.Hs.Chip identified 21 up-regulated gene sets (GS) in high membranous CAIX expression and 29 up-regulated GS in low membranous CAIX. Of those, 5 GS were up-regulated with FDR < 25% and there was no significant down-regulated GS (**Figure 3.13 and Supplement Table 3 and 4**). The GSEA results for cytoplasmic CAIX were similar to membranous CAIX with 8 GS upregulated with FDR < 25% and insignificant downregulation (**Figure 3.14 and Supplement Table 5 and 6**). Overall, GSEA of *hypoxia*, *glycolysis*, *G2M checkpoint*, *MTORC1 signalling* and *unfolded protein response* overlapped between membranous and cytoplasmic CAIX phenotypes (**Figure 3.15**).

Leading-edge analysis and enrichment map analysis showed *PPFIA4, NDRG1* and *VEGFA* genes expressed in DEGs were also significant in the hypoxia and glycolysis GSEA.

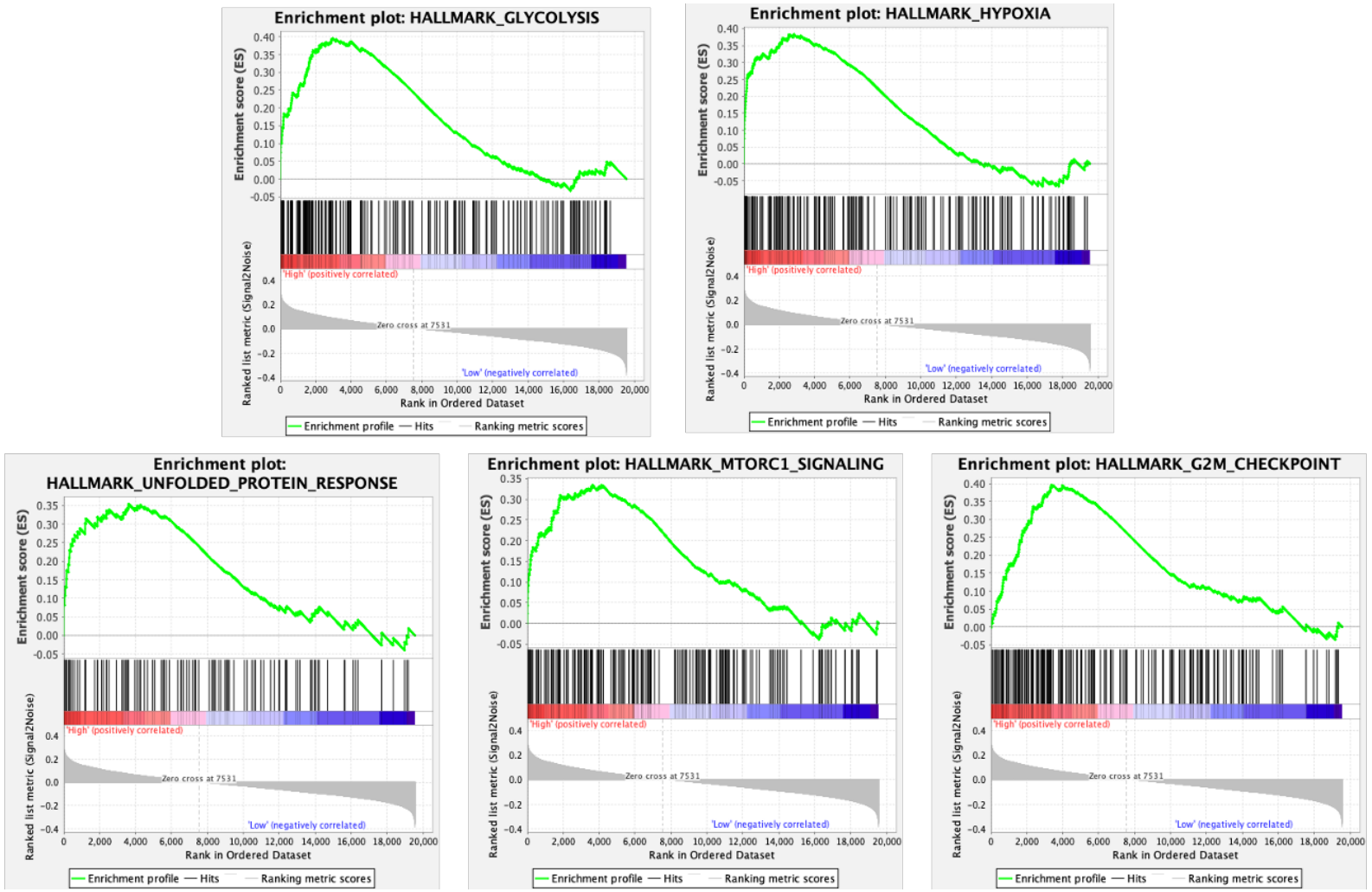

Figure 3.13- GSEA upregulation in high membranous CAIX phenotypes

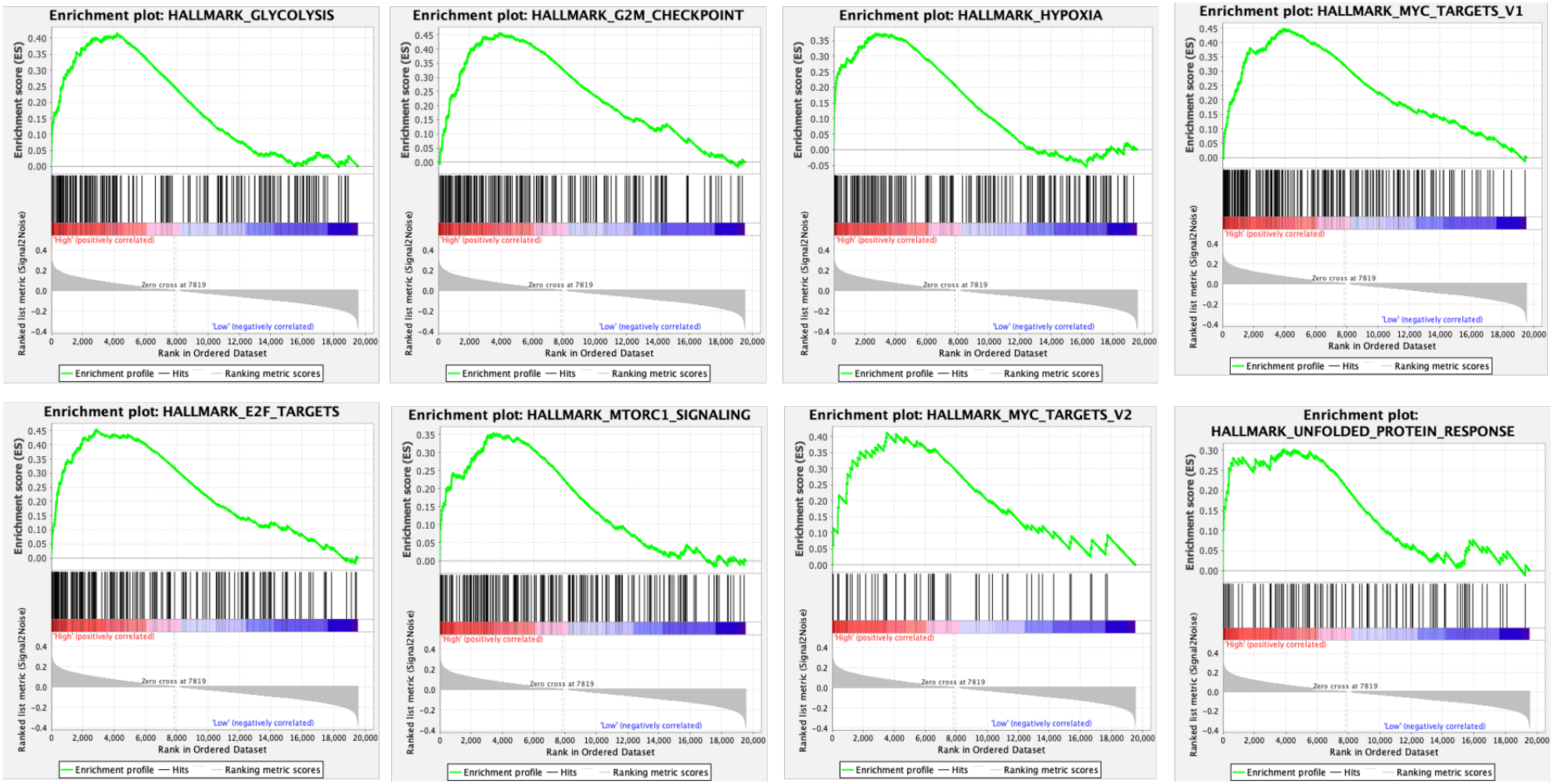

Figure 3.14- GSEA upregulation in high cytoplasmic CAIX phenotypes

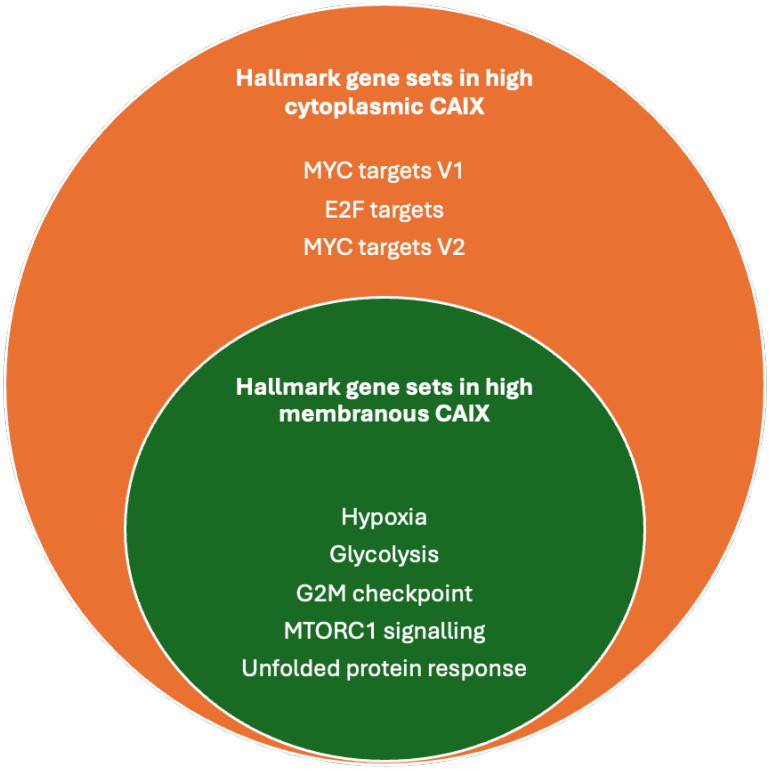

Figure 3.15-Venn diagram of overall hallmark gene sets upregulated in high CAIX expression with FDR < 25%

3.4.4 Protein-Protein Interaction (PPI) network construction

The STRING online database was applied for PPI analysis which used the top 5 significant up and down-regulated genes from DEGs for membranous and cytoplasmic CAIX (accessed at https://string-db.org/cgi/network?taskId=bYsmxBGn2WWa&sessionId=bRh9rplhyWYw). The PPI enrichment P value was 0.0032 suggesting that these targeted genes had significant interaction. The black line indicates *CA9*, *VEGFA* and *NDRG1* co-expression as evidenced by a database provided by STRING shown as the green line, however, *PPFIA4* were not associated with the others (**Figure 3.16**). CA9 is also linked to the downregulated gene *ESR1* based on non-human experiments.

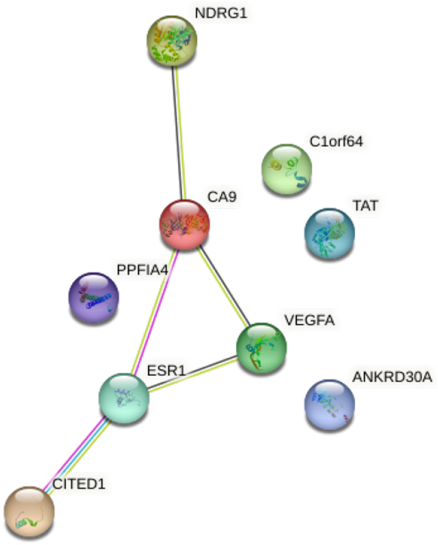

Figure 3.16 -PPI analysis of CAIX expression. The thickness of the edge indicates the strength of data that supported the interaction between the two proteins. The proteins were derived from significant DEGs of membrane and cytoplasmic CAIX expression. The colour line represents black for gene co-expression, pink for experimental evidence, green for co-mentioned in the PubMed database and blue for curated database association.

3.4.5 Validation of 4 hypoxia gene signatures in the Glasgow breast cancer cohort ER/PR-negative subgroup

Verification of the 4 upregulated genes from high CAIX expression with survival outcomes in the ER/PR-negative cohort was performed. This revealed that high *VEGFA* mRNA, *PPFIA4* mRNA and *NDRG1* mRNA but not *CA9* mRNA are significantly predictive of poor CSS (**Figure 3.17**).

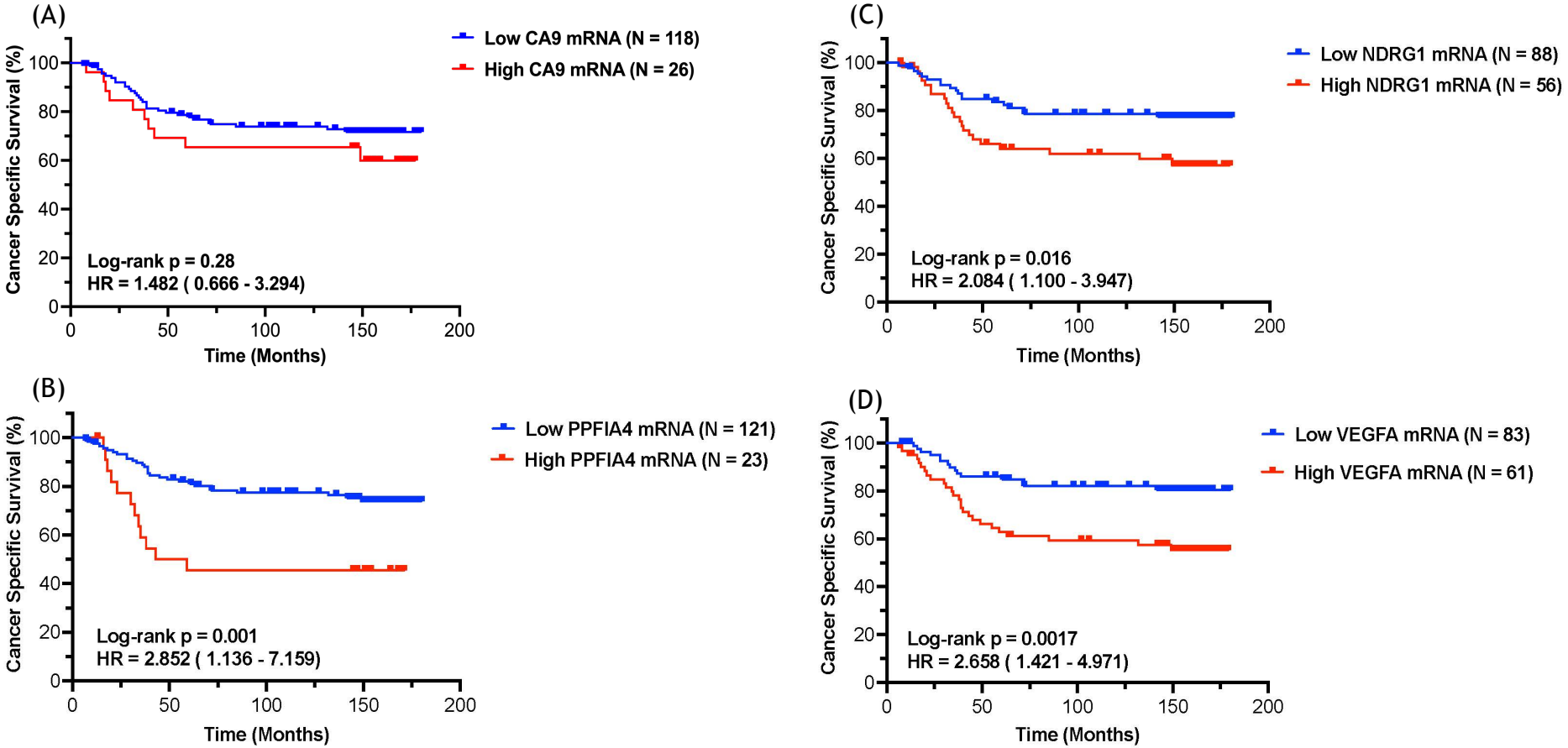

Figure 3.17 -Cancer specific survival based on the expression of (A) *CA9* mRNA (B) *PPFIA4* mRNA (C) *NDRG1* mRNA and (D) *VEGFA* mRNA

3.4.6 The correlation between CAIX and genes of interest

To understand hypoxia in terms of the up regulated genes associated with CAIX expression, the public biomedical ontology "cBioportal" was used to analyse the relationships between these genes (accessed at https://www.cbioportal.org/study/summary?id=brca_metabric). METABRIC dataset, that includes all breast cancer subtypes, was selected because it is the largest cohort with 2509 breast samples. Overall patients had no somatic mutations in these genes but carried DNA copy number alterations. 24% of patients had *PPFIA4* gene amplification followed by 23% *NDRG1* gene amplification, 2% *VEGFA* gene amplification and 1% CA9 gene amplification.

Co-expression between *CA9* and the genes of interest was evaluated using Spearman's correlation and the results were low to moderate at 0.362 for *NDRG1*, 0.338 for *PPFIA4* and 0.364 for *VEGFA*. However, when focusing only on the 554 ER-negative patients, 33% of patients had *NDRG1* gene amplification, 14% had *PPFIA4* gene amplification, 5% had *VEGFA* amplification and 2% had *CA9* gene amplification. This showed that *NDRG1* might be a predisposing gene that regulates aggression in ER-negative breast cancer subtypes. There was a strong Spearman's correlation between *CA9* and *PPFIA4* at 0.637, *NDRG1* at 0.594 and *VEGFA* at 0.520.

In the TNBC subgroup (270 patients), 33% of patients carried *NDRG1* gene amplification, 11% *PPFIA4* gene amplification, 7% *VEGFA* amplification and 3% *CA9* gene amplification. The Spearman's correlation was 0.612 with *PPFIA4*, 0.555 with *NDRG1* and 0.515 with *VEGFA*. In the HER-2 overexpression subgroup (114 patients), 32% had *NDRG1* gene amplification, 19% had *PPFIA4* gene amplification, 2% had *VEGFA* gene amplification and <1% had *CA9* gene amplification. The Spearman's correlation was 0.678 with *NDRG1*, 0.688 with *PPFIA4* and 0.566 with *VEGFA*. This is in contrast to the ER-positive/HER-2 negative cohort (1329 patients), where 27% of patients had *PPFIA4* gene amplification, 20% *NDRG1* gene amplification, 0.5% *CA9* gene amplification and 0.4% *VEGFA* gene amplification. The Spearman's correlation was 0.240 with *PPFIA4*, 0.214 with *VEGFA* and 0.156

with *NDRG1*. This provides further evidence that hypoxia-related genes *especially NDRG1* and *PPFIA4*, play a role in the ER-negative subgroup (**Table 3.3**).

Table 3.3 -The Spearman correlation between CA9 and 4 upregulated genes from TCGA database

	CA9				
Genes	**All subtypes**	**ER-positive**	**ER-negative**	**TNBC**	**HER2-enriched**
NDRG1	0.362 (p=3.33e-62)	0.156 (p=1.23e-9)	0.594 (p=3.29e-43)	0.555 (p=7.44e-27)	0.678 (p=4.99e-18)
PPFIA4	0.338 (p=2.91e-54)	0.24 (p=4.48e-21)	0.637 (p=2.46e-51)	0.612 (p=1.07e-33)	0.688 (p=1.00e-18)
VEGFA	0.364 (p=4.63e-63)	0.214 (p=5.44e-17)	0.520 (p=8.17e-32)	0.515 (p=9.68e-23)	0.566 (p=7.42e-12)

3.5 Discussion

Tumour hypoxia drives metastasis and treatment resistance and is primarily identified by HIF-1α expression, a key regulator of the low-oxygen response (303). However, HIF-1α has a short half-life of approximately 5 minutes, thus may be less sensitive to detection, particularly in patient tissue samples (250). In addition to HIF-1α, CAIX is a potential marker for identifying hypoxia as it requires HIF-1α activation and has a longer half-life of approximately 2-3 days (199). This chapter demonstrated that CAIX may be a promising breast cancer prognostic marker, especially in ER/PR negative subgroups. It was found that *CA9, NDRG1, PPFIA4* and *VEGFA* genes were significantly differentially expressed in tumours with high CAIX expression. High CAIX-expressing tumours were also enriched for hypoxia, glycolysis, G2M checkpoint, MTORC1 and unfolded protein response signalling pathways. These genes, at the mRNA level, were primarily investigated in the Glasgow breast cancer cohort, and all except *CA9* mRNA were associated with CSS.

Although CAIX is a transmembrane protein, it can be internalised to the cytoplasm under conditions of stress such as hypoxia or stimulation with a monoclonal antibody (333, 334). Previous studies reported that scoring CAIX in both the tumour cell membrane and cytoplasm could help predict breast cancer survival outcomes (318, 320, 323, 335). However, none of the studies reported survival data for membrane-bound CAIX or cytoplasmic CAIX individually. This

present study demonstrated that high CAIX expression as detected by IHC, whether in the tumour cell membrane or cytoplasm, can predict poor OS in breast cancer patients and reported the significance of cytoplasmic CAIX as an independent factor for overall survival. Cytoplasmic CAIX expression has also been observed in other cancers, including prostate cancer, squamous cell carcinoma of the head and neck, and non-small cell lung cancer (336, 337, 338). Its presence has been associated with high-grade disease, chemoresistance, and poor prognosis. Targeted CAIX treatment has not been widely explored however, SLC-0111 a specific small-molecule CAIX inhibitor, is in a phase Ib clinical study for advanced pancreatic cancer (NCT03450018). These data highlight the importance of hypoxia-associated CAIX in cancer biology.

CAIX has been extensively studied and has a well-established prognostic role in many cancers. The meta-analysis focused specifically on breast cancer, strengthening its role as a poor prognostic marker, affecting both OS and DFS, particularly in TNBC. However, due to lacking subgroup analysis for HER-2 positive cases, it remains uncertain whether CAIX plays a similar role in that subtype. It has been hypothesised that CAIX may have a compensatory or mediating role in ER-negative disease, suggesting that its impact is more pronounced in ER-negative breast cancer compared to ER-positive cases. In addition, the molecular background of high CAIX expression remains poorly understood. Transcriptomic analysis is a preferential method used to gain a deeper understanding of what is driving the high CAIX profile. There are several transcriptomic approaches such as microarrays and RNA-seq (339). However, this study used the TempO-Seq platform, which is a whole transcriptome expression assay. The advantage of this technique is that it can be performed using FFPE samples. Differential gene expression, which compared high and low CAIX expression (whether from cytoplasm or membrane) identified similar upregulated genes, *CA9, NDRG1, PPFIA4* and *VEGFA*, and overlapped some downregulated genes. This highlights the upregulation of these genes in conjunction with high CAIX expression underscores a coordinated response to hypoxic stress within tumours.

The main function of CAIX in pH regulation has been well established. Cancer cells obtain energy from oxidative phosphorylation in mitochondria or aerobic glycolysis where the end products are CO_2 and lactate, respectively (340). Both CO_2 and lactate decrease intracellular pH and this needs to be reversed.

Transmembrane CAIX works in conjunction with other acid/base transporters to regulate the pH both intracellular and extracellular by converting external CO_2 to H^+ and HCO_3^-, which results in extracellular acidosis (253). CAIX expression is largely based on HIF-1α activation and not only serves as a pH regulator but also participates in tumour migration and invasion (197).

The rapid proliferation of cancer cells increases oxygen and nutrient demand. Thus, new blood vessels are required, and the key regulator for neovascularisation is HIF-1α. As tumours grow, they contain regions of ischemia and necrosis, leading HIF-1α to promote angiogenesis by activating VEGF transcription. In humans, the VEGF family comprises VEGF-A to VEGF-F, placenta growth factor (PlGF) and endocrine gland-derived vascular endothelial growth factor (EG-VEGFA) (341). VEGF-A is the most potent pro-angiogenic factor and, when combined with its receptor VEGFR1/2, triggers multiple signalling pathways, such as, TSAd-Src-PI3K/AKT1/survivin and NCK-P53-MAPK (342). Overall activation of VEGFA/VEGFR cascade contributes to angiogenesis, enhance vascular permeability, cell migration and cell proliferation (342, 343). CAIX and VEGFA are both hypoxia-responsive genes and high expression in breast cancer tissue predicts adverse survival outcomes (204, 344). Additionally, CAIX knockdown improved the effectiveness of the anti-VEGFA treatment (Bevacizumab) by reducing tumour volume in colonic and glioblastoma xenograft models (345). This suggests that hypoxia-responsive genes interact and affect the function of each other.

Protein Tyrosine Phosphatase, Receptor Type, F Polypeptide (PTPRF), Interacting Protein Alpha 4 (PPFIA4) or liprin-alpha-4 is a member of the liprin family. It can be induced under hypoxic conditions by HIF-1α directly activating the *PPFIA4* gene as there is a HRE at the promoter region that HIF-1α can bind to, as demonstrated through reporter assays and chromatin immunoprecipitation studies (346). PPFIA4 expression promotes cancer cell proliferation, cell-cell adhesion and migration (347, 348). In addition, PPFI4 is associated with treatment failure in small-cell lung cancer models and this effect was reversed by silencing PPFIA4 (348). However, no study has reported a correlation between CAIX and PPFIA4.

N-myc down-regulated gene 1 (NDRG1) belongs to the NDRG family comprising of 4 members. Its expression is regulated by cellular stress including

hypoxia (278). NDRG1 is regulated by HIF-1α through binding sites within the promotor area which was demonstrated by ChIP analysis using the A549 lung cancer cell line (281). The function of NDRG1 has been controversial mostly depending on the type of cancer as well as the context of each cancer. In breast cancer research, findings have been inconclusive. Earlier studies highlighted an anti-oncogenic role, showing that it suppressed cancer proliferation, invasion, and migration. However, more recent studies have reported contrasting results (349).

String analysis showed that all upregulated genes except *PPFIA4* were associated with each other and are involved in hypoxia so it may be hypothesised that their interaction occurs under hypoxic conditions. Gene set enrichment analysis was conducted to gain further insight into the potential pathways involved. Five signalling pathways with FDR<0.25 overlapped between high cytoplasmic and membrane CAIX including hypoxia, glycolysis, G2M checkpoint, MTORC1 and unfolded protein response signalling pathways. However, when the criteria were made more stringent with FDR < 0.25 and NOM-P < 0.05, only hypoxia, glycolysis, and MTORC1 pathways remained significant.

Hypoxia activates the transcription of *CA9* and related genes as mentioned above. Glycolysis is a metabolic alteration related to hypoxia. CAIX plays a major role in optimising intra- and extracellular pH in cancer during aerobic glycolysis. VEGFA activation enhances glycolysis through neuropilin-1 (NRP-1), while the gene expression of VEGFA is linked to lactate dehydrogenase A (LDHA) and glucose transporter 1 (Glut-1), both essential glycolytic genes (350). However, few studies have reported the outcome of NDRG1-associated glycolysis. In pancreatic cancer cell lines, NDRG1 expression decreased glycolysis-related enzymes, for example, GLUT-1, LDHA, HK2 and PDK-1, and promoted mitochondrial respiration (351). Previous results using HCC cell lines demonstrated a similar pattern, silencing NDRG1 decreased glucose uptake and lactic acid production in hypoxia (352). mTORC1 is one of 2 mTORC forms that are stimulated by many signalling pathways. (353). Hypoxia impairs the mTOR inhibitor efficacy and can be reversed when inhibiting CAIX (354).

Cancer-specific survival for the ER-negative breast cancer cohort with respect to the mRNA levels of the 4 upregulated genes was initially analysed to determine the significance of these genes in the cohort. With the exception of

CA9, high levels of mRNA were significantly associated with inferior CSS. The results underlined the potential of these genes as prognostic markers in ER-negative breast cancer. Although *CA9* mRNA CSS was discordant from CAIX protein expression, this was probably caused by post-transcriptional modification of mRNA and mRNA level does not reflect biological function (355). Another possibility is that different clones of cells within the same tumour express different levels of mRNA and protein due to epigenetic heterogeneity. Data from the other 3 genes should be investigated at the protein level to confirm the findings of this study. In addition, this section demonstrated a moderate positive correlation between CAIX expression and upregulated markers from the transcriptome, with this correlation being potentiated in the ER-negative subgroup. This suggests that these genes may play a more dominant role in the aggressive features of the disease. High VEGFA protein expression associated with lymph node metastasis and poor OS in small cell lung cancer, renal cell carcinoma (356, 357). NDRG1 protein expression has shown varying prognostic significance; while it predicted poor survival in hepatocellular carcinoma, it served as a good prognostic indicator in colorectal cancer (358, 359, 360). Currently, no study has examined PPFIA protein expression by IHC to predict survival outcomes. However, *PPFIA4* mRNA related to poor OS and DFS in colorectal cancer and cholangiocarcinoma (361, 362).

In conclusion, this present study underlined the importance of hypoxia through CAIX expression in the ER-negative breast cancer subgroup. An additional 3 upregulated genes from the transcriptomic analysis were identified as candidates for promoting tumour aggressiveness in addition to CAIX that probably involves hypoxia and metabolic alteration. The following chapter investigates the regulation of these genes in response to hypoxia.

Chapter 4 : Hypoxia-induced expression of CAIX, NDRG1, VEGFA, and PPFIA4

4.1 Introduction

Cellular hypoxia is a common feature in solid malignancy contributing to tumour aggressiveness by promoting cell proliferation, angiogenesis, invasion, apoptosis and metabolic alteration (363). Hypoxia-inducible factor-1α (HIF-1a) is a master transcription factor which is undegraded in an oxygen-deprived environment and subsequently activates the hypoxia-responsive targeted genes at the hypoxia-response elements (HREs)(364). Breast cancer is one of 10 cancers with a high hypoxic score (365). The oxygen level in breast cancer tissue is approximately 1% compared to over 10% in normal breast parenchyma (366, 367). This suggests that hypoxia contributes to the aggressive nature of breast cancer.

The previous chapter reported on the transcriptomic data from CAIX expression, and an additional 3 significantly differentially expressed genes that were upregulated in tissue with high CAIX expression; NDRG1, PPFIA4 and VEGFA. CAIX has been well established as one of the genes strongly induced under hypoxic conditions and has been validated as a marker of acute or chronic hypoxia (368, 369). In addition, VEGFA expression has been shown to be regulated under hypoxic conditions through HIF-1α activation (370). A meta-analysis from Su et al., including 22 papers, reported that VEGFA overexpression was related to lymph node metastasis (risk ratio [RR] = 1.28 [95% CI 1.04-1.58]) (371). The expression of CAIX and CAIX-associated markers identified from transcriptomic data, particularly NDRG1 and PPFIA4 has not yet been determined under conditions of low oxygen.

This chapter examined the response of CA9, NDRG1, PPFIA4 and VEGFA mRNA levels, along with their corresponding protein levels to in vitro hypoxia in a panel of human breast cancer cell lines; MDA-MB-231 (for TNBC subtypes), SK-BR-3 (for HER-2 enriched subtype) and MCF-7 (for ER-positive subtype). As these cell lines are widely accepted as representative models of TNBC, HER2-enriched and ER-positive subtypes, respectively.

MDA-MB-231 ($2.5x10^5$ cells), SK-BR-3 ($2.5x10^5$ cells) and MCF-7 ($3.0x10^5$ cells) were seeded in 6 well-plate 24 hours before the experiment. Cells were incubated under normoxic (21% O_2, 5% CO_2, 74% N_2) or hypoxic (1% O_2, 5% CO_2,

94% N_2) conditions for specific time points. Lysates were prepared from one set of plates for protein analysis, while mRNA was isolated from another set. mRNA levels were analysed using qPCR, while protein levels were assessed via western blot.

4.2 The expression of CAIX, NDRG1, PPFIA4, VEGFA and HIF-1α is induced under hypoxic conditions in MDA-MB-231, SK-BR-3 and MCF-7 cell lines

4.2.1 CA9 mRNA and protein expression in response to 1% oxygen

The level of CA9 mRNA increased over time peaking at 48 hours in 1% oxygen for all of the breast cancer cell lines. In the MDA-MB-231 cell line, CA9 mRNA was detected from 4 hours onwards, and the levels gradually increased until they peaked at 48 hours (

Figure 4.1 F). In normoxia, 20% oxygen, CA9 mRNA levels were very low across all time points. However, CA9 mRNA levels were higher in hypoxia than normoxia at every time point and this was significant from 16 hours onward. The pattern of CA9 mRNA expression in SK-BR-3 was similar to MDA-MB-231 with maximal expression at 48 hours, and it was significantly upregulated from 16 hours onwards (**Figure 4.2 F**)**.** The MCF-7 cell line showed a comparable pattern, reaching its peak at 48 hours; however, CA9 mRNA levels increased significantly at 8 hours, which was earlier than observed in the MDA-MB-231 and SK-BR-3 cell lines (**Figure 4.3 F**) **.**

CAIX protein levels were concordant with the mRNA levels. In MDA-MB-231 and SK-BR-3 cell lines, CAIX protein expression, began to increase at 4 hours and reached its highest level at 48 hours and this was significantly different from normoxia at 16 hours (

Figure 4.1 A and C & Figure 4.2 **A and C)**. Although CAIX protein level in the MCF-7 cell line was elevated, the difference was only significantly different from normoxia at 48 hours (**Figure 4.3 A and C**).

4.2.2 NDRG1 mRNA and protein expression in response to 1% oxygen

NDRG1 mRNA expression progressively increased in all breast cancer cell lines, with a peak observed at 48 hours in 1% oxygen conditions. In the MDA-MB-231 cell line, NDRG1 mRNA was detectable from 4 hours and its levels progressively increased although slightly dropped at 24 hours but still peaked at 48 hours under hypoxic conditions **(**

Figure 4.1 G). However, NDRG1 mRNA levels remained very low at all time points under normoxic conditions. NDRG1 mRNA levels were higher in hypoxia than normoxia at every time point and this was significant at 16 hours and 24 hours. NDRG1 mRNA expression in SK-BR-3 increased progressively, reaching its peak at 48 hours, with a significant upregulation observed specifically at 48 hours under hypoxic conditions **(Figure 4.2 G)**. The MCF-7 cell line showed a comparable pattern to MD-MB-231, reaching its peak at 48 hours; however, NDRG1 mRNA levels increased significantly at 8 hours and 48 hours (**Figure 4.3 G**)

NDRG1 protein levels consistently increased over time in all breast cancer cell lines. In MDA-MB-231, SK-BR-3 and MCF-7 cell lines, the NDRG1 protein expression levels increased from 4 hours onward and reached their highest level at 48 hours. They were significantly different from normoxia starting at 16 hours to 48 hours (

Figure 4.1-Figure 4.3 A and D).

4.2.3 PPFIA4 mRNA and protein expression in response to 1% oxygen

PPFIA4 mRNA levels in all breast cancer cell lines were generally higher in hypoxia than in normoxia at all time points, although they fluctuated over time. The peak PPFIA4 mRNA level occurred at 4 hours in the MDA-MB-231 and MCF-7 cell lines (

Figure 4.1 H &Figure 4.3 H), while in the SK-BR-3 cell line, the highest level was observed at 48 hours **(Figure 4.2 H).** However, PPFIA4 protein levels were not able to be detected by western blot.

4.2.4 VEGFA mRNA and protein expression in response to 1% oxygen

VEGFA mRNA levels in all breast cancer cell lines were typically higher in hypoxia than in normoxia at each time point, with some fluctuations observed over time. The highest level of VEGFA mRNA for MDA-MB-231 occurred at 16 hours (

Figure 4.1 I), for SK-BR-3 at 48 hours (**Figure 4.2 I**) and MCF-7 at 4 hours (**Figure 4.3 I**). However, VEGFA protein levels were not able to be detected by western blot.

4.2.5 HIF-1α mRNA and protein expression in response to 1% oxygen

To confirm the hypoxic conditions, HIF-1α was also evaluated at both mRNA and protein levels. In MDA-MB-231, SK-BR-3 and MCF-7 cell lines, HIF-1α mRNA levels under hypoxic conditions were significantly lower than those observed in normoxia at all time points except 4 hours (

Figure 4.1 E & Figure 4.3 E). HIF-1α mRNA expression in SK-BR-3 exhibited a similar pattern, although the disparity between normoxia and hypoxia was less pronounced compared to the other two cell lines **(Figure 4.2 E)**

HIF-1α protein levels as assessed by western blotting were discordant with mRNA levels assessed by qPCR. Although the levels of HIF-1α mRNA in MDA-MB-231 and MCF-7 cell lines were lower in hypoxia than in normoxia at all time points, HIF-1α protein level was significantly higher at 4 and 8 hours in hypoxia than in normoxia before decreasing at longer time points. In the SK-BR-3 cell line, HIF-1α protein levels were consistently higher under hypoxia than normoxia at all time points, although the difference did not reach statistical significance **(**

Figure 4.1-Figure 4.3 A and B)

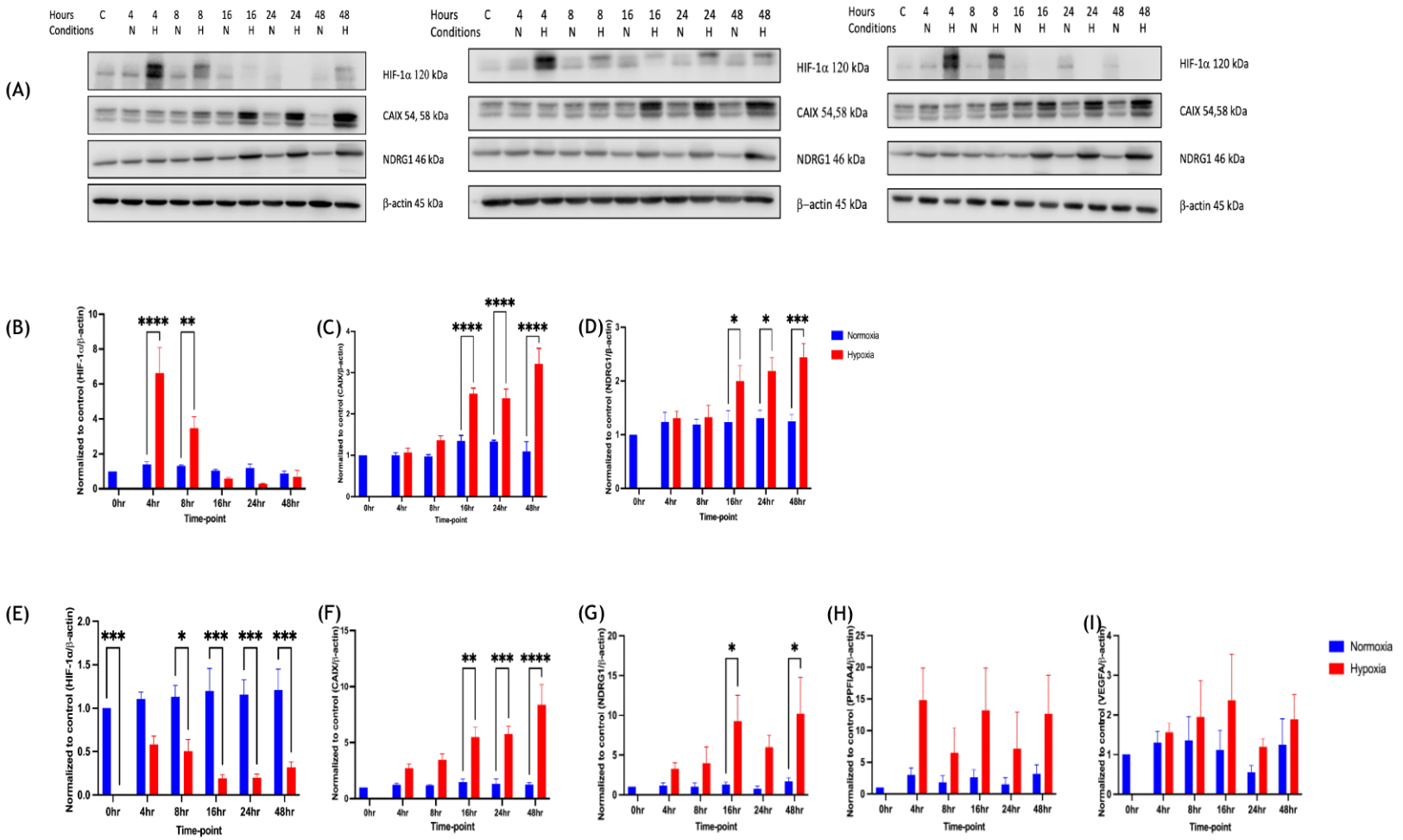

Figure 4.1- CAIX, NDRG1, PPFIA4, VEGFA and HIF-1α expression in normoxia and 1% O_2 hypoxia conditions in the MDA-MB-231 cell line. A; western blot of three independent biological replicates for HIF-1a, CAIX, and NDRG1 at time points 0-, 4-, 8-, 16, 24- and 48 hours. B-D;

the quantitative measurement of each protein from the western blots (B) HIF-1α, (C) CAIX and (D) NDRG1. Beta-actin was used as a control, and all were normalised to 0 hours (control). E-I; q-PCR results for (E) HIF-1a, (F) CAIX, (G) NDRG1, (H) PPFIA4 and (I) VEGFA. Beta-actin was used as a control, and all were normalised to 0 hours (control). Two-way ANOVA was used to compare between groups with different time points. Data were mean+/-SEM. *P≤0.05, **P≤0.01, ***P≤0.001 and ****P≤0.0001.

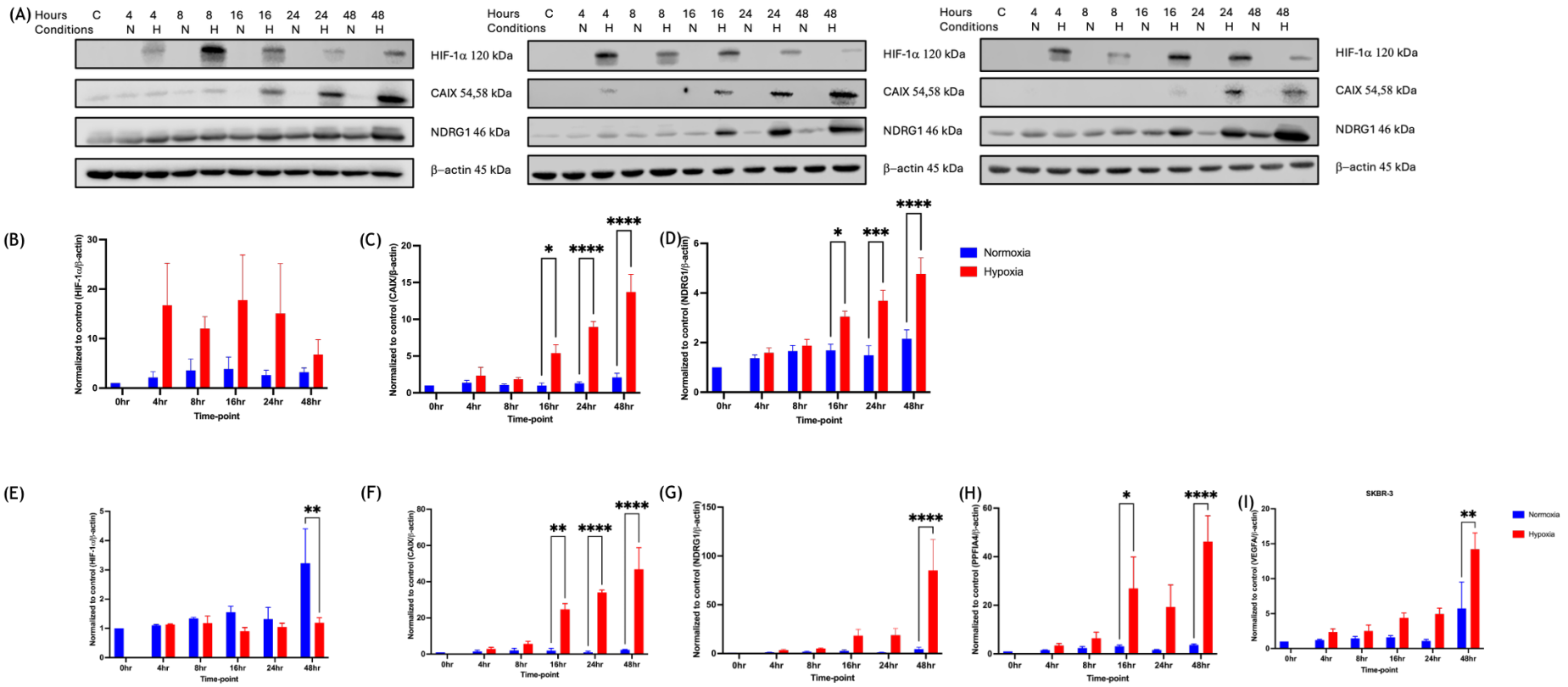

Figure 4.2-CAIX, NDRG1, PPFIA4, VEGFA and HIF-1α expression in normoxia and 1% O_2 hypoxia conditions in the SK-BR-3 cell line. A; western blot of three independent biological replicates for HIF-1a, CAIX, and NDRG1 at time points 0-, 4-, 8-, 16, 24- and 48 hours. B-D;

the quantitative measurement of each protein from the western blots (B) HIF-1α, (C) CAIX and (D) NDRG1. Beta-actin was used as a control, and all were normalised to 0 hours (control). E-I; q-PCR results for (E) HIF-1a, (F) CAIX, (G) NDRG1, (H) PPFIA4 and (I) VEGFA. Beta-actin was used as a control, and all were normalised to 0 hours (control). Two-way ANOVA was used to compare between groups with different time points. Data were mean+/-SEM. *P≤0.05, **P≤0.01, ***P≤0.001 and ****P≤0.00

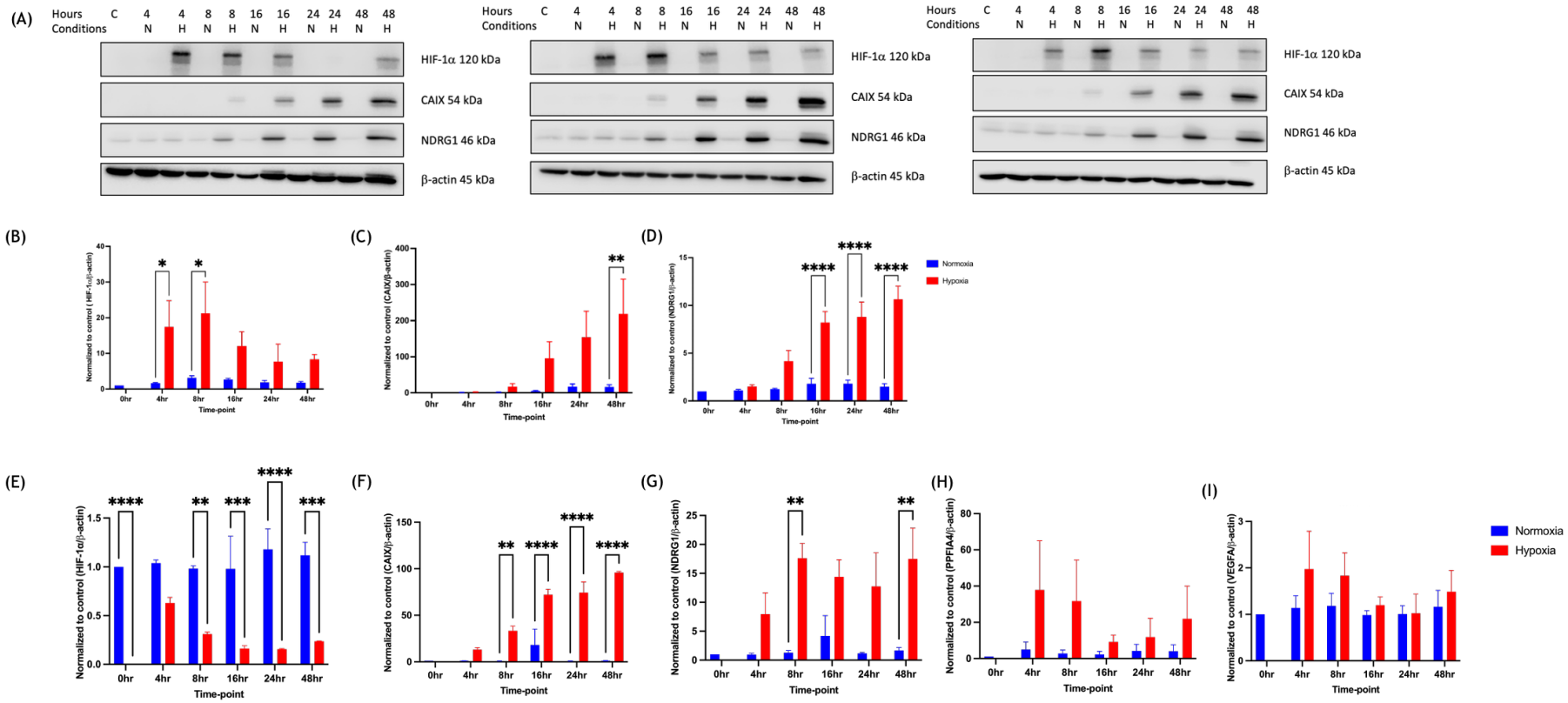

Figure 4.3-CAIX, NDRG1, PPFIA4, VEGFA and HIF-1α expression in normoxia and 1% O_2 hypoxia conditions in the MCF-7 cell line. A; western blot of three independent biological replicates for HIF-1a, CAIX, and NDRG1 at time points 0-, 4-, 8-, 16, 24- and 48 hours. B-D; the

quantitative measurement of each protein from the western blots (B) HIF-1α, (C) CAIX and (D) NDRG1. Beta-actin was used as a control, and all were normalised to 0 hours (control). E-I; q-PCR results for (E) HIF-1a, (F) CAIX, (G) NDRG1, (H) PPFIA4 and (I) VEGFA. Beta-actin was used as a control, and all were normalised to 0 hours (control). Two-way ANOVA was used to compare between groups with different time points. Data were mean+/-SEM. *P≤0.05, **P≤0.01, ***P≤0.001 and ****P≤0.0001.

4.3 Discussion

In this chapter, qPCR and western blotting were used to determine if the mRNA and protein expression of the genes identified by TempO-Seq as being upregulated in CAIX high tissue were upregulated in response to hypoxia. By using both qPCR and Western blot, this study assessed whether mRNA expression changes translated into protein levels. Consistent results between the two methods suggest effective mRNA translation, while discrepancies indicate potential post-transcriptional or post-translational regulation (372, 373). The response of all three genes to hypoxia was examined in 3 representative breast cancer cell lines: MDA-MB-2321, SK-BR-3 and MCF-7. CAIX, NDRG1, PPFIA4, VEGFA and HIF-1α were increased at either the mRNA or protein level. Pathological hypoxia varies depending on the type of cancer, the oxygen level and hypoxia exposure time (374). In breast cancer, the median value of the partial pressure of oxygen (PO_2) is 10 mm Hg (~1% O_2), while in normal breast tissue it is 65 mm Hg (>10% O_2) (180). Cancer cells exhibit varied responses to different periods of hypoxic exposure. Acute hypoxia results from a brief period of reduced oxygen availability (ranging from minutes to a few hours) and is generally reversible. In contrast, chronic hypoxia involves extended periods of low oxygen, typically lasting more than 24 hours, which imposes significant adaptive pressures on cancer cells (374, 375). The biological consequences vary between acute hypoxia and chronic hypoxia. Acute hypoxia allows cells to accumulate genomic instabilities and induce aggressive phenotypes, whereas chronic hypoxia results in a regressive change and selective pressures on cancer cells (376). Therefore, the experiments reported in this chapter utilised 1% O_2, with acute hypoxia defined as ≤ 24 hours and chronic hypoxia as >24 hours, to observe the function of CA9-associated genes. HIF-1α expression was measured to verify that the cell lines were exposed to hypoxic conditions.

The results revealed that CAIX mRNA and protein levels matched each other. This suggests hypoxia influences CAIX regulation largely based at the transcriptional level, and in this case, mRNA levels are a reliable indicator of protein expression. CAIX expression in tumour cells was typically minimal under

normoxic conditions but was significantly elevated during hypoxia. CAIX levels progressively increased following hypoxia induction, from 4 hours to 48 hours, across all representative breast cancer subtypes. CAIX protein expression was elevated from 16 hours and peaked at 48 hours. Similar results were reported in studies by Stiehl et al. and Tafreshi et al. who both found that CAIX increased at 16 hours (377, 378). This suggests that CAIX expression occurs across all breast cancer subtypes, and its sustained induction under prolonged hypoxia indicates that CAIX serves as a marker of chronic hypoxia and plays a role in mediating aerobic glycolysis. It is widely accepted that CAIX is dependent on HIF-1a transcription (198). The CA9 gene contains HRE at the promotor site where HIF-1a activates transcription (198, 379). CAIX expression increases more gradually compared to HIF-1α because, during the acute phase, HIF-1α first activates the transcription of hypoxia-related genes, including CAIX, which takes several hours to become detectable (198, 380). The function of CAIX is mainly to control the pH of the tumour by hydrating HCO_3^{2-} resulting in extracellular acidity (253). CAIX also works with other transporters that are involved in aerobic glycolysis, EMT, angiogenesis and invasive mechanisms (305). This underlies the importance of hypoxia, as represented by CAIX, in all breast cancer subtypes.

NDRG1 expression at both the mRNA and protein levels increased under hypoxic conditions in all breast cancer cell lines. This suggests that NDRG1 regulation under hypoxia is primarily driven at the transcriptional level, with mRNA levels serving as a reliable reflection of protein expression. NDRG1 induction was strongly related to the amount of oxygen and the duration of hypoxia. At 1% oxygenation, NDRG1 protein exhibited a similar pattern to CAIX with a dramatic increase at 16 hours and peaking at 48 hours in all breast cancer cell lines. The results are similar to those of Li et al. who found that NDRG1 protein increased at 24 hours after the induction of hypoxia in the MCF-7 cell line (282). This is the first report of NDRG1 expression at both mRNA and protein levels at specific time points in three representative breast cancer cell lines. This suggests that NDRG1 may be a marker of chronic hypoxia in breast cancer as NDRG1 responds to hypoxia, a process known to be dependent on HIF-1α activation via HRE in the NDRG1 promoter region (232, 381, 382). Thus, NDRG1 expression could be regulated by HIF-1α in hypoxia.

HIF-1α mRNA levels did not match the protein levels. HIF-1α mRNA was suppressed, particularly in extended periods of hypoxia, while HIF-1 protein was upregulated in hypoxia in all breast cancer cell lines. The reduction in mRNA levels may be due to the binding of Repressor Element 1-Silencing Transcription factor (REST) to the HIF-1α promoter resulting in reduced HIF-1α mRNA (383). HIF-1α mRNA stability is dependent on tristetraprolin (TTP) which, in a study using endothelial cells, was found to block HIF-1α transcription at HIF-1α 3'UTR (384). Antisense HIF-1α (aHIF) has been shown to escalate mRNA degradation through uncovered AU-rich elements in the HIF-1α 3'UTR in lung cancer, lymphocytes and renal cancer cell models (385, 386). Protein levels increase rapidly between 4 -8 hours then decrease in MDA-MB-231 and MCF-7, although in SK-BR-3 cells the increase was observed up to 16 hours. These results are consistent with other studies that report that HIF-1 protein expression peaks typically around 4–8 hours and gradually decreases until undetectable around 18–24 hours (385, 387, 388). It may be that this increase in HIF-1α protein expression corresponds to acute hypoxia mediated by the negative feedback of HIF-1α mRNA in prolonged hypoxia to prevent -HIF-1α overexpression that might be harmful to cancer cells (389).

HIF-1a is unstable thus, it is not surprising that HIF-1a is not widely used as a single surrogate hypoxic marker in clinics (390). HIF-1a activates the transcription of hypoxia-targeted genes including CA9, NDRG1, PPFIA4 and VEGFA predominantly in prolonged hypoxia. HIF-1a rapidly activates transcription of those targeted genes that support cell survival during a prolonged period at low oxygen levels (391).

The limitations of this chapter are that PPFIA4 and VEGFA expression could not be validated at the protein level by western blot. Although PPFIA4 mRNA and VEGFA mRNA levels were higher in hypoxia than normoxia at different time points, the protein expression of PPFIA4 and VEGFA was not detected. For PPFIA4, this was probably due to the very low expression of PPFIA4 in breast cancer. The data from the human protein atlas showed that PPFIA4 proteins are enriched in the brain and duodenum and are not detected in breast tissue (392). Additionally, breast cancer cell lines have very low expression of PPFIA4 mRNA. Another possible cause may be the low affinity of the antibody to the PPFIA4 protein. For VEGFA, VEGFA mRNA persisted over time indicating that it was necessary for

cellular adaptation in prolonged hypoxia. However, this study could not determine a precise molecular weight for VEGFA at the protein level, as multiple bands were observed on western blots. This might be explained by poor antibody specificity.

In conclusion, this chapter demonstrates that the upregulated genes; CA9, NDRG1, PPFIA4 and VEGFA, from the ER-negative breast cancer cohort, can be induced by hypoxia in a time-dependent manner. The co-expression of CAIX and NDRG1 at both mRNA and protein levels during extended periods of hypoxia suggests a potential functional interaction in the cellular response, where they may modulate the activity of each other.Thus, NDRG1 is a candidate gene for further analysis to further elucidate its actions in breast cancer biology.

Chapter 5 : Expression of NDRG1 in the Glasgow breast cancer cohort

5.1 Introduction

The previous chapter demonstrated that NDRG1 is related to hypoxia signature genes and is expressed under hypoxic conditions. The TCGA was initially used to explore the importance of NDRG1 in breast cancer patients. The results showed that high NDRG1 mRNA predicted significantly worse OS (HR=1.4, 95%CI; 1.16-1.69, log-rank p=0.00046) and RFS (HR=1.42, 95%CI; 1.28-1.57, log-rank p=1.6e-11). This suggested a prognostic role for NDRG1 in breast cancer.

A potential prognostic role for NDGR1 is controversial and differs between different types of cancer. While high NDRG1 predicted poor prognosis in lung and gynaecologic malignancies, it becomes a protective factor in urogenital, colorectal and brain cancers. In breast cancer, early studies reported that NDRG1 had an inverse correlation with lymph node and bone metastasis(393). Survival analysis in 85 breast cancer patients revealed that those with high NDRG1 expression had better 5-year disease-free survival (DFS) compared to the low NDRG1 expression group (393). In contrast, in inflammatory breast cancer, which is the most aggressive form of breast cancer, it was found that NDRG1 expression related to poor OS and DFS (394). Lopez-Tejada et al reported that in TNBC patients, OS was inferior in those with high NDRG1 (297). Thus, NDRG1 predicts prognosis differently depending on the cancer type and location.

This chapter aimed to investigate the prognostic role of NDRG1 in the Glasgow breast cancer cohort, which includes all breast cancer subtypes. NDRG1 protein expression was assessed using immunohistochemistry (IHC) on tissue microarrays (TMA) to evaluate its correlation with clinicopathological factors and survival outcomes. Additionally, transcriptomic analysis was performed to explore gene expression patterns related to NDRG1.

Antibody specificity was determined by western blot and cell pellet analysis, comparing normoxic and hypoxic conditions, as well as NDRG1 overexpression and knockdown models. Transcriptomic data from bulk RNA sequencing (TempO-Seq®) were reanalysed to identify differentially expressed genes associated with high and low NDRG1 expression using DESeq2 in R.

5.2 NDGR1 antibody specificity

Cell pellets and western blotting were used to determine antibody specificity. NDRG1 expression was compared between hypoxia and normoxia. The MDA-MB-231 cell line was cultured in both 1% O_2 and 20% O_2 for up to 48 hours to activate the expression of NDRG1 before preparing cell pellets and lysates.

A single band of predicted size (46 kDa) was observed when MDA-MB-231 cell lysates were run on a western blot and probed with anti-NDRG1. Expression increased in hypoxia for the prolonged incubated time. NDRG1 was silenced under hypoxic conditions for 48 hours, resulting in a significant reduction in NDRG1 protein expression compared to the scramble control (SC) and the hypoxic cell culture control (Ct) (**Figure 5.1 A**). IHC was performed on MDA-MB-231 pellets and the hypoxic cell pellet had a higher intensity of cytoplasmic staining than the normoxic cell pellet. NDRG1 expression was predominantly in the cytoplasm rather than nucleus or membrane indicating that its functions are in the cytoplasm (**Figure 5.1 B**).

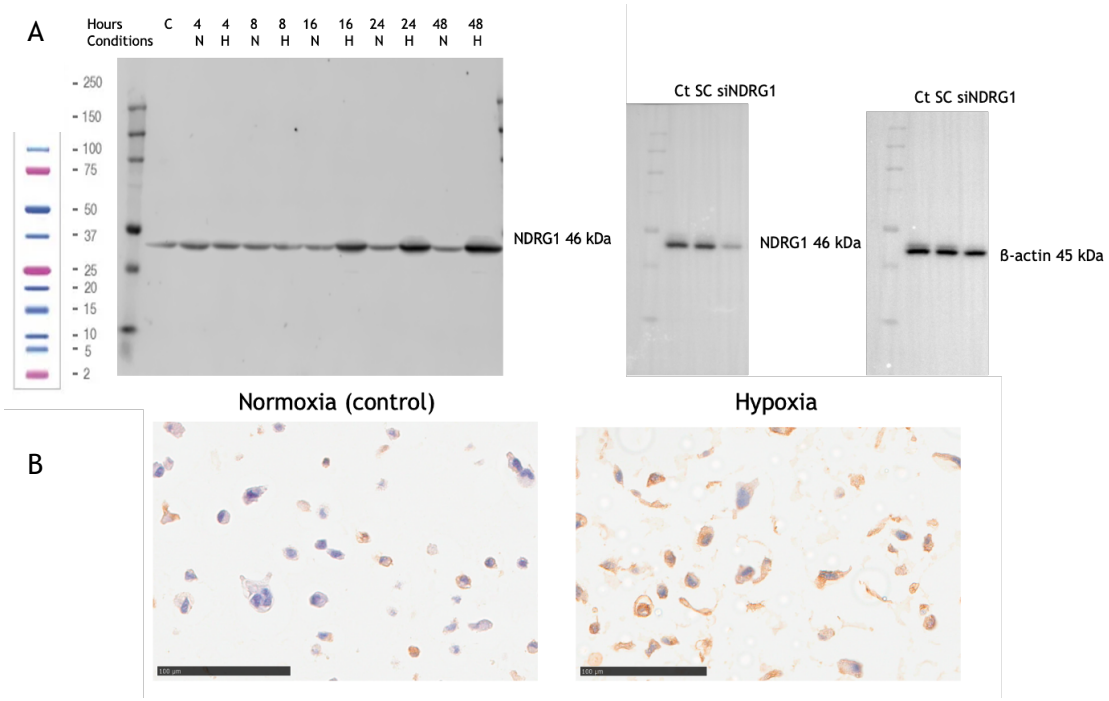

Figure 5.1-NDGR1 antibody specificity (A) Single band of the expected size (46 kDa) was observed in MDA-MB-231 cell lysates under both hypoxic and normoxic conditions. Lysates from siNDRG1-treated MDA-MB-231 cells showed reduced expression compared to both the hypoxic and scrambled controls. ß-Actin was used as a loading control. (B) Cell pellets prepared under hypoxic and normoxic conditions were stained with an NDRG1 antibody. Hypoxic pellets showed stronger cytoplasmic staining compared to normoxic pellets.*Ct, hypoxic cell culture control; SC, scramble control

5.3 Expression and clinical outcomes of NDRG1 in the Glasgow breast cancer cohort

This study followed the main criteria for REMARK **(395)**. The Glasgow breast cohort is comprised of tissue from 850 invasive breast cancer collected between 1980 and 1998. After excluding patients with missing TMA cores, 435 patients remained. Clinicopathological variables included age, tumour size, histologic grade, ER status, PR status, HER2 status, and nodal metastasis status were available. The diagram of eligible patients is illustrated in **Figure 5.2**.

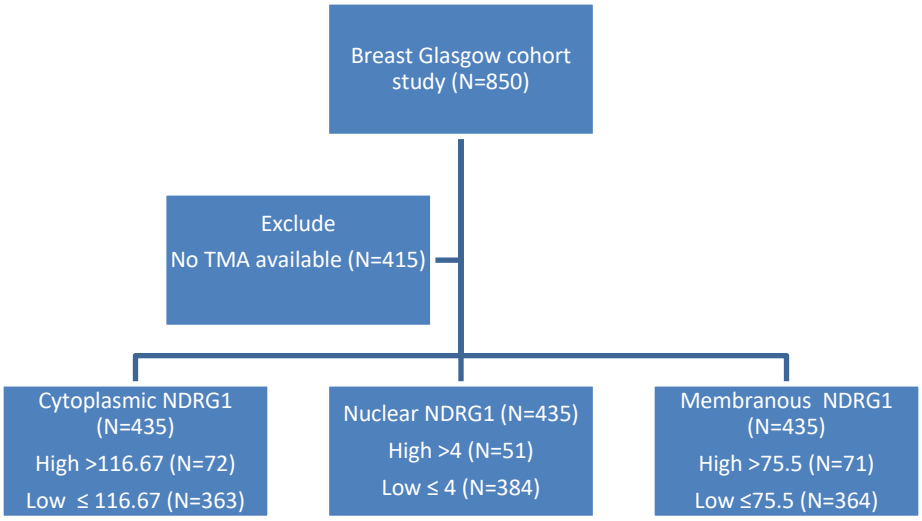

Figure 5.2-Consort diagram showing the number of patients included in the analysis for different cellular compartments

Patients were mostly diagnosed after 50 years of age (69.2%) and histologically, most were invasive ductal cancers (90.3%). Over 50% of patients had T1 lesions; 234 patients (53.8%) followed by T2; 168 patients (38.6%) and T3; 33 patients (7.6%). The proportion of grade II was the highest, with 206 patients (47.4%) followed by grade III with 138 patients (31.7%) and grade I with 91 patients (20.9%). Lymph node metastasis was present in 188 patients (43.2%). The majority of patients were ER-positive (78.9%), PR-positive (55.2%), HER-2 negative (80%) and had low Ki-67 (61.8%). Luminal subtypes were the most commonly diagnosis, luminal A (47.4%) and luminal B (29%), followed by TNBC (11.0%) and HER-2 enriched (8.9%). Adjuvant endocrine therapy was given to 321 patients (73.8%), chemotherapy to 165 patients (37.9%) and radiation was given to 187 patients (43.0%). Two hundred thirty-nine (54.9%) patients were alive, and 336 patients (77.2%) had no recurrence. The median CSS survival was 176 months (range 1-180 months) (**Table 5.1**).

Table 5.1-Clinicopathological characteristics of the whole Glasgow breast cancer cohort who achieve NDRG1 staining

Clinicopathological factors	All breast cancer subtypes (N=435)
Age, yr	
≤50	134 (30.8%)
>50	301 (69.2%)
Histological types	
Ductal	393 (90.3%)
Lobular	27 (6.2%)
Other	15 (3.4%)
Tumour size, mm	
≤20	234 (53.8%)
>20-50	168 (38.6%)
>50	33 (7.6%)
Tumour grade	
I	91 (20.9%)
II	206 (47.4%)
III	138 (31.7%)
Nodal involvement	
No	240 (55.2%)
Yes	188 (43.2%)
NA	7 (1.6%)
ER status	
Negative (<1%)	91 (20.9%)
Positive (≥1%)	434 (78.9%)
NA	1 (0.2%)
PR status	
Negative (<1%)	194 (44.6%)
Positive (≥1%)	240 (55.2%)
NA	1 (0.2%)
HER-2 status	
Negative	348 (80%)
Positive	79 (18.2%)
NA	8 (1.8%)
Ki-67	
≤14%	269 (61.8%)
<14%	150 (34.5%)
NA	16 (3.7%)
Breast cancer subtypes	
Luminal A	206 (47.4%)
Luminal B	126 (29%)
HER-2 enriched	36 (8.3%)
TNBC	48 (11.0%)
NA	19 (4.4%)
Adjuvant endocrine treatment	
No	43 (9.9%)
Yes	321 (73.8%)
NA	71 (16.3%)
Adjuvant chemotherapy	
No	268 (61.6%)
Yes	165 (37.9%)
NA	2 (0.5%)
Adjuvant radiation	
No	246 (56.6%)
Yes	187 (43.0%)
NA	2 (0.5%)
Status	
Alive	239 (54.9%)
Breast cancer related death	88 (20.2%)
Non breast cancer related death	85 (19.5%)
NA	23 (5.3%)
Recurrence status	
No	336 (77.2%)
Local	21 (4.8%)
Distant	58 (13.3%)
Both local and distant	6 (1.4%)
NA	14 (3.2%)

The weighted histoscore for NDRG1 for each cellular compartment (membrane, cytoplasm and nucleus) was determined **(Figure 5.3**). NDRG1 showed no staining in the membrane for 190 patients (43.67%), in the cytoplasm for 145 patients (33.33%), and in the nucleus for 349 patients (80.23%). The median weighted histoscore for membrane was 2.5 (IQ=0,50.00, min-max=0-275) and for cytoplasm was 31 (IQ=0,100, min-max=0-208). Nuclear staining was rarely observed, with 349 samples of the specimens being negative, this resulted in the median score being 0 (IQ=0,0, min-max=0-295). For all cellular locations there was a good correlation between observers with an ICCC score of 0.929 for nuclear expression (WN and JQ), 0.882 for cytoplasmic expression and 0.855 for membranous expression (WN and KP). Bland Altman and scatter plots were also constructed to confirm that the score was not biased between scorers; membrane (p=0.123) ,cytoplasm (p=0.245), and nucleus (p=0.10), respectively (**Figure 5.4 B-D**). The cut-point was determined by R package using "survminer" which can maximise log-rank statistics to select the optimal cut-point for continuous variables. The cut-point for membranous NDRG1 was 75.5 ,cytoplasmic NDRG1 was 116.67, and nuclear NDRG1 was 4 (**Figure 5.4 B-D**).

A

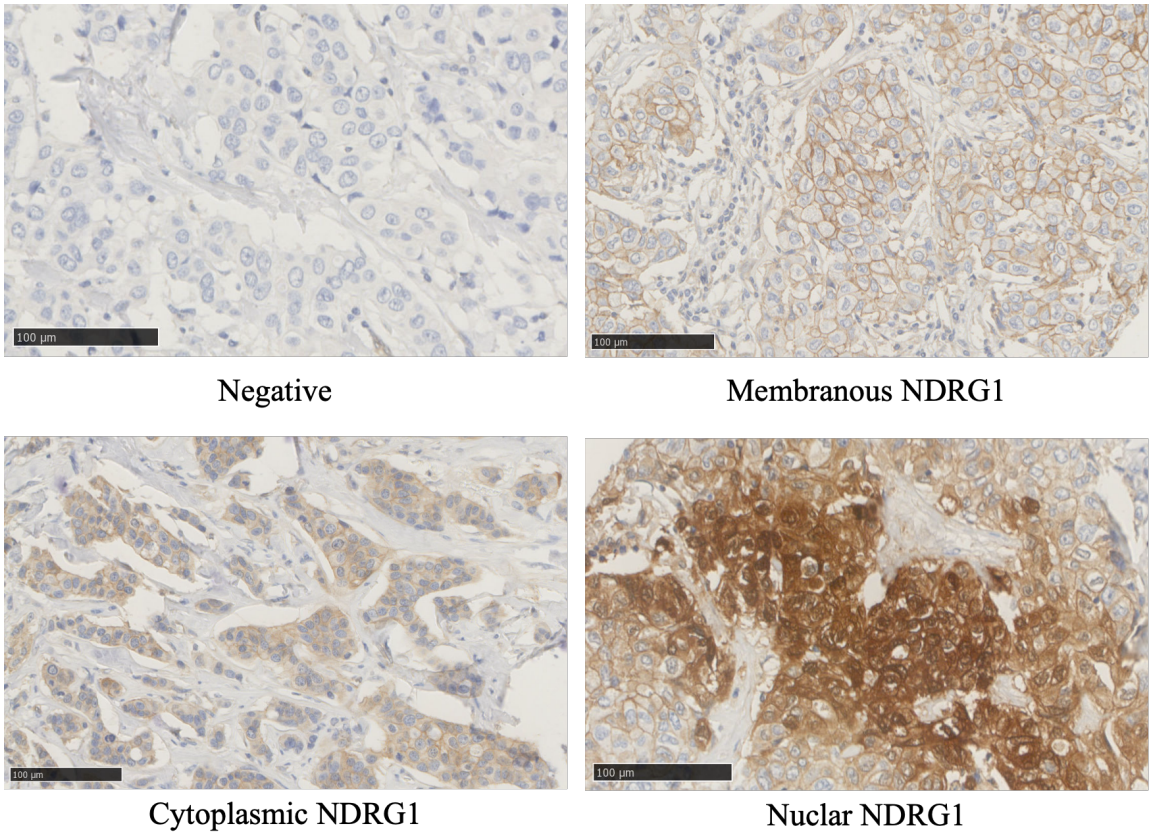

Figure 5.3-Representative image of NDRG1 expression showing its subcellular localisation (images captured at 20x magnification with 100 µm scale bar).

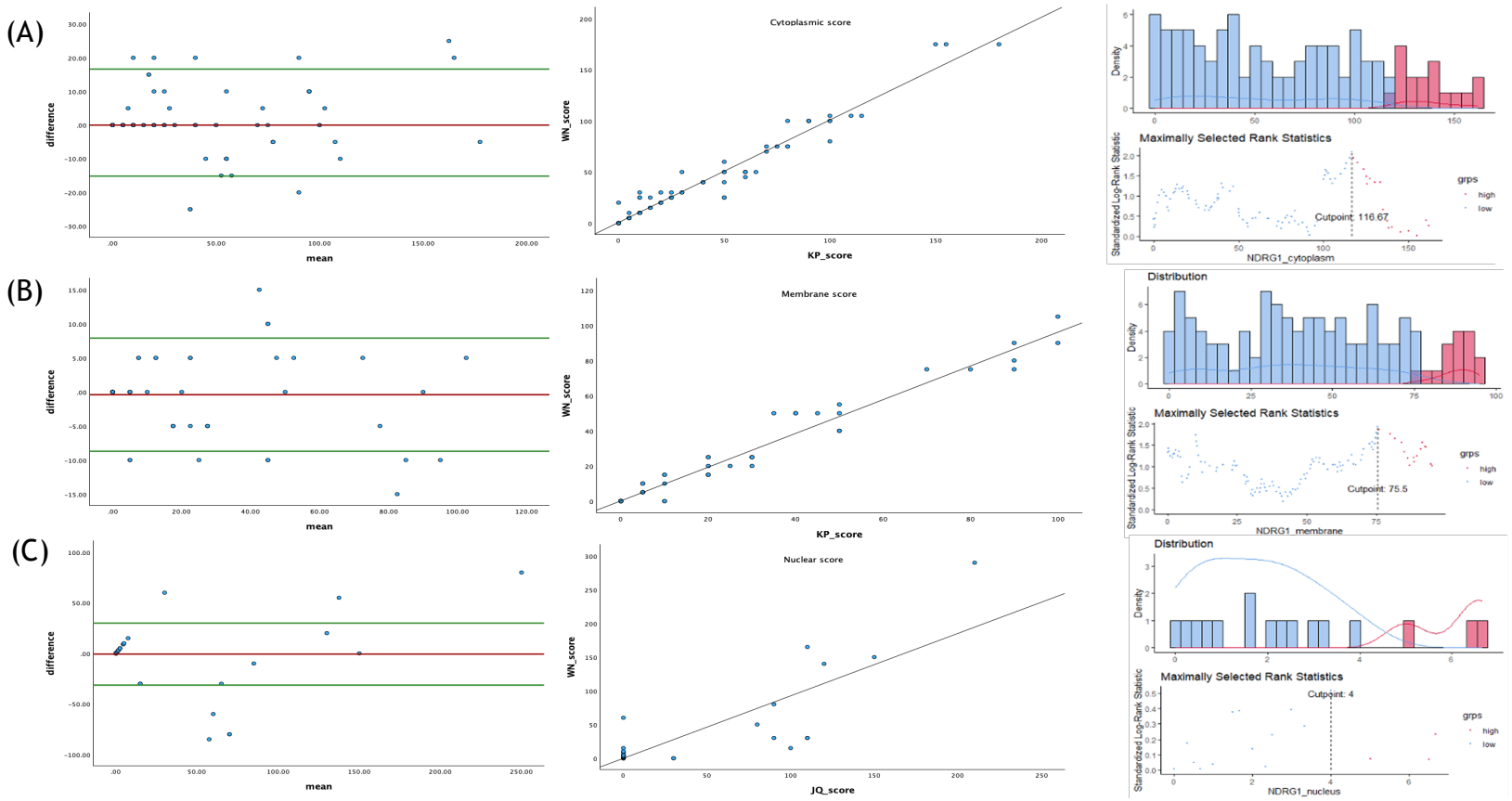

Figure 5.4- The Bland Altman plot, scatter plot and the cut-point of cytoplasmic NDRG1 (A), membranous NDRG1 (B) and nuclear NDRG1 (C), respectively

5.3.1 NDGR1 status and clinicopathological factors

The correlation between cytoplasmic NDRG1 status and clinicopathological characteristics was analysed using the Chi-square test and showed a significant statistical difference with tumour grade ($p < 0.001$) and molecular subtypes ($p < 0.001$) (**Table 5.2**).

Table 5.2-Cytoplasmic NDRG1 expression in the whole Glasgow breast cancer cohort

Clinicopathological factors	**Cytoplasmic NDRG1 expression**		**p-value**
	Low	**High**	
Age, yr ≤50 >50	 115 (85.8%) 248 (82.4%)	 19 (14.2%) 53 (17.6%)	0.374
Tumour size, mm ≤20 >20-50 >50	 199 (85.0%) 137 (81.5%) 27 (81.8%)	 35 (15.0%) 31 (18.5%) 6 (18.2%)	0.627
Tumour grade I II III	 85 (93.4%) 178 (86.4%) 100 (72.5%)	 6 (6.6%) 28 (13.6%) 38 (27.5%)	<0.001
Nodal involvement No Yes	 201 (83.8%) 156 (83.0%)	 39 (16.2%) 32 (17.0%)	0.965
Lymphoinvasion No Yes	 143 (88.3%) 73 (82.0%)	 19 (11.7%) 16 (18.0%)	0.172
Molecular subtypes Luminal A Luminal B HER-2 enriched TNBC	 188 (91.3%) 103 (81.7%) 26 (72.2%) 28 (58.3%)	 18 (8.7%) 23 (18.3%) 10 (27.8%) 20 (41.7%)	<0.001
Chemotherapy treatment No Yes	 223 (83.2%) 138 (83.6%)	 45 (16.8%) 27 (16.4%)	0.691
Radiation No yes	 198 (80.5%) 163 (87.3%)	 48 (19.5%) 24 (12.8%)	0.444

Nuclear NDRG1 was similarly significantly associated with tumour grade ($p < 0.001$) and molecular subtypes ($p < 0.001$) (**Table 5.3**).

Table 5.3-Nuclear NDRG1 expression in the whole Glasgow breast cancer cohort

Clinicopathological factors	Nuclear NDRG1 expression		p-value
	Low	High	
Age, yr ≤50 >50	 120 (89.6%) 264 (87.7%)	 14 (10.4%) 37 (12.3%)	0.581
Tumour size, mm ≤20 >20-50 >50	 212 (90.6%) 143 (85.1%) 29 (87.9%)	 22 (9.4%) 25 (14.9%) 4 (12.1%)	0.245
Tumour grade I II III	 85 (93.4%) 191 (92.7%) 108 (78.3%)	 6 (6.6%) 15 (7.3%) 30 (21.7%)	<0.001
Nodal status Negative Positive	 210 (87.5%) 168 (89.4%)	 30 (12.5%) 20 (10.6%)	0.819
Lymphoinvasion No Yes	 146 (90.1%) 80 (89.9%)	 16 (9.9%) 9 (10.1%)	0.285
Molecular subtypes Luminal A Luminal B HER2 enriched TNBC	 193 (93.7%) 109 (86.5%) 32 (88.9%) 33 (68.8%)	 13 (6.3%) 17 (13.5%) 4 (11.1%) 15 (31.3%)	<0.001
Chemotherapy treatment No Yes	 233 (86.9%) 149 (90.3%)	 35 (13.1%) 16 (9.7%)	0.441
Radiation No yes	 211 (85.8%) 171 (85.8%)	 35 (14.2%) 16 (14.2%)	0.143

In contrast, membranous NDRG1 was significantly related to nodal status ($p < 0.001$) (**Table 5.4**).

Table 5.4-Membranous NDRG1 expression in the whole Glasgow breast cancer cohort

Clinicopathological factors	Membranous NDRG1 expression		p-value
	Low	High	
Age, yr			
≤50	112 (84.8%)	20 (15.2%)	0.653
>50	251 (83.1%)	51 (16.9%)	
Tumour size, mm			
≤20	201 (83.8%)	39 (16.2%)	0.976
>20-50	139 (83.7%)	27 (16.3%)	
>50	23 (82.1%)	5 (17.9%)	
Tumour grade			
I	74 (82.2%)	16 (17.8%)	0.684
II	179 (85.2%)	31 (14.8%)	
III	110 (82.1%)	24 (17.9%)	
Nodal status			
Negative	177 (74.7%)	60 (25.3%)	<0.001
Positive	182 (95.8%)	8 (4.2%)	
Lymphoinvasion			
No	132 (80.0%)	33 (20.0%)	0.285
Yes	71 (85.5%)	12 (14.5%)	
Molecular subtypes			
Luminal A	172 (82.3%)	37 (17.7%)	0.422
Luminal B	104 (87.4%)	15 (12.6%)	
HER2 enriched	28 (77.8%)	8 (22.2%)	
TNBC	39 (79.6%)	10 (20.4%)	
Chemotherapy treatment			
No	222 (82.2%)	48 (17.8%)	0.432
Yes	139 (85.8%)	23 (14.2%)	
Radiation			
No	205 (81.0%)	48 (19.0%)	0.162
yes	156 (87.2%)	23 (12.8%)	

5.3.2 Combined cytoplasmic and membrane NDRG1 score is an independent factor for DFS

The Kaplan-Meier curve showed that patients with high cytoplasmic -high membranous NDRG1 had significantly lower CSS but not OS compared to the low cytoplasmic-low membranous NDRG1 group (HR = 1.945, 95% CI: 1.096-3.451, p = 0.022) (**Figure 5.5**).

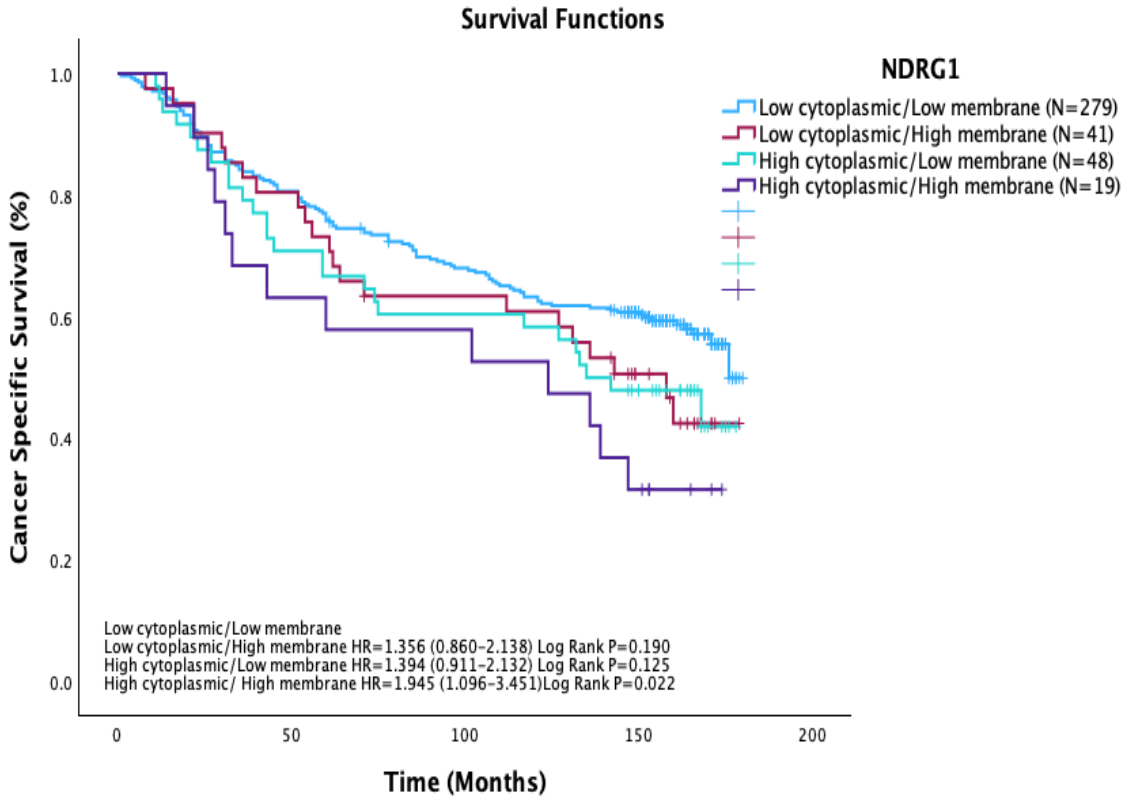

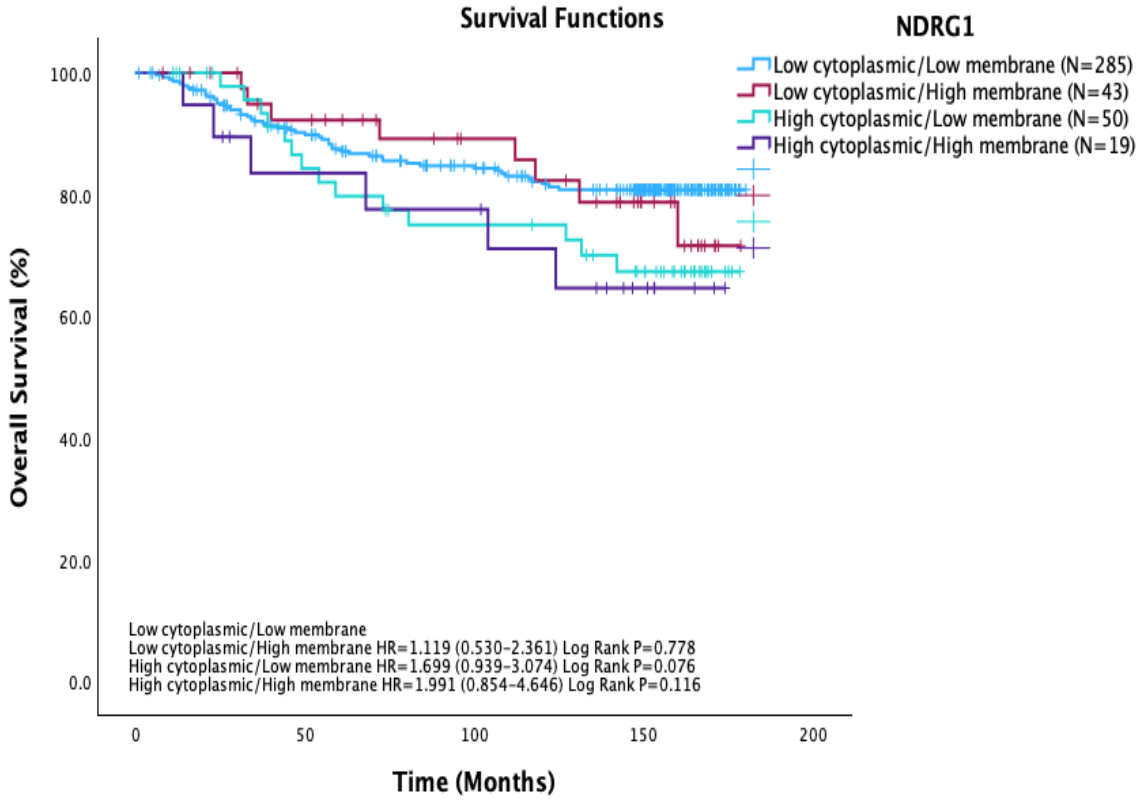

Figure 5.5-(A) Cancer-specific survival and (B) Overall survival for combined cytoplasmic and membranous NDRG1 expression

In univariate analysis for CSS, older than 50 years old, larger tumour size > 2 cm, positive lymph node metastasis, non-luminal A subtypes and both high cytoplasmic-nuclear NDRG1 were associated with poorer CSS. In multivariate analysis, age, tumour size > 5 cm, positive nodal metastasis, HER2-overexpression subtype and low cytoplasmic-high membranous NDRG1 were independent prognostic factors for CSS (**Table 5.5**). However, the combination of cytoplasmic and membranous NDRG1 did not affect OS either in univariate or multivariate analysis (**Table 5.6**).

Table 5.5-Univariate and multivariate analysis of combined cytoplasmic and membranous NDRG1 and clinicopathological factors in the Glasgow breast cancer cohort for CSS

Clinicopathological factors	Univariate CSS			Multivariate CSS		
	HR	CI	p-value	HR	CI	p-value
Age (≤50 vs 50) (N=129 vs 287)	1.693	1.205-2.397	0.002	1.879	1.295-2.728	<0.001
Tumour size, mm ≤20 (N=222) >20-50 (N=162) >50 (N=32)	 1 1.520 2.260	 1.125-2.054 1.400-3.647	 0.006 <0.001	 1 1.176 2.334	 0.845-1.638 1.361-4.000	 0.337 0.002
Tumour grade I (N=85) II (N=199) III (N=132)	 1 0.940 1.347	 0.641-1.379 0.906-2.001	 0.752 1.141			
Nodal involvement (Positive vs negative) (N=180 vs 229)	1.919	1.435-2.565	<0.001	2.176	1.538-3.077	<0.001
Breast cancer subtypes Luminal A (N=194) Luminal B (N=122) HER-2 enriched (N=35) TNBC (N=48)	 1 1.663 2.298 1.675	 1.187-2.330 1.424-3.707 1.070-2.623	 0.003 <0.001 0.024	 1 1.365 1.838 1.549	 0.955-1.949 1.118-3.023 0.949-2.530	 0.088 0.016 0.080
Combined cytoplasmic and membrane NDRG1 -Both-low (N=279) -Low cytoplasmic/High membrane (N=41) -High cytoplasmic/Low membrane (N=48) -Both-high (N=19)	 1 1.356 1.394 1.945	 0.860-2.138 0.911-2.132 1.096-3.451	 0.191 0.126 0.023	 1 1.935 1.255 1.679	 1.173-3.192 0.799-1.971 0.905-3.115	 0.010 0.325 0.100

Table 5.6-Univariate and multivariate analysis of combined cytoplasmic and membranous NDRG1 and clinicopathological factors in the Glasgow breast cancer cohort for OS

Clinicopathological factors	Univariate OS			Multivariate OS		
	HR	CI	p-value	HR	CI	p-value
Age (≤50 vs 50) (N=133 vs 293)	1.173	0.742-1.855	0.495			
Tumour size, mm ≤20 (N-228) >20-50 (N=166) >50 (N=32)	 1 1.897 4.519	 1.194-3.012 2.446-8.350	 0.007 <0.001	 1 1.357 3.337	 0.839-2.196 1.748-6.371	 0.214 <0.001
Tumour grade I (N=87) II (N=203) III (N=136)	 1 1.354 2.740	 0.688-2.666 1.410-5.322	 0.381 0.003	 1 0.992 1.463	 0.481-2.047 0.681-3.141	 0.983 0.329
Nodal involvement (Positive vs negative) (N=185 vs 234)	2.988	1.915-4.662	<0.001	2.564	1.614-4.071	<0.001
Breast cancer subtypes Luminal A (N=199) Luminal B (N=125) HER-2 enriched (N=36) TNBC (N=48)	 1 2.293 2.900 2.957	 1.371-3.835 1.432-5.873 1.586-5.513	 0.002 0.003 <0.001	 1 2.109 3.097 2.877	 1.259-3.534 1.517-6.319 1.541-5.373	 0.005 0.002 <0.001
Combined cytoplasmic and membrane NDRG1 -Both-low (N=285) -Low cytoplasmic/High membrane (N=43) -High cytoplasmic/Low membrane (N=50) Both-high (N=19)	 1 1.119 1.699 1.991	 0.530-2.361 0.939-3.074 0.854-4.646	 0.768 0.080 0.111			

Individual cellular localisation was assessed separately, but the findings were largely insignificant and are summarised briefly here. To determine NDRG1 association with clinical outcomes, Kaplan-Meier survival analysis was performed. High and low NDRG1 expression were compared by log-rank test. High cytoplasmic NDRG1 resulted in poorer CSS when compared to low cytoplasmic NDRG1 (HR = 1.542, 95% CI: 1.092-2.179, p = 0.013), however, no significant difference was observed for nuclear NDRG1 (HR = 0.915, 95% CI: 0.581-1.440, p = 0.701) or membranous NDRG1 (HR = 1.404, 95% CI: 0.987-1.997, p = 0.059) (**Figure 5.6**).

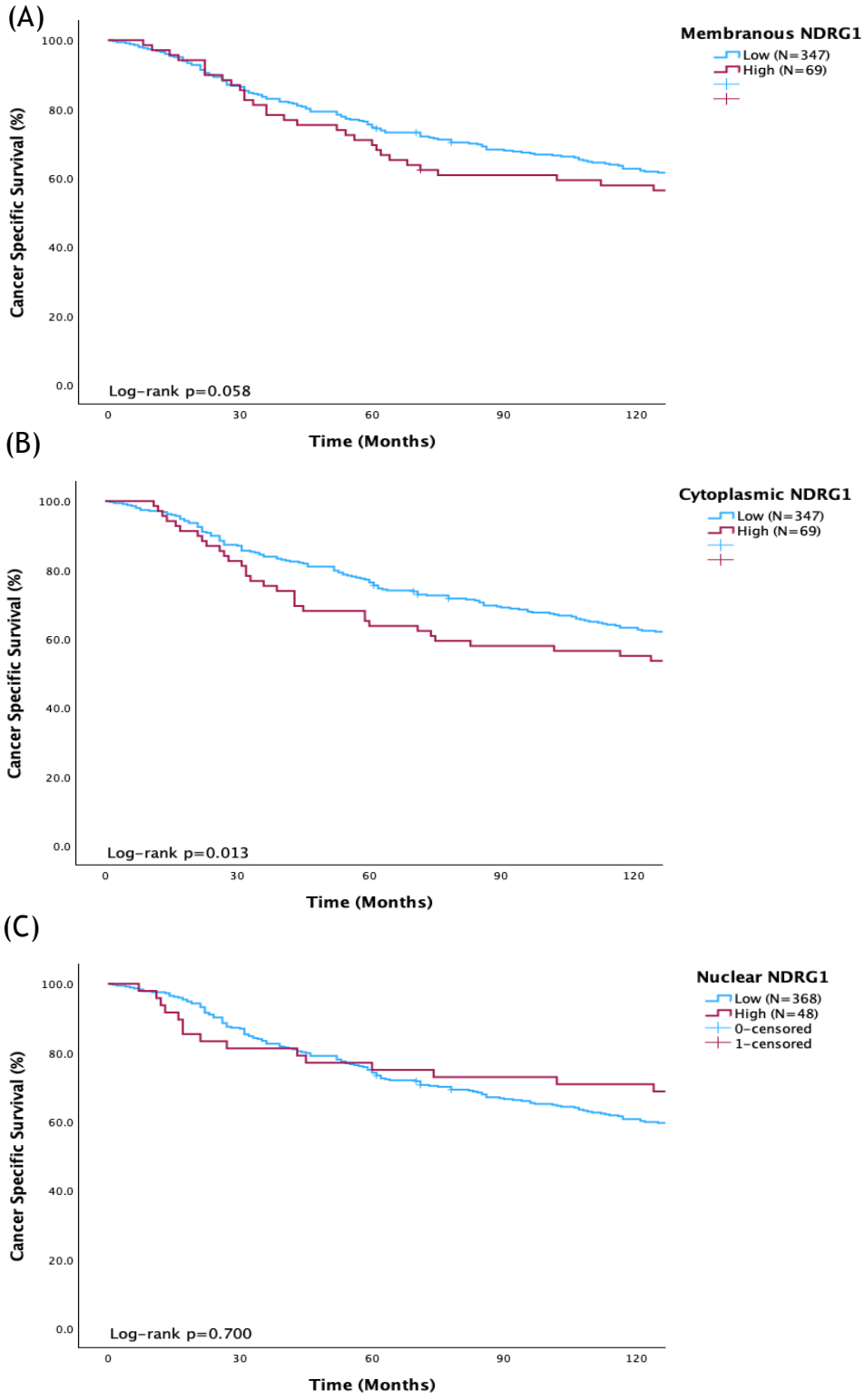

Figure 5.6-Cancer-specific survival at each cellular location for NDRG1 staining (A) membrane NDRG1, (B) cytoplasmic NDRG1 and (C) nuclear NDRG1

High cytoplasmic NDRG1 status was also significantly associated with inferior OS compared to low cytoplasmic NDRG1 (HR = 1.712, 95% CI: 1.049-2.795, p = 0.032) and there was no significant correlation between nuclear NDRG1 or membranous NDRG1 with OS (**Figure 5.7**).

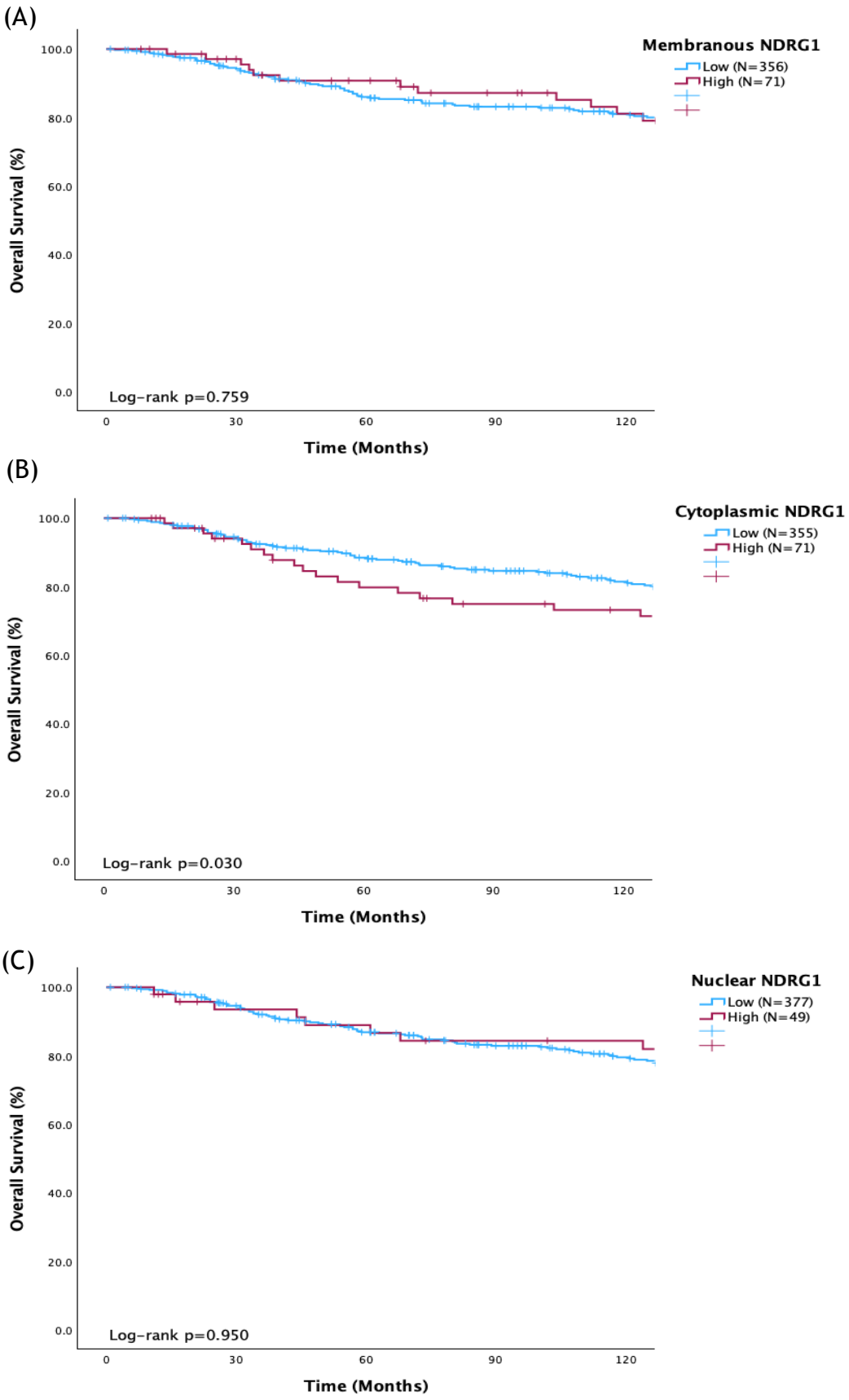

Figure 5.7-Overall survival at each cellular location for NDRG1 staining (A) membranous NDRG1, (B) cytoplasmic NDRG1 and (C) nuclear NDRG1

As only cytoplasmic NDRG1 appeared to predict breast cancer prognosis, its significance was assessed based on different breast cancer molecular subtypes. However, the findings suggested that cytoplasmic NDRG1 could not differentiate prognosis in any specific subtype for either CSS or OS; luminal A (log-rank p = 0.619 and 0.362), luminal B (log-rank p = 0.474 and 0.629), TNBC (log-rank p = 0.497 and 0.464) and HER-2 enriched (log-rank p = 0.120 and 0.123) (**Figure 5.8 and Figure 5.9**).

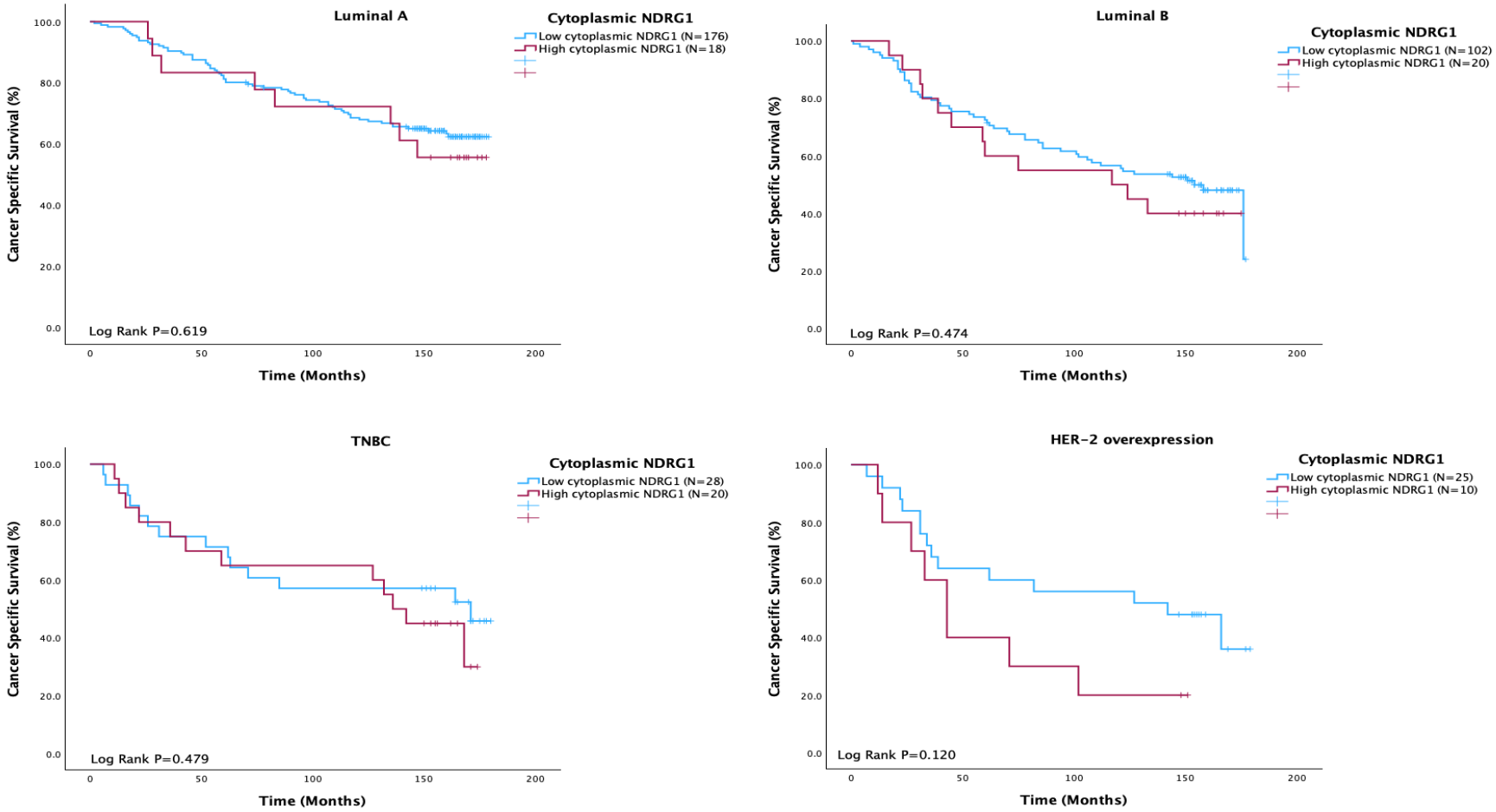

Figure 5.8-The CSS plots by breast molecular subtype, stratified by cytoplasmic NDRG1 expression

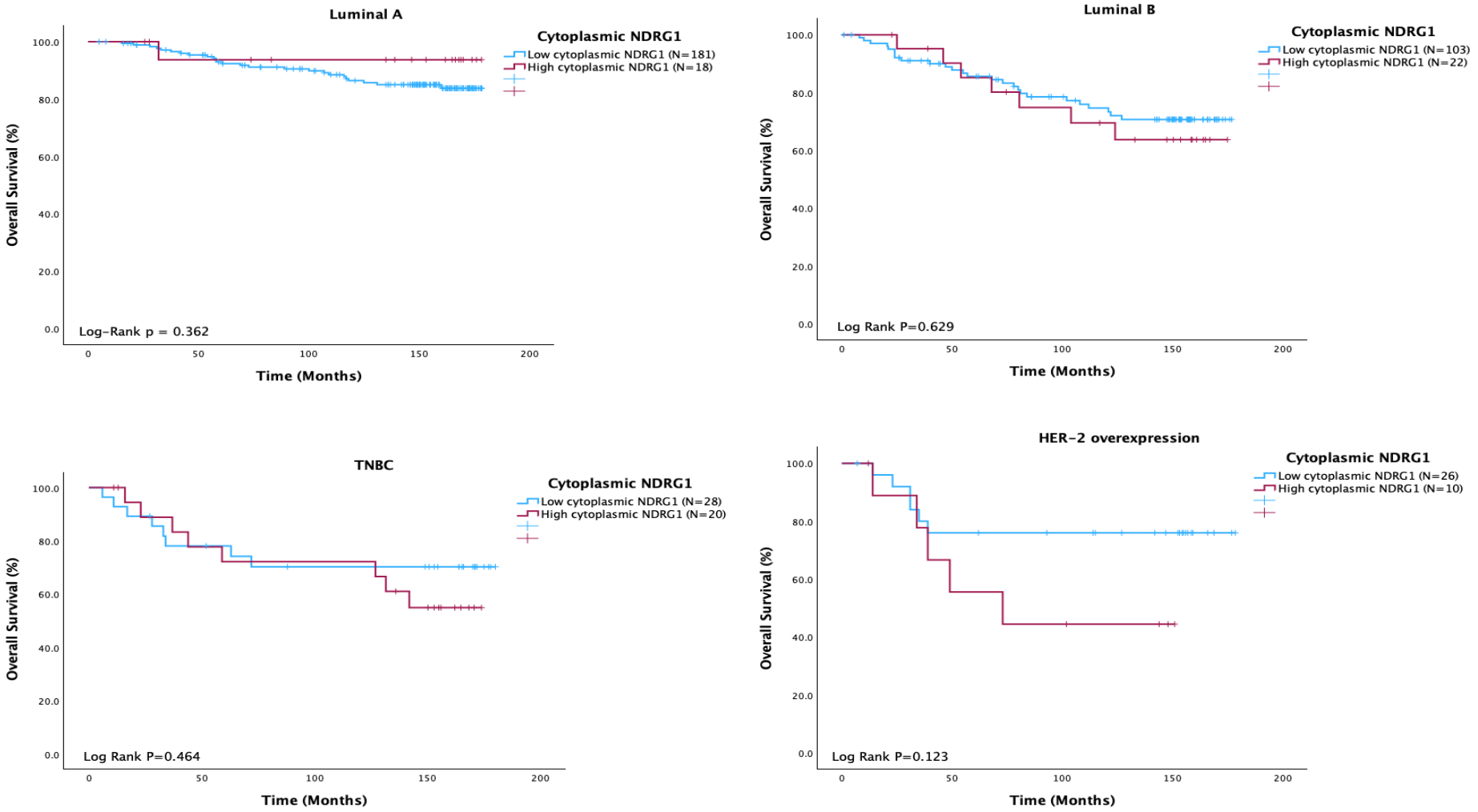

Figure 5.9- The OS plots by breast molecular subtype, stratified by cytoplasmic NDRG1 expression

Additionally, NDRG1 expression did not significantly impact survival outcomes within the ER subgroups (**Figure 5.10**). In the ER-positive subgroup, there was no significant difference in CSS (log-rank p = 0.206) or OS (log-rank p = 0.765). Similarly, in the ER-negative subgroup, the association with CSS (log-rank p = 0.108) and OS (log-rank p = 0.057) was not statistically significant.

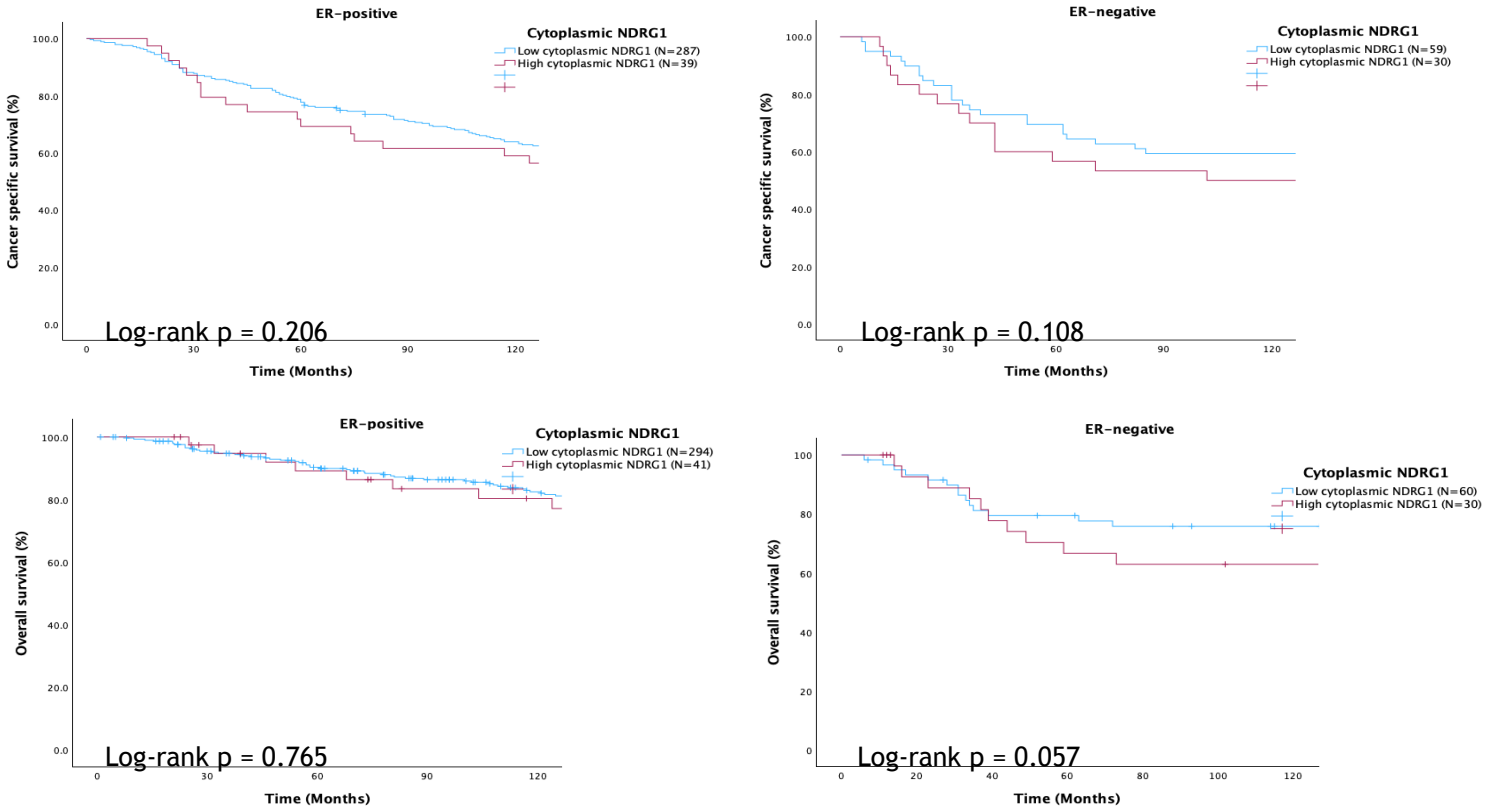

Figure 5.10-Kaplan-Meir survival plots for cytoplasmic NDGR1 expression and ER-expression (A) CSS and (B) OS.

In univariate analysis for CSS, older ≥ 50 years (HR = 1.693, 95% CI: 1.205-2.397, p = 0.002), tumour size > 2 cm (HR = 1.520, 95% CI: 1.125-2.054, p = 0.006), positive nodal metastasis (HR = 1.919, 95% CI: 1.435-2.565, p < 0.001), non-luminal A subtype, and high cytoplasmic NDRG1 (HR = 1.542, 95% CI: 1.092-2.179, p = 0.014) were related to poorer CSS. However, in multivariate analysis, age, tumour size, nodal status, and molecular subtypes were independent prognostic factors for CSS (**Table 5.7**).

Table 5.7-Univariate and multivariate analysis of NDRG1 and clinicopathological factors in the Glasgow breast cancer cohort for CSS

Clinicopathological factors	Univariate CSS			Multivariate CSS		
	HR	CI	p-value	HR	CI	p-value
Age (≤50 vs 50) (N=129 vs 287)	1.693	1.205-2.397	0.002	1.893	1.320-2.716	<0.001
Tumour size, mm ≤20 (N=222) >20-50 (N=162) >50 (N=32)	 1 1.520 2.260	 1.125-2.054 1.400-3.647	 0.006 <0.001	 1 1.250 2.088	 0.907-1.721 1.264-3.448	 0.172 0.004
Tumour grade I (N=85) II (N=199) III (N=132)	 1 0.940 1.347	 0.641-1.379 0.906-2.001	 0.752 1.141			
Nodal involvement (Positive vs negative) (N=180 vs 229)	1.919	1.435-2.565	<0.001	1.846	1.357-2.511	<0.001
Breast cancer subtypes Luminal A (N=194) Luminal B (N=122) HER-2 enriched (N=35) TNBC (N=48)	 1 1.663 2.298 1.675	 1.187-2.330 1.424-3.707 1.070-2.623	 0.003 <0.001 0.024	 1 1.530 2.059 1.864	 1.088-2.151 1.264-3.355 1.181-2.940	 0.014 0.004 0.007
Cytoplasmic NDRG1 (High vs Low) (N=69 vs 347)	1.542	1.092-2.179	0.014	1.292	0.886-1.885	0.183
Membranous NDRG1 (High vs Low) (N=69 vs 347)	1.404	0.987-1.997	0.059			
Nucleus NDRG1 (High vs Low) (N=48 vs 368)	0.915	0.581-1.440	0.701			

Univariate analysis for OS demonstrated that tumour size > 2cm (HR = 1.897, 95% CI: 1.194-3.012, p = 0.007), grade III tumour (HR = 2.740, 95% CI: 1.410-5.322, p = 0.003), positive nodal metastasis (HR = 2.988, 95% CI: 1.915-4.662, p < 0.001), non-luminal A subtypes and cytoplasmic NDRG1(HR = 1.712, 95% CI: 1.049-2.795, p = 0.032) were associated with unfavourable OS (**Table 5.8**). In

multivariate analysis, the independent prognostic factors were tumour size > 5 cm, positive nodal status and non-luminal A subtypes (**Table 5.8**).

Table 5.8-Univariate and multivariate analysis of NDRG1 and clinicopathological factors in the Glasgow breast cancer cohort for OS

Clinicopathological factors	Univariate OS			Multivariate OS		
	HR	CI	p-value	HR	CI	p-value
Age (≤50 vs 50) (N=133 vs 293)	1.173	0.742-1.855	0.495			
Tumour size, mm ≤20 (N-228) >20-50 (N=166) >50 (N=32)	 1 1.897 4.519	 1.194-3.012 2.446-8.350	 0.007 <0.001	 1 1.357 3.337	 0.839-2.196 1.748-6.371	 0.214 <0.001
Tumour grade I (N=87) II (N=203) III (N=136)	 1 1.354 2.740	 0.688-2.666 1.410-5.322	 0.381 0.003	 1 0.992 1.463	 0.481-2.047 0.681-3.141	 0.983 0.329
Nodal involvement (Positive vs negative) (N=185 vs 234)	2.988	1.915-4.662	<0.001	2.564	1.614-4.071	<0.001
Breast cancer subtypes Luminal A (N=199) Luminal B (N=125) HER-2 enriched (N=36) TNBC (N=48)	 1 2.293 2.900 2.957	 1.371-3.835 1.432-5.873 1.586-5.513	 0.002 0.003 <0.001	 1 2.109 3.097 2.877	 1.259-3.534 1.517-6.319 1.541-5.373	 0.005 0.002 <0.001
Cytoplasmic NDRG1 (High vs Low) (N=71 vs 355)	1.712	1.049-2.795	0.032	1.441	0.851-2.440	0.174
Membranous NDRG1 (High vs Low) (N=71 vs 356)	0.914	0.514-1.625	0.759			
Nucleus NDRG1 (High vs Low) (N=49 vs 377)	0.979	0.507-1.892	0.950			

5.4 Gene signatures associated with high and low NDRG1

To further understand NDRG1 function, transcriptomic data using bulk RNA seq (TempO-Seq®) was reanalysed. The DESeq2 package was used to determine differential gene expression between high versus low NDRG1 expression in each molecular subtype (**Table 5.9**). There was no gene overlap between each molecular subtype for either upregulated or downregulated genes. However, the TNBC subtype carried upregulated *NDRG1* and this suggests that NDRG1 is more likely to play a role in mediating TNBC as compared to other subtypes.

Table 5.9-The signature genes associated with high versus low NDRG1 expression in each breast cancer molecular subtype

Molecular Subtypes	Upregulated genes	Downregulated genes
Luminal A	ERBB2	FGF14, IGHV2-70D, IGHV3-74, CPB1, KRT5, KRT14, TPH1, IGKV4-1, TAT, IGLV3-9, IL9, PRR33, ALX4, OR10Z1, DUSP15, IGKC
Luminal B		IGLV4-60, COL17A1, PXDNL, CYSRT1
HER2 enriched	LGALS12	IL5, KRT10, SIX5, ANXA6, PTH2R
TNBC	NDRG1, MUCL1, NFASC, SGK2	TVP23B, TAS2R4, IDO1, CST1, ABCC11, CCN5, TOX3, TRAF3IP1, LRRC1, CST4, BNIPL, CEACAM6

To enhance sensitivity, the analysis was broadened to compare ER-negative and ER-positive subtypes. The upregulated genes with a significant adjusted p-value of 0.05 included *NDRG1, VEGFA, PPFIA4, AARD, EGLN3, LOXL2., FXYD5, SLPI* and *MFGE8* (**Figure 5.11** and **5.12 A-I**) while downregulated genes included *CXCL14, IGLV1, IGHA1, IGHV1-18, IGLC3, IGHV3-33* and *LTF* (**Figure 5.11** and **5.13 A-G**).

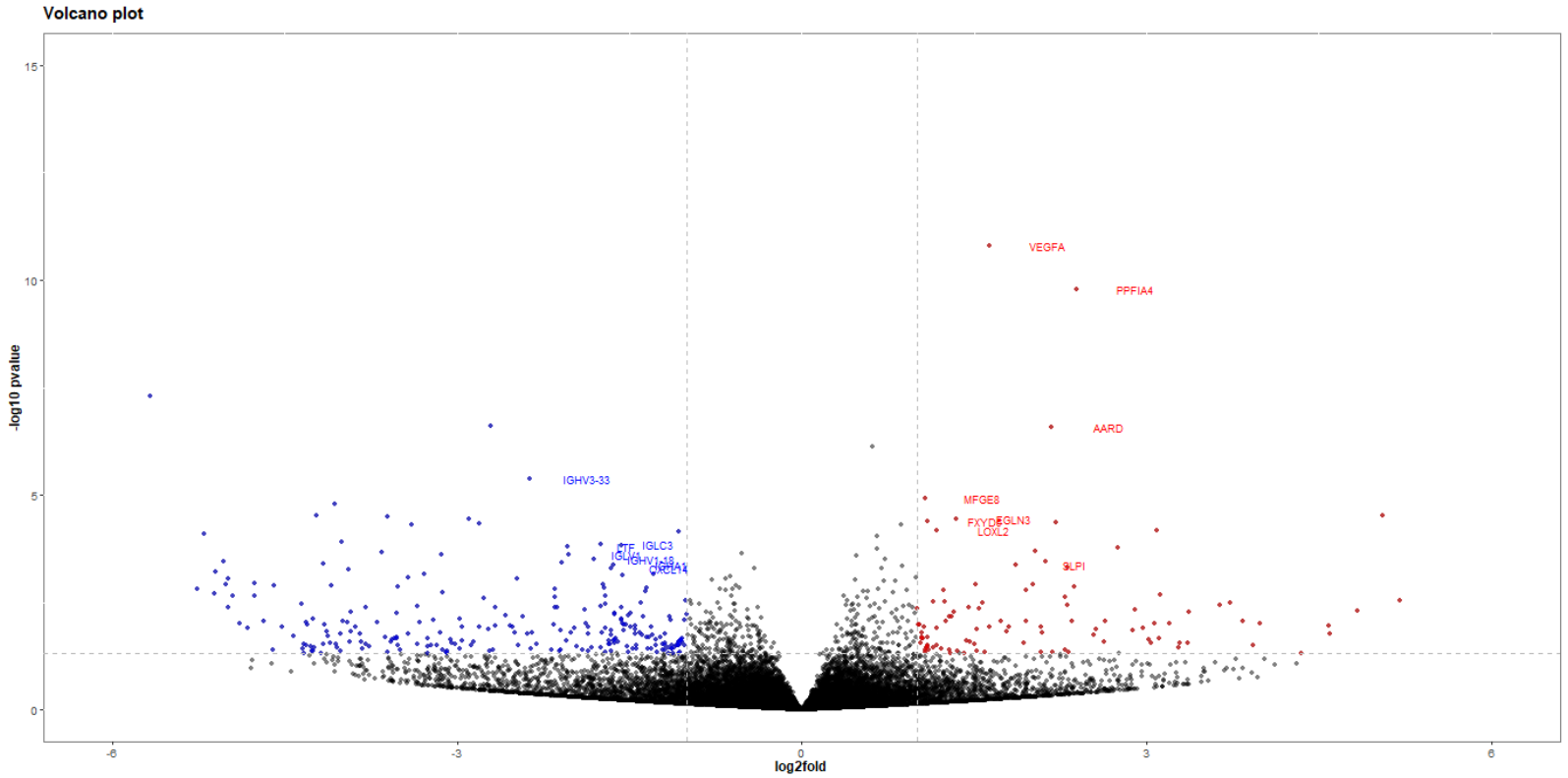

Figure 5.11-Volcano plot representation of differential expression analysis of genes for high and low NDRG1 expression. Red and blue dots mark the genes with significantly increased or decreased expression respectively in high NDRG1 compared to low NDRG1 expression samples (p adj. < 0.05). The x-axis shows log2 fold-changes in expression and the y-axis shows the -log 10 of a gene being differentially expression

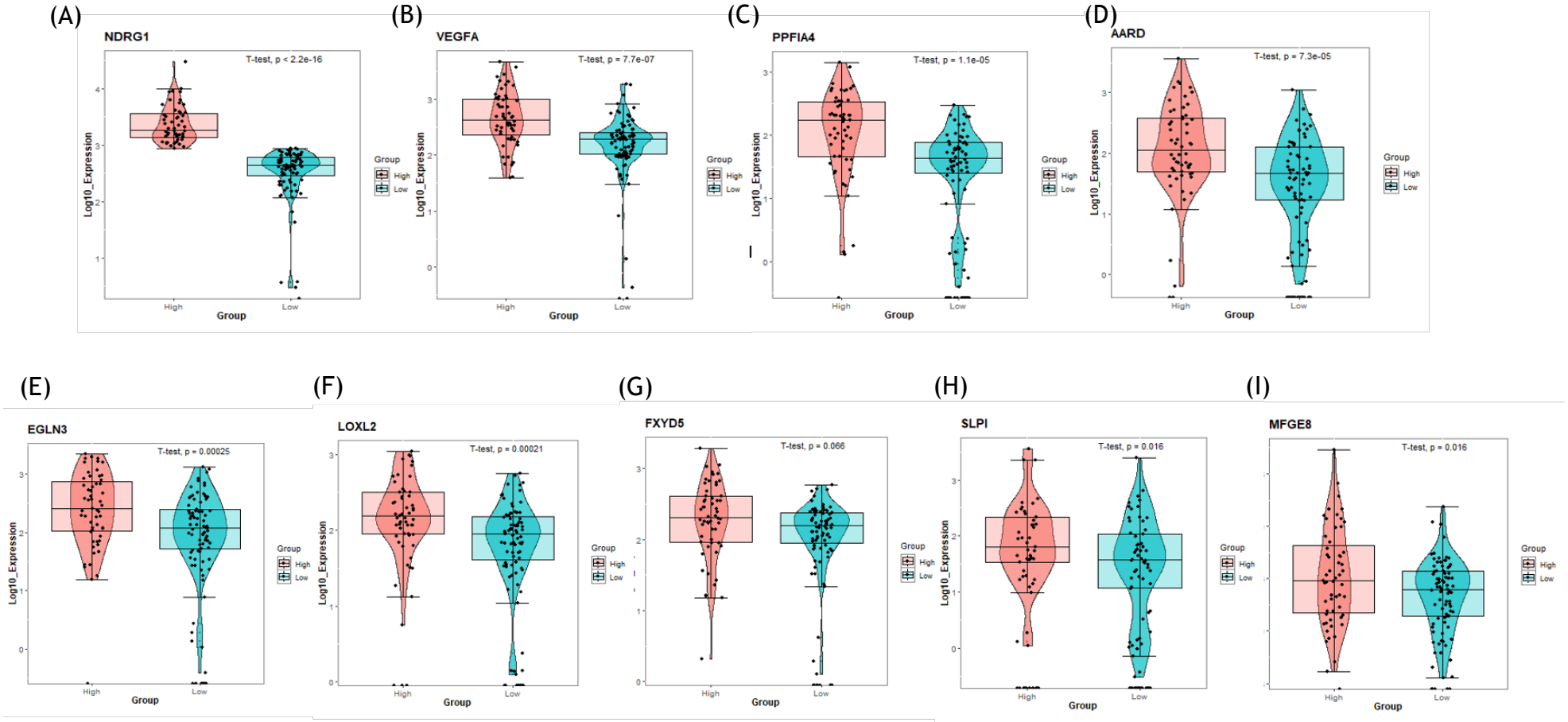

Figure 5.12 - Violin plots of upregulated significant p-adj. DEGs relating to NDRG1 expression phenotypes; (A) *NDRG1*, (B) *VEGFA*, (C) *PPFIA4*, (D) *AARD*, (E) *EGLN3*, (F) *LOXL2*, (G) *FXYD5*, (H) *SLPI* and (I) *MFGE8*

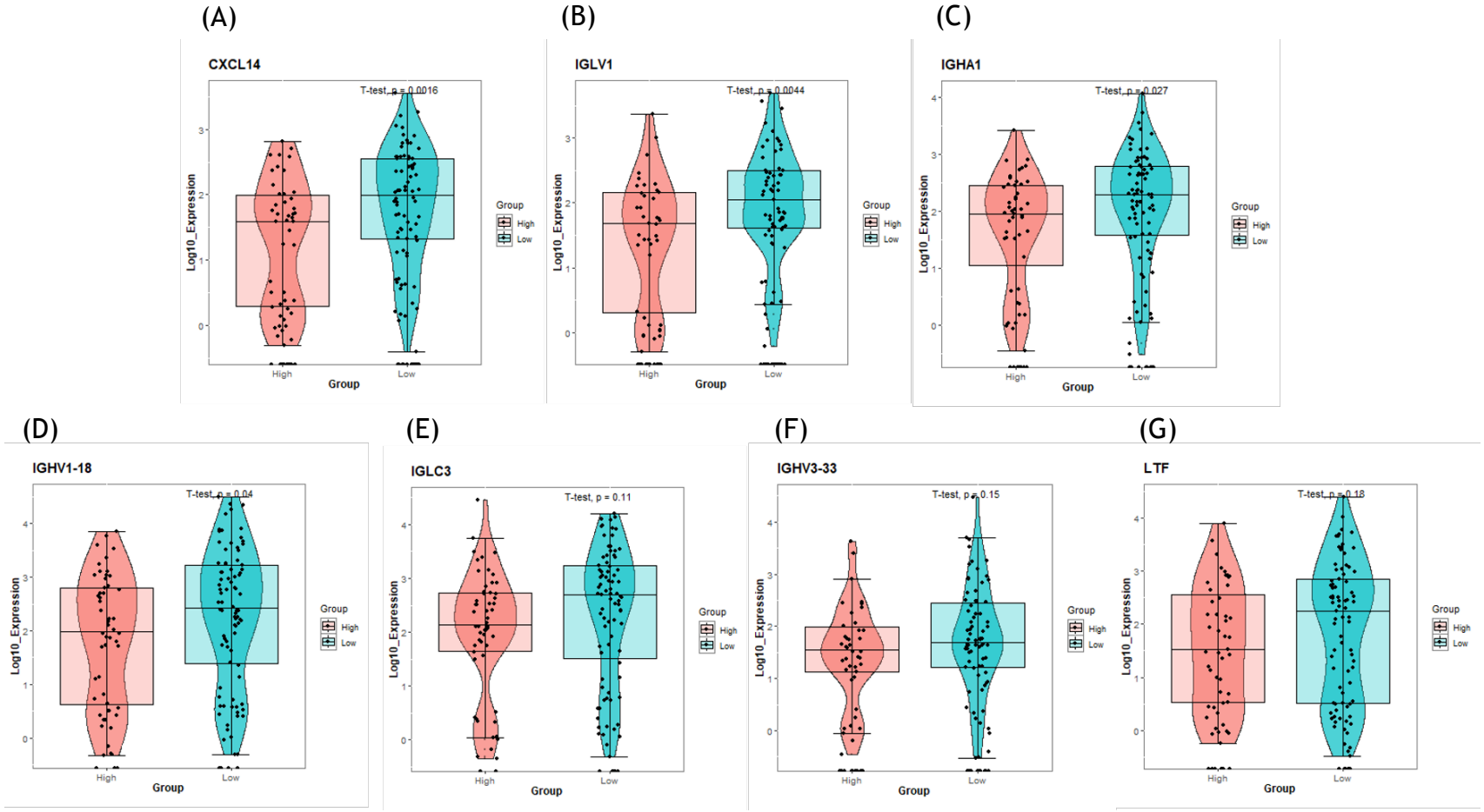

Figure 5.13- Violin plots of downregulated significant p-adj. DEGs related to NDRG1expression phenotypes included (A) *CXCL14*, (B) *IGLV1*, (C) *IGHA1*, (D) *IGHV1-18*, (E) *IGLC3*, (F) *IGHV3-33* and (G) *LTF*

The KM-plotter was used to determine the RFS of significant differential genes, however, *AARD* and *IGHV1-18* were not identified from this plot. *NDRG1* (p=1.6e-11), *VEGFA* (p=2.6e-10), *PPFIA4* (p=0.0005) and *SLP1* (p=2.1e-05) in the upregulated group (**Figure 5.14**) and all except *IGLC3* in the downregulated group (**Figure 5.15**) were significantly associated with survival outcomes.

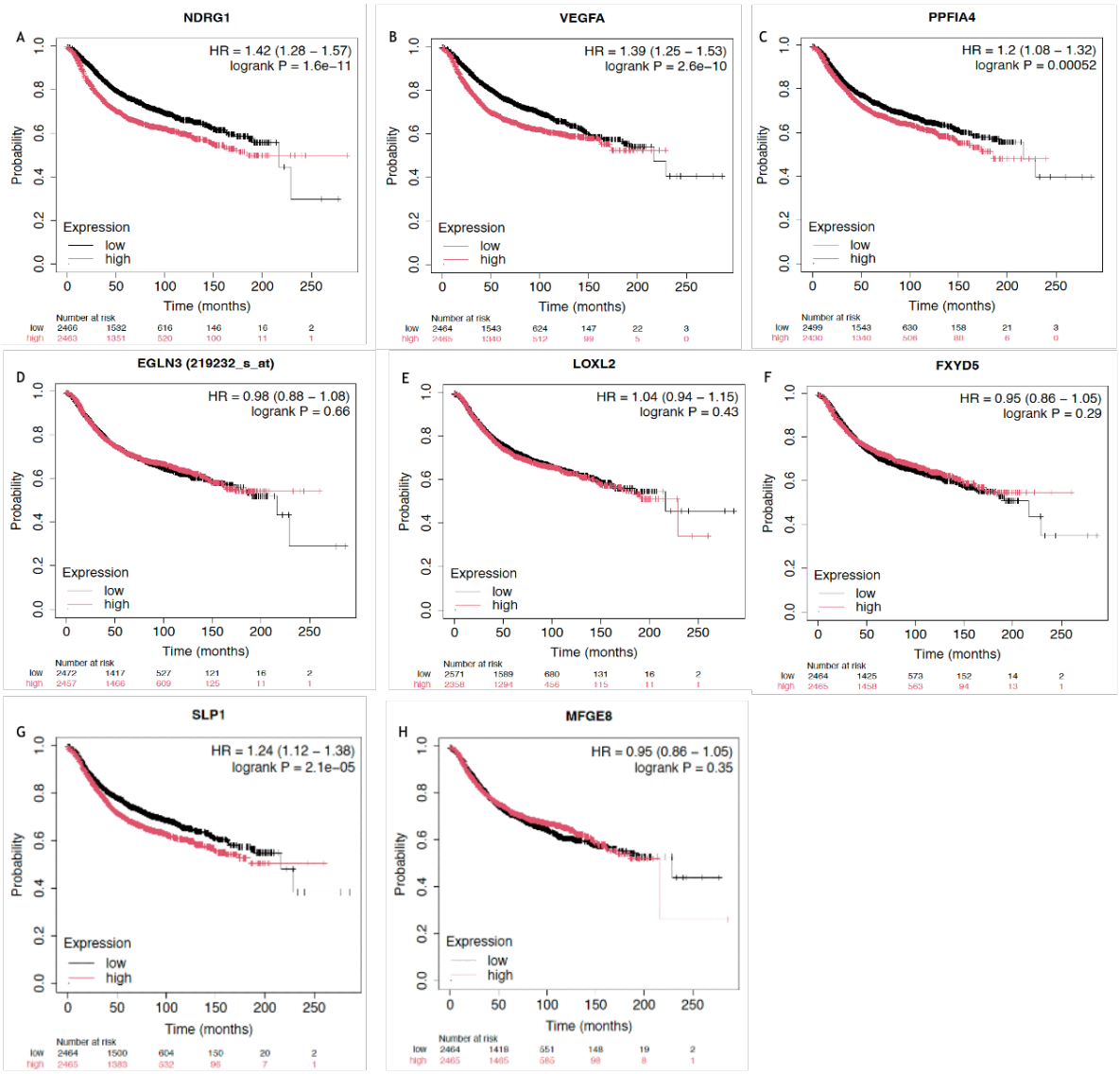

Figure 5.14-The RFS of upregulated significant DEGs from KM-plotter; (A) *NDRG1*, (B) *VEGFA*, (C) *PPFIA4*, (D) *EGLN3*, (E) *LOXL2*, (F) *FXYD5*, (G) *SLPI* and (H) *MFGE8*

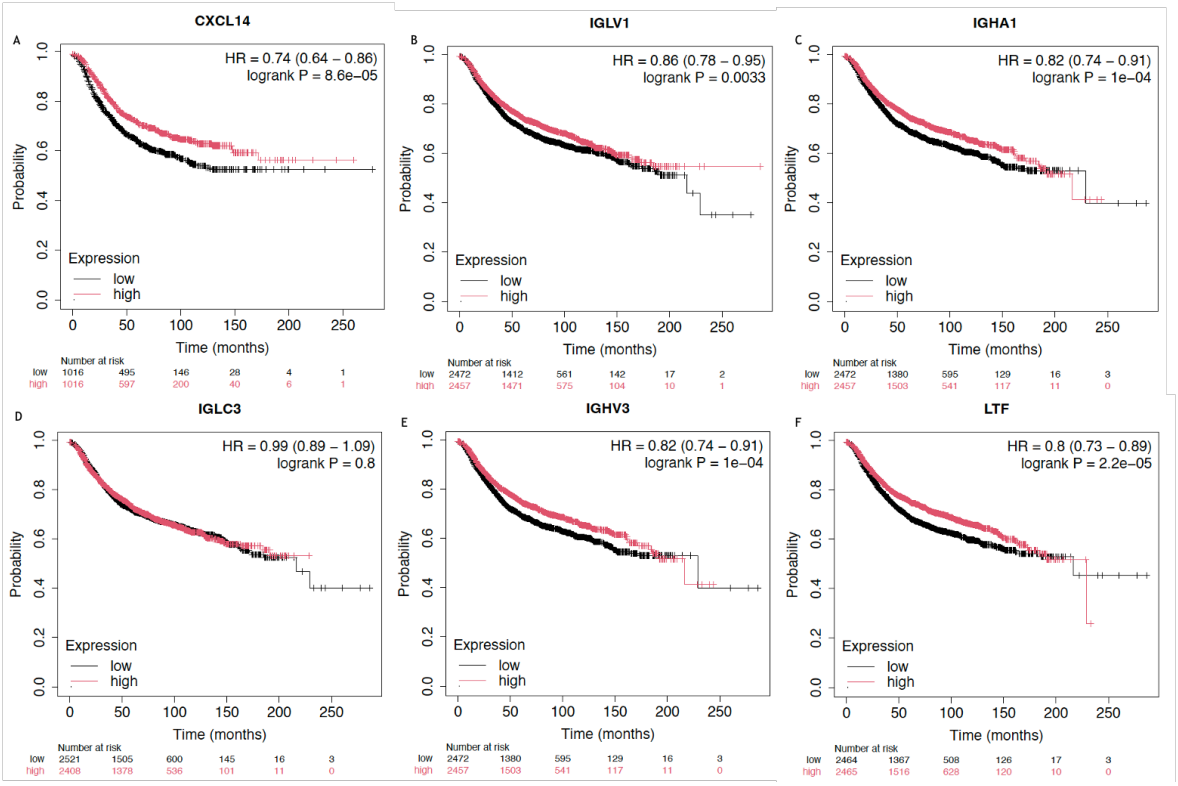

Figure 5.15-The RFS of downregulated significant DEGs from KM-plotter; (A) *CXCL14,* (B) *IGLV1,* (C) *IGHA1,* (D) *IGLC3,* (E) *IGHV3-33* and (F) *LTF*

5.5 Discussion

Although several biomarkers have been used to predict prognosis and treatment response in breast cancer, it remains the most common cause of cancer death in women across the world. Thus, novel markers are still needed. Hypoxia-related markers are of interest because hypoxia is a common feature in breast cancer. NDRG1 was predominantly localised in the cytoplasm and membrane, with a smaller proportion found in the nucleus. These findings align with predictions from PSORT, a program for subcellular localisation analysis, which identified NDRG1 distribution as 47.8% in the cytoplasm, 26.1% in the nucleus, and 8.7% in the mitochondria (396). This suggests that NDRG1 primarily functions in the cytoplasm and membrane of tumour cells. Cytoplasmic NDRG1 expression increased under 1% oxygen conditions in SUM102 cells, and its overexpression has been linked to vesicle transport (397). In colorectal cancer, cytoplasmic NDRG1 positivity was higher in primary tumour tissues compared to regional lymph node metastases (398). Additionally, in hepatocellular carcinoma (HCC) cell lines, cytoplasmic NDRG1 promoted tumour growth by inducing ß-catenin nuclear

localisation through competitive binding with glycogen synthase kinase-3β (GSK-3β) and the orphan nuclear receptor (Nur77) (399).

Membranous NDRG1 may be localised near adherens junctions and desmosomes (400). Under hypoxic conditions, cytoplasmic NDRG1 redistributes to the cell membrane and nucleus, as observed in trophoblast cells (401). In liver cancer, membrane-associated NDRG1 levels were higher in cancerous regions compared to adjacent degenerative tissues, suggesting its potential role in determining the extent of liver injury (402).

The proportion of NDRG1 nuclear expression observed in this study was relatively low compared its expression in other cellular compartments. This finding is consistent with other studies, which reported NDRG1 nuclear expression in approximately 10-20% of cases (297, 403, 404). Moreover, Joshi et al. compared matched primary breast cancer and breast cancer-related brain metastasis samples and found that metastatic brain tissue exhibited higher NDRG1 expression than the corresponding primary breast cancer tissue (404). This suggests that NDRG1 is more highly expressed in aggressive forms of breast cancer. Although nuclear NDRG1 expression was less prominent, its translocation to the nucleus appears to be involved in the DNA damage response in a p53-dependent manner. NDRG1 was primarily identified in the G1 and G2-M phases of the cell cycle, and its introduction into human cancer cells inhibited cell proliferation (405). Conversely, silencing nuclear NDRG1 in Caki-1 cells (clear cell renal cell carcinoma) promoted cell proliferation (406). Additionally, Lachat proposed that nuclear NDRG1 expression in prostate cancer cells may protect against ischemic damage under hypoxic conditions (407).

The results from this study suggest that NDRG1 protein is related to aggressive pathological features. Cytoplasmic and nuclear NDRG1 protein expression was significantly associated with high tumour grade and more aggressive molecular subtypes, while membranous NDRG1 was associated with negative nodal status.

These results are in agreement with other studies ; however, most did not perform separate analyses based on subcellular localisation and primarily examined NDRG1 expression in the cytoplasm and membrane. Nagai et al.

reported high NDRG1 and low SPARC expression were related to nodal metastasis and ER- and PR-negative status (408). Villodre et al. studied NDRG1 in inflammatory breast cancer patients and found that NDRG1 significantly associated with higher tumour grade and the TNBC molecular subtype (300). Zeng et al. utilised iTRAQ proteomics analysis to identify metastatic-associated markers. NDRG1 was downregulated and was associated with high-grade tumours, however, NDRG1 did not predict survival outcomes in their cohort (409). Although NDRG1 protein expression is correlated with poor pathological factors, only 2 reports, from Nagai et al and Villodre et al., showed that NDRG1 expression was an independent factor for survival outcomes. Their findings differed from this study, in that NDRG1 was associated with CSS and OS in univariate analysis, but this association was not observed in multivariate analysis. This was probably due to the strong correlation between NDRG1 and pathological factors including tumour grade and molecular subtypes in the breast cancer cohort. The subgroup analysis of 4 molecular subtypes of breast cancer showed no association between survival in each subtype and NDRG1 expression, however, it may be that high NDRG1 in the HER-2 enriched subtype had inferior CSS compared to low NDRG1.

The transcriptomic data for NDRG1 expression in the ER-negative subgroup showed a trend similar to that of CAIX, as discussed in Chapter 3. Specifically, the genes NDRG1, PPFIA, and VEGFA were found to be upregulated. However, the CA9 gene, which codes for CAIX, was not identified in the NDRG1 classification. This suggested their functions are interconnected under hypoxic conditions to promote tumour growth, survival and metastasis, particularly in aggressive breast cancer phenotypes. As discussed in Chapter 3, the function and interaction of PPFI4 with other genes is less understood and no study has reported the co-expression of PPFIA4 with them. *NDRG1, VEGFA and CA9* are involved throughout the hypoxia pathway. In Chapter 4, the results demonstrated that *NDRG1* and *CA9* were co-expressed in hypoxia, and they might influence the expression of each other. CA9 and VEGFA are typically co-expressed in response to hypoxia promoting angiogenesis and modulating pH (345). Other upregulated genes, including Alanine and Arginine Rich Domain Containing Protein (AARD), Egl-9 Family Hypoxia-Inducible Factor 3 (EGLN3), Lysyl Oxidase-Like 2 (LOXL2), and FXYD5, are upregulated under hypoxic conditions except AARD (410). These genes contribute to various cancer-related processes. The function of AARD remains

largely uncharacterised, *AARD* mRNA predicted prognosis in gastric cancer (411). EGLN3 modulates HIF stability, apoptosis, and differentiation (412). It is involved in both tumour suppression and adaptation to hypoxia, depending on the cancer type (413). LOXL2 is an extracellular matrix-modifying enzyme that promotes epithelial-to-mesenchymal transition (EMT), invasion, and metastasis under hypoxic conditions (410, 414). It enhances collagen crosslinking, creating a tumour-supportive microenvironment (415). FXYD5 regulates ion transport and cell adhesion (416). Hypoxia-induced FXYD5 expression is associated with tumour aggressiveness, increased metastasis, and resistance to apoptosis (417).

In contrast, several immune-related genes are downregulated under hypoxia, potentially facilitating immune evasion and tumour progression. These include immunoglobulin genes (IGLV1, IGHA1, IGHV1-18, IGLC3, IGHV3-33). These encode components of the B-cell receptor and immunoglobulin chains, which are critical for adaptive immune responses (418). Their downregulation may impair antibody production and tumour immune surveillance. CXCL14 (C-X-C Motif Chemokine Ligand 14) functions as a tumour suppressor chemokine involved in immune cell recruitment and angiogenesis inhibition (419). Reduced expression is associated with poor immune infiltration and enhanced tumour growth. LTF (Lactotransferrin) is an iron-binding glycoprotein with antimicrobial, anti-inflammatory, and tumour-suppressive properties (420). Its downregulation is linked to increased cancer cell proliferation and reduced immune activation.

Overall, the upregulation of hypoxia-responsive genes promotes tumour growth, survival, and metastasis, while the downregulation of immune-related genes weakens immune surveillance, enabling tumour progression.

The limitations of this study were, first, the absence of a standard cut-point for NDRG1 expression, which may have over- or underestimated the power of NDRG1 to predict survival outcomes. The choice of threshold can significantly influence the interpretation of biomarker impact, and this variability highlights the need for standardised criteria in future studies. Second, the relative sample size was small, particularly in TNBC and HER-2 enriched subtypes, in which it might be expected that NDRG1 would affect survival outcomes, so a limited number of cases could reduce the statistical power to detect meaningful

associations. Third, no validation cohort was available to validate the reproducibility and robustness of our findings, which is essential for biomarker studies to ensure broader applicability. Additionally, the Glasgow breast cancer cohort utilised in this study was derived from cases diagnosed between 1995 and 1998, a period characterised by substantially different treatment standards compared to today. At that time, adjuvant HER-2 targeted treatment and neoadjuvant treatment were not yet in routine clinical use. Likewise, modern endocrine therapies and chemotherapy regimens have undergone considerable evolution since then. These differences in therapeutic approach may influence survival outcomes and limit the extent to which our results can be extrapolated to current patient populations receiving contemporary treatment. Consequently, while this cohort provides valuable historical insights, validation in more recent cohorts with up-to-date clinical management is necessary to fully understand the prognostic role of NDRG1 in breast cancer.

In conclusion, the results suggest that NDRG1 has the potential to be a prognostic marker in breast cancer. Validation or larger cohorts of breast cancer subtypes are required to confirm the results and to further follow the REMARK criteria.

Chapter 6 : The functions of NDRG1

6.1 Introduction

Hypoxia is a hallmark of solid malignancy including breast cancer (421). The reduced blood supply to the tumour results in cellular stress and activates adaptive survival mechanisms, such as proliferation, invasion, angiogenesis and metabolic reprogramming (421, 422). The previous chapters demonstrated the significance of NDRG1 in terms of hypoxic-regulated genes and biomarkers of poor prognosis in breast cancer and underlined the importance of NDRG1 in breast cancer particularly in the hypoxia context. However, the functions of NDRG1 have still to be elucidated.

Some studies have previously reported that NDRG1 was a tumour suppressor in breast cancer (293, 298, 393, 423) . However, other studies have demonstrated the opposite (298). Early studies reported NDRG1 overexpression decreased the invasive properties of MDA-MB-468 cells. This was supported by IHC analysis from surgical breast cancer patients, where NDRG1 had an inverse correlation with lymph node and bone metastasis (393). The oncogenic T-box 2 (T-box 2) promotes cell proliferation by suppressing NDRG1 through the interaction of T-box 2 and early growth response gene 1(EGR1), particularly in the MCF-7 cell line(293). Reoxygenated MCF-7 cells had low expression of NDRG1 and enhanced cell migration, and this effect was reduced when NDRG1 was overexpressed (423). The migration and invasion of breast cancer can be activated through the phosphorylation of multiple kinases, including EGFR, AKT and ERK1/2 when knocking down SGK1/NDRG1 in T47D and MDA-MB-231 cell lines (424). NDRG1 has also been reported to be involved in epithelial-mesenchymal transition (EMT) by blocking the Wnt receptor LRP6 (298) (**Figure 6.1**). Survival analysis of 85 breast cancer patients revealed that those with high NDRG1 expression had a better 5-year disease-free survival (DFS) compared to those with low NDRG1 expression (393).

In contrast, reports have demonstrated tumour promotor properties for NDRG1. Blocking NDRG1 in the MCF-7 cell line under hypoxic conditions prevented cell proliferation, cell migration and enhanced cell cycle arrest (282). This has also been shown in TNBC cell lines (MDA-MB-231 and SUM-159) and the HER2 cell line SK-BR-3 where silencing NDRG1 suppressed cell proliferation but had no effect

on migration (292, 425). In the inflammatory breast cancer model, the most aggressive clinical form of breast cancer, it was found that NDRG1 was involved in driving brain metastasis and this was diminished when NDRG1 was reduced (426) (**Figure 6.1**). NDRG1 may also be associated with treatment resistance. The AKT inhibitor "Capivasertib" has recently been approved by the FDA for use in ER+/HER2- locally advanced or advanced breast cancer (427). However, a previous study reported high SGK1 and phosphorylated NDRG1 serve as predictors of AKT inhibitor resistance (428). Several studies have indicated that high NDRG1 expression is associated with worse OS, metastatic-free survival and RFS (299, 425, 429, 430). Thus, the function and role of NDGR1 in breast cancer progression and prognosis are inconsistent.

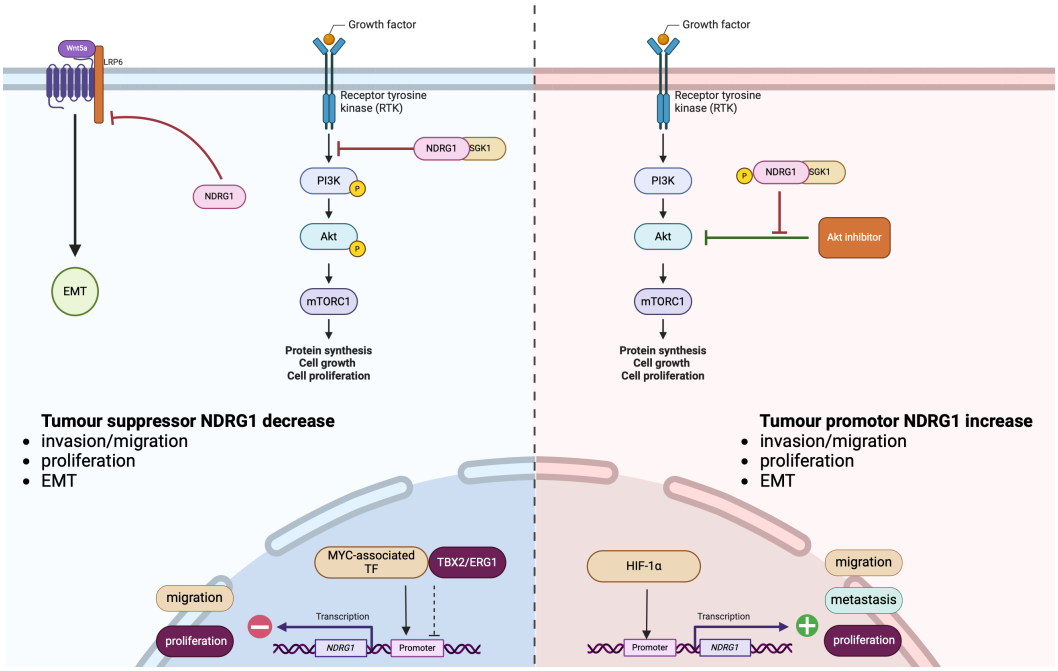

Figure 6.1-Summary of NDRG1 function as presented in the NDRG1 literature (Created with BioRender.com)

This study aimed to investigate the functions of NDRG1 in breast cancer in vitro. The bulk RNAseq transcriptomic data from Chapter 3 showed that upregulated genes including NDRG1 correlated with gene set enrichment for both hypoxia and glycolysis. NDRG1 protein expressions predominantly localised in the cytoplasm and membrane, suggesting that its function is likely cytoplasm-based. The hypothesis is that NDRG1 expression acts as a tumour enhancer and that when

inhibited, it rescues cancer glycolysis in addition to having a proliferative function.

To test this hypothesis, MDA-MB-231 and MCF-7 cells were seeded at 15,000 cells/well in Seahorse XF 96 cell culture microplates for glycolysis stress and mitochondrial stress tests, or in 96-well plates for lactate, ATP, and WST-1 assays. After 48 hours, experiments were conducted following the protocols outlined in Chapter 2. Each experiment was performed for three biological replicates, with at least three technical replicates, and medium-only samples served as negative controls.

6.2 Silencing NDRG1 optimisation

Before investigating the function of NDRG1, selective and optimised silencing was performed under hypoxic conditions, which are known to induce NDRG1 overexpression. Following hypoxic exposure, cells were assessed to evaluate the knockdown efficiency, with results presented in **Figure 6.2**.

In MDA-MB-231 cells, silencing was conducted at varying time points (24 and 48 hours) and concentrations (5 nM, 10 nM, 15 nM and 25 nM). The results indicated that NDRG1 mRNA and protein levels were more effectively reduced after 48 hours compared to 24 hours. The optimal concentration was 5 nM RNAi duplex concentration, achieving an 81% reduction in mRNA and an 80% reduction in protein expression (**Figure 6.2A**). Based on this optimisation, MCF-7 cells were assessed under hypoxic conditions solely at 48 hours, where 5 nM siNDRG1 was also found to be the most effective, reducing NDRG1 expression by 70% at the mRNA level and achieving complete (100%) protein knockdown (**Figure 6.2B**).

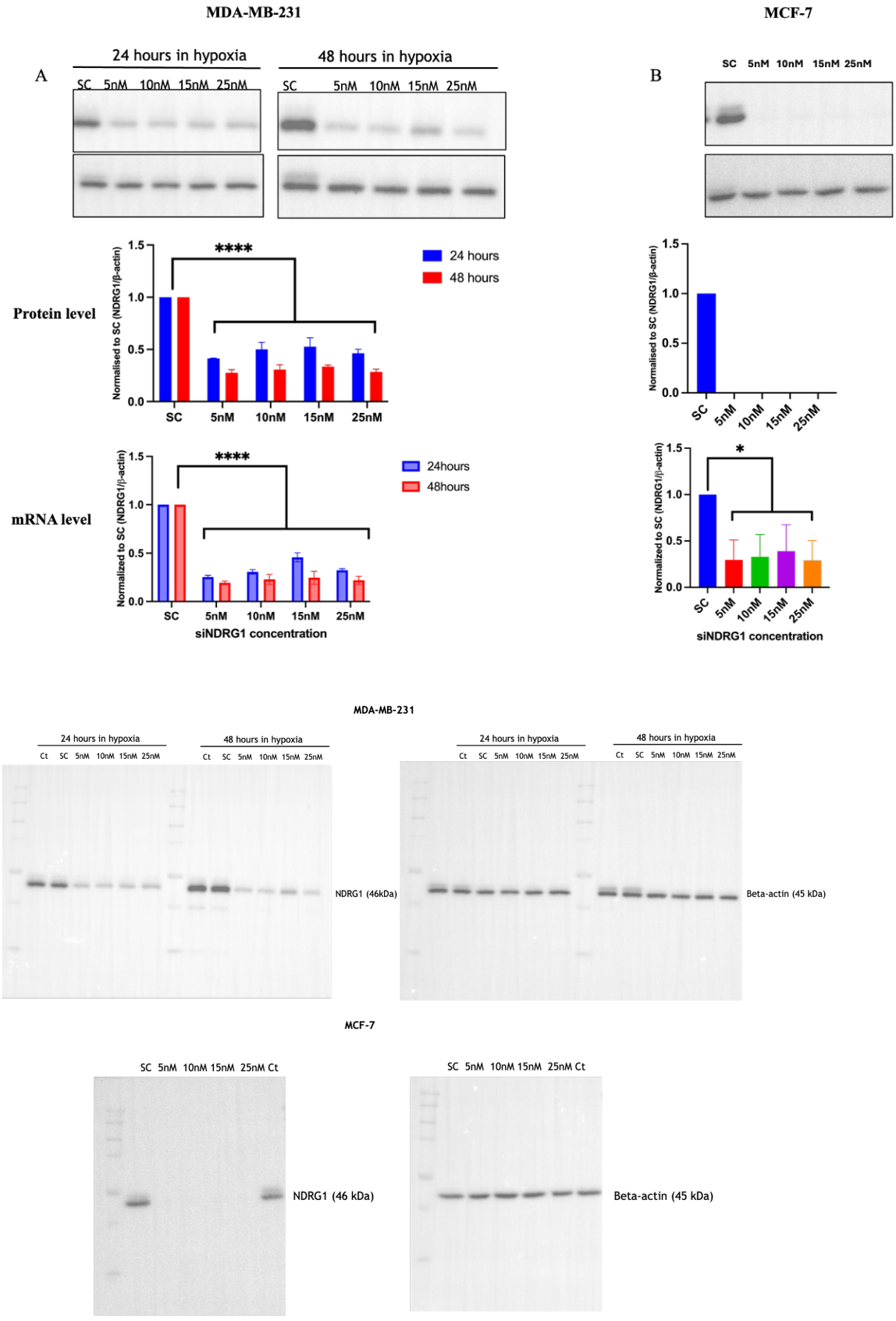

Figure 6. 2-The optimisation of siNDRG1 in (A) MDA-MB-231 and (B) MCF-7 in hypoxic conditions. Scramble was used as control. The experiments were performed in triplicate.*p < 0.05, ****p < 0.0001

Cell viability was evaluated using the trypan blue exclusion test to ensure that silencing did not induce cytotoxicity (**Table 6.1**). Based on these findings, 5 nM siNDRG1 was selected for further experiments in both MDA-MB-231 and MCF-7 cell lines.

Table 6. 1-The cell viability results for NDRG1 silencing optimisation

Cell viability (%)	SC	RNAi duplex concentration			
		5nM	10nM	15nM	25nM
MDA-MB-231	95%	94%	96%	92%	97%
MCF-7	94%	99%	95%	91%	96%

6.3 The role of NDRG1 in breast cancer cell energy production

Cancer cells obtain energy from mitochondrial respiration and glycolysis, and this is dependent on cellular context. Briefly, one glucose molecule enters the glycolysis pathway and produces 2 ATPs with pyruvate, which is converted to the end product lactate plus a proton by lactate dehydrogenase. Pyruvate enters the mitochondria as a substrate in the tricarboxylic acid cycle (TCA) cycle, and the proton enters the inner membrane at the electron transport chain that consists of complex I-IV. This step transfers electrons sequentially, cooperating with $FADH_2$ and NADPH to generate ATP. Altogether mitochondrial respiration provides 36 ATP molecules, H_2O and CO_2, with the latter converted to carbonic acid and H^+. To measure the bioenergetics of breast cancer cells mediated by NDRG1, the Seahorse analyser was used to estimate the real-time metabolic dependence of breast cancer cells. The Glycolysis stress test was used to determine NDRG1 mediated glycolysis. The Mito stress test was also used to determine if NDRG1 mediated mitochondrial respiration.

6.3.1 Silencing NDRG1 associated with glycolytic reduction in MDA-MB-231 and MCF-7 cell lines under hypoxic conditions

To determine the role of NDRG1 in glycolysis, the XF Glycolysis Stress test was performed. This test involved the cells becoming stressed by inhibiting the glycolysis pathway sequentially (**Figure 6.3**). Prior to the assay, glucose-containing media was removed and replaced with a glucose-free medium. Glucose was then injected, and cells underwent glycolysis to produce pyruvate, ATP, NADH, water, and protons. This glucose-induced response is the rate of glycolysis under basal conditions. Then oligomycin was injected to inhibit mitochondrial ATP respiration. This step allows cells to utilise only glycolysis and therefore measures the maximal glycolytic capacity. 2-deoxy-glucose (2-DG) was the final injection and this inhibits glycolysis by competitive binding with hexokinase, the first enzyme in the glycolytic pathway. This step disrupts the glycolysis pathway resulting in decreased ECAR confirming the ECAR produced in the experiment comes from glycolysis and the glycolytic reserve can be calculated for this.

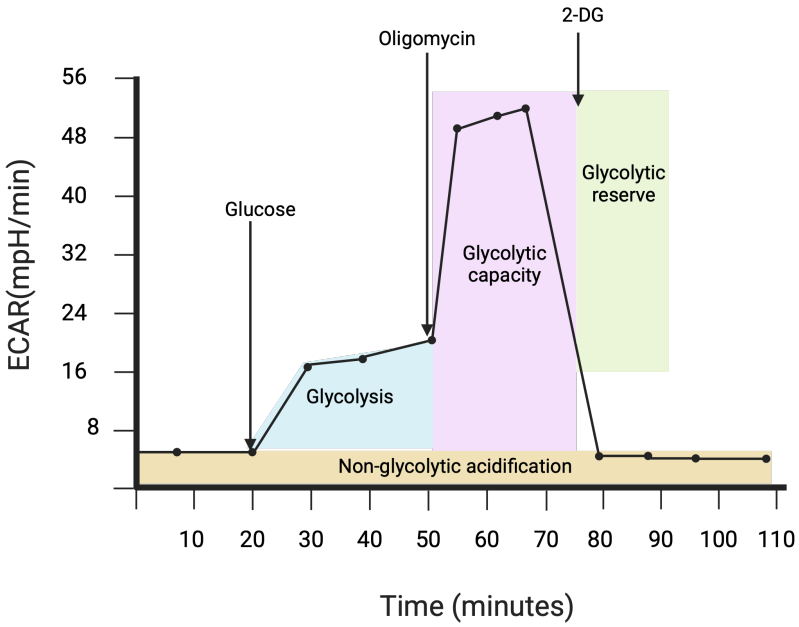

Figure 6.3-The Glycolysis stress test (courtesy of Agilent Seahorse XF Glycolysis Stress Test Kit User Guide)

This was performed in two cell lines (MDA-MB-231 and MCF-7) for both hypoxic and normoxic conditions. In the MDA-MB-231 cell line, NDRG1 did not mediate the glycolytic pathways in hypoxia and siNDRG1 decreased non-glycolytic

acidification. However, siNDRG1 significantly elevated glycolysis and glycolytic capacity under normoxic conditions (**Figure 6.4**).

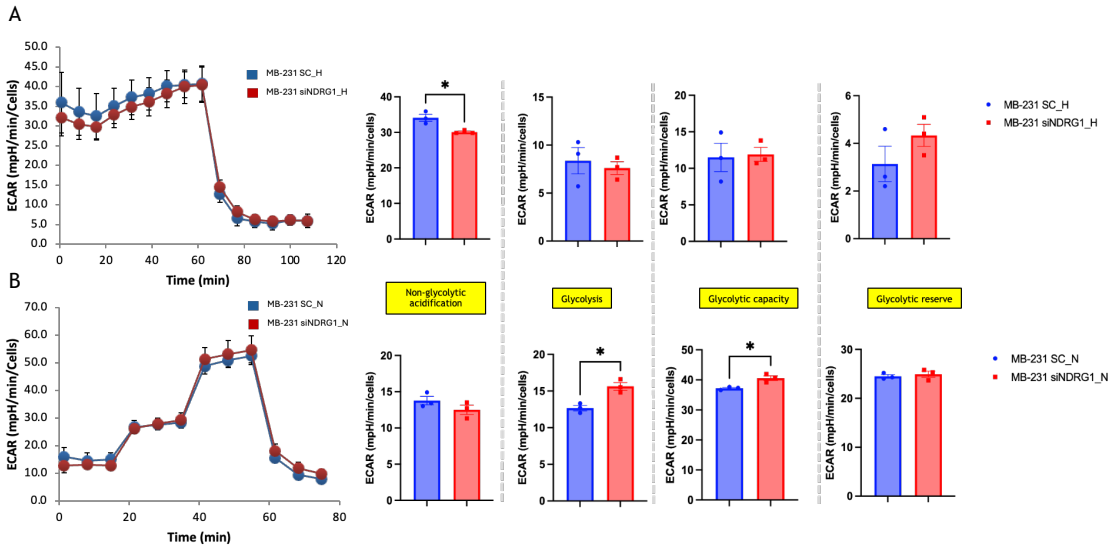

Figure 6.4-The Glycolysis stress test results for the MDA-MB-231 cell line in (A) hypoxia and (B) normoxia. The experiment was performed with three biological replicates, each with 4-6 technical replicates. Student T-test was used to compare SC vs siNDRG1. Data were mean+/-SEM. *P≤0.05.

In contrast, siNDRG1 significantly increased glycolysis, glycolytic capacity and glycolytic reserve under hypoxic conditions in the MCF-7 breast cancer cell line while appearing to have no role in normoxia (**Figure 6.5**).

A

B

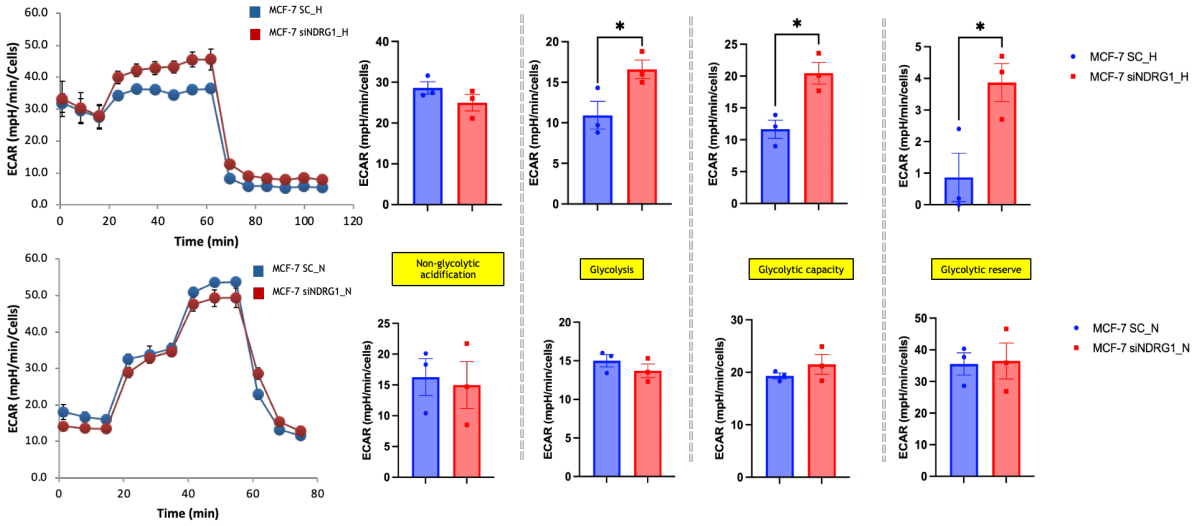

Figure 6.5-The Glycolysis stress test results for MCF-7 cell line in (A) hypoxia and (B) normoxia. The experiment was performed with three biological replicates, each with 4-6 technical replicates. Student T-test was used to compare SC vs siNDRG1. Data were mean+/-SEM. *P≤0.05.

To validate the glycolysis stress test, lactate, the end product of glycolysis, was measured from conditioned cell culture medium using the Lactate-Glo™ Assay (**Figure 6.6**). The results showed that silencing NDRG1 expression can significantly reduce lactate production in MDA-MB-231 and MCF-7 cell lines in hypoxia. Interestingly, silencing NDRG1 in the MCF-7 cell line paradoxically increased lactate release in normoxia; however, this was not observed in MDA-MB-231 cells. Overall, glycolysis was predominant in hypoxia rather than in normoxia, particularly in MCF-7 cells. Although the metabolic program in MDA-MB-231 seemed to exploit glycolysis regardless of oxygen level, NDRG1 expression had an effect on glycolysis only under hypoxic conditions.

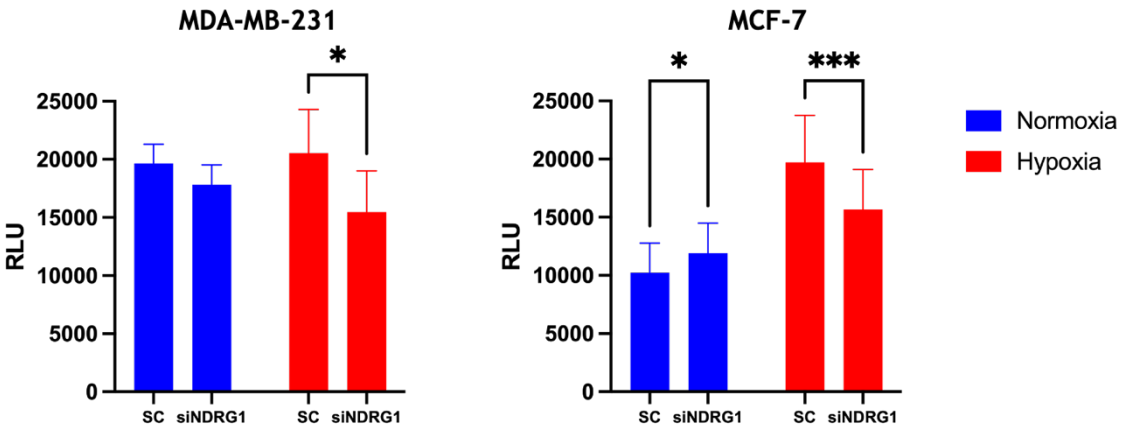

Figure 6.6- Lactate production in culture medium from MDA-MB-231 and MCF-7 cell lines measured using the Lactate-Glo™ Assay under normoxic and hypoxic conditions. Two-way ANOVA was used to compare SC vs siNDRG1. Data were mean+/-SEM. *P≤0.05 and ***P≤0.001.

6.3.2 Silencing NDRG1 associated with reduction of glycolysis in MDA-MB-231 and MCF-7 cell lines under hypoxic conditions

To determine the role of NDRG1 in mitochondrial respiration, the Mito Stress test was performed (**Figure 6.7**). Oligomycin, an inhibitor of ATP synthase was injected. By blocking ATP production, oligomycin decreases oxygen consumption, thereby giving a value for basal respiration. Carbonyl cyanide-4-(trifluoromethoxy) phenylhydrazone (FCCP) was introduced. This is an uncoupling agent that disrupts the proton gradient and collapses the mitochondrial membrane potential, allowing unrestricted electron flow through the electron transport chain (ETC)and leads to maximal oxygen consumption by complex V. The FCCP step enables protons to freely cross into the mitochondrial matrix, driving the mitochondria to maximise oxygen utilisation for ATP production and unrestricted ETC activity. Subsequently, rotenone and antimycin A were injected to inhibit complex I and complex III, respectively. This step halts mitochondrial activity, and the spare respiratory capacity and non-mitochondrial respiration can be determined.

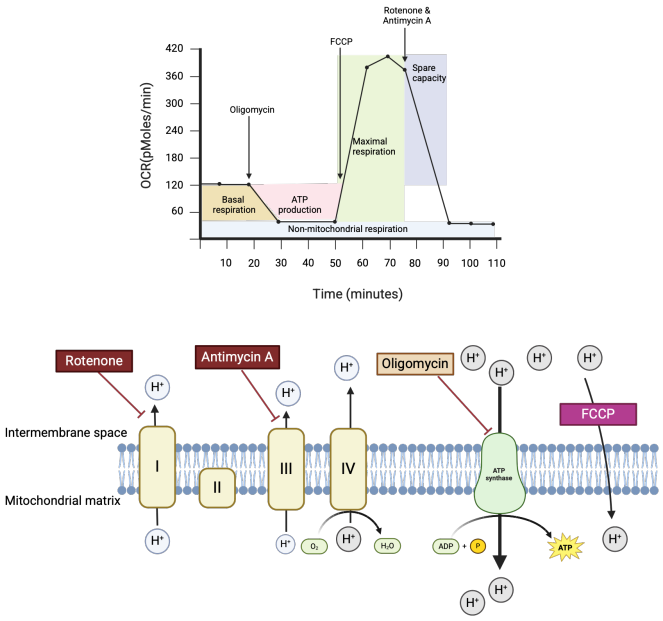

Figure 6.7-The Mito Stress test (courtesy of Seahorse XF Cell Mito Stress Test Kit User Guide)

In the MDA-MB-231 cell line, NDRG1 did not affect mitochondrial respiration in either hypoxia or normoxia (**Figure 6.8**).

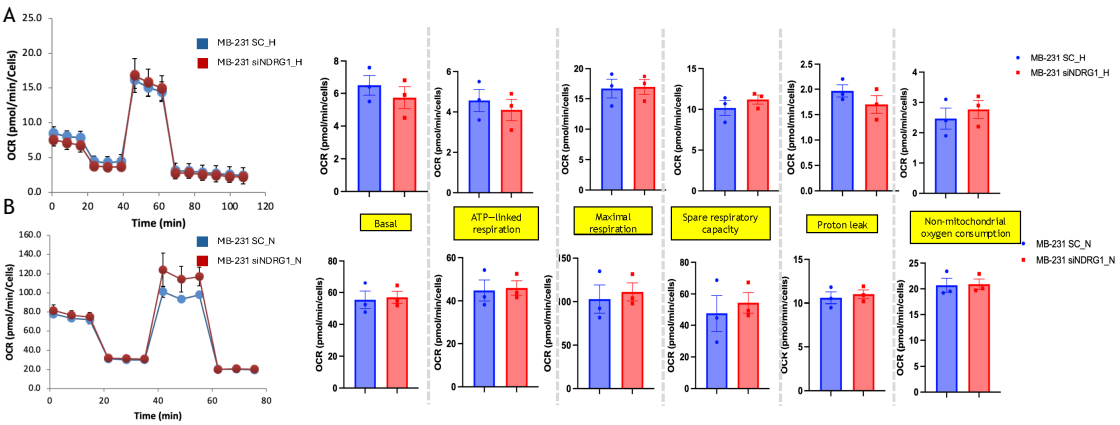

Figure 6.8-The Mito Stress test results for the MDA-MB-231 cell line in (A) hypoxia and (B) normoxia. The experiment was performed for three biological replicates, each with 4–6 technical replicates. Student T-test was used to compare SC vs siNDRG1. Data were mean+/-SEM.

In contrast, siNDRG1 significantly increased basal respiration, maximal respiration, non-mitochondrial consumption and ATP production under hypoxic

conditions in MCF-7 breast cancer cell line. However, no effect was observed in normoxia (**Figure 6.9**).

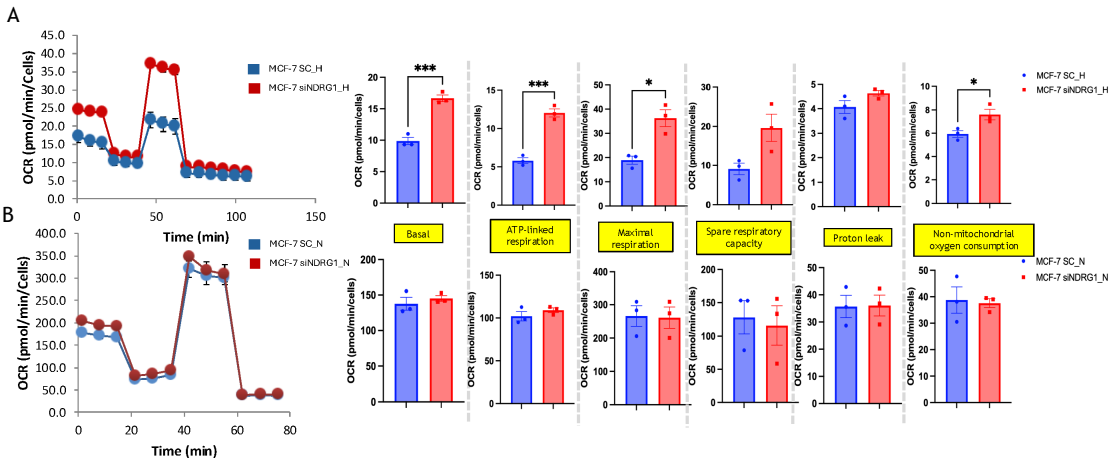

Figure 6.9-The Mito Stress test results for the MCF-7 cell line in (A) hypoxia and (B) normoxia. The experiment was performed for three biological replicates, each with 4–6 technical replicates. Student T-test was used to compare SC vs siNDRG1. Data were mean+/-SEM. *P≤0.05 and ***P≤0.001.

To validate the Mito Stress test, the extracellular ATP was measured by using the luminescent ATP Detection Assay Kit (Abcam 113849). The results showed that silencing NDRG1 expression significantly increases ATP production in MCF-7 cell lines under hypoxic conditions but had no effect in MDA-MB-231 cells. NDGR1 had no effect on either cell line in normoxia (**Figure 6.10**).

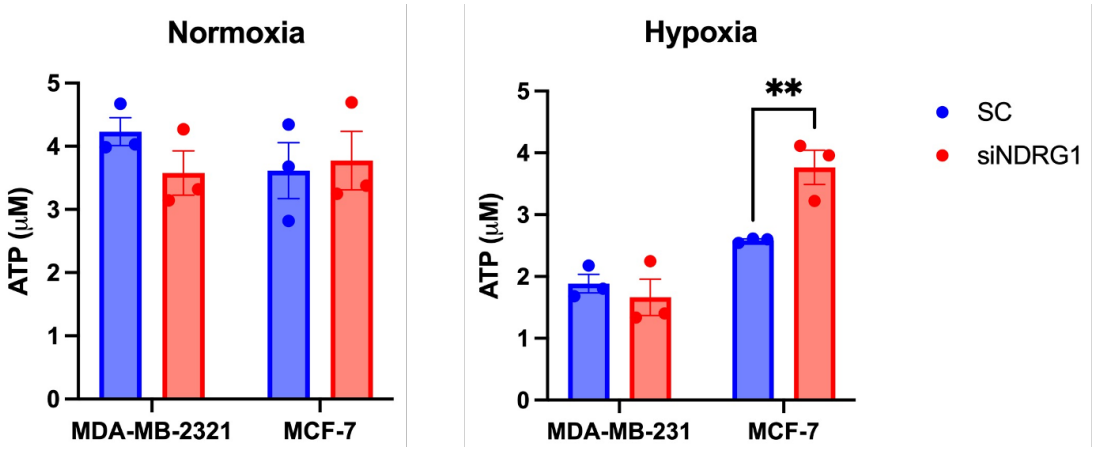

Figure 6.10- ATP production of MDA-MB-231 and MCF-7 cell lines was determined by the Luminescent ATP Detection Assay Kit under normoxic and hypoxic conditions. The was performed for three biological replicates, each with 3

technical replicates. Student T-test was used to compare SC vs siNDRG1. Data were mean+/-SEM. **P=0.0002.

6.4 Hypoxia promotes cell proliferation independently of NDRG1 expression

To determine if NDRG1 mediates breast cancer proliferation, a WST-1 assay was performed after incubating MDA-MB-231 and MCF-7 cell lines under hypoxic and normoxic conditions. Cell proliferation on was measured at a single time point (48 hours) following treatment. As expected, the proliferation of MDA-MB-231 and MCF-7 breast cancer cell lines was significantly higher in hypoxia than in normoxia but independent of NDRG1 expression (**Figure 6.11**). When NDGR1 was silenced in MDA-MB-231 cells, proliferation was slightly decreased when compared to the scrambled control in both normoxia and hypoxia. However, in MCF-7 cells silencing resulted in a slight increase in proliferation. Statistical significance was not achieved for either cell line.

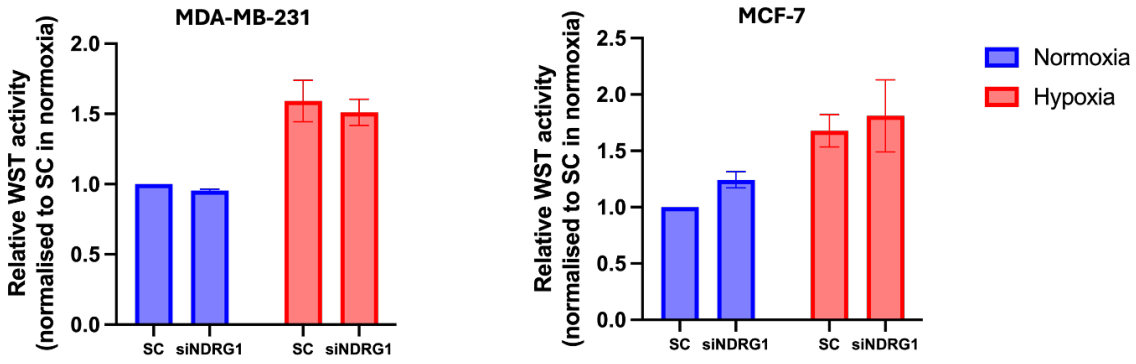

Figure 6.11-The proliferative activity of MDA-MB-231 and MCF-7 cell lines determined by WST-1 assay under normoxic and hypoxic conditions. Cells were incubated for 48 hours, and proliferation was measured at a single time point. The experiment was performed for three biological replicates, each with three technical replicates. Student T-test was used to compare SC vs siNDRG1. Data were mean+/-SEM.

6.5 Discussion

NDGR1 was first identified in an autosomal recessive disease called Charcot-Marie-Tooth neuropathy type 4 (CMT4). The *NDRG1* gene is one of the predisposing genes that contribute to CMT4D phenotypes (431). NDRG1 mutation causes demyelinating neuropathy which initially presents with distal motor impairment followed by proximal motor impairment concomitant with sensorineural hearing loss (432). However, the underlying mechanisms by which NDGR1 destroys the myelin have not been completely identified. Li et al. proposed homozygous NDRG1 missense variants at c.437T>C (p.Leu146Pro) and c.701G>A (p.Arg234Gln) resulting in alteration of intracellular protein trafficking and decreased uptake of low-density lipoprotein receptor subsequently resulting in a deficit of myelination (433).

The role of NDRG1 in cancer has been investigated however its exact functions are still controversial. Many studies agree that NDRG1 functions differently depending on the cancer type. NDRG1 expression in lung cancer, HCC, gastric and cervical cancer favours tumour promotion while in colon, prostate and ovarian cancer favours tumour suppression (434, 435, 436, 437, 438, 439). Early breast cancer studies reported NDRG1 as a tumour suppressor while subsequent and updated studies reported that NDRG1 acts as a tumour activator. The difference in NDGR1 functions is not restricted to tumour origin but also varies within subtypes of the same tumour. As discussed in the introduction section, the role of NDRG1 in breast cancer is still under debate. In this study, following on from the bulk transcriptomic data, it was found that NDRG1 is upregulated in hypoxia. However, the role of NDGR1 in breast cancer under hypoxic conditions has not been elucidated.

The results presented in this chapter suggest that NDGR1 may modulate metabolic pathways in breast cancer. Metabolism in hypoxia generally shifts toward glycolysis and mitochondrial respiration is suppressed. The basal level of ECAR was higher while OCR was lower under hypoxic conditions in both cell lines. However, hypoxia-induced NDRG1 has a different metabolic role in different cell lines, particularly under hypoxic conditions. NDRG1 expression was less likely to

mediate metabolic activity in normoxia, however, its expression affected metabolism differently in hypoxia dependent on specific cellular characteristics.

MDA-MB-231 metabolism relies more on glycolysis than mitochondrial respiration. Glycolysis activity was measured and the results showed that NDRG1 status did not affect ECAR, however, silencing NDGR1 decreased lactate production as measured by the lactate assay. This can be explained by the XF Glycolysis Stress test which determines ECAR including protons and reflects overall glycolytic activity but does not fully account for downstream pathways such as lactate production. This may imply that NDRG1 is specific to lactate regulation rather than playing a central role in glycolysis or ATP production. NDRG1 might mediate the exportation of lactate extracellularly via the lactate transporter (i.e. MCT) or by altering lactate dehydrogenase (LDH). The absence of NDRG1 decreased MCT and lactate dehydrogenase function leading to a decrease in extracellular lactate levels.

To understand and gain insight into the role of NDRG1 in the metabolic profile of MDA-MB-231 cells, mitochondrial respiration was investigated. The results from the XF Mito Stress test showed that NDRG1 did not affect mitochondrial respiration. Mitochondrial respiration was already suppressed under hypoxic conditions, with HIF-1a, a key hypoxic regulator, probably driving metabolic reprogramming. Therefore, any subtle change in OCR from being NDRG1 dependent might not be detected.

Hypoxia disrupts mitochondrial function and OXPHOS by blocking pyruvate entry into the TCA cycle. This is a consequence of HIF-1 activating PDK and subsequently inhibiting PDH, the enzyme that converts pyruvate to acetyl-CoA (440). In addition, hypoxic conditions increase lipid droplet accumulation which limits fatty acid oxidation in mitochondria(441). Thus, NDRG1 does not play a role in mitochondrial function, suggesting that, MDA-MB-231 cells exploit compensatory pathways in hypoxia other than mitochondrial respiration. This may also explain why the XF Mito Stress test could not detect any changes when NDGR1 was silenced. Further evidence for this was provided by the ATP assay, with ATP production being independent of NDRG1 expression. Thus, in MDA-MB-231 cells, NDRG1 may not be directly involved in mitochondrial respiration. Inhibition of NDRG1 disrupted glycolysis only under hypoxic conditions. This assumes ATP

production was mostly obtained from glycolysis, which is usually a small amount compared to oxidative phosphorylation). Although silencing NDGR1 reduced glycolysis, it was not sufficient to switch to OXPHOS. Hence, the intracellular ATP level was not increased. Instead, there might be an energy deficit as normoxic conditions resulted in more ATP than in hypoxic conditions.

The MCF-7 cell line was more adaptable under stress conditions such as hypoxia. Under hypoxic conditions, MCF-7 cells rely on glycolysis. The Glycolysis Stress test revealed that silencing NDGR1 increased ECAR, however, the lactate assay results show the opposite. This suggests that high ECAR probably results from redundant protons producing a high ECAR even with low lactate output. This was confirmed by the increasing OCR observed in the XF Mito Stress test in which CO_2, a proton source, was emitted from mitochondrial respiration. In the lactate assay silencing NDGR1 significantly decreased lactate output and significantly increased ATP production. However, NDRG1 might also regulate lactate production as in MDA-MB-231 cells. For the MCF-7 cell line, it may be concluded that NDRG1 is necessary to maintain glycolysis in hypoxia and inhibition of NDRG1 can rescue mitochondrial respiration with a shift away from glycolysis.

Although NDRG1 has been shown to mediate many functions in cancer, for example, proliferation, migration, apoptosis, angiogenesis and lipid metabolism, the role of NDRG1 in glycolysis has not been examined in breast cancer under hypoxic conditions. The results described in this chapter are the first to report that NDRG1 mediates glycolysis under hypoxic conditions. Liu et al. studied NDRG1 in two pancreatic cancer cell lines MIA PaCa-2 and PANC-1 in normoxia and found that overexpressed NDRG1 decreased extracellular acid production while increasing the rate of oxygen consumption. This referred to NDRG1 shifting cellular metabolism from glycolysis to utilise mitochondrial respiration (351). Another study from Guo determined the ECAR of two HCC cell lines Huh7 and Hep3B, and they showed that silencing NDRG1 in hypoxia inhibited glycolysis activity (442). The results reported here are similar to those of Guo. It may be that NDRG1 functions depend on the type of cell and, the cancer environment may play a pivotal role in NDRG1 activity. However, the results are in contrast to those of Jadhav et al. who knocked out NDRG1 in both MCF-7 and MCD-MB-231 cell lines in normoxia and evaluated ECAR and OCR activity. They proposed that the absence of NDRG1 in MCF-7 cells led to an increase in both ECAR and OCR, whereas in MDA-

MB-231 cells, it decreased ECAR without affecting OCR (443). This suggests that environmental conditions may mediate NDRG1 functions and the underlying mechanisms responsible for this activity warrant investigation.

The proliferation of both breast cancer cell lines is not dependent on NDRG1 regardless of expression. Although silencing NDGR1 decreased glycolysis, it did not independently decrease the proliferation of the cells. This study suggests that hypoxia drives tumorigenesis by accelerating cancer cell proliferation as compared to normoxic conditions. However, other genes can increase cancer cell proliferation independently of NDRG1. It may be that even if NDRG1 is not a predominant factor, it might facilitate signalling pathways for example, PI3K/mTOR, p53 and MYC, that are involved in promoting proliferation in hypoxic conditions. The results reported here are similar to those for pancreatic (444), prostatic (445) and colon (446) in vitro studies where cells in which NDGR1 had been knocked down had a similar growth rate to the control group. In a lung cancer model, Azuma et al. also reported that silencing NDRG1 did not affect tumour growth in vitro but reduced tumour volume in a xenograft model. This suggested that NDRG1 possibly interacts with other factors such as angiogenic factors (434).

This study demonstrated that NDRG1 modulates glycolysis under hypoxic conditions. The inhibition of NDRG1 reduced glycolysis and increased mitochondrial respiration depending on cellular subtypes. Although NDRG1 was identified from ER-negative breast cancer samples, its metabolic function was predisposed to MCF-7 cell lines (ER-positive) rather than MDA-MB-231 (TNBC). This may be due to NDRG1 being produced by other cell types. An investigation into the role of NDGR1 in the stroma would provide further information.

One limitation of this study was the inability to directly compare normoxic and hypoxic conditions using the XF analyser, as hypoxic conditions require a specialized chamber set to an oxygen level of 3% O_2. Additionally, the timing of the experiments may have influenced the results, given that cancer cell metabolism is a dynamic process. Measuring at a single time point could obscure the effects of NDRG1. This is particularly relevant for real-time XF analysis, which may explain the inconsistencies observed between the XF analyser results and the endpoint measurements obtained from lactate and ATP assay kits.

In summary, NDRG1 plays a different role in the metabolic plasticity of breast cancer under hypoxic conditions. It is predisposed to play a role in regulating mitochondrial metabolism only in MCF-7 cells (ER-positive). Silencing NDGR1 could enhance mitochondrial ATP generation by activating or upregulating OXPHOS components, while NDRG1 might interact with downstream pathways of lactate excretion in glycolysis (**Figure 6.11**).

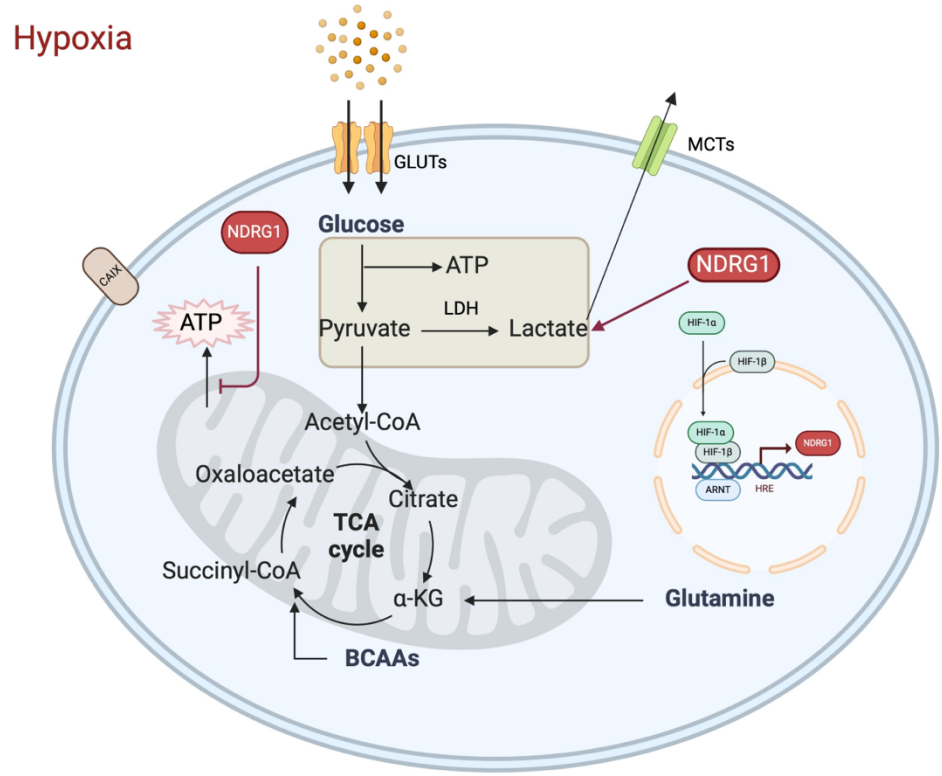

Figure 6.12-The role of NDRG1 in regulating metabolic function in breast cancer cells under hypoxic conditions (Created with BioRender.com)

Chapter 7 : General Discussion

7.1 General discussion and future perspective

Breast cancer is the most commonly diagnosed cancer and also the leading cause of cancer death among women worldwide (1). Currently, the screening programs, diagnostic techniques, surgical techniques, adjuvant systemic treatment and radiation therapy have been improved exponentially. This has resulted in decreasing morbidity and mortality from breast cancer. The improvements are mainly due to an increase in the knowledge of the molecular background and genetic associations of breast cancer tumorigenesis (142, 143). However, most of the evidence relies on tumour molecular subtypes and less so on the tumour environment, despite it being the source of many factors that drive the aggression of the disease or eventually lead to resistance to therapy (447, 448).

ER-negative or non-luminal breast cancers, including triple-negative breast cancer (TNBC) and HER2-enriched subtypes, exhibit aggressive tumour characteristics such as high grade and high proliferative index. These subtypes also have distinct intrinsic molecular profiles (449, 450). While luminal breast cancers express ER-related genes, HER2-enriched tumours are defined by ErbB2 oncogene overexpression. Additionally, 80% of TNBC cases belong to the basal-like intrinsic subtype, characterised by the expression of keratin 5/17, integrin-ß4, and laminin gene clusters. At the transcriptional level, TNBC frequently exhibits hyperactivation of key oncogenic transcription factors, including HIF-1α/ARNT, which drive proliferation, metabolic reprogramming, and therapy resistance (149). This suggests that hypoxia-induced mechanisms contribute to the aggressive nature of certain breast cancer subtypes. Transcriptomic analyses of 31 breast cancer cell lines, covering all four intrinsic subtypes, confirmed distinct hypoxia-responsive gene expression patterns., Hypoxia-conserved genes were upregulated more in basal-like compared to luminal-like breast cancers, correlating with poor prognosis (181). However, despite the clear role of hypoxia in tumour progression, no hypoxia-targeted therapies or interventions have been established as standard treatments for breast cancer.

HIF-1 is a crucial transcription factor in hypoxia but has a short half-life of a few minutes (192). HIF-1 is expressed in both normal and tumour tissues, thus

used of inhibitors may cause off target toxicity. (451). These other alternative targets should be considered. Carbonic anhydrase 9 (CAIX) is an enzyme that equilibrates pH for optimal cancer cell survival under hypoxic conditions, and its transcription is regulated by HIF-1α (241, 245). CAIX protein expression has a longer half-life of up to 24-48 hours with stability after reoxygenation and is almost exclusive to cancerous tissue (251). Thus, it is an attractive therapeutic target for cancers that are hypoxia-enriched. Currently, SLC-0111, a specific CAIX inhibitor, is undergoing a phase I clinical trial for advanced-stage solid cancer and the results showed that it is safe and can inhibit tumour progression in some patients (452). Thus, a broad understanding of the molecular background of CAIX expression is required.

The previous data supported the finding that CAIX expression is a poor prognostic marker in many cancers, including breast cancer (251). Dr. Suad A.K. Shamis, a previous PhD student, also reported that CAIX expression is a negative prognosticator for survival outcomes in the Glasgow breast cancer cohort. The present study specifically focuses on the ER-negative subgroup that included the two most aggressive subtypes, TNBC and HER-2 enriched, as they have poorer oncologic outcomes than ER-positive subtypes and have limited treatment modalities. Thus, the thesis started with validation of the role of the prognostic marker CAIX in ER-negative subtypes before exploring the molecular background and identifying the novel therapeutic markers associated with hypoxia in breast cancer.

7.2 Tissue-based study-CAIX and NDRG1

Protein expression of CAIX in The Glasgow breast cancer cohort was initially analysed to determine the prognostic role of CAIX, specifically in the ER-negative subgroup. These results agreed with previous studies in the literature reporting the use of CAIX as a prognostic marker whether in all subtypes or in specific subgroups (204). In Chapter 3, it was demonstrated that high CAIX immunostaining predicted unfavourable CSS, OS and RFS in the full Glasgow breast cancer cohort but only predicted poor OS in ER-negative breast cancer. Cytoplasmic CAIX expression was shown to be an independent factor for OS in ER-negative subgroup. This suggests that CAIX serves as an indicator of overall outcomes in breast cancer

patients rather than being specific to disease progression alone. These results are reliable, as they are based on a long-term follow-up period of 12.53 years. Thus, CAIX expression may play a role in the aggressive features of tumours or may indicate which patients are likely not to respond to treatment.

NDRG1 was identified as a signature gene in high CAIX expression. However, the role of NDRG1 in breast cancer remains controversial. Some studies suggest that NDRG1 functions as a tumour suppressor (293, 393, 423, 453) , while others indicate a tumour-promoting role (282, 292, 298, 424).

Some studies link NDRG1 overexpression to reduced metastasis (453) and inhibition of migration via Wnt signalling suppression (294). Others report that TBX2-mediated repression of NDRG1 promotes proliferation (393) and that low NDRG1 after reoxygenation enhances migration (293). Additionally, SGK1/NDRG1 axis activation has been associated with increased EGFR, AKT1, and ERK1/2 phosphorylation, promoting migration (454). Conversely, studies suggest NDRG1 supports tumour progression. Its suppression in hypoxia inhibits proliferation and migration (298), while in TNBC and HER2+ cells, NDRG1 silencing reduces proliferation but not migration (454). In inflammatory breast cancer, NDRG1 drives brain metastasis (282) and is linked to AKT inhibitor resistance (292) and poor survival outcomes (300, 429). Given these conflicting roles, it was hypothesised that NDRG1 could serve as a prognostic marker under hypoxic conditions and the aim was to investigate its oncological impact using a patient tissue cohort.

In Chapter 5, it was demonstrated the high cytoplasmic NDRG1 associated with poorer CSS and OS in the full Glasgow breast cancer cohort, even though it was not an independent factor for those outcomes. These results were concordant with other studies that investigated the prognostic role of NDRG1 in breast cancer (297, 300, 394). However, NDRG1 expression did not significantly distinguish survival outcomes based on ER status or molecular subtypes. This suggested that NDRG1 generally mediated the aggressive phenotypes rather than molecular subtype-specific pathways. It is also possible that NDGR1 might affect the conditions in the tumour microenvironment, such as hypoxia or acidity, which would not be exclusive to ER-negative or ER-positive cancer.

There are several limitations to the tissue-based study. Although TMAs are efficient and cost-effective for IHC analysis, they might not fully represent the whole tumour population. The limited core size might not represent intratumoural variability across different tumour regions, thus leading to sampling bias. Another limitation was the lack of recommended cut-point method. This study used R's surminer package to determine the most significant survival-related cut-off. It calculates the maximally selected rank statistics, which is similar to the minimum p-value approach, and it can decrease subjective bias by selecting a cut-off value that might occur if (Receiver Operating Characteristic) ROC was used. Although ROC, minimum p-value and mean/median value are commonly used, they also have some limitations. ROC needs a large sample size for reliable outcomes, while minimum p-value might introduce multiple testing bias, and the mean/median value might not capture the threshold that truly correlates with clinical outcomes. Therefore, future work should include validation of the selected cut-off in an independent cohort.

7.3 Transcriptomic analysis

One of the objectives of this thesis was to identify the signature genes related to CAIX expression. It was hypothesised that these differentially expressed signature genes share distinct biological functions in tumours with high CAIX expression. Four significantly upregulated genes were identified, *NDRG1, CA9, VEGFA* and *PPFIA4* and 20s downregulated genes that were differentially expressed between high and low CAIX expression in ER-negative breast cancer tissue samples. In Chapter 4, these upregulated genes were validated at the mRNA level and protein level using qPCR and Western blot techniques to compare expression in normoxic and hypoxic conditions. All four genes showed significant overexpression in hypoxia (vs. normoxia) at the mRNA level, with NDRG1 and CAIX expression also elevated at the protein level. In addition, the functional enrichment analysis from GSEA also had relevance to the biological function of CAIX, which is associated with hypoxia and glycolysis.

In this study, NDRG1 was selected for further study as it met stringent criteria (p-adjusted < 0.05, |log2FC| > 1) for meaningful biological expression. Additionally, it was the only gene, aside from CA9, validated at the protein level.

Although the results were validated, Tempo-Seq is a bulk RNA-seq method that averages gene expression across all cell types in the sample. As a result, cell-type heterogeneity could obscure cell-specific effects. Additionally, Tempo-Seq probes approximately 22,000 genes and does not provide full-length transcript information, potentially missing novel or unexpected transcripts. Therefore, further study of the biological relevance of NDRG1 should be investigated carefully.

7.4 In vitro studies

The in vitro studies were conducted to validate the biological functions of NDRG1 obtained from transcriptomic analysis. In Chapter 3, the signature genes (*NDRG1, CA9, VEGFA* and *PPFIA4*) were identified when CAIX was expressed. This suggested that the regulation and functions of those genes favoured hypoxia. 1% O_2 was chosen as to represent hypoxic conditions as at this level, it mimics the existing O_2 tension in breast cancer tissue. In Chapter 4, the aim was to determine how these genes were regulated, with the hypothesis that they are upregulated under hypoxic conditions. MDA-MB-231, SKBR3, and MCF-7 cells, representing TNBC, HER2-enriched, and ER-positive subtypes, respectively, were used to assess the expression at both mRNA and protein levels. The results confirmed that the expression of all four genes was higher under hypoxic conditions (1% oxygen). This was consistent across all subtypes at mRNA level and for CAIX and NDRG1 at protein level. A longer incubation under hypoxic conditions led to higher expression. This was consistent with CAIX expression, especially NDRG1 which increased along with CAIX at up to 48 hours in hypoxia at the protein level. This suggests a close relationship or coordinated function between the two and both could be promising hypoxic markers particularly in chronic hypoxia exposure. Future work should consider multiplex IHC to identify if both are co-localised, enabling a better understanding of protein expression profiles and their correlations across different cell types.

Another objective of this thesis was to identify the functions of the targeted genes. NDRG1 was selected because it was the only gene that was overexpressed at the protein level. This step was crucial, as many cellular functions rely on proteins rather than mRNA, and mRNA levels do not always correlate with protein

expression due to post-transcriptional modifications (355). In Chapter 6, it was hypothesised that NDRG1 expression is involved in glycolytic function and that the absence of NDRG1 would reduce aerobic glycolysis. This hypothesis was based on evidence that CAIX plays a role in pH equilibration under metabolic disturbances in low-oxygen conditions. Aerobic glycolysis is a hallmark of cancer metabolism, where cells shift from mitochondrial respiration to glycolysis despite the presence of oxygen. While mitochondrial respiration fully oxidizes glucose to produce 36 ATP, with CO_2 and H_2O as byproducts, aerobic glycolysis (Warburg effect) generates only 2 ATP per molecule of glucose, producing lactate as the end product (239). This hypothesis was further supported when GSEA revealed that signature genes in CAIX-high cells were associated with glycolysis-enriched pathways. As CAIX is implicated in aerobic glycolysis, it is proposed that NDRG1 may function similarly to CAIX in regulating this metabolic shift.

In this study, the metabolism of breast cancer cells was assessed using Seahorse assays under hypoxic conditions, along with additional assays such as lactate production and ATP production assays to minimize potential biases from any single test. In terms of glucose metabolism, NDRG1 was found not to significantly mediate glycolysis in the MDA-MB-231 cell line, based on real-time analysis using Seahorse assays. However, silencing NDRG1 did lead to a reduction in overall lactate production as measured by lactate assays. Interestingly, while silencing NDRG1 increased extracellular acidification (ECAR) in the Seahorse assays, this did not align with the lactate assay data, which showed a reduction in final lactate production. These results suggest that NDRG1 inhibition may reduce lactate production, although this effect was not fully captured by the Seahorse assay. The discrepancy between Seahorse ECAR and lactate production assays might be explained by the complexity of cancer cell metabolism particularly under stress like hypoxia. ECAR measured acid production that is commonly linked to lactate, the end product of glycolysis. However, there are other sources of acids such as mitochondrial activity that release CO_2 or result in shunting to other pathways i.e. glutaminolysis (455, 456). The lactate assays measure the final lactate output from glycolysis. It is possible that glycolysis is still active (by ECAR) but the distribution of lactate could be altered upon silencing NDRG1. For example, pyruvate, the intermediate metabolite of glycolysis, could be diverted away from lactate production toward other pathways such as TCA cycle or

silencing NDRG1 might disturb the lactate dehydrogenase function resulting in decreased lactate production. Additionally, HIF-1α expression usually governs the adaptive response of cancer cells under low oxygen levels so it might reprogram to alternative pathways such as glutamine metabolism. To investigate this further, metabolomic analysis using mass spectrometry methods could be undertaken and this may provide more insight into the metabolic change in NDRG1-silenced cells. The lactate dehydrogenase activity assay may help clarify whether a reduction in lactate production is due to lower enzymatic activity or a shift in metabolite flux.

One possible explanation for the observed increase in ECAR without a corresponding increase in lactate production is that the increased acidification may result from excessive proton production during mitochondrial respiration rather than glycolysis. To explore this, the oxygen consumption rate (OCR) was measured using Seahorse assays, which provide insight into mitochondrial function and the role of oxidative phosphorylation. The results revealed that OCR did not change in the MDA-MB-231 cell line regardless of whether NDRG1 was present or silenced. However, silencing NDRG1 increased OCR under hypoxic conditions in the MCF-7 cell line, suggesting that NDRG1 silencing may promote mitochondrial respiration in MCF-7 cells. These findings were consistent with the ATP production assays, which showed that silencing NDRG1 enhanced ATP production in MCF-7 cells but did not significantly affect ATP levels in MDA-MB-231 cells. This suggests that the increase in ECAR observed in MCF-7 cells in the absence of NDRG1 may be linked to an increase in OCR, which produces CO_2 , thereby contributing to the observed acidification of the extracellular environment.

From the metabolic function experiments, it can be concluded that NDRG1 expression influences the metabolic activity of breast cancer cells under hypoxic conditions in a molecular context-dependent manner. In MDA-MB-231 cells, silencing NDRG1 reduced glycolysis but had no impact on mitochondrial respiration. Although ECAR remained unchanged, lactate production decreased, suggesting that NDRG1 silencing may slow glycolytic activity without disrupting overall acid production. This implies that NDRG1 loss may alter pyruvate fate, potentially redirecting it into other metabolic pathways such as the TCA cycle or

glutamine metabolism, or it might reduce lactate export. The involvement of Na+/H+ exchangers or MCT transporters in compensatory acid regulation under hypoxia could explain why ECAR remained stable despite reduced lactate production (457).

MDA-MB-231 cells do not rely on mitochondrial respiration, and this metabolic preference is not mediated by NDRG1 (458, 459). OCR and ATP production remained unchanged under hypoxia, which is reasonable given that MDA-MB-231cell metabolism primarily depends on glycolysis and alternative pathways such as lipid metabolism or glutaminolysis. Further investigation should explore alternative metabolic pathways, including fatty acid oxidation, lactate export activity, and pH regulation transporters. For MCF-7 cells, the results clearly indicate that silencing NDRG1 shifts metabolic pathways from aerobic glycolysis toward mitochondrial respiration.

Proliferation assays using WST-1 were conducted to determine whether NDRG1 silencing affects breast cancer cell growth under different oxygen conditions. It was hypothesised that if silencing NDRG1 enhances metabolic efficiency, it may suppress proliferation, a key cancer phenotype. However, no significant changes in proliferation were observed following NDRG1 knockdown, regardless of oxygen levels. This result suggests that while NDRG1 silencing alters metabolism, proliferation is not always directly linked to metabolic shifts. It is also possible that breast cancer cells compensate by utilizing alternative nutrient sources, such as glutamine or fatty acids, to sustain growth. Additionally, the WST-1 assay may not be sensitive enough to detect subtle changes or may require a longer observation period for differences to become apparent. Another explanation is that NDRG1 may not play a direct role in proliferation but could instead influence other cellular processes such as survival, migration, or invasion. To further investigate these possibilities, additional long-term assays, such as colony formation over 7–14 days, should be considered. Furthermore, alternative approaches, including cell cycle analysis via flow cytometry and real-time proliferation tracking through live-cell imaging, may provide deeper insights. These experiments should be carefully designed to ensure stable gene silencing over extended periods, particularly under hypoxic conditions, to accurately assess the long-term effects of NDRG1 depletion on breast cancer cell proliferation.

7.5 Future investigation

7.5.1 Validation of NDRG1 as a prognostic marker in independent cohorts

To ensure the reproducibility and reliability of NDRG1 as a prognostic marker in breast cancer, it is crucial to validate the findings in independent patient cohorts. This validation would strengthen the robustness of the results and allow for a more comprehensive correlation between NDRG1 expression and clinical parameters, such as survival outcomes and treatment response. Additionally, confirming NDRG1 expression patterns in different cohorts reinforces its biological relevance and supports the proposed mechanisms underlying its role in breast cancer progression.

7.5.2 Exploring Alternative Metabolic Pathways

The metabolic role of NDRG1 in breast cancer under hypoxic conditions is complex, and current experiments may not fully capture its broader metabolic impact. This challenge is further compounded by the ability of cancer cells to adapt to hypoxic stress, leading to metabolic flexibility. Investigating alternative pathways, such as fatty acid oxidation and glutamine metabolism, could provide additional insights into NDRG1-mediated metabolic regulation. Employing advanced techniques like metabolomic profiling and isotope tracing using ^{13}C-glucose could help delineate metabolic fluxes within glycolysis and the TCA cycle, offering a deeper understanding of the role of NDGR1 in cancer metabolism.

7.5.3 Transcriptomic Analysis of NDRG1

Bulk RNA sequencing can serve as a powerful tool to identify gene expression changes associated with NDRG1 modulation. By analysing transcriptomic profiles, potential pathways can be identified that NDRG1 exploits to regulate cellular metabolism and other oncogenic processes. This approach will help generate new hypotheses and guide further functional validation experiments.

Spatial transcriptomics (ST) in breast cancer tissue samples preserves the spatial context within the tumour microenvironment. Unlike bulk RNA-Seq,

which averages gene expression across entire samples, ST can differentiate gene expression patterns along hypoxic gradients, pinpointing hypoxia-associated markers in specific tumour subregions. This may be particularly valuable in understanding how NDRG1 interacts with hypoxia-driven pathways and contributes to tumour heterogeneity, metastasis, and treatment resistance. By integrating bulk RNA-Seq and ST, a more comprehensive view of the role of NDRG1 in breast cancer progression may be obtained, leading to more precise therapeutic targeting strategies.

7.6 Conclusion

Breast cancer remains a leading cause of cancer-related mortality, with tumour hypoxia contributing to progression and therapy resistance. This study validated CAIX as a poor prognostic marker in ER-negative breast cancer and identified NDRG1 as a hypoxia-related gene associated with CAIX expression. Functional studies demonstrated that NDRG1 influences metabolic adaptation under hypoxic conditions, particularly in glycolysis and mitochondrial respiration, in a molecular context-dependent manner. While NDRG1 silencing altered metabolic pathways, its impact on proliferation was limited, suggesting alternative roles in tumour aggressiveness. These findings provide a foundation for future research into the prognostic value of NDGR1, its metabolic functions, and therapeutic potential in breast cancer.

References

1. World Health O. Global breast cancer initiative implementation framework: assessing, strengthening and scaling up of services for the early detection and management of breast cancer: executive summary. Geneva: World Health Organization; 2023 2023.
2. Ferlay J LM, Ervik M, Lam F, Colombet M, Mery L et al. Cancer tomorrow: International Agency for Research on Cancer; 2020 [Available from: https://gco.iarc.fr/tomorrow.
3. UK CR. 2017-2019 [Available from: https://www.cancerresearchuk.org/health-professional/cancer-statistics/statistics-by-cancer-type/breast-cancer/mortality.
4. Giaquinto AN, Sung H, Miller KD, Kramer JL, Newman LA, Minihan A, et al. Breast Cancer Statistics, 2022. CA: A Cancer Journal for Clinicians. 2022;72(6):524-41.
5. Chen HL, Zhou MQ, Tian W, Meng KX, He HF. Effect of Age on Breast Cancer Patient Prognoses: A Population-Based Study Using the SEER 18 Database. PLoS One. 2016;11(10):e0165409.
6. Johnson RH, Anders CK, Litton JK, Ruddy KJ, Bleyer A. Breast cancer in adolescents and young adults. Pediatr Blood Cancer. 2018;65(12):e27397.
7. He X-M, Zou D-H. The association of young age with local recurrence in women with early-stage breast cancer after breast-conserving therapy: a meta-analysis. Scientific Reports. 2017;7(1):11058.
8. Biganzoli L, Battisti NML, Wildiers H, McCartney A, Colloca G, Kunkler IH, et al. Updated recommendations regarding the management of older patients with breast cancer: a joint paper from the European Society of Breast Cancer Specialists (EUSOMA) and the International Society of Geriatric Oncology (SIOG). The Lancet Oncology. 2021;22(7):e327-e40.
9. Bagegni NA, Peterson LL. Chapter Two - Age-related disparities in older women with breast cancer. In: Ford ME, Esnaola NF, Salley JD, editors. Advances in Cancer Research. 146: Academic Press; 2020. p. 23-56.
10. Warner E, Foulkes W, Goodwin P, Meschino W, Blondal J, Paterson C, et al. Prevalence and Penetrance of BRCA1 and BRCA2 Gene Mutations in Unselected Ashkenazi Jewish Women With Breast Cancer. JNCI: Journal of the National Cancer Institute. 1999;91(14):1241-7.
11. Jatoi I, Sung H, Jemal A. The Emergence of the Racial Disparity in U.S. Breast-Cancer Mortality. New England Journal of Medicine. 2022;386(25):2349-52.
12. Giordano SH. Breast Cancer in Men. New England Journal of Medicine. 2018;378(24):2311-20.
13. Yao N, Shi W, Liu T, Siyin ST, Wang W, Duan N, et al. Clinicopathologic characteristics and prognosis for male breast cancer compared to female breast cancer. Scientific Reports. 2022;12(1):220.
14. Ottini L, Masala G, D'Amico C, Mancini B, Saieva C, Aceto G, et al. BRCA1 and BRCA2 mutation status and tumor characteristics in male breast cancer: a population-based study in Italy. Cancer Res. 2003;63(2):342-7.
15. Tung N, Battelli C, Allen B, Kaldate R, Bhatnagar S, Bowles K, et al. Frequency of mutations in individuals with breast cancer referred for BRCA1 and BRCA2 testing using next-generation sequencing with a 25-gene panel. Cancer. 2015;121(1):25-33.

16. Mahdavi M, Nassiri M, Kooshyar MM, Vakili-Azghandi M, Avan A, Sandry R, et al. Hereditary breast cancer; Genetic penetrance and current status with BRCA. J Cell Physiol. 2019;234(5):5741-50.
17. Mavaddat N, Barrowdale D, Andrulis IL, Domchek SM, Eccles D, Nevanlinna H, et al. Pathology of breast and ovarian cancers among BRCA1 and BRCA2 mutation carriers: results from the Consortium of Investigators of Modifiers of BRCA1/2 (CIMBA). Cancer Epidemiol Biomarkers Prev. 2012;21(1):134-47.
18. Daly MB, Pal T, Berry MP, Buys SS, Dickson P, Domchek SM, et al. Genetic/Familial High-Risk Assessment: Breast, Ovarian, and Pancreatic, Version 2.2021, NCCN Clinical Practice Guidelines in Oncology. Journal of the National Comprehensive Cancer Network. 2021;19(1):77-102.
19. Nara M, Ishihara S, Kitano A, Tamura N, Aruga T, Kobayashi D, et al. Does breast-conserving surgery with radiotherapy in BRCA-mutation carriers significantly increase ipsilateral breast tumor recurrence? A systematic review and meta-analysis. Breast Cancer. 2022;29(3):394-401.
20. Metcalfe K, Lynch HT, Ghadirian P, Tung N, Olivotto I, Warner E, et al. Contralateral Breast Cancer in BRCA1 and BRCA2 Mutation Carriers. Journal of Clinical Oncology. 2004;22(12):2328-35.
21. Huber-Keener KJ. Cancer genetics and breast cancer. Best Practice & Research Clinical Obstetrics & Gynaecology. 2022;82:3-11.
22. Kim EJ, Park HS, Kim JY, Kim SI, Cho YU, Park BW. Assessment of the Prognostic Staging System of American Joint Committee on Cancer 8th Edition for Breast Cancer: Comparisons with the Conventional Anatomic Staging System. J Breast Cancer. 2020;23(1):59-68.
23. Goldhirsch A, Glick JH, Gelber RD, Senn H-J. Meeting Highlights: International Consensus Panel on the Treatment of Primary Breast Cancer. JNCI: Journal of the National Cancer Institute. 1998;90(21):1601-8.
24. Rakha EA, Tse GM, Quinn CM. An update on the pathological classification of breast cancer. Histopathology. 2023;82(1):5-16.
25. Oldenhuis CN, Oosting SF, Gietema JA, de Vries EG. Prognostic versus predictive value of biomarkers in oncology. Eur J Cancer. 2008;44(7):946-53.
26. Cardoso F, Kyriakides S, Ohno S, Penault-Llorca F, Poortmans P, Rubio IT, et al. Early breast cancer: ESMO Clinical Practice Guidelines for diagnosis, treatment and follow-up[†]. Annals of Oncology. 2019;30(8):1194-220.
27. Howlader N, Cronin KA, Kurian AW, Andridge R. Differences in Breast Cancer Survival by Molecular Subtypes in the United States. Cancer Epidemiology, Biomarkers & Prevention. 2018;27(6):619-26.
28. Sopik V, Sun P, Narod SA. The prognostic effect of estrogen receptor status differs for younger versus older breast cancer patients. Breast Cancer Res Treat. 2017;165(2):391-402.
29. Van Asten K, Slembrouck L, Olbrecht S, Jongen L, Brouckaert O, Wildiers H, et al. Prognostic Value of the Progesterone Receptor by Subtype in Patients with Estrogen Receptor-Positive, HER-2 Negative Breast Cancer. Oncologist. 2019;24(2):165-71.
30. Borg A, Tandon AK, Sigurdsson H, Clark GM, Fernö M, Fuqua SA, et al. HER-2/neu amplification predicts poor survival in node-positive breast cancer. Cancer Res. 1990;50(14):4332-7.
31. Romond EH, Perez EA, Bryant J, Suman VJ, Geyer CE, Davidson NE, et al. Trastuzumab plus Adjuvant Chemotherapy for Operable HER2-Positive Breast Cancer. New England Journal of Medicine. 2005;353(16):1673-84.

32. Hassing CMS, Nielsen DL, Knoop AS, Tvedskov THF, Kroman N, Lænkholm A-V, et al. Adjuvant treatment with trastuzumab of patients with HER2-positive, T1a-bN0M0 breast tumors: A systematic review and meta-analysis. Critical Reviews in Oncology/Hematology. 2023;184:103952.
33. Early Breast Cancer Trialists' Collaborative G. Relevance of breast cancer hormone receptors and other factors to the efficacy of adjuvant tamoxifen: patient-level meta-analysis of randomised trials. The Lancet. 2011;378(9793):771-84.
34. Bekes I, Huober J. Extended Adjuvant Endocrine Therapy in Early Breast Cancer Patients-Review and Perspectives. Cancers (Basel). 2023;15(16).
35. Miller I, Min M, Yang C, Tian C, Gookin S, Carter D, et al. Ki67 is a Graded Rather than a Binary Marker of Proliferation versus Quiescence. Cell Reports. 2018;24(5):1105-12.e5.
36. Ki-67 expression is associated with poor prognosis in early-stage breast cancer. Nature Clinical Practice Oncology. 2007;4(8):445-.
37. Goldhirsch A, Winer EP, Coates AS, Gelber RD, Piccart-Gebhart M, Thürlimann B, et al. Personalizing the treatment of women with early breast cancer: highlights of the St Gallen International Expert Consensus on the Primary Therapy of Early Breast Cancer 2013. Annals of Oncology. 2013;24(9):2206-23.
38. Nielsen TO, Leung SCY, Rimm DL, Dodson A, Acs B, Badve S, et al. Assessment of Ki67 in Breast Cancer: Updated Recommendations From the International Ki67 in Breast Cancer Working Group. J Natl Cancer Inst. 2021;113(7):808-19.
39. Conforti F, Nekljudova V, Sala I, Ascari R, Solbach C, Untch M, et al. Surrogate End Points for Overall Survival in Neoadjuvant Randomized Clinical Trials for Early Breast Cancer. Journal of Clinical Oncology.0(0):JCO-24-01360.
40. Huang M, O'Shaughnessy J, Zhao J, Haiderali A, Cortés J, Ramsey SD, et al. Association of Pathologic Complete Response with Long-Term Survival Outcomes in Triple-Negative Breast Cancer: A Meta-Analysis. Cancer Research. 2020;80(24):5427-34.
41. Schmid P, Cortes J, Dent R, Pusztai L, McArthur H, Kümmel S, et al. Event-free Survival with Pembrolizumab in Early Triple-Negative Breast Cancer. New England Journal of Medicine. 2022;386(6):556-67.
42. Swain SM, Macharia H, Cortes J, Dang C, Gianni L, Hurvitz SA, et al. Event-Free Survival in Patients with Early HER2-Positive Breast Cancer with a Pathological Complete Response after HER2-Targeted Therapy: A Pooled Analysis. Cancers (Basel). 2022;14(20).
43. Gianni L, Pienkowski T, Im YH, Roman L, Tseng LM, Liu MC, et al. Efficacy and safety of neoadjuvant pertuzumab and trastuzumab in women with locally advanced, inflammatory, or early HER2-positive breast cancer (NeoSphere): a randomised multicentre, open-label, phase 2 trial. Lancet Oncol. 2012;13(1):25-32.
44. Huang L, Pang D, Yang H, Li W, Wang S, Cui S, et al. Neoadjuvant-adjuvant pertuzumab in HER2-positive early breast cancer: final analysis of the randomized phase III PEONY trial. Nat Commun. 2024;15(1):2153.
45. Spring LM, Fell G, Arfe A, Sharma C, Greenup R, Reynolds KL, et al. Pathologic Complete Response after Neoadjuvant Chemotherapy and Impact on Breast Cancer Recurrence and Survival: A Comprehensive Meta-analysis. Clin Cancer Res. 2020;26(12):2838-48.
46. Passarelli MN, Newcomb PA, Hampton JM, Trentham-Dietz A, Titus LJ, Egan KM, et al. Cigarette Smoking Before and After Breast Cancer Diagnosis: Mortality

From Breast Cancer and Smoking-Related Diseases. J Clin Oncol. 2016;34(12):1315-22.
47. Duan W, Li S, Meng X, Sun Y, Jia C. Smoking and survival of breast cancer patients: A meta-analysis of cohort studies. The Breast. 2017;33:117-24.
48. LoConte NK, Brewster AM, Kaur JS, Merrill JK, Alberg AJ. Alcohol and Cancer: A Statement of the American Society of Clinical Oncology. J Clin Oncol. 2018;36(1):83-93.
49. Kwan ML, Kushi LH, Weltzien E, Tam EK, Castillo A, Sweeney C, et al. Alcohol consumption and breast cancer recurrence and survival among women with early-stage breast cancer: the life after cancer epidemiology study. J Clin Oncol. 2010;28(29):4410-6.
50. Zeinomar N, Qin B, Amin S, Lin Y, Xu B, Chanumolu D, et al. Association of Cigarette Smoking and Alcohol Consumption With Subsequent Mortality Among Black Breast Cancer Survivors in New Jersey. JAMA Network Open. 2023;6(1):e2252371-e.
51. De Cicco P, Catani MV, Gasperi V, Sibilano M, Quaglietta M, Savini I. Nutrition and Breast Cancer: A Literature Review on Prevention, Treatment and Recurrence. Nutrients. 2019;11(7):1514.
52. Kang HJ, Lee SY, Lee DY, Kang JH, Kim JH, Kim HW, et al. Main mechanisms for carcinogenic heterocyclic amine reduction in cooked meat by natural materials. Meat Science. 2022;183:108663.
53. Snyderwine EG, Yu M, Schut HAJ, Knight-Jones L, Kimura S. Effect of CYP1A2 deficiency on heterocyclic amine DNA adduct levels in mice. Food and Chemical Toxicology. 2002;40(10):1529-33.
54. Farvid MS, Stern MC, Norat T, Sasazuki S, Vineis P, Weijenberg MP, et al. Consumption of red and processed meat and breast cancer incidence: A systematic review and meta-analysis of prospective studies. International Journal of Cancer. 2018;143(11):2787-99.
55. Schlesinger S, Chan DSM, Vingeliene S, Vieira AR, Abar L, Polemiti E, et al. Carbohydrates, glycemic index, glycemic load, and breast cancer risk: a systematic review and dose-response meta-analysis of prospective studies. Nutr Rev. 2017;75(6):420-41.
56. Lodi M, Kiehl A, Qu FL, Gabriele V, Tomasetto C, Mathelin C. Lipid Intake and Breast Cancer Risk: Is There a Link? A New Focus and Meta-Analysis. Eur J Breast Health. 2022;18(2):108-26.
57. Devericks EN, Carson MS, McCullough LE, Coleman MF, Hursting SD. The obesity-breast cancer link: a multidisciplinary perspective. Cancer and Metastasis Reviews. 2022;41(3):607-25.
58. Mohanty SS, Mohanty PK. Obesity as potential breast cancer risk factor for postmenopausal women. Genes Dis. 2021;8(2):117-23.
59. Morad SA, Cabot MC. Ceramide-orchestrated signalling in cancer cells. Nat Rev Cancer. 2013;13(1):51-65.
60. Saponaro C, Gaggini M, Carli F, Gastaldelli A. The Subtle Balance between Lipolysis and Lipogenesis: A Critical Point in Metabolic Homeostasis. Nutrients. 2015;7(11):9453-74.
61. Koundouros N, Poulogiannis G. Reprogramming of fatty acid metabolism in cancer. British Journal of Cancer. 2020;122(1):4-22.
62. Bhardwaj P, Au CC, Benito-Martin A, Ladumor H, Oshchepkova S, Moges R, et al. Estrogens and breast cancer: Mechanisms involved in obesity-related development, growth and progression. J Steroid Biochem Mol Biol. 2019;189:161-70.

63. Lohmann AE, Soldera SV, Pimentel I, Ribnikar D, Ennis M, Amir E, et al. Association of Obesity With Breast Cancer Outcome in Relation to Cancer Subtypes: A Meta-Analysis. JNCI: Journal of the National Cancer Institute. 2021;113(11):1465-75.
64. UK CR. Breast cancer statistics [Available from: https://www.cancerresearchuk.org/health-professional/cancer-statistics/statistics-by-cancer-type/breast-cancer#heading-Eight.
65. Lundqvist A, Andersson E, Ahlberg I, Nilbert M, Gerdtham U. Socioeconomic inequalities in breast cancer incidence and mortality in Europe-a systematic review and meta-analysis. Eur J Public Health. 2016;26(5):804-13.
66. Smith D, Thomson K, Bambra C, Todd A. The breast cancer paradox: A systematic review of the association between area-level deprivation and breast cancer screening uptake in Europe. Cancer Epidemiol. 2019;60:77-85.
67. Selli C, Dixon JM, Sims AH. Accurate prediction of response to endocrine therapy in breast cancer patients: current and future biomarkers. Breast Cancer Research. 2016;18(1):118.
68. Russo J, Russo IH. The role of estrogen in the initiation of breast cancer. J Steroid Biochem Mol Biol. 2006;102(1-5):89-96.
69. Huang B, Omoto Y, Iwase H, Yamashita H, Toyama T, Coombes RC, et al. Differential expression of estrogen receptor α, β1, and β2 in lobular and ductal breast cancer. Proc Natl Acad Sci U S A. 2014;111(5):1933-8.
70. Yaşar P, Ayaz G, User SD, Güpür G, Muyan M. Molecular mechanism of estrogen-estrogen receptor signaling. Reprod Med Biol. 2017;16(1):4-20.
71. Louie MC, Sevigny MB. Steroid hormone receptors as prognostic markers in breast cancer. Am J Cancer Res. 2017;7(8):1617-36.
72. Khan JA, Bellance C, Guiochon-Mantel A, Lombès M, Loosfelt H. Differential Regulation of Breast Cancer-Associated Genes by Progesterone Receptor Isoforms PRA and PRB in a New Bi-Inducible Breast Cancer Cell Line. PLOS ONE. 2012;7(9):e45993.
73. Bleach R, McIlroy M. The Divergent Function of Androgen Receptor in Breast Cancer; Analysis of Steroid Mediators and Tumor Intracrinology. Front Endocrinol (Lausanne). 2018;9:594.
74. Schuler LA, O'Leary KA. Prolactin: The Third Hormone in Breast Cancer. Front Endocrinol (Lausanne). 2022;13:910978.
75. KONTOMANOLIS EN, KOUTRAS A, SYLLAIOS A, SCHIZAS D, MASTORAKI A, GARMPIS N, et al. Role of Oncogenes and Tumor-suppressor Genes in Carcinogenesis: A Review. Anticancer Research. 2020;40(11):6009-15.
76. Loibl S, Gianni L. HER2-positive breast cancer. The Lancet. 2017;389(10087):2415-29.
77. Cordo Russo RI, Chervo MF, Madera S, Charreau EH, Elizalde PV. Nuclear ErbB-2: a Novel Therapeutic Target in ErbB-2-Positive Breast Cancer? Hormones and Cancer. 2019;10(2):64-70.
78. Wee P, Wang Z. Epidermal Growth Factor Receptor Cell Proliferation Signaling Pathways. Cancers. 2017;9(5):52.
79. Chen H, Liu H, Qing G. Targeting oncogenic Myc as a strategy for cancer treatment. Signal Transduction and Targeted Therapy. 2018;3(1):5.
80. Lee EYHP, Muller WJ. Oncogenes and Tumor Suppressor Genes. Cold Spring Harbor Perspectives in Biology. 2010;2(10).
81. Osborne C, Wilson P, Tripathy D. Oncogenes and Tumor Suppressor Genes in Breast Cancer: Potential Diagnostic and Therapeutic Applications. The Oncologist. 2004;9(4):361-77.

82. Chen X, Zhang T, Su W, Dou Z, Zhao D, Jin X, et al. Mutant p53 in cancer: from molecular mechanism to therapeutic modulation. Cell Death & Disease. 2022;13(11):974.
83. Marvalim C, Datta A, Lee SC. Role of p53 in breast cancer progression: An insight into p53 targeted therapy. Theranostics. 2023;13(4):1421-42.
84. Gorodetska I, Kozeretska I, Dubrovska A. BRCA Genes: The Role in Genome Stability, Cancer Stemness and Therapy Resistance. Journal of Cancer. 2019;10(9):2109-27.
85. Buocikova V, Rios-Mondragon I, Pilalis E, Chatziioannou A, Miklikova S, Mego M, et al. Epigenetics in Breast Cancer Therapy—New Strategies and Future Nanomedicine Perspectives. Cancers. 2020;12(12):3622.
86. Guo Q, Zhou Y, Xie T, Yuan Y, Li H, Shi W, et al. Tumor microenvironment of cancer stem cells: Perspectives on cancer stem cell targeting. Genes & Diseases. 2024;11(3):101043.
87. Gonzalez H, Hagerling C, Werb Z. Roles of the immune system in cancer: from tumor initiation to metastatic progression. Genes Dev. 2018;32(19-20):1267-84.
88. Loibl S, André F, Bachelot T, Barrios CH, Bergh J, Burstein HJ, et al. Early breast cancer: ESMO Clinical Practice Guideline for diagnosis, treatment and follow-up[☆]. Annals of Oncology. 2024;35(2):159-82.
89. Veronesi U, Cascinelli N, Mariani L, Greco M, Saccozzi R, Luini A, et al. Twenty-Year Follow-up of a Randomized Study Comparing Breast-Conserving Surgery with Radical Mastectomy for Early Breast Cancer. New England Journal of Medicine. 2002;347(16):1227-32.
90. National Comprehensive Cancer Network. Breast Cancer (Version 4.2024) [Available from: https://www.nccn.org/professionals/physician_gls/pdf/breast.pdf.
91. Soran A, Ozmen V, Ozbas S, Karanlik H, Muslumanoglu M, Igci A, et al. Randomized Trial Comparing Resection of Primary Tumor with No Surgery in Stage IV Breast Cancer at Presentation: Protocol MF07-01. Annals of Surgical Oncology. 2018;25(11):3141-9.
92. Chatterjee A, Serniak N, Czerniecki BJ. Sentinel lymph node biopsy in breast cancer: a work in progress. Cancer J. 2015;21(1):7-10.
93. Giuliano AE, Ballman KV, McCall L, Beitsch PD, Brennan MB, Kelemen PR, et al. Effect of Axillary Dissection vs No Axillary Dissection on 10-Year Overall Survival Among Women With Invasive Breast Cancer and Sentinel Node Metastasis: The ACOSOG Z0011 (Alliance) Randomized Clinical Trial. Jama. 2017;318(10):918-26.
94. Cavalcante FP, Millen EC, Zerwes FP, Novita GG. Role of Axillary Surgery After Neoadjuvant Chemotherapy. JCO Global Oncology. 2020(6):238-41.
95. Kuemmel S, Heil J, Bruzas S, Breit E, Schindowski D, Harrach H, et al. Safety of Targeted Axillary Dissection After Neoadjuvant Therapy in Patients With Node-Positive Breast Cancer. JAMA Surgery. 2023;158(8):807-15.
96. Minami CA, Bryan AF, Freedman RA, Revette AC, Schonberg MA, King TA, et al. Assessment of Oncologists' Perspectives on Omission of Sentinel Lymph Node Biopsy in Women 70 Years and Older With Early-Stage Hormone Receptor-Positive Breast Cancer. JAMA Netw Open. 2022;5(8):e2228524.
97. Shah C, Al-Hilli Z, Vicini F. Advances in Breast Cancer Radiotherapy: Implications for Current and Future Practice. JCO Oncology Practice. 2021;17(12):697-706.
98. Fisher B, Anderson S, Bryant J, Margolese RG, Deutsch M, Fisher ER, et al. Twenty-Year Follow-up of a Randomized Trial Comparing Total Mastectomy,

Lumpectomy, and Lumpectomy plus Irradiation for the Treatment of Invasive Breast Cancer. New England Journal of Medicine. 2002;347(16):1233-41.
99. Bartels SAL, Donker M, Poncet C, Sauvé N, Straver ME, Velde CJHvd, et al. Radiotherapy or Surgery of the Axilla After a Positive Sentinel Node in Breast Cancer: 10-Year Results of the Randomized Controlled EORTC 10981-22023 AMAROS Trial. Journal of Clinical Oncology. 2023;41(12):2159-65.
100. Strnad V, Ott OJ, Hildebrandt G, Kauer-Dorner D, Knauerhase H, Major T, et al. 5-year results of accelerated partial breast irradiation using sole interstitial multicatheter brachytherapy versus whole-breast irradiation with boost after breast-conserving surgery for low-risk invasive and in-situ carcinoma of the female breast: a randomised, phase 3, non-inferiority trial. The Lancet. 2016;387(10015):229-38.
101. Haussmann J, Corradini S, Nestle-Kraemling C, Bölke E, Njanang FJD, Tamaskovics B, et al. Recent advances in radiotherapy of breast cancer. Radiation Oncology. 2020;15(1):71.
102. Sousa C, Cruz M, Neto A, Pereira K, Peixoto M, Bastos J, et al. Neoadjuvant radiotherapy in the approach of locally advanced breast cancer. ESMO Open. 2020;5(2).
103. Ciocon SLB, Sousa C, Marta GN, Kwan JYY. Palliative radiation therapy for locally advanced breast cancer. Curr Opin Support Palliat Care. 2025;19(1):41-50.
104. Corti C, Batra-Sharma H, Kelsten M, Shatsky RA, Garrido-Castro AC, Gradishar WJ. Systemic Therapy in Breast Cancer. American Society of Clinical Oncology Educational Book. 2024;44(3):e432442.
105. Wang J, Wu SG. Breast Cancer: An Overview of Current Therapeutic Strategies, Challenge, and Perspectives. Breast Cancer (Dove Med Press). 2023;15:721-30.
106. Linders AN, Dias IB, López Fernández T, Tocchetti CG, Bomer N, Van der Meer P. A review of the pathophysiological mechanisms of doxorubicin-induced cardiotoxicity and aging. npj Aging. 2024;10(1):9.
107. Jawad B, Poudel L, Podgornik R, Steinmetz NF, Ching WY. Molecular mechanism and binding free energy of doxorubicin intercalation in DNA. Phys Chem Chem Phys. 2019;21(7):3877-93.
108. Ichikawa Y, Ghanefar M, Bayeva M, Wu R, Khechaduri A, Naga Prasad SV, et al. Cardiotoxicity of doxorubicin is mediated through mitochondrial iron accumulation. J Clin Invest. 2014;124(2):617-30.
109. Parness J, Horwitz SB. Taxol binds to polymerized tubulin in vitro. J Cell Biol. 1981;91(2 Pt 1):479-87.
110. Noll DM, Mason TM, Miller PS. Formation and repair of interstrand cross-links in DNA. Chem Rev. 2006;106(2):277-301.
111. Blanchette P, Sivajohanathan D, Bartlett J, Eisen A, Feilotter H, Pezo R, et al. Clinical Utility of Multigene Profiling Assays in Early-Stage Invasive Breast Cancer: An Ontario Health (Cancer Care Ontario) Clinical Practice Guideline. Curr Oncol. 2022;29(4):2599-615.
112. Pistilli B, Lohrisch C, Sheade J, Fleming GF. Personalizing Adjuvant Endocrine Therapy for Early-Stage Hormone Receptor–Positive Breast Cancer. American Society of Clinical Oncology Educational Book. 2022(42):60-72.
113. Effects of chemotherapy and hormonal therapy for early breast cancer on recurrence and 15-year survival: an overview of the randomised trials. The Lancet. 2005;365(9472):1687-717.
114. Miller WR. Aromatase inhibitors: mechanism of action and role in the treatment of breast cancer. Semin Oncol. 2003;30(4 Suppl 14):3-11.

115. Aromatase inhibitors versus tamoxifen in early breast cancer: patient-level meta-analysis of the randomised trials. The Lancet. 2015;386(10001):1341-52.
116. Rachner TD, Göbel A, Jaschke NP, Hofbauer LC. Challenges in Preventing Bone Loss Induced by Aromatase Inhibitors. The Journal of Clinical Endocrinology & Metabolism. 2020;105(10):3122-33.
117. Pagani O, Walley BA, Fleming GF, Colleoni M, Láng I, Gomez HL, et al. Adjuvant Exemestane With Ovarian Suppression in Premenopausal Breast Cancer: Long-Term Follow-Up of the Combined TEXT and SOFT Trials. Journal of Clinical Oncology. 2023;41(7):1376-82.
118. Francis PA, Regan MM, Fleming GF, Láng I, Ciruelos E, Bellet M, et al. Adjuvant Ovarian Suppression in Premenopausal Breast Cancer. New England Journal of Medicine. 2015;372(5):436-46.
119. Slamon DJ, Clark GM, Wong SG, Levin WJ, Ullrich A, McGuire WL. Human Breast Cancer: Correlation of Relapse and Survival with Amplification of the HER-2/neu Oncogene. Science. 1987;235(4785):177-82.
120. Sawyers CL. Herceptin: A First Assault on Oncogenes that Launched a Revolution. Cell. 2019;179(1):8-12.
121. Trastuzumab for early-stage, HER2-positive breast cancer: a meta-analysis of 13 864 women in seven randomised trials. Lancet Oncol. 2021;22(8):1139-50.
122. Geyer CE, Forster J, Lindquist D, Chan S, Romieu CG, Pienkowski T, et al. Lapatinib plus Capecitabine for HER2-Positive Advanced Breast Cancer. New England Journal of Medicine. 2006;355(26):2733-43.
123. Verma S, Miles D, Gianni L, Krop IE, Welslau M, Baselga J, et al. Trastuzumab Emtansine for HER2-Positive Advanced Breast Cancer. New England Journal of Medicine. 2012;367(19):1783-91.
124. Hudis CA. Trastuzumab — Mechanism of Action and Use in Clinical Practice. New England Journal of Medicine. 2007;357(1):39-51.
125. Franklin MC, Carey KD, Vajdos FF, Leahy DJ, de Vos AM, Sliwkowski MX. Insights into ErbB signaling from the structure of the ErbB2-pertuzumab complex. Cancer Cell. 2004;5(4):317-28.
126. Swain SM, Baselga J, Kim S-B, Ro J, Semiglazov V, Campone M, et al. Pertuzumab, Trastuzumab, and Docetaxel in HER2-Positive Metastatic Breast Cancer. New England Journal of Medicine. 2015;372(8):724-34.
127. Gianni L, Pienkowski T, Im YH, Tseng LM, Liu MC, Lluch A, et al. 5-year analysis of neoadjuvant pertuzumab and trastuzumab in patients with locally advanced, inflammatory, or early-stage HER2-positive breast cancer (NeoSphere): a multicentre, open-label, phase 2 randomised trial. Lancet Oncol. 2016;17(6):791-800.
128. Wang X, Zhao S, Xin Q, Zhang Y, Wang K, Li M. Recent progress of CDK4/6 inhibitors' current practice in breast cancer. Cancer Gene Therapy. 2024;31(9):1283-91.
129. Klein ME, Kovatcheva M, Davis LE, Tap WD, Koff A. CDK4/6 Inhibitors: The Mechanism of Action May Not Be as Simple as Once Thought. Cancer Cell. 2018;34(1):9-20.
130. Slamon DJ, Stroyakovskiy D, Yardley DA, Huang C-S, Fasching PA, Crown J, et al. Ribociclib and endocrine therapy as adjuvant treatment in patients with HR+/HER2- early breast cancer: Primary results from the phase III NATALEE trial. Journal of Clinical Oncology. 2023;41(17_suppl):LBA500-LBA.
131. Johnston SRD, Toi M, O'Shaughnessy J, Rastogi P, Campone M, Neven P, et al. Abemaciclib plus endocrine therapy for hormone receptor-positive, HER2-negative, node-positive, high-risk early breast cancer (monarchE): results from a

preplanned interim analysis of a randomised, open-label, phase 3 trial. Lancet Oncol. 2023;24(1):77-90.
132. Lu YS, Im SA, Colleoni M, Franke F, Bardia A, Cardoso F, et al. Updated Overall Survival of Ribociclib plus Endocrine Therapy versus Endocrine Therapy Alone in Pre- and Perimenopausal Patients with HR+/HER2- Advanced Breast Cancer in MONALEESA-7: A Phase III Randomized Clinical Trial. Clin Cancer Res. 2022;28(5):851-9.
133. Zhou T, Zhang J. Therapeutic advances and application of PARP inhibitors in breast cancer. Transl Oncol. 2025;57:102410.
134. Patel AG, Sarkaria JN, Kaufmann SH. Nonhomologous end joining drives poly(ADP-ribose) polymerase (PARP) inhibitor lethality in homologous recombination-deficient cells. Proceedings of the National Academy of Sciences. 2011;108(8):3406-11.
135. Schmid P, Adams S, Rugo HS, Schneeweiss A, Barrios CH, Iwata H, et al. Atezolizumab and Nab-Paclitaxel in Advanced Triple-Negative Breast Cancer. New England Journal of Medicine. 2018;379(22):2108-21.
136. Schmid P, Cortes J, Pusztai L, McArthur H, Kümmel S, Bergh J, et al. Pembrolizumab for Early Triple-Negative Breast Cancer. New England Journal of Medicine. 2020;382(9):810-21.
137. Mittendorf EA, Zhang H, Barrios CH, Saji S, Jung KH, Hegg R, et al. Neoadjuvant atezolizumab in combination with sequential nab-paclitaxel and anthracycline-based chemotherapy versus placebo and chemotherapy in patients with early-stage triple-negative breast cancer (IMpassion031): a randomised, double-blind, phase 3 trial. The Lancet. 2020;396(10257):1090-100.
138. Diéras V, Miles D, Verma S, Pegram M, Welslau M, Baselga J, et al. Trastuzumab emtansine versus capecitabine plus lapatinib in patients with previously treated HER2-positive advanced breast cancer (EMILIA): a descriptive analysis of final overall survival results from a randomised, open-label, phase 3 trial. The Lancet Oncology. 2017;18(6):732-42.
139. Curigliano G, Romieu G, Campone M, Dorval T, Duck L, Canon JL, et al. A phase I/II trial of the safety and clinical activity of a HER2-protein based immunotherapeutic for treating women with HER2-positive metastatic breast cancer. Breast Cancer Res Treat. 2016;156(2):301-10.
140. McArthur HL, Leal JHS, Page DB, Abaya CD, Basho RK, Phillips M, et al. Neoadjuvant HER2-targeted therapy +/- immunotherapy with pembrolizumab (neoHIP): An open-label randomized phase II trial. Journal of Clinical Oncology. 2022;40(16_suppl):TPS624-TPS.
141. Rugo HS, Delord J-P, Im S-A, Ott PA, Piha-Paul SA, Bedard PL, et al. Safety and Antitumor Activity of Pembrolizumab in Patients with Estrogen Receptor–Positive/Human Epidermal Growth Factor Receptor 2–Negative Advanced Breast Cancer. Clinical Cancer Research. 2018;24(12):2804-11.
142. Perou CM, Sørlie T, Eisen MB, van de Rijn M, Jeffrey SS, Rees CA, et al. Molecular portraits of human breast tumours. Nature. 2000;406(6797):747-52.
143. Sørlie T, Perou CM, Tibshirani R, Aas T, Geisler S, Johnsen H, et al. Gene expression patterns of breast carcinomas distinguish tumor subclasses with clinical implications. Proc Natl Acad Sci U S A. 2001;98(19):10869-74.
144. Sotiriou C, Wirapati P, Loi S, Harris A, Fox S, Smeds J, et al. Gene Expression Profiling in Breast Cancer: Understanding the Molecular Basis of Histologic Grade To Improve Prognosis. JNCI: Journal of the National Cancer Institute. 2006;98(4):262-72.

145. van 't Veer LJ, Dai H, van de Vijver MJ, He YD, Hart AAM, Mao M, et al. Gene expression profiling predicts clinical outcome of breast cancer. Nature. 2002;415(6871):530-6.
146. Wirapati P, Sotiriou C, Kunkel S, Farmer P, Pradervand S, Haibe-Kains B, et al. Meta-analysis of gene expression profiles in breast cancer: toward a unified understanding of breast cancer subtyping and prognosis signatures. Breast Cancer Research. 2008;10(4):R65.
147. Goldhirsch A, Wood WC, Gelber RD, Coates AS, Thürlimann B, Senn HJ. Progress and promise: highlights of the international expert consensus on the primary therapy of early breast cancer 2007. Annals of Oncology. 2007;18(7):1133-44.
148. Acheampong T, Kehm RD, Terry MB, Argov EL, Tehranifar P. Incidence Trends of Breast Cancer Molecular Subtypes by Age and Race/Ethnicity in the US From 2010 to 2016. JAMA Network Open. 2020;3(8):e2013226-e.
149. Comprehensive molecular portraits of human breast tumours. Nature. 2012;490(7418):61-70.
150. Nielsen TO, Jensen MB, Burugu S, Gao D, Jørgensen CL, Balslev E, et al. High-Risk Premenopausal Luminal A Breast Cancer Patients Derive no Benefit from Adjuvant Cyclophosphamide-based Chemotherapy: Results from the DBCG77B Clinical Trial. Clin Cancer Res. 2017;23(4):946-53.
151. Yu NY, Iftimi A, Yau C, Tobin NP, van ’t Veer L, Hoadley KA, et al. Assessment of Long-term Distant Recurrence-Free Survival Associated With Tamoxifen Therapy in Postmenopausal Patients With Luminal A or Luminal B Breast Cancer. JAMA Oncology. 2019;5(9):1304-9.
152. Ahn HJ, Jung SJ, Kim TH, Oh MK, Yoon HK. Differences in Clinical Outcomes between Luminal A and B Type Breast Cancers according to the St. Gallen Consensus 2013. J Breast Cancer. 2015;18(2):149-59.
153. Yang ZJ, Liu YX, Huang Y, Chen ZJ, Zhang HZ, Yu Y, et al. The regrouping of Luminal B (HER2 negative), a better discriminator of outcome and recurrence score. Cancer Med. 2023;12(3):2493-504.
154. McVeigh TP, Kerin MJ. Clinical use of the Oncotype DX genomic test to guide treatment decisions for patients with invasive breast cancer. Breast Cancer (Dove Med Press). 2017;9:393-400.
155. Sparano JA, Gray RJ, Makower DF, Pritchard KI, Albain KS, Hayes DF, et al. Adjuvant Chemotherapy Guided by a 21-Gene Expression Assay in Breast Cancer. N Engl J Med. 2018;379(2):111-21.
156. Sparano JA, Gray RJ, Ravdin PM, Makower DF, Pritchard KI, Albain KS, et al. Clinical and Genomic Risk to Guide the Use of Adjuvant Therapy for Breast Cancer. New England Journal of Medicine. 2019;380(25):2395-405.
157. Parise CA, Caggiano V. Breast Cancer Survival Defined by the ER/PR/HER2 Subtypes and a Surrogate Classification according to Tumor Grade and Immunohistochemical Biomarkers. Journal of Cancer Epidemiology. 2014;2014:469251.
158. Pegram M, Jackisch C, Johnston SRD. Estrogen/HER2 receptor crosstalk in breast cancer: combination therapies to improve outcomes for patients with hormone receptor-positive/HER2-positive breast cancer. npj Breast Cancer. 2023;9(1):45.
159. Kurokawa H, Lenferink AEG, Simpson JF, Pisacane PI, Sliwkowski MX, Forbes JT, et al. Inhibition of HER2/neu (erbB-2) and Mitogen-activated Protein Kinases Enhances Tamoxifen Action against HER2-overexpressing, Tamoxifen-resistant Breast Cancer Cells1. Cancer Research. 2000;60(20):5887-94.

160. Prat A, Perou CM. Deconstructing the molecular portraits of breast cancer. Mol Oncol. 2011;5(1):5-23.
161. Ahn S, Woo JW, Lee K, Park SY. HER2 status in breast cancer: changes in guidelines and complicating factors for interpretation. J Pathol Transl Med. 2020;54(1):34-44.
162. Wang J, Xu B. Targeted therapeutic options and future perspectives for HER2-positive breast cancer. Signal Transduction and Targeted Therapy. 2019;4(1):34.
163. Schlam I, Swain SM. HER2-positive breast cancer and tyrosine kinase inhibitors: the time is now. npj Breast Cancer. 2021;7(1):56.
164. National Comprehensive Cancer Network. Breast Cancer (Version 4.2023) 2023 [Available from: https://www.nccn.org/professionals/physician_gls/pdf/breast.pdf.
165. Dowling GP, Keelan S, Toomey S, Daly GR, Hennessy BT, Hill ADK. Review of the status of neoadjuvant therapy in HER2-positive breast cancer. Front Oncol. 2023;13:1066007.
166. Bradley R, Braybrooke J, Gray R, Hills R, Liu Z, Peto R, et al. Trastuzumab for early-stage, HER2-positive breast cancer: a meta-analysis of 13 864 women in seven randomised trials. The Lancet Oncology. 2021;22(8):1139-50.
167. Gianni L, Eiermann W, Semiglazov V, Lluch A, Tjulandin S, Zambetti M, et al. Neoadjuvant and adjuvant trastuzumab in patients with HER2-positive locally advanced breast cancer (NOAH): follow-up of a randomised controlled superiority trial with a parallel HER2-negative cohort. The Lancet Oncology. 2014;15(6):640-7.
168. Nader-Marta G, Martins-Branco D, de Azambuja E. How we treat patients with metastatic HER2-positive breast cancer. ESMO Open. 2022;7(1):100343.
169. Yin L, Duan J-J, Bian X-W, Yu S-c. Triple-negative breast cancer molecular subtyping and treatment progress. Breast Cancer Research. 2020;22(1):61.
170. Lehmann BD, Pietenpol JA, Tan AR. Triple-Negative Breast Cancer: Molecular Subtypes and New Targets for Therapy. American Society of Clinical Oncology Educational Book. 2015(35):e31-e9.
171. Zhou L, Yu C-W. Epigenetic modulations in triple-negative breast cancer: Therapeutic implications for tumor microenvironment. Pharmacological Research. 2024;204:107205.
172. Cortes J, Rugo HS, Cescon DW, Im S-A, Yusof MM, Gallardo C, et al. Pembrolizumab plus Chemotherapy in Advanced Triple-Negative Breast Cancer. New England Journal of Medicine. 2022;387(3):217-26.
173. Tutt ANJ, Garber JE, Kaufman B, Viale G, Fumagalli D, Rastogi P, et al. Adjuvant Olaparib for Patients with BRCA1- or BRCA2-Mutated Breast Cancer. New England Journal of Medicine. 2021;384(25):2394-405.
174. Bardia A, Hurvitz SA, Tolaney SM, Loirat D, Punie K, Oliveira M, et al. Sacituzumab Govitecan in Metastatic Triple-Negative Breast Cancer. New England Journal of Medicine. 2021;384(16):1529-41.
175. Nuncia-Cantarero M, Nieto-Jiménez C, Burgos M, Montero JC, Ocaña A, Galán-Moya EM. The tyrosine kinase inhibitor dasatinib blocks tumour growth, invasion and recurrence potential by interrupting the communication between cancer cells and their surrounding microenvironment in triple negative breast cancer. Annals of Oncology. 2019;30:v10.
176. Rampurwala M, Wisinski KB, O'Regan R. Role of the androgen receptor in triple-negative breast cancer. Clin Adv Hematol Oncol. 2016;14(3):186-93.

177. Mazzeo R, Sears J, Palmero L, Bolzonello S, Davis AA, Gerratana L, et al. Liquid biopsy in triple-negative breast cancer: unlocking the potential of precision oncology. ESMO Open. 2024;9(10).
178. Zaikova E, Cheng BYC, Cerda V, Kong E, Lai D, Lum A, et al. Circulating tumour mutation detection in triple-negative breast cancer as an adjunct to tissue response assessment. npj Breast Cancer. 2024;10(1):3.
179. Chen Z, Han F, Du Y, Shi H, Zhou W. Hypoxic microenvironment in cancer: molecular mechanisms and therapeutic interventions. Signal Transduct Target Ther. 2023;8(1):70.
180. Vaupel P, Höckel M, Mayer A. Detection and characterization of tumor hypoxia using pO2 histography. Antioxid Redox Signal. 2007;9(8):1221-35.
181. Ye IC, Fertig EJ, DiGiacomo JW, Considine M, Godet I, Gilkes DM. Molecular Portrait of Hypoxia in Breast Cancer: A Prognostic Signature and Novel HIF-Regulated Genes. Mol Cancer Res. 2018;16(12):1889-901.
182. Cimmino F, Avitabile M, Lasorsa VA, Montella A, Pezone L, Cantalupo S, et al. HIF-1 transcription activity: HIF1A driven response in normoxia and in hypoxia. BMC Medical Genetics. 2019;20(1):37.
183. Vaupel P. The role of hypoxia-induced factors in tumor progression. Oncologist. 2004;9 Suppl 5:10-7.
184. Semenza GL. Defining the role of hypoxia-inducible factor 1 in cancer biology and therapeutics. Oncogene. 2010;29(5):625-34.
185. Semenza GL. Hypoxia, clonal selection, and the role of HIF-1 in tumor progression. Crit Rev Biochem Mol Biol. 2000;35(2):71-103.
186. Höckel M, Vaupel P. Tumor Hypoxia: Definitions and Current Clinical, Biologic, and Molecular Aspects. JNCI: Journal of the National Cancer Institute. 2001;93(4):266-76.
187. Ivan M, Fishel ML, Tudoran OM, Pollok KE, Wu X, Smith PJ. Hypoxia signaling: Challenges and opportunities for cancer therapy. Seminars in Cancer Biology. 2022;85:185-95.
188. Nordsmark M, Bentzen SM, Overgaard J. Measurement of Human Tumour Oxygenation Status by a Polarographic Needle Electrode: An analysis of inter- and intratumour heterogeneity. Acta Oncologica. 1994;33(4):383-9.
189. Hopf HW, Hunt TK. Comparison of Clark Electrode and Optode for Measurement of Tissue Oxygen Tension. In: Vaupel P, Zander R, Bruley DF, editors. Oxygen Transport to Tissue XV. Boston, MA: Springer US; 1994. p. 841-7.
190. Hammond EM, Asselin MC, Forster D, O'Connor JPB, Senra JM, Williams KJ. The Meaning, Measurement and Modification of Hypoxia in the Laboratory and the Clinic. Clinical Oncology. 2014;26(5):277-88.
191. Godet I, Doctorman S, Wu F, Gilkes DM. Detection of Hypoxia in Cancer Models: Significance, Challenges, and Advances. Cells. 2022;11(4).
192. Wang GL, Jiang BH, Rue EA, Semenza GL. Hypoxia-inducible factor 1 is a basic-helix-loop-helix-PAS heterodimer regulated by cellular O2 tension. Proceedings of the National Academy of Sciences. 1995;92(12):5510-4.
193. Shi Y, Gilkes DM. HIF-1 and HIF-2 in cancer: structure, regulation, and therapeutic prospects. Cellular and Molecular Life Sciences. 2025;82(1):44.
194. dos Santos M, Mercante AM, Louro ID, Gonçalves AJ, de Carvalho MB, da Silva EH, et al. HIF1-alpha expression predicts survival of patients with squamous cell carcinoma of the oral cavity. PLoS One. 2012;7(9):e45228.
195. Gruber G, Greiner RH, Hlushchuk R, Aebersold DM, Altermatt HJ, Berclaz G, et al. Hypoxia-inducible factor 1 alpha in high-risk breast cancer: an independent prognostic parameter? Breast Cancer Research. 2004;6(3):R191.

196. Baba Y, Nosho K, Shima K, Irahara N, Chan AT, Meyerhardt JA, et al. HIF1A overexpression is associated with poor prognosis in a cohort of 731 colorectal cancers. Am J Pathol. 2010;176(5):2292-301.
197. McDonald PC, Dedhar S. Carbonic Anhydrase IX (CAIX) as a Mediator of Hypoxia-Induced Stress Response in Cancer Cells. In: Frost SC, McKenna R, editors. Carbonic Anhydrase: Mechanism, Regulation, Links to Disease, and Industrial Applications. Dordrecht: Springer Netherlands; 2014. p. 255-69.
198. Kaluz S, Kaluzová M, Liao SY, Lerman M, Stanbridge EJ. Transcriptional control of the tumor- and hypoxia-marker carbonic anhydrase 9: A one transcription factor (HIF-1) show? Biochim Biophys Acta. 2009;1795(2):162-72.
199. Li J, Zhang G, Wang X, Li XF. Is carbonic anhydrase IX a validated target for molecular imaging of cancer and hypoxia? Future Oncol. 2015;11(10):1531-41.
200. Kirkpatrick JP, Rabbani ZN, Bentley RC, Hardee ME, Karol S, Meyer J, et al. Elevated CAIX Expression is Associated with an Increased Risk of Distant Failure in Early-Stage Cervical Cancer. Biomark Insights. 2008;3:45-55.
201. Lorenzo-Pouso AI, Gallas-Torreira M, Pérez-Sayáns M, Chamorro-Petronacci CM, Alvarez-Calderon O, Takkouche B, et al. Prognostic value of CAIX expression in oral squamous cell carcinoma: a systematic review and meta-analysis. J Enzyme Inhib Med Chem. 2020;35(1):1258-66.
202. Ilie M, Mazure NM, Hofman V, Ammadi RE, Ortholan C, Bonnetaud C, et al. High levels of carbonic anhydrase IX in tumour tissue and plasma are biomarkers of poor prognostic in patients with non-small cell lung cancer. Br J Cancer. 2010;102(11):1627-35.
203. Ong CHC, Lee DY, Lee B, Li H, Lim JCT, Lim JX, et al. Hypoxia-regulated carbonic anhydrase IX (CAIX) protein is an independent prognostic indicator in triple negative breast cancer. Breast Cancer Res. 2022;24(1):38.
204. Numprasit W, Yangngam S, Prasopsiri J, Quinn JA, Edwards J, Thuwajit C. Carbonic anhydrase IX-related tumoral hypoxia predicts worse prognosis in breast cancer: A systematic review and meta-analysis. Frontiers in Medicine. 2023;10.
205. Hayashi M, Sakata M, Takeda T, Yamamoto T, Okamoto Y, Sawada K, et al. Induction of glucose transporter 1 expression through hypoxia-inducible factor 1α under hypoxic conditions in trophoblast-derived cells. Journal of Endocrinology. 2004;183(1):145-54.
206. Yu M, Yongzhi H, Chen S, Luo X, Lin Y, Zhou Y, et al. The prognostic value of GLUT1 in cancers: a systematic review and meta-analysis. Oncotarget. 2017;8(26):43356-67.
207. Le QT, Courter D. Clinical biomarkers for hypoxia targeting. Cancer Metastasis Rev. 2008;27(3):351-62.
208. Salven P, Mänpää H, Orpana A, Alitalo K, Joensuu H. Serum vascular endothelial growth factor is often elevated in disseminated cancer. Clin Cancer Res. 1997;3(5):647-51.
209. Petrik D, Lavori PW, Cao H, Zhu Y, Wong P, Christofferson E, et al. Plasma osteopontin is an independent prognostic marker for head and neck cancers. J Clin Oncol. 2006;24(33):5291-7.
210. Tatum JL. Hypoxia: Importance in tumor biology, noninvasive measurement by imaging, and value of its measurement in the management of cancer therapy. International Journal of Radiation Biology. 2006;82(10):699-757.
211. Jensen RL, Mumert ML, Gillespie DL, Kinney AY, Schabel MC, Salzman KL. Preoperative dynamic contrast-enhanced MRI correlates with molecular markers of hypoxia and vascularity in specific areas of intratumoral microenvironment and is predictive of patient outcome. Neuro-Oncology. 2013;16(2):280-91.

212. Baudelet C, Gallez B. How does blood oxygen level-dependent (BOLD) contrast correlate with oxygen partial pressure (pO2) inside tumors? Magnetic Resonance in Medicine. 2002;48(6):980-6.
213. Toma-Dasu I, Dasu A. Modelling Tumour Oxygenation, Reoxygenation and Implications on Treatment Outcome. Computational and Mathematical Methods in Medicine. 2013;2013(1):141087.
214. Wang LV, Hu S. Photoacoustic Tomography: In Vivo Imaging from Organelles to Organs. Science. 2012;335(6075):1458-62.
215. Chapman JD. Hypoxic sensitizers--implications for radiation therapy. N Engl J Med. 1979;301(26):1429-32.
216. Raleigh JA, Calkins-Adams DP, Rinker LH, Ballenger CA, Weissler MC, Fowler WC, Jr., et al. Hypoxia and vascular endothelial growth factor expression in human squamous cell carcinomas using pimonidazole as a hypoxia marker. Cancer Res. 1998;58(17):3765-8.
217. Evans SM, Hahn S, Pook DR, Jenkins WT, Chalian AA, Zhang P, et al. Detection of hypoxia in human squamous cell carcinoma by EF5 binding. Cancer Res. 2000;60(7):2018-24.
218. Liao D, Johnson RS. Hypoxia: A key regulator of angiogenesis in cancer. Cancer and Metastasis Reviews. 2007;26(2):281-90.
219. Pugh CW, Ratcliffe PJ. Regulation of angiogenesis by hypoxia: role of the HIF system. Nat Med. 2003;9(6):677-84.
220. Fukumura D, Kashiwagi S, Jain RK. The role of nitric oxide in tumour progression. Nat Rev Cancer. 2006;6(7):521-34.
221. Shi Y-h, Wang Y-x, Bingle L, Gong L-h, Heng W-j, Li Y, et al. In vitro study of HIF-1 activation and VEGF release by bFGF in the T47D breast cancer cell line under normoxic conditions: involvement of PI-3K/Akt and MEK1/ERK pathways. The Journal of Pathology. 2005;205(4):530-6.
222. Befani C, Liakos P. The role of hypoxia-inducible factor-2 alpha in angiogenesis. Journal of Cellular Physiology. 2018;233(12):9087-98.
223. Loboda A, Jozkowicz A, Dulak J. HIF-1 versus HIF-2 — Is one more important than the other? Vascular Pharmacology. 2012;56(5):245-51.
224. Magnussen AL, Mills IG. Vascular normalisation as the stepping stone into tumour microenvironment transformation. British Journal of Cancer. 2021;125(3):324-36.
225. Cheng H, Wang M, Su J, Li Y, Long J, Chu J, et al. Lipid Metabolism and Cancer. Life (Basel). 2022;12(6).
226. Chen M, Huang J. The expanded role of fatty acid metabolism in cancer: new aspects and targets. Precis Clin Med. 2019;2(3):183-91.
227. Snaebjornsson MT, Janaki-Raman S, Schulze A. Greasing the Wheels of the Cancer Machine: The Role of Lipid Metabolism in Cancer. Cell Metab. 2020;31(1):62-76.
228. Shi L, Tu BP. Acetyl-CoA and the regulation of metabolism: mechanisms and consequences. Curr Opin Cell Biol. 2015;33:125-31.
229. Röhrig F, Schulze A. The multifaceted roles of fatty acid synthesis in cancer. Nature Reviews Cancer. 2016;16(11):732-49.
230. Wakil SJ, Abu-Elheiga LA. Fatty acid metabolism: target for metabolic syndrome. Journal of Lipid Research. 2009;50:S138-S43.
231. Munir R, Lisec J, Swinnen JV, Zaidi N. Lipid metabolism in cancer cells under metabolic stress. British Journal of Cancer. 2019;120(12):1090-8.
232. Cangul H. Hypoxia upregulates the expression of the NDRG1 gene leading to its overexpression in various human cancers. BMC Genet. 2004;5:27.

233. Sevinsky CJ, Khan F, Kokabee L, Darehshouri A, Maddipati KR, Conklin DS. NDRG1 regulates neutral lipid metabolism in breast cancer cells. Breast Cancer Res. 2018;20(1):55.
234. Klawitter J, Shokati T, Moll V, Christians U, Klawitter J. Effects of lovastatin on breast cancer cells: a proteo-metabonomic study. Breast Cancer Research. 2010;12(2):R16.
235. Herst PM, Berridge MV. Cell surface oxygen consumption: A major contributor to cellular oxygen consumption in glycolytic cancer cell lines. Biochimica et Biophysica Acta (BBA) - Bioenergetics. 2007;1767(2):170-7.
236. Lee M, Yoon JH. Metabolic interplay between glycolysis and mitochondrial oxidation: The reverse Warburg effect and its therapeutic implication. World J Biol Chem. 2015;6(3):148-61.
237. Martínez-Reyes I, Chandel NS. Cancer metabolism: looking forward. Nature Reviews Cancer. 2021;21(10):669-80.
238. Cui XG, Han ZT, He SH, Wu XD, Chen TR, Shao CH, et al. HIF1/2α mediates hypoxia-induced LDHA expression in human pancreatic cancer cells. Oncotarget. 2017;8(15):24840-52.
239. Liberti MV, Locasale JW. The Warburg Effect: How Does it Benefit Cancer Cells? Trends Biochem Sci. 2016;41(3):211-8.
240. Ibrahim-Hashim A, Estrella V. Acidosis and cancer: from mechanism to neutralization. Cancer Metastasis Rev. 2019;38(1-2):149-55.
241. Sedlakova O, Svastova E, Takacova M, Kopacek J, Pastorek J, Pastorekova S. Carbonic anhydrase IX, a hypoxia-induced catalytic component of the pH regulating machinery in tumors. Front Physiol. 2014;4:400.
242. Queen A, Bhutto HN, Yousuf M, Syed MA, Hassan MI. Carbonic anhydrase IX: A tumor acidification switch in heterogeneity and chemokine regulation. Semin Cancer Biol. 2022;86(Pt 3):899-913.
243. Li Y, Wang H, Oosterwijk E, Selman Y, Mira JC, Medrano T, et al. Antibody-specific detection of CAIX in breast and prostate cancers. Biochem Biophys Res Commun. 2009;386(3):488-92.
244. Swietach P, Hulikova A, Vaughan-Jones RD, Harris AL. New insights into the physiological role of carbonic anhydrase IX in tumour pH regulation. Oncogene. 2010;29(50):6509-21.
245. Koltai T. CHAPTER X part I: COMPLEMENTARY PHARMACOLOGICAL INTERVENTIONS. 2018.
246. Laderoute KR. The interaction between HIF-1 and AP-1 transcription factors in response to low oxygen. Semin Cell Dev Biol. 2005;16(4-5):502-13.
247. Kaluz S, Kaluzová M, Stanbridge EJ. Rational design of minimal hypoxia-inducible enhancers. Biochem Biophys Res Commun. 2008;370(4):613-8.
248. Kaluz S, Kaluzová M, Stanbridge EJ. The role of extracellular signal-regulated protein kinase in transcriptional regulation of the hypoxia marker carbonic anhydrase IX. J Cell Biochem. 2006;97(1):207-16.
249. Shamis SAK, McMillan DC, Edwards J. The relationship between hypoxia-inducible factor 1α (HIF-1α) and patient survival in breast cancer: Systematic review and meta-analysis. Critical reviews in oncology/hematology. 2021;159:103231.
250. Huang LE, Gu J, Schau M, Bunn HF. Regulation of hypoxia-inducible factor 1alpha is mediated by an O2-dependent degradation domain via the ubiquitin-proteasome pathway. Proc Natl Acad Sci U S A. 1998;95(14):7987-92.
251. van Kuijk SJ, Yaromina A, Houben R, Niemans R, Lambin P, Dubois LJ. Prognostic Significance of Carbonic Anhydrase IX Expression in Cancer Patients: A Meta-Analysis. Front Oncol. 2016;6:69.

252. Pastorekova S, Gillies RJ. The role of carbonic anhydrase IX in cancer development: links to hypoxia, acidosis, and beyond. Cancer Metastasis Rev. 2019;38(1-2):65-77.
253. Becker HM. Carbonic anhydrase IX and acid transport in cancer. Br J Cancer. 2020;122(2):157-67.
254. Jamali S, Klier M, Ames S, Felipe Barros L, McKenna R, Deitmer JW, et al. Hypoxia-induced carbonic anhydrase IX facilitates lactate flux in human breast cancer cells by non-catalytic function. Scientific Reports. 2015;5(1):13605.
255. van Gisbergen MW, Offermans K, Voets AM, Lieuwes NG, Biemans R, Hoffmann RF, et al. Mitochondrial Dysfunction Inhibits Hypoxia-Induced HIF-1α Stabilization and Expression of Its Downstream Targets. Frontiers in Oncology. 2020;10.
256. Benej M, Svastova E, Banova R, Kopacek J, Gibadulinova A, Kery M, et al. CA IX Stabilizes Intracellular pH to Maintain Metabolic Reprogramming and Proliferation in Hypoxia. Front Oncol. 2020;10:1462.
257. Pillai S, Mahmud I, Mahar R, Griffith C, Langsen M, Nguyen J, et al. Lipogenesis mediated by OGR1 regulates metabolic adaptation to acid stress in cancer cells via autophagy. Cell Rep. 2022;39(6):110796.
258. Venkateswaran G, McDonald PC, Chafe SC, Brown WS, Gerbec ZJ, Awrey SJ, et al. A Carbonic Anhydrase IX/SLC1A5 Axis Regulates Glutamine Metabolism Dependent Ferroptosis in Hypoxic Tumor Cells. Mol Cancer Ther. 2023;22(10):1228-42.
259. Kreuzer M, Banerjee A, Birts CN, Darley M, Tavassoli A, Ivan M, et al. Glycolysis, via NADH-dependent dimerisation of CtBPs, regulates hypoxia-induced expression of CAIX and stem-like breast cancer cell survival. FEBS Lett. 2020;594(18):2988-3001.
260. Mendler AN, Hu B, Prinz PU, Kreutz M, Gottfried E, Noessner E. Tumor lactic acidosis suppresses CTL function by inhibition of p38 and JNK/c-Jun activation. Int J Cancer. 2012;131(3):633-40.
261. Bosticardo M, Ariotti S, Losana G, Bernabei P, Forni G, Novelli F. Biased activation of human T lymphocytes due to low extracellular pH is antagonized by B7/CD28 costimulation. Eur J Immunol. 2001;31(9):2829-38.
262. Huber V, Camisaschi C, Berzi A, Ferro S, Lugini L, Triulzi T, et al. Cancer acidity: An ultimate frontier of tumor immune escape and a novel target of immunomodulation. Semin Cancer Biol. 2017;43:74-89.
263. Chafe SC, McDonald PC, Saberi S, Nemirovsky O, Venkateswaran G, Burugu S, et al. Targeting Hypoxia-Induced Carbonic Anhydrase IX Enhances Immune-Checkpoint Blockade Locally and Systemically. Cancer Immunol Res. 2019;7(7):1064-78.
264. Yang MH, Wu MZ, Chiou SH, Chen PM, Chang SY, Liu CJ, et al. Direct regulation of TWIST by HIF-1alpha promotes metastasis. Nat Cell Biol. 2008;10(3):295-305.
265. Zhang W, Shi X, Peng Y, Wu M, Zhang P, Xie R, et al. HIF-1α Promotes Epithelial-Mesenchymal Transition and Metastasis through Direct Regulation of ZEB1 in Colorectal Cancer. PLoS One. 2015;10(6):e0129603.
266. Storci G, Sansone P, Mari S, D'Uva G, Tavolari S, Guarnieri T, et al. TNFalpha up-regulates SLUG via the NF-kappaB/HIF1alpha axis, which imparts breast cancer cells with a stem cell-like phenotype. J Cell Physiol. 2010;225(3):682-91.
267. Luo D, Wang J, Li J, Post M. Mouse snail is a target gene for HIF. Mol Cancer Res. 2011;9(2):234-45.
268. Tam SY, Wu VWC, Law HKW. Hypoxia-Induced Epithelial-Mesenchymal Transition in Cancers: HIF-1α and Beyond. Front Oncol. 2020;10:486.

269. Riemann A, Rauschner M, Gießelmann M, Reime S, Haupt V, Thews O. Extracellular Acidosis Modulates the Expression of Epithelial-Mesenchymal Transition (EMT) Markers and Adhesion of Epithelial and Tumor Cells. Neoplasia. 2019;21(5):450-8.
270. Suzuki A, Maeda T, Baba Y, Shimamura K, Kato Y. Acidic extracellular pH promotes epithelial mesenchymal transition in Lewis lung carcinoma model. Cancer Cell International. 2014;14(1):129.
271. Svastová E, Zilka N, Zat'ovicová M, Gibadulinová A, Ciampor F, Pastorek J, et al. Carbonic anhydrase IX reduces E-cadherin-mediated adhesion of MDCK cells via interaction with beta-catenin. Exp Cell Res. 2003;290(2):332-45.
272. Swayampakula M, McDonald PC, Vallejo M, Coyaud E, Chafe SC, Westerback A, et al. The interactome of metabolic enzyme carbonic anhydrase IX reveals novel roles in tumor cell migration and invadopodia/MMP14-mediated invasion. Oncogene. 2017;36(45):6244-61.
273. Qu X, Zhai Y, Wei H, Zhang C, Xing G, Yu Y, et al. Characterization and expression of three novel differentiation-related genes belong to the human NDRG gene family. Molecular and Cellular Biochemistry. 2002;229(1):35-44.
274. Shaw E, McCue LA, Lawrence CE, Dordick JS. Identification of a novel class in the alpha/beta hydrolase fold superfamily: the N-myc differentiation-related proteins. Proteins. 2002;47(2):163-8.
275. Zhao W, Tang R, Huang Y, Wang W, Zhou Z, Gu S, et al. Cloning and expression pattern of the human NDRG3 gene. Biochim Biophys Acta. 2001;1519(1-2):134-8.
276. Kokame K, Kato H, Miyata T. Homocysteine-respondent genes in vascular endothelial cells identified by differential display analysis. GRP78/BiP and novel genes. J Biol Chem. 1996;271(47):29659-65.
277. Kurdistani SK, Arizti P, Reimer CL, Sugrue MM, Aaronson SA, Lee SW. Inhibition of tumor cell growth by RTP/rit42 and its responsiveness to p53 and DNA damage. Cancer Res. 1998;58(19):4439-44.
278. Ellen TP, Ke Q, Zhang P, Costa M. NDRG1, a growth and cancer related gene: regulation of gene expression and function in normal and disease states. Carcinogenesis. 2008;29(1):2-8.
279. Salnikow K, Kluz T, Costa M, Piquemal D, Demidenko ZN, Xie K, et al. The regulation of hypoxic genes by calcium involves c-Jun/AP-1, which cooperates with hypoxia-inducible factor 1 in response to hypoxia. Mol Cell Biol. 2002;22(6):1734-41.
280. Ryan HE, Lo J, Johnson RS. HIF-1 alpha is required for solid tumor formation and embryonic vascularization. Embo j. 1998;17(11):3005-15.
281. Wang Q, Li L-H, Gao G-D, Wang G, Qu L, Li J-G, et al. HIF-1α up-regulates NDRG1 expression through binding to NDRG1 promoter, leading to proliferation of lung cancer A549 cells. Molecular Biology Reports. 2013;40(5):3723-9.
282. Li EY, Huang WY, Chang YC, Tsai MH, Chuang EY, Kuok QY, et al. Aryl Hydrocarbon Receptor Activates NDRG1 Transcription under Hypoxia in Breast Cancer Cells. Sci Rep. 2016;6:20808.
283. Lederman HM, Cohen A, Lee JWW. Deferoxamine: A reversible S-phase inhibitor of human lymphocyte proliferation. Blood. 1984;64(3):748-53.
284. Jaakkola P, Mole DR, Tian Y-M, Wilson MI, Gielbert J, Gaskell SJ, et al. Targeting of HIF-α to the von Hippel-Lindau Ubiquitylation Complex by O₂-Regulated Prolyl Hydroxylation. Science. 2001;292(5516):468-72.
285. Lane DJ, Saletta F, Suryo Rahmanto Y, Kovacevic Z, Richardson DR. N-myc downstream regulated 1 (NDRG1) is regulated by eukaryotic initiation factor 3a

(eIF3a) during cellular stress caused by iron depletion. PLoS One. 2013;8(2):e57273.
286. Salnikow K, Su W, Blagosklonny MV, Costa M. Carcinogenic metals induce hypoxia-inducible factor-stimulated transcription by reactive oxygen species-independent mechanism. Cancer Res. 2000;60(13):3375-8.
287. Stein S, Thomas EK, Herzog B, Westfall MD, Rocheleau JV, Jackson RS, 2nd, et al. NDRG1 is necessary for p53-dependent apoptosis. J Biol Chem. 2004;279(47):48930-40.
288. Bandyopadhyay S, Pai SK, Hirota S, Hosobe S, Tsukada T, Miura K, et al. PTEN up-regulates the tumor metastasis suppressor gene Drg-1 in prostate and breast cancer. Cancer Res. 2004;64(21):7655-60.
289. Zhang P, Tchou-Wong K-M, Costa M. Egr-1 Mediates Hypoxia-Inducible Transcription of the NDRG1 Gene through an Overlapping Egr-1/Sp1 Binding Site in the Promoter. Cancer Research. 2007;67(19):9125-33.
290. Zhang J, Chen S, Zhang W, Zhang J, Liu X, Shi H, et al. Human differentiation-related gene NDRG1 is a Myc downstream-regulated gene that is repressed by Myc on the core promoter region. Gene. 2008;417(1):5-12.
291. Chiang K-C, Yeh C-N, Chung L-C, Feng T-H, Sun C-C, Chen M-F, et al. WNT-1 inducible signaling pathway protein-1 enhances growth and tumorigenesis in human breast cancer. Scientific Reports. 2015;5(1):8686.
292. Mishra A, Bonello M, Byron A, Langdon SP, Sims AH. Evaluation of Gene Expression Data From Cybrids and Tumours Highlights Elevated NDRG1-Driven Proliferation in Triple-Negative Breast Cancer. Breast Cancer (Auckl). 2020;14:1178223420934447.
293. Redmond KL, Crawford NT, Farmer H, D'Costa ZC, O'Brien GJ, Buckley NE, et al. T-box 2 represses NDRG1 through an EGR1-dependent mechanism to drive the proliferation of breast cancer cells. Oncogene. 2010;29(22):3252-62.
294. Lai LC, Su YY, Chen KC, Tsai MH, Sher YP, Lu TP, et al. Down-regulation of NDRG1 promotes migration of cancer cells during reoxygenation. PLoS One. 2011;6(8):e24375.
295. Wang Z, Liu Q, Chen Q, Zhu R, Zhu H-g. [Overexpression of NDRG1: relationship with proliferative activity and invasiveness of breast cancer cell line and breast cancer metastasis]. Zhonghua Bing Li Xue Za Zhi. 2006;35(6):333-8.
296. Tian S, Wang X, Proud CG. Oncogenic MNK signalling regulates the metastasis suppressor NDRG1. Oncotarget. 2017;8(28).
297. López-Tejada A, Griñán-Lisón C, González-González A, Cara FE, Luque RJ, Rosa-Garrido C, et al. TGFß Governs the Pleiotropic Activity of NDRG1 in Triple-Negative Breast Cancer Progression. Int J Biol Sci. 2023;19(1):204-24.
298. Liu W, Xing F, Iiizumi-Gairani M, Okuda H, Watabe M, Pai SK, et al. N-myc downstream regulated gene 1 modulates Wnt-β-catenin signalling and pleiotropically suppresses metastasis. EMBO Mol Med. 2012;4(2):93-108.
299. Berghoff AS, Liao Y, Karreman MA, Ilhan-Mutlu A, Gunkel K, Sprick MR, et al. Identification and Characterization of Cancer Cells That Initiate Metastases to the Brain and Other Organs. Mol Cancer Res. 2021;19(4):688-701.
300. Villodre ES, Hu X, Eckhardt BL, Larson R, Huo L, Yoon EC, et al. NDRG1 in Aggressive Breast Cancer Progression and Brain Metastasis. J Natl Cancer Inst. 2022;114(4):579-91.
301. Abascal MF, Elia A, Alvarez M, Pataccini G, Sequeira G, Riggio M, et al. Progesterone receptor isoform ratio dictates antiprogestin/progestin effects on breast cancer growth and metastases: A role for NDRG1. International Journal of Cancer. 2022;150(9):1481-96.

302. Chemist A. ChemSpider SyntheticPages 2001 [Available from: http://cssp.chemspider.com/123.
303. Semenza GL. Targeting HIF-1 for cancer therapy. Nature Reviews Cancer. 2003;3(10):721-32.
304. Wigerup C, Påhlman S, Bexell D. Therapeutic targeting of hypoxia and hypoxia-inducible factors in cancer. Pharmacology & Therapeutics. 2016;164:152-69.
305. Pastorekova S, Gillies RJ. The role of carbonic anhydrase IX in cancer development: links to hypoxia, acidosis, and beyond. Cancer and Metastasis Reviews. 2019;38(1):65-77.
306. Shamis SAK. The relationship between hypoxia, hypoxia gene signature and survival in patients with breast cancer: University of Glasgow.; 2023.
307. Shamis SAK, Quinn J, Mallon EEA, Edwards J, McMillan DC. The Relationship Between the Tumor Cell Expression of Hypoxic Markers and Survival in Patients With ER-positive Invasive Ductal Breast Cancer. Journal of Histochemistry & Cytochemistry. 2022;70(7):479-94.
308. Li Y, Chen X, Zhou Z, Li Q, Westover KD, Wang M, et al. Dynamic surveillance of tamoxifen-resistance in ER-positive breast cancer by CAIX-targeted ultrasound imaging. Cancer Medicine. 2020;9(7):2414-26.
309. Alves W, Bonatelli M, Dufloth R, Kerr LM, Carrara GFA, da Costa RFA, et al. CAIX is a predictor of pathological complete response and is associated with higher survival in locally advanced breast cancer submitted to neoadjuvant chemotherapy. BMC Cancer. 2019;19(1):1173.
310. Ozretic P, Alvir I, Sarcevic B, Vujaskovic Z, Rendic-Miocevic Z, Roguljic A, et al. Apoptosis regulator Bcl-2 is an independent prognostic marker for worse overall survival in triple-negative breast cancer patients. Int J Biol Markers. 2018;33(1):109-15.
311. Jin MS, Lee H, Park IA, Chung YR, Im SA, Lee KH, et al. Overexpression of HIF1α and CAXI predicts poor outcome in early-stage triple negative breast cancer. Virchows Arch. 2016;469(2):183-90.
312. Chu CY, Jin YT, Zhang W, Yu J, Yang HP, Wang HY, et al. CA IX is upregulated in CoCl2-induced hypoxia and associated with cell invasive potential and a poor prognosis of breast cancer. Int J Oncol. 2016;48(1):271-80.
313. Samaka RM, Abd El-Wahed MM, Al Sharaky DR, Shehata MA, Hegazy SE, Aleskandarany MA. Overexpression of Carbonic Anhydrase IX is a Dismal Prognostic Marker in Breast Carcinoma in Egyptian Patients. Appl Immunohistochem Mol Morphol. 2016;24(6):405-13.
314. Aomatsu N, Yashiro M, Kashiwagi S, Kawajiri H, Takashima T, Ohsawa M, et al. Carbonic anhydrase 9 is associated with chemosensitivity and prognosis in breast cancer patients treated with taxane and anthracycline. BMC Cancer. 2014;14(1):400.
315. Deb S, Johansson I, Byrne D, Nilsson C, Constable L, Fjällskog ML, et al. Nuclear HIF1A expression is strongly prognostic in sporadic but not familial male breast cancer. Mod Pathol. 2014;27(9):1223-30.
316. Kim HM, Jung WH, Koo JS. Site-specific metabolic phenotypes in metastatic breast cancer. Journal of Translational Medicine. 2014;12(1):354.
317. Noh S, Kim JY, Koo JS. Metabolic differences in estrogen receptor-negative breast cancer based on androgen receptor status. Tumour Biol. 2014;35(8):8179-92.
318. Betof AS, Rabbani ZN, Hardee ME, Kim SJ, Broadwater G, Bentley RC, et al. Carbonic anhydrase IX is a predictive marker of doxorubicin resistance in early-

stage breast cancer independent of HER2 and TOP2A amplification. Br J Cancer. 2012;106(5):916-22.
319. Kaya AO, Gunel N, Benekli M, Akyurek N, Buyukberber S, Tatli H, et al. Hypoxia inducible factor-1 alpha and carbonic anhydrase IX overexpression are associated with poor survival in breast cancer patients. J buon. 2012;17(4):663-8.
320. Beketic-Oreskovic L, Ozretic P, Rabbani ZN, Jackson IL, Sarcevic B, Levanat S, et al. Prognostic significance of carbonic anhydrase IX (CA-IX), endoglin (CD105) and 8-hydroxy-2'-deoxyguanosine (8-OHdG) in breast cancer patients. Pathol Oncol Res. 2011;17(3):593-603.
321. Lou Y, McDonald PC, Oloumi A, Chia S, Ostlund C, Ahmadi A, et al. Targeting tumor hypoxia: suppression of breast tumor growth and metastasis by novel carbonic anhydrase IX inhibitors. Cancer Res. 2011;71(9):3364-76.
322. Pinheiro C, Sousa B, Albergaria A, Paredes J, Dufloth R, Vieira D, et al. GLUT1 and CAIX expression profiles in breast cancer correlate with adverse prognostic factors and MCT1 overexpression. Histol Histopathol. 2011;26(10):1279-86.
323. Jubb AM, Soilleux EJ, Turley H, Steers G, Parker A, Low I, et al. Expression of vascular notch ligand delta-like 4 and inflammatory markers in breast cancer. Am J Pathol. 2010;176(4):2019-28.
324. Tan EY, Yan M, Campo L, Han C, Takano E, Turley H, et al. The key hypoxia regulated gene CAIX is upregulated in basal-like breast tumours and is associated with resistance to chemotherapy. Br J Cancer. 2009;100(2):405-11.
325. Crabb SJ, Bajdik CD, Leung S, Speers CH, Kennecke H, Huntsman DG, et al. Can clinically relevant prognostic subsets of breast cancer patients with four or more involved axillary lymph nodes be identified through immunohistochemical biomarkers? A tissue microarray feasibility study. Breast Cancer Research. 2008;10(1):R6.
326. Kyndi M, Sørensen FB, Knudsen H, Alsner J, Overgaard M, Nielsen HM, et al. Carbonic anhydrase IX and response to postmastectomy radiotherapy in high-risk breast cancer: a subgroup analysis of the DBCG82 b and c trials. Breast Cancer Res. 2008;10(2):R24.
327. Hussain SA, Ganesan R, Reynolds G, Gross L, Stevens A, Pastorek J, et al. Hypoxia-regulated carbonic anhydrase IX expression is associated with poor survival in patients with invasive breast cancer. Br J Cancer. 2007;96(1):104-9.
328. Trastour C, Benizri E, Ettore F, Ramaioli A, Chamorey E, Pouysségur J, et al. HIF-1alpha and CA IX staining in invasive breast carcinomas: prognosis and treatment outcome. Int J Cancer. 2007;120(7):1451-8.
329. Brennan DJ, Jirstrom K, Kronblad A, Millikan RC, Landberg G, Duffy MJ, et al. CA IX is an independent prognostic marker in premenopausal breast cancer patients with one to three positive lymph nodes and a putative marker of radiation resistance. Clin Cancer Res. 2006;12(21):6421-31.
330. Generali D, Berruti A, Brizzi MP, Campo L, Bonardi S, Wigfield S, et al. Hypoxia-inducible factor-1alpha expression predicts a poor response to primary chemoendocrine therapy and disease-free survival in primary human breast cancer. Clin Cancer Res. 2006;12(15):4562-8.
331. Tomes L, Emberley E, Niu Y, Troup S, Pastorek J, Strange K, et al. Necrosis and hypoxia in invasive breast carcinoma. Breast Cancer Res Treat. 2003;81(1):61-9.
332. Chia SK, Wykoff CC, Watson PH, Han C, Leek RD, Pastorek J, et al. Prognostic significance of a novel hypoxia-regulated marker, carbonic anhydrase IX, in invasive breast carcinoma. J Clin Oncol. 2001;19(16):3660-8.

333. Bourseau-Guilmain E, Menard JA, Lindqvist E, Indira Chandran V, Christianson HC, Cerezo Magaña M, et al. Hypoxia regulates global membrane protein endocytosis through caveolin-1 in cancer cells. Nature Communications. 2016;7(1):11371.
334. Zatovicova M, Jelenska L, Hulikova A, Csaderova L, Ditte Z, Ditte P, et al. Carbonic anhydrase IX as an anticancer therapy target: preclinical evaluation of internalizing monoclonal antibody directed to catalytic domain. Curr Pharm Des. 2010;16(29):3255-63.
335. Jin M-S, Lee H, Park IA, Chung YR, Im S-A, Lee K-H, et al. Overexpression of HIF1α and CAXI predicts poor outcome in early-stage triple negative breast cancer. Virchows Archiv. 2016;469(2):183-90.
336. Ambrosio MR, Di Serio C, Danza G, Rocca BJ, Ginori A, Prudovsky I, et al. Carbonic anhydrase IX is a marker of hypoxia and correlates with higher Gleason scores and ISUP grading in prostate cancer. Diagnostic Pathology. 2016;11(1):45.
337. Le QT, Kong C, Lavori PW, O'Byrne K, Erler JT, Huang X, et al. Expression and prognostic significance of a panel of tissue hypoxia markers in head-and-neck squamous cell carcinomas. Int J Radiat Oncol Biol Phys. 2007;69(1):167-75.
338. Swinson DE, Jones JL, Richardson D, Wykoff C, Turley H, Pastorek J, et al. Carbonic anhydrase IX expression, a novel surrogate marker of tumor hypoxia, is associated with a poor prognosis in non-small-cell lung cancer. J Clin Oncol. 2003;21(3):473-82.
339. Lowe R, Shirley N, Bleackley M, Dolan S, Shafee T. Transcriptomics technologies. PLoS Comput Biol. 2017;13(5):e1005457.
340. Bedi M, Ray M, Ghosh A. Active mitochondrial respiration in cancer: a target for the drug. Molecular and Cellular Biochemistry. 2022;477(2):345-61.
341. Melincovici CS, Boşca AB, Şuşman S, Mărginean M, Mihu C, Istrate M, et al. Vascular endothelial growth factor (VEGF) – key factor in normal and pathological angiogenesis. Romanian Journal of Morphology and Embryology. 2018;59(2):455-67.
342. Ghalehbandi S, Yuzugulen J, Pranjol MZI, Pourgholami MH. The role of VEGF in cancer-induced angiogenesis and research progress of drugs targeting VEGF. European Journal of Pharmacology. 2023;949:175586.
343. Shibuya M. Vascular Endothelial Growth Factor (VEGF) and Its Receptor (VEGFR) Signaling in Angiogenesis: A Crucial Target for Anti- and Pro-Angiogenic Therapies. Genes Cancer. 2011;2(12):1097-105.
344. Maae E, Olsen DA, Steffensen KD, Jakobsen EH, Brandslund I, Sørensen FB, et al. Prognostic impact of placenta growth factor and vascular endothelial growth factor A in patients with breast cancer. Breast Cancer Res Treat. 2012;133(1):257-65.
345. McIntyre A, Patiar S, Wigfield S, Li J-l, Ledaki I, Turley H, et al. Carbonic Anhydrase IX Promotes Tumor Growth and Necrosis In Vivo and Inhibition Enhances Anti-VEGF Therapy. Clinical Cancer Research. 2012;18(11):3100-11.
346. Mattauch S, Sachs M, Behrens J. Liprin-α4 is a new hypoxia-inducible target gene required for maintenance of cell-cell contacts. Exp Cell Res. 2010;316(17):2883-92.
347. Yamasaki A, Nakayama K, Imaizumi A, Kawamoto M, Fujimura A, Oyama Y, et al. Liprin-α4 as a Possible New Therapeutic Target for Pancreatic Cancer. Anticancer Res. 2017;37(12):6649-54.
348. Onishi H, Yamasaki A, Nakamura K, Ichimiya S, Yanai K, Umebayashi M, et al. Liprin-α4 as a New Therapeutic Target for SCLC as an Upstream Mediator of HIF1α. Anticancer Res. 2019;39(3):1179-84.

349. Villodre ES, Nguyen APN, Debeb BG. NDRGs in Breast Cancer: A Review and In Silico Analysis. Cancers (Basel). 2024;16(7).
350. Azuma M, Shi MM, Jacques CJ, Barrett C, Danenberg KD, Iqbal S, et al. Tumor VEGFA gene expression is associated with serum lactate dehydrogenase (LDH) levels and intratumoral mRNA expression of genes involved in glycolysis in patients with metastatic colorectal cancer (mCRC). Journal of Clinical Oncology. 2006;24(18_suppl):3530-.
351. Liu W, Zhang B, Hu Q, Qin Y, Xu W, Shi S, et al. A new facet of NDRG1 in pancreatic ductal adenocarcinoma: Suppression of glycolytic metabolism. Int J Oncol. 2017;50(5):1792-800.
352. Guo YJ, Pan WW, Liu SB, Shen ZF, Xu Y, Hu LL. ERK/MAPK signalling pathway and tumorigenesis (Review). Exp Ther Med. 2020;19(3):1997-2007.
353. Zou Z, Tao T, Li H, Zhu X. mTOR signaling pathway and mTOR inhibitors in cancer: progress and challenges. Cell & Bioscience. 2020;10(1):31.
354. Faes S, Planche A, Uldry E, Santoro T, Pythoud C, Stehle JC, et al. Targeting carbonic anhydrase IX improves the anti-cancer efficacy of mTOR inhibitors. Oncotarget. 2016;7(24):36666-80.
355. Liu Y, Beyer A, Aebersold R. On the Dependency of Cellular Protein Levels on mRNA Abundance. Cell. 2016;165(3):535-50.
356. Kotulak-Chrzaszcz A, Kiezun J, Czajkowski M, Matuszewski M, Klacz J, Krazinski BE, et al. The immunoreactivity of GLI1 and VEGFA is a potential prognostic factor in kidney renal clear cell carcinoma. BMC Cancer. 2023;23(1):1110.
357. Chen P, Zhu J, Liu DY, Li HY, Xu N, Hou M. Over-expression of survivin and VEGF in small-cell lung cancer may predict the poorer prognosis. Med Oncol. 2014;31(1):775.
358. Han F, Cao D, Zhu X, Shen L, Wu J, Chen Y, et al. Construction and validation of a prognostic model for hepatocellular carcinoma: Inflammatory ferroptosis and mitochondrial metabolism indicate a poor prognosis. Frontiers in Oncology. 2023;12.
359. Xu X, Liu Z, Wang J, Xie H, Li J, Cao J, et al. Global proteomic profiling in multistep hepatocarcinogenesis and identification of PARP1 as a novel molecular marker in hepatocellular carcinoma. Oncotarget. 2016;7(12):13730-41.
360. Zhang S, Yu C, Yang X, Hong H, Lu J, Hu W, et al. N-myc downstream-regulated gene 1 inhibits the proliferation of colorectal cancer through emulative antagonizing NEDD4-mediated ubiquitylation of p21. Journal of Experimental & Clinical Cancer Research. 2019;38(1):490.
361. Fu F, Niu R, Zheng M, Yang X, Fan L, Fu W, et al. Clinicopathological Significances and Prognostic Value of PPFIA4 in Colorectal Cancer. J Cancer. 2023;14(1):24-34.
362. Sun Q, Wang H, Xiao B, Xue D, Wang G. Development and Validation of a 6-Gene Hypoxia-Related Prognostic Signature For Cholangiocarcinoma. Front Oncol. 2022;12:954366.
363. Lee P, Chandel NS, Simon MC. Cellular adaptation to hypoxia through hypoxia inducible factors and beyond. Nature Reviews Molecular Cell Biology. 2020;21(5):268-83.
364. Kallio PJ, Pongratz I, Gradin K, McGuire J, Poellinger L. Activation of hypoxia-inducible factor 1α: Posttranscriptional regulation and conformational change by recruitment of the Arnt transcription factor. Proceedings of the National Academy of Sciences. 1997;94(11):5667-72.

365. Bhandari V, Li CH, Bristow RG, Boutros PC, Aaltonen LA, Abascal F, et al. Divergent mutational processes distinguish hypoxic and normoxic tumours. Nature Communications. 2020;11(1):737.
366. Vaupel P, Schlenger K, Knoop C, Höckel M. Oxygenation of human tumors: evaluation of tissue oxygen distribution in breast cancers by computerized O2 tension measurements. Cancer Res. 1991;51(12):3316-22.
367. Chun YS, Adusumilli PS, Fong Y. Employing tumor hypoxia for oncolytic therapy in breast cancer. J Mammary Gland Biol Neoplasia. 2005;10(4):311-8.
368. McDonald PC, Winum J-Y, Supuran CT, Dedhar S. Recent Developments in Targeting Carbonic Anhydrase IX for Cancer Therapeutics. Oncotarget. 2012;3(1).
369. Vordermark D, Kaffer A, Riedl S, Katzer A, Flentje M. Characterization of carbonic anhydrase IX (CA IX) as an endogenous marker of chronic hypoxia in live human tumor cells. Int J Radiat Oncol Biol Phys. 2005;61(4):1197-207.
370. Du J, Xu R, Hu Z, Tian Y, Zhu Y, Gu L, et al. PI3K and ERK-induced Rac1 activation mediates hypoxia-induced HIF-1?? expression in MCF-7 breast cancer cells. PloS one. 2011;6:e25213.
371. Su F, Liu B, Chen M, Xiao J, Li X, Lv X, et al. Association between VEGF-A, C and D Expression and lymph Node Involvement in Breast Cancer: A Meta-Analysis. The International Journal of Biological Markers. 2016;31(3):235-44.
372. Vogel C, Silva GM, Marcotte EM. Protein Expression Regulation under Oxidative Stress*. Molecular & Cellular Proteomics. 2011;10(12):M111.009217.
373. Tian Q, Stepaniants SB, Mao M, Weng L, Feetham MC, Doyle MJ, et al. Integrated Genomic and Proteomic Analyses of Gene Expression in Mammalian Cells *. Molecular & Cellular Proteomics. 2004;3(10):960-9.
374. Saxena K, Jolly MK. Acute vs. Chronic vs. Cyclic Hypoxia: Their Differential Dynamics, Molecular Mechanisms, and Effects on Tumor Progression. Biomolecules. 2019;9(8):339.
375. Liu Q, Palmgren VAC, Danen EH, Le Dévédec SE. Acute vs. chronic vs. intermittent hypoxia in breast Cancer: a review on its application in in vitro research. Mol Biol Rep. 2022;49(11):10961-73.
376. Bayer C, Vaupel P. Acute versus chronic hypoxia in tumors. Strahlentherapie und Onkologie. 2012;188(7):616-27.
377. Stiehl DP, Bordoli MR, Abreu-Rodríguez I, Wollenick K, Schraml P, Gradin K, et al. Non-canonical HIF-2α function drives autonomous breast cancer cell growth via an AREG–EGFR/ErbB4 autocrine loop. Oncogene. 2012;31(18):2283-97.
378. Tafreshi NK, Lloyd MC, Proemsey JB, Bui MM, Kim J, Gillies RJ, et al. Evaluation of CAIX and CAXII Expression in Breast Cancer at Varied O2 Levels: CAIX is the Superior Surrogate Imaging Biomarker of Tumor Hypoxia. Mol Imaging Biol. 2016;18(2):219-31.
379. Wykoff CC, Beasley NJ, Watson PH, Turner KJ, Pastorek J, Sibtain A, et al. Hypoxia-inducible expression of tumor-associated carbonic anhydrases. Cancer Res. 2000;60(24):7075-83.
380. Sobhanifar S, Aquino-Parsons C, Stanbridge EJ, Olive P. Reduced Expression of Hypoxia-Inducible Factor-1α in Perinecrotic Regions of Solid Tumors. Cancer Research. 2005;65(16):7259-66.
381. Zhang ZY, Zhang SL, Chen HL, Mao YQ, Li ZM, Kong CY, et al. The up-regulation of NDRG1 by HIF counteracts the cancer-promoting effect of HIF in VHL-deficient clear cell renal cell carcinoma. Cell Prolif. 2020;53(7):e12853.
382. Ellen TP, Ke Q, Zhang P, Costa M. NDRG1, a growth and cancer related gene: regulation of gene expression and function in normal and disease states. Carcinogenesis. 2007;29(1):2-8.

383. Cavadas MAS, Mesnieres M, Crifo B, Manresa MC, Selfridge AC, Scholz CC, et al. REST mediates resolution of HIF-dependent gene expression in prolonged hypoxia. Scientific Reports. 2015;5(1):17851.
384. Chamboredon S, Ciais D, Desroches-Castan A, Savi P, Bono F, Feige J-J, et al. Hypoxia-inducible factor-1α mRNA: a new target for destabilization by tristetraprolin in endothelial cells. Molecular Biology of the Cell. 2011;22(18):3366-78.
385. Uchida T, Rossignol F, Matthay MA, Mounier R, Couette S, Clottes E, et al. Prolonged Hypoxia Differentially Regulates Hypoxia-inducible Factor (HIF)-1α and HIF-2α Expression in Lung Epithelial Cells: IMPLICATION OF NATURAL ANTISENSE HIF-1α*. Journal of Biological Chemistry. 2004;279(15):14871-8.
386. Rossignol F, Vaché C, Clottes E. Natural antisense transcripts of hypoxia-inducible factor 1alpha are detected in different normal and tumour human tissues. Gene. 2002;299(1-2):135-40.
387. Bartoszewski R, Moszyńska A, Serocki M, Cabaj A, Polten A, Ochocka R, et al. Primary endothelial cell-specific regulation of hypoxia-inducible factor (HIF)-1 and HIF-2 and their target gene expression profiles during hypoxia. Faseb j. 2019;33(7):7929-41.
388. Koh MY, Lemos R, Jr, Liu X, Powis G. The Hypoxia-Associated Factor Switches Cells from HIF-1α- to HIF-2α-Dependent Signaling Promoting Stem Cell Characteristics, Aggressive Tumor Growth and Invasion. Cancer Research. 2011;71(11):4015-27.
389. Bruning U, Cerone L, Neufeld Z, Fitzpatrick SF, Cheong A, Scholz CC, et al. MicroRNA-155 promotes resolution of hypoxia-inducible factor 1alpha activity during prolonged hypoxia. Mol Cell Biol. 2011;31(19):4087-96.
390. Salceda S, Caro J. Hypoxia-inducible Factor 1α (HIF-1α) Protein Is Rapidly Degraded by the Ubiquitin-Proteasome System under Normoxic Conditions: ITS STABILIZATION BY HYPOXIA DEPENDS ON REDOX-INDUCED CHANGES *. Journal of Biological Chemistry. 1997;272(36):22642-7.
391. Zhao Y, Xing C, Deng Y, Ye C, Peng H. HIF-1α signaling: Essential roles in tumorigenesis and implications in targeted therapies. Genes & Diseases. 2024;11(1):234-51.
392. Atlas HP. **PPFIA4 - The Human Protein Atlas** 2025 [Available from: https://www.proteinatlas.org/search/PPFIA4.
393. Bandyopadhyay S, Pai SK, Hirota S, Hosobe S, Takano Y, Saito K, et al. Role of the putative tumor metastasis suppressor gene Drg-1 in breast cancer progression. Oncogene. 2004;23(33):5675-81.
394. Villodre ES, Gong Y, Hu X, Huo L, Yoon EC, Ueno NT, et al. NDRG1 Expression Is an Independent Prognostic Factor in Inflammatory Breast Cancer. Cancers. 2020;12(12):3711.
395. Altman DG, McShane LM, Sauerbrei W, Taube SE. Reporting Recommendations for Tumor Marker Prognostic Studies (REMARK): explanation and elaboration. PLoS Med. 2012;9(5):e1001216.
396. Nakai K, Horton P. PSORT: A program for detecting sorting signals in proteins and predicting their subcellular localization. Trends in Biochemical Sciences. 1999;24(1):34-5.
397. Askautrud HA, Gjernes E, Gunnes G, Sletten M, Ross DT, Børresen-Dale AL, et al. Global gene expression analysis reveals a link between NDRG1 and vesicle transport. PLoS One. 2014;9(1):e87268.
398. Song Y, Lv L, Du J, Yue L, Cao L. Correlation of N-myc downstream-regulated gene 1 subcellular localization and lymph node metastases of colorectal

neoplasms. Biochemical and Biophysical Research Communications. 2013;439(2):241-6.
399. Lu W-J, Chua M-S, Wei W, So SK. NDRG1 promotes growth of hepatocellular carcinoma cells by directly interacting with GSK-3ß and Nur77 to prevent ß-catenin degradation. Oncotarget. 2015;6(30).
400. Sibold S, Roh V, Keogh A, Studer P, Tiffon C, Angst E, et al. Hypoxia increases cytoplasmic expression of NDRG1, but is insufficient for its membrane localization in human hepatocellular carcinoma. FEBS Letters. 2007;581(5):989-94.
401. Shi X-H, Larkin JC, Chen B, Sadovsky Y. The Expression and Localization of N-Myc Downstream-Regulated Gene 1 in Human Trophoblasts. PLOS ONE. 2013;8(9):e75473.
402. Song Y, Wu G, Zhang M, Kong Q, Du J, Zheng Y, et al. N-myc downstream-regulated gene 1 inhibits the proliferation and invasion of hepatocellular carcinoma cells via the regulation of integrin ß3. Oncol Lett. 2017;13(5):3599-607.
403. Saponaro C, Damato M, Stanca E, Aboulouard S, Zito FA, De Summa S, et al. Unraveling the protein kinase C/NDRG1 signaling network in breast cancer. Cell & Bioscience. 2024;14(1):156.
404. Joshi V, Stacey A, Feng Y, Kalita-de Croft P, Duijf PH, Simpson PT, et al. NDRG1 is a prognostic biomarker in breast cancer and breast cancer brain metastasis. J Pathol Clin Res. 2024;10(2):e12364.
405. Kurdistani SK, Arizti P, Reimer CL, Sugrue MM, Aaronson SA, Lee SW. Inhibition of tumor cell growth by RTP/rit42 and its responsiveness to p53 and DNA damage. Cancer Research. 1998;58(19):4439-44.
406. Hosoya N, Sakumoto M, Nakamura Y, Narisawa T, Bilim V, Motoyama T, et al. Proteomics identified nuclear N-myc downstream-regulated gene 1 as a prognostic tissue biomarker candidate in renal cell carcinoma. Biochimica et Biophysica Acta (BBA) - Proteins and Proteomics. 2013;1834(12):2630-9.
407. Lachat P, Shaw P, Gebhard S, van Belzen N, Chaubert P, Bosman FT. Expression of NDRG1, a differentiation-related gene, in human tissues. Histochemistry and Cell Biology. 2002;118(5):399-408.
408. Nagai MA, Gerhard R, Fregnani JHTG, Nonogaki S, Rierger RB, Netto MM, et al. Prognostic value of NDRG1 and SPARC protein expression in breast cancer patients. Breast Cancer Research and Treatment. 2011;126(1):1-14.
409. Zeng L, Deng X, Zhong J, Yuan L, Tao X, Zhang S, et al. Prognostic value of biomarkers EpCAM and αB-crystallin associated with lymphatic metastasis in breast cancer by iTRAQ analysis. BMC Cancer. 2019;19(1):831.
410. Fan Z, Zheng W, Li H, Wu W, Liu X, Sun Z, et al. LOXL2 upregulates hypoxia-inducible factor-1α signaling through Snail-FBP1 axis in hepatocellular carcinoma cells. Oncol Rep. 2020;43(5):1641-9.
411. Yin L, Feng S, Sun Y, Jiang Y, Tang C, Sun D. Identification of a five m6A-relevant mRNAs signature and risk score for the prognostication of gastric cancer. J Gastrointest Oncol. 2022;13(5):2234-48.
412. Appelhoff RJ, Tian YM, Raval RR, Turley H, Harris AL, Pugh CW, et al. Differential function of the prolyl hydroxylases PHD1, PHD2, and PHD3 in the regulation of hypoxia-inducible factor. J Biol Chem. 2004;279(37):38458-65.
413. Strocchi S, Reggiani F, Gobbi G, Ciarrocchi A, Sancisi V. The multifaceted role of EGLN family prolyl hydroxylases in cancer: going beyond HIF regulation. Oncogene. 2022;41(29):3665-79.

414. Cuevas EP, Eraso P, Mazón MJ, Santos V, Moreno-Bueno G, Cano A, et al. LOXL2 drives epithelial-mesenchymal transition via activation of IRE1-XBP1 signalling pathway. Scientific Reports. 2017;7(1):44988.
415. Wen B, Xu LY, Li EM. LOXL2 in cancer: regulation, downstream effectors and novel roles. Biochim Biophys Acta Rev Cancer. 2020;1874(2):188435.
416. Nam JS, Hirohashi S, Wakefield LM. Dysadherin: a new player in cancer progression. Cancer Lett. 2007;255(2):161-9.
417. Niinivirta A, Salo T, Åström P, Juurikka K, Risteli M. Prognostic value of dysadherin in cancer: A systematic review and meta-analysis. Front Oncol. 2022;12:945992.
418. Dunn-Walters D, Townsend C, Sinclair E, Stewart A. Immunoglobulin gene analysis as a tool for investigating human immune responses. Immunol Rev. 2018;284(1):132-47.
419. Liu Y, Qing C, Xiaotang W, Youlin Y, and Zhang H. Effect of chemokine CXCL14 on in vitro angiogenesis of human hepatocellular carcinoma cells. Archives of Physiology and Biochemistry. 2022;128(5):1316-22.
420. Bukowska-Ośko I, Sulejczak D, Kaczyńska K, Kleczkowska P, Kramkowski K, Popiel M, et al. Lactoferrin as a Human Genome "Guardian"-An Overall Point of View. Int J Mol Sci. 2022;23(9).
421. Ruan K, Song G, Ouyang G. Role of hypoxia in the hallmarks of human cancer. J Cell Biochem. 2009;107(6):1053-62.
422. Brian MO. Hypoxia-inducible factor in cancer: from pathway regulation to therapeutic opportunity. BMJ Oncology. 2024;3(1):e000154.
423. Lai L-C, Su Y-Y, Chen K-C, Tsai M-H, Sher Y-P, Lu T-P, et al. Down-Regulation of NDRG1 Promotes Migration of Cancer Cells during Reoxygenation. PLOS ONE. 2011;6(8):e24375.
424. Godbole M, Togar T, Patel K, Dharavath B, Yadav N, Janjuha S, et al. Up-regulation of the kinase gene SGK1 by progesterone activates the AP-1–NDRG1 axis in both PR-positive and -negative breast cancer cells. Journal of Biological Chemistry. 2018;293(50):19263-76.
425. Sevinsky CJ, Khan F, Kokabee L, Darehshouri A, Maddipati KR, Conklin DS. NDRG1 regulates neutral lipid metabolism in breast cancer cells. Breast Cancer Research. 2018;20(1):55.
426. Villodre ES, Hu X, Eckhardt BL, Larson R, Huo L, Yoon EC, et al. NDRG1 in Aggressive Breast Cancer Progression and Brain Metastasis. JNCI: Journal of the National Cancer Institute. 2021;114(4):579-91.
427. Turner NC, Oliveira M, Howell SJ, Dalenc F, Cortes J, Moreno HLG, et al. Capivasertib in Hormone Receptor–Positive Advanced Breast Cancer. New England Journal of Medicine. 2023;388(22):2058-70.
428. Sommer EM, Dry H, Cross D, Guichard S, Davies BR, Alessi DR. Elevated SGK1 predicts resistance of breast cancer cells to Akt inhibitors. Biochem J. 2013;452(3):499-508.
429. de Nonneville A, Finetti P, Mamessier E, Bertucci F. RE: NDRG1 in Aggressive Breast Cancer Progression and Brain Metastasis. J Natl Cancer Inst. 2022;114(7):1046-7.
430. Nagai MA, Gerhard R, Fregnani JH, Nonogaki S, Rierger RB, Netto MM, et al. Prognostic value of NDRG1 and SPARC protein expression in breast cancer patients. Breast Cancer Res Treat. 2011;126(1):1-14.
431. Echaniz-Laguna A, Degos B, Bonnet C, Latour P, Hamadouche T, Lévy N, et al. NDRG1-linked Charcot-Marie-Tooth disease (CMT4D) with central nervous system involvement. Neuromuscul Disord. 2007;17(2):163-8.

432. Ricard E, Mathis S, Magdelaine C, Delisle M-B, Magy L, Funalot B, et al. CMT4D (NDRG1 mutation): genotype–phenotype correlations. Journal of the Peripheral Nervous System. 2013;18(3):261-5.
433. Li L-X, Liu G-L, Liu Z-J, Lu C, Wu Z-Y. Identification and functional characterization of two missense mutations in NDRG1 associated with Charcot-Marie-Tooth disease type 4D. Human Mutation. 2017;38(11):1569-78.
434. Azuma K, Kawahara A, Hattori S, Taira T, Tsurutani J, Watari K, et al. NDRG1/Cap43/Drg-1 may Predict Tumor Angiogenesis and Poor Outcome in Patients with Lung Cancer. Journal of Thoracic Oncology. 2012;7(5):779-89.
435. Cheng J, Xie H-Y, Xu X, Wu J, Wei X, Su R, et al. NDRG1 as a biomarker for metastasis, recurrence and of poor prognosis in hepatocellular carcinoma. Cancer Letters. 2011;310(1):35-45.
436. Dong X, Hong Y, Sun H, Chen C, Zhao X, Sun B. NDRG1 suppresses vasculogenic mimicry and tumor aggressiveness in gastric carcinoma. Oncol Lett. 2019;18(3):3003-16.
437. Nishio S, Ushijima K, Tsuda N, Takemoto S, Kawano K, Yamaguchi T, et al. Cap43/NDRG1/Drg-1 is a molecular target for angiogenesis and a prognostic indicator in cervical adenocarcinoma. Cancer Letters. 2008;264(1):36-43.
438. Bandyopadhyay S, Wang Y, Zhan R, Pai SK, Watabe M, Iiizumi M, et al. The Tumor Metastasis Suppressor Gene Drg-1 Down-regulates the Expression of Activating Transcription Factor 3 in Prostate Cancer. Cancer Research. 2006;66(24):11983-90.
439. Terada A, Tsuda N, Tasaki S, Park J, Nasu H, Tasaki K, et al. N-Myc Downstream Regulated Gene-1 May Play an Important Role in the Prognosis of Ovarian Cancer, in Its Association with Beta-Catenin. The Kurume Medical Journal. 2022;69(1.2):39-46.
440. Ježek J, Plecitá-Hlavatá L, Ježek P. Aglycemic HepG2 Cells Switch From Aminotransferase Glutaminolytic Pathway of Pyruvate Utilization to Complete Krebs Cycle at Hypoxia. Frontiers in Endocrinology. 2018;9.
441. Bensaad K, Favaro E, Lewis Caroline A, Peck B, Lord S, Collins Jennifer M, et al. Fatty Acid Uptake and Lipid Storage Induced by HIF-1α Contribute to Cell Growth and Survival after Hypoxia-Reoxygenation. Cell Reports. 2014;9(1):349-65.
442. Guo D-D, Xie K-F, Luo X-J. Hypoxia-induced elevated NDRG1 mediates apoptosis through reprograming mitochondrial fission in HCC. Gene. 2020;741:144552.
443. Jadhav SB, Vondrackova M, Potomova P, Sandoval-Acuña C, Smigova J, Klanicova K, et al. NDRG1 acts as an oncogene in triple-negative breast cancer and its loss sensitizes cells to mitochondrial iron chelation. Frontiers in Pharmacology. 2024;15.
444. Maruyama Y, Ono M, Kawahara A, Yokoyama T, Basaki Y, Kage M, et al. Tumor growth suppression in pancreatic cancer by a putative metastasis suppressor gene Cap43/NDRG1/Drg-1 through modulation of angiogenesis. Cancer Res. 2006;66(12):6233-42.
445. Bandyopadhyay S, Pai SK, Gross SC, Hirota S, Hosobe S, Miura K, et al. The Drg-1 gene suppresses tumor metastasis in prostate cancer. Cancer Res. 2003;63(8):1731-6.
446. Guan RJ, Ford HL, Fu Y, Li Y, Shaw LM, Pardee AB. Drg-1 as a differentiation-related, putative metastatic suppressor gene in human colon cancer. Cancer Res. 2000;60(3):749-55.
447. Li Y, Zhao L, Li XF. Hypoxia and the Tumor Microenvironment. Technol Cancer Res Treat. 2021;20:15330338211036304.

448. Baghban R, Roshangar L, Jahanban-Esfahlan R, Seidi K, Ebrahimi-Kalan A, Jaymand M, et al. Tumor microenvironment complexity and therapeutic implications at a glance. Cell Communication and Signaling. 2020;18(1):59.
449. Qiu J, Xue X, Hu C, Xu H, Kou D, Li R, et al. Comparison of Clinicopathological Features and Prognosis in Triple-Negative and Non-Triple Negative Breast Cancer. Journal of Cancer. 2016;7(2):167-73.
450. Agarwal G, Nanda G, Lal P, Mishra A, Agarwal A, Agrawal V, et al. Outcomes of Triple-Negative Breast Cancers (TNBC) Compared with Non-TNBC: Does the Survival Vary for All Stages? World Journal of Surgery. 2016;40(6):1362-72.
451. Qannita RA, Alalami AI, Harb AA, Aleidi SM, Taneera J, Abu-Gharbieh E, et al. Targeting Hypoxia-Inducible Factor-1 (HIF-1) in Cancer: Emerging Therapeutic Strategies and Pathway Regulation. Pharmaceuticals. 2024;17(2):195.
452. McDonald PC, Chia S, Bedard PL, Chu Q, Lyle M, Tang L, et al. A Phase 1 Study of SLC-0111, a Novel Inhibitor of Carbonic Anhydrase IX, in Patients With Advanced Solid Tumors. Am J Clin Oncol. 2020;43(7):484-90.
453. Melotte V, Qu X, Ongenaert M, van Criekinge W, de Bruïne AP, Baldwin HS, et al. The N-myc downstream regulated gene (NDRG) family: diverse functions, multiple applications. Faseb j. 2010;24(11):4153-66.
454. Godbole M, Togar T, Patel K, Dharavath B, Yadav N, Janjuha S, et al. Up-regulation of the kinase gene SGK1 by progesterone activates the AP-1-NDRG1 axis in both PR-positive and -negative breast cancer cells. J Biol Chem. 2018;293(50):19263-76.
455. Metallo CM, Gameiro PA, Bell EL, Mattaini KR, Yang J, Hiller K, et al. Reductive glutamine metabolism by IDH1 mediates lipogenesis under hypoxia. Nature. 2012;481(7381):380-4.
456. Wang S-F, Tseng L-M, Lee H-C. Role of mitochondrial alterations in human cancer progression and cancer immunity. Journal of Biomedical Science. 2023;30(1):61.
457. Blaszczak W, Williams H, Swietach P. Autoregulation of H(+)/lactate efflux prevents monocarboxylate transport (MCT) inhibitors from reducing glycolytic lactic acid production. Br J Cancer. 2022;127(7):1365-77.
458. Cappelletti V, Iorio E, Miodini P, Silvestri M, Dugo M, Daidone MG. Metabolic Footprints and Molecular Subtypes in Breast Cancer. Dis Markers. 2017;2017:7687851.
459. Gong Y, Ji P, Yang Y-S, Xie S, Yu T-J, Xiao Y, et al. Metabolic-Pathway-Based Subtyping of Triple-Negative Breast Cancer Reveals Potential Therapeutic Targets. Cell Metabolism. 2021;33(1):51-64.e9.

Appendix

Supplement Table 1 -Significant differential gene expression by membranous CAIX phenotype

Genes	Description	log2FoldChange	p-value	padj
Downregulated genes				
SRARP	Steroid Receptor Associated And Regulated Protein	-6.730941483	1.39E-09	2.31E-05
ESR1	Estrogen receptor 1	-2.247297235	3.06E-08	0.000127255
CITED1	Cbp/P300 Interacting Transactivator With Glu/Asp Rich Carboxy-Terminal Domain 1	-5.261697233	1.88E-07	0.000521142
ANKRD30B	Ankyrin Repeat Domain 30B	-3.918370991	4.88E-07	0.00115856
ANKRD30A	Ankyrin Repeat Domain 30A	-2.655852534	2.00E-06	0.004157766
TAT	Tyrosine Aminotransferase	-4.869276215	9.55E-06	0.017639682
ZNF774	Zinc Finger Protein 774	-5.429364141	1.44E-05	0.023768086
CCL14	C-C Motif Chemokine Ligand 14	-4.814973121	1.57E-05	0.023768086
MRO	Maestro	-4.191217016	1.89E-05	0.024901604
HPD	4-Hydroxyphenylpyruvate Dioxygenase	-4.794840307	1.95E-05	0.024901604
TFF1	Trefoil Factor 1	-2.581144142	2.16E-05	0.024908967
PLP1	Proteolipid Protein 1	-3.434090822	2.25E-05	0.024908967
DLGAP1	DLG Associated Protein 1	-3.693517564	2.71E-05	0.028140986
TCN1	Transcobalamin 1	-4.820533759	3.03E-05	0.0296116
RP1	RP1 Axonemal Microtubule Associated	-4.964821386	3.47E-05	0.031134313
TLCD3B	TLC Domain Containing 3B	-5.522626014	3.68E-05	0.031134313
RNASE2	Ribonuclease A Family Member 2	-5.255114913	3.89E-05	0.031134313
NR2E3	Nuclear Receptor Subfamily 2 Group E Member 3	-4.239056396	4.10E-05	0.031134313
Upregulated genes				
VEGFA	Vascular Endothelial Growth Factor A	1.535211386	2.53E-08	0.000127255
NDRG1	N-Myc Downstream Regulated 1	1.494050585	3.01E-08	0.000127255
CA9	Carbonic Anhydrase 9	3.931068964	1.10E-07	0.000366427
PPFIA4	PTPRF Interacting Protein Alpha 4	1.753757657	4.12E-05	0.031134313

Supplement Table 2 -Significant differential gene expression by cytoplasmic CAIX phenotype

Genes	Description	log2FoldChange	p-value	padj
Downregulated genes				
SRARP	Steroid Receptor Associated And Regulated Protein	-6.716174622	3.15E-09	2.97E-05
ESR1	Estrogen receptor 1	-2.214606651	5.06E-08	0.000317471
CITED1	Cbp/P300 Interacting Transactivator With Glu/Asp Rich Carboxy-Terminal Domain 1	-5.296501082	1.52E-07	0.000713074
SERHL	Serine Hydrolase Like (Pseudogene)	-4.512189172	2.57E-06	0.008065646
CCL21	C-C Motif Chemokine Ligand 21	-4.991903739	3.92E-06	0.010538069
TAT	Tyrosine Aminotransferase	-4.90929435	7.88E-06	0.016468991
ANKRD30A	Ankyrin Repeat Domain 30A	-2.481067794	9.89E-06	0.018598634
ZNF774	Zinc Finger Protein 774	-5.46974017	1.22E-05	0.020853032
CCL14	C-C Motif Chemokine Ligand 14	-4.814196828	1.58E-05	0.02482105
CYP2B6	Cytochrome P450 Family 2 Subfamily B Member 6	-3.829799741	1.84E-05	0.02482105
DUSP4	Dual Specificity Phosphatase 4	-1.452965962	1.85E-05	0.02482105
GAGE2D	G Antigen 2D	-5.19519447	2.20E-05	0.026594399
HPD	4-Hydroxyphenylpyruvate Dioxygenase	-4.758923615	2.28E-05	0.026594399
NDP	Norrin Cystine Knot Growth Factor NDP	-5.437066769	2.40E-05	0.026594399
DLGAP1	DLG Associated Protein 1	-3.699592919	2.63E-05	0.027457314
DPEP1	Dipeptidase 1	-4.805319435	3.22E-05	0.031106614
IGHE	Immunoglobulin Heavy Constant Epsilon	-5.181979236	3.31E-05	0.031106614
TLCD3B	TLC Domain Containing 3B	-5.492195838	4.12E-05	0.035721244
RNASE2	Ribonuclease A Family Member 2	-5.226017853	4.37E-05	0.035721244
NR2E3	Nuclear Receptor Subfamily 2 Group E Member 3	-4.249361245	5.29E-05	0.041476433
PLP1	Proteolipid Protein 1	-3.269690505	5.72E-05	0.042995603
TFF1	Trefoil Factor 1	-2.446134521	6.02E-05	0.04354308
Upregulated genes				
CA9	Carbonic Anhydrase 9	4.357222413	1.22E-09	2.30E-05
NDRG1	N-Myc Downstream Regulated 1	1.318114718	1.67E-06	0.006298496
VEGFA	Vascular Endothelial Growth Factor A	1.286168777	5.74E-06	0.013503974
PPFIA4	PTPRF Interacting Protein Alpha 4	1.752481162	4.18E-05	0.035721244

Supplement Table 3 -GSEA upregulation in high membranous CAIX phenotypes

NAME	SIZE	ES	NES	NOM p-val	FDR q-val	FWER p-val	RANK AT MAX	LEADING EDGE
HALLMARK_GLYCOLYSIS	199	0.39513183	1.8753251	0	0.04594927	0.039	2967	tags=36%, list=15%, signal=42%
HALLMARK_HYPOXIA	199	0.38372898	1.7551321	0	0.07490486	0.102	2831	tags=32%, list=14%, signal=37%
HALLMARK_UNFOLDED_PROTEIN_RESPONSE	110	0.35417414	1.6110482	0.02148438	0.13569893	0.26	3613	tags=31%, list=18%, signal=38%
HALLMARK_MTORC1_SIGNALING	199	0.33434698	1.5702895	0.01030928	0.13547967	0.322	4127	tags=34%, list=21%, signal=43%
HALLMARK_G2M_CHECKPOINT	196	0.395975	1.5529281	0.07520326	0.11838117	0.344	3373	tags=40%, list=17%, signal=48%
HALLMARK_E2F_TARGETS	199	0.3617335	1.3188211	0.1910569	0.35788438	0.746	3547	tags=38%, list=18%, signal=46%
HALLMARK_PROTEIN_SECRETION	96	0.298855	1.3002328	0.11247443	0.338291	0.775	3414	tags=30%, list=17%, signal=36%
HALLMARK_MYC_TARGETS_V1	196	0.30509573	1.1524593	0.31620553	0.58927786	0.93	4285	tags=36%, list=22%, signal=46%
HALLMARK_INFLAMMATORY_RESPONSE	200	0.25010774	1.131108	0.23796791	0.57722545	0.944	2315	tags=21%, list=12%, signal=24%
HALLMARK_TNFA_SIGNALING_VIA_NFKB	200	0.24788262	1.1301398	0.2740047	0.521228	0.944	4308	tags=35%, list=22%, signal=44%
HALLMARK_IL6_JAK_STAT3_SIGNALING	87	0.26194957	1.0865954	0.30769232	0.56653464	0.971	2944	tags=26%, list=15%, signal=31%
HALLMARK_MYC_TARGETS_V2	57	0.28896573	1.0338529	0.38945234	0.6370077	0.984	4673	tags=39%, list=24%, signal=51%
HALLMARK_INTERFERON_GAMMA_RESPONSE	200	0.25949427	0.960536	0.46021506	0.76464796	0.997	4290	tags=33%, list=22%, signal=41%
HALLMARK_PEROXISOME	104	0.21231098	0.9575546	0.5106838	0.71933514	0.997	4383	tags=29%, list=22%, signal=37%
HALLMARK_PI3K_AKT_MTOR_SIGNALING	105	0.19794741	0.9444388	0.5646552	0.7044079	0.999	3126	tags=23%, list=16%, signal=27%
HALLMARK_CHOLESTEROL_HOMEOSTASIS	74	0.22116321	0.9055415	0.58313817	0.7470519	0.999	3202	tags=26%, list=16%, signal=31%
HALLMARK_INTERFERON_ALPHA_RESPONSE	97	0.281708	0.89604485	0.5242105	0.72406673	0.999	5415	tags=45%, list=28%, signal=62%
HALLMARK_MITOTIC_SPINDLE	199	0.17352897	0.85770154	0.67469877	0.7676376	1	3971	tags=27%, list=20%, signal=33%
HALLMARK_P53_PATHWAY	199	0.16492909	0.84857047	0.8	0.74737245	1	4156	tags=28%, list=21%, signal=35%
HALLMARK_UV_RESPONSE_UP	157	0.16655733	0.82434005	0.802381	0.7578162	1	1931	tags=14%, list=10%, signal=15%
HALLMARK_NOTCH_SIGNALING	32	0.17854649	0.66670716	0.92436975	0.9397782	1	3465	tags=28%, list=18%, signal=34%

Supplement Table 4 -GSEA upregulation in low membranous CAIX phenotypes

NAME	SIZE	ES	NES	NOM p-val	FDR q-val	FWER p-val	RANK AT MAX	LEADING EDGE
HALLMARK_ESTROGEN_RESPONSE_LATE	199	-0.3147107	-1.4431971	0.03305785	1	0.585	4827	tags=34%, list=25%, signal=44%
HALLMARK_HEDGEHOG_SIGNALING	36	-0.4163052	-1.4350357	0.09142857	0.7806811 3	0.599	5174	tags=50%, list=26%, signal=68%
HALLMARK_ESTROGEN_RESPONSE_EARLY	199	-0.2969864	-1.3482305	0.09437086	0.8668083	0.763	5724	tags=35%, list=29%, signal=49%
HALLMARK_UV_RESPONSE_DN	144	-0.2894502	-1.318559	0.10076046	0.7539323	0.817	2963	tags=24%, list=15%, signal=28%
HALLMARK_PANCREAS_BETA_CELLS	40	-0.3970611	-1.3157325	0.09515571	0.6098846	0.819	5181	tags=45%, list=27%, signal=61%
HALLMARK_APICAL_JUNCTION	200	-0.2706217	-1.2926586	0.09122203	0.5768631	0.852	4519	tags=29%, list=23%, signal=37%
HALLMARK_TGF_BETA_SIGNALING	54	-0.3074085	-1.2574397	0.14671814	0.5938926 3	0.894	2722	tags=22%, list=14%, signal=26%
HALLMARK_HEME_METABOLISM	198	-0.2554413	-1.2405211	0.08739496	0.5592435 6	0.911	4729	tags=28%, list=24%, signal=37%
HALLMARK_MYOGENESIS	200	-0.2798489	-1.2069066	0.18485916	0.5922915 3	0.952	5111	tags=31%, list=26%, signal=42%
HALLMARK_FATTY_ACID_METABOLISM	157	-0.2623038	-1.1672881	0.21621622	0.6366716 6	0.969	4729	tags=27%, list=24%, signal=36%
HALLMARK_WNT_BETA_CATENIN_SIGNALING	40	-0.3240318	-1.1630597	0.2591171	0.5889001	0.971	1517	tags=15%, list=8%, signal=16%
HALLMARK_SPERMATOGENESIS	133	-0.3109175	-1.1465137	0.31161973	0.5795629 6	0.978	2987	tags=26%, list=15%, signal=30%
HALLMARK_IL2_STAT5_SIGNALING	199	-0.2306657	-1.1249272	0.25694445	0.5918976 7	0.985	7015	tags=41%, list=36%, signal=64%
HALLMARK_XENOBIOTIC_METABOLISM	198	-0.2517068	-1.1120967	0.29064038	0.5791225	0.988	5334	tags=31%, list=27%, signal=43%
HALLMARK_KRAS_SIGNALING_DN	200	-0.2387865	-1.0832132	0.2734694	0.6087203	0.992	5663	tags=34%, list=29%, signal=47%
HALLMARK_ADIPOGENESIS	200	-0.2278966	-1.0520827	0.35580525	0.641996	0.995	6215	tags=35%, list=32%, signal=50%
HALLMARK_BILE_ACID_METABOLISM	112	-0.2415176	-1.0243344	0.4219745	0.6684038	0.997	6912	tags=43%, list=35%, signal=66%
HALLMARK_ANDROGEN_RESPONSE	100	-0.2306757	-0.9964119	0.45610687	0.6988015	0.998	3997	tags=22%, list=20%, signal=28%
HALLMARK_KRAS_SIGNALING_UP	200	-0.2126112	-0.9541004	0.5217391	0.7666241	0.999	3241	tags=21%, list=17%, signal=24%
HALLMARK_COAGULATION	138	-0.236732	-0.9508869	0.5293132	0.7356087 6	0.999	5172	tags=30%, list=26%, signal=41%
HALLMARK_EPITHELIAL_MESENCHYMAL_TRANSITION	199	-0.2487456	-0.9402458	0.48549324	0.7252025	0.999	4174	tags=27%, list=21%, signal=34%
HALLMARK_OXIDATIVE_PHOSPHORYLATION	200	-0.2074308	-0.9351191	0.5229885	0.7047888	0.999	5140	tags=25%, list=26%, signal=33%
HALLMARK_ANGIOGENESIS	36	-0.2566556	-0.8642703	0.63486236	0.8351422 5	1	6602	tags=47%, list=34%, signal=71%
HALLMARK_DNA_REPAIR	149	-0.1717273	-0.8469355	0.7892791	0.8359991	1	3505	tags=17%, list=18%, signal=21%
HALLMARK_APOPTOSIS	161	-0.1682821	-0.8079891	0.81441444	0.8805889	1	8510	tags=47%, list=44%, signal=83%
HALLMARK_APICAL_SURFACE	44	-0.1983588	-0.7527425	0.8454861	0.9435712 7	1	4033	tags=23%, list=21%, signal=29%
HALLMARK_COMPLEMENT	200	-0.1656472	-0.7230923	0.8929889	0.9503098	1	5759	tags=26%, list=29%, signal=37%
HALLMARK_ALLOGRAFT_REJECTION	198	-0.1775241	-0.6915078	0.845735	0.9511618	1	4307	tags=23%, list=22%, signal=29%
HALLMARK_REACTIVE_OXYGEN_SPECIES_PATHWAY	49	-0.1409608	-0.5465397	0.98659	0.9906406 4	1	7824	tags=43%, list=40%, signal=71%

Supplement Table 5 -GSEA upregulation in (A) high cytoplasmic CAIX phenotype

NAME	SIZE	ES (A)	NES	NOM p-val	FDR q-val	FWER p-val	RANK AT MAX	LEADING EDGE
HALLMARK_GLYCOLYSIS	199	0.4143493	2.0369215	0	0.01243518	0.01	4189	tags=47%, list=21%, signal=59%
HALLMARK_G2M_CHECKPOINT	196	0.45505375	1.7886003	0.02217742	0.07421745	0.092	3952	tags=45%, list=20%, signal=56%
HALLMARK_HYPOXIA	199	0.37221092	1.7196947	0.01101322	0.07900678	0.144	2677	tags=30%, list=14%, signal=35%
HALLMARK_MYC_TARGETS_V1	196	0.4466585	1.7170775	0.04474708	0.05990833	0.147	3884	tags=40%, list=20%, signal=49%
HALLMARK_E2F_TARGETS	199	0.45281842	1.7016056	0.04696673	0.0526749	0.157	2872	tags=36%, list=15%, signal=42%
HALLMARK_MTORC1_SIGNALING	199	0.35389692	1.6963289	0.01369863	0.04445372	0.158	3418	tags=31%, list=17%, signal=37%
HALLMARK_MYC_TARGETS_V2	57	0.41095605	1.452326	0.094	0.15857527	0.523	3522	tags=35%, list=18%, signal=43%
HALLMARK_UNFOLDED_PROTEIN_RESPONSE	110	0.3029765	1.3896102	0.06883365	0.19335818	0.616	3870	tags=27%, list=20%, signal=34%
HALLMARK_MITOTIC_SPINDLE	199	0.2630452	1.3018863	0.11066398	0.26639915	0.779	3050	tags=27%, list=16%, signal=31%
HALLMARK_PROTEIN_SECRETION	96	0.27606317	1.1888931	0.21792261	0.4096032	0.905	4637	tags=33%, list=24%, signal=43%
HALLMARK_TNFA_SIGNALING_VIA_NFKB	200	0.24716406	1.1438549	0.23695652	0.45209247	0.938	3960	tags=32%, list=20%, signal=40%
HALLMARK_INFLAMMATORY_RESPONSE	200	0.23185244	1.0642068	0.34916866	0.5771066	0.973	2263	tags=21%, list=12%, signal=23%
HALLMARK_PI3K_AKT_MTOR_SIGNALING	105	0.19897474	0.9318994	0.58744395	0.84682494	0.994	3782	tags=26%, list=19%, signal=32%
HALLMARK_UV_RESPONSE_UP	157	0.18036202	0.89406526	0.69161	0.89541674	0.997	3072	tags=20%, list=16%, signal=23%
HALLMARK_P53_PATHWAY	199	0.16585517	0.841608	0.80733943	0.9685858	0.998	3666	tags=24%, list=19%, signal=29%
HALLMARK_IL6_JAK_STAT3_SIGNALING	87	0.20116939	0.82867306	0.72139305	0.93736774	0.999	4412	tags=32%, list=23%, signal=41%
HALLMARK_INTERFERON_GAMMA_RESPONSE	200	0.22489603	0.81734633	0.625	0.9060411	0.999	4181	tags=29%, list=21%, signal=37%
HALLMARK_NOTCH_SIGNALING	32	0.22671387	0.81674427	0.7389474	0.8575536	0.999	4126	tags=31%, list=21%, signal=40%
HALLMARK_CHOLESTEROL_HOMEOSTASIS	74	0.18785994	0.7757436	0.78289473	0.89141417	1	3091	tags=22%, list=16%, signal=26%
HALLMARK_DNA_REPAIR	149	0.15390153	0.7668101	0.9136842	0.8607339	1	3224	tags=18%, list=16%, signal=22%
HALLMARK_INTERFERON_ALPHA_RESPONSE	97	0.2275122	0.7240996	0.68333334	0.8799708	1	4727	tags=34%, list=24%, signal=45%

Supplement Table 6 -GSEA upregulation in low cytoplasmic CAIX phenotypes

NAME	SIZE	ES	NES	NOM p-val	FDR q-val	FWER p-val	RANK AT MAX	LEADING EDGE
HALLMARK_ESTROGEN_RESPONSE_EARLY	199	-0.37291828	-1.7144226	0.00499168	0.2729393	0.169	5347	tags=41%, list=27%, signal=55%
HALLMARK_ESTROGEN_RESPONSE_LATE	199	-0.33231783	-1.5443743	0.010033445	0.41924748	0.422	5343	tags=39%, list=27%, signal=53%
HALLMARK_HEDGEHOG_SIGNALING	36	-0.40824935	-1.3972507	0.093406595	0.67727315	0.702	4818	tags=47%, list=25%, signal=63%
HALLMARK_FATTY_ACID_METABOLISM	157	-0.29156384	-1.2939596	0.1305842	0.88345325	0.859	4267	tags=28%, list=22%, signal=36%
HALLMARK_WNT_BETA_CATENIN_SIGNALING	40	-0.36070424	-1.2903236	0.13333334	0.71927685	0.865	2343	tags=20%, list=12%, signal=23%
HALLMARK_XENOBIOTIC_METABOLISM	198	-0.28694087	-1.2688013	0.12962963	0.66308665	0.879	6648	tags=42%, list=34%, signal=63%
HALLMARK_UV_RESPONSE_DN	144	-0.28177524	-1.2685577	0.1592233	0.5690697	0.88	3656	tags=28%, list=19%, signal=34%
HALLMARK_ANDROGEN_RESPONSE	100	-0.2920259	-1.2678763	0.14772727	0.4996323	0.88	6093	tags=36%, list=31%, signal=52%
HALLMARK_MYOGENESIS	200	-0.28287044	-1.2375011	0.14354838	0.5142405	0.908	4185	tags=28%, list=21%, signal=35%
HALLMARK_APICAL_JUNCTION	200	-0.25705713	-1.2236216	0.1539735	0.49366423	0.921	4530	tags=28%, list=23%, signal=35%
HALLMARK_PANCREAS_BETA_CELLS	40	-0.36582193	-1.2001393	0.17905405	0.4952107	0.936	5794	tags=50%, list=30%, signal=71%
HALLMARK_IL2_STAT5_SIGNALING	199	-0.23261893	-1.1357423	0.22934233	0.6007097	0.965	6853	tags=42%, list=35%, signal=64%
HALLMARK_KRAS_SIGNALING_DN	200	-0.24514544	-1.1102254	0.2109589	0.61863416	0.973	5509	tags=36%, list=28%, signal=49%
HALLMARK_HEME_METABOLISM	198	-0.22686306	-1.1050631	0.2641844	0.586437	0.973	4497	tags=26%, list=23%, signal=34%
HALLMARK_COAGULATION	138	-0.27055877	-1.0926878	0.3310811	0.5758598	0.978	4755	tags=31%, list=24%, signal=41%
HALLMARK_BILE_ACID_METABOLISM	112	-0.25683874	-1.072482	0.31010452	0.58615947	0.986	5505	tags=37%, list=28%, signal=51%
HALLMARK_TGF_BETA_SIGNALING	54	-0.25955224	-1.0487874	0.36312848	0.6074953	0.991	5960	tags=33%, list=30%, signal=48%
HALLMARK_ADIPOGENESIS	200	-0.2193614	-1.0395517	0.38103756	0.59606373	0.994	6587	tags=37%, list=34%, signal=55%
HALLMARK_KRAS_SIGNALING_UP	200	-0.22636119	-1.0245341	0.39523	0.59427464	0.996	3296	tags=20%, list=17%, signal=24%
HALLMARK_ANGIOGENESIS	36	-0.2794628	-0.95356643	0.48924732	0.7235988	0.999	7351	tags=53%, list=38%, signal=84%
HALLMARK_SPERMATOGENESIS	133	-0.24824794	-0.91902745	0.5774411	0.7727129	1	2940	tags=22%, list=15%, signal=25%
HALLMARK_APOPTOSIS	161	-0.1813729	-0.88577867	0.6536412	0.81637925	1	4529	tags=24%, list=23%, signal=30%
HALLMARK_EPITHELIAL_MESENCHYMAL_TRANSITION	199	-0.22015992	-0.83626974	0.59225094	0.8962157	1	4453	tags=28%, list=23%, signal=35%
HALLMARK_COMPLEMENT	200	-0.18534465	-0.8085565	0.75135136	0.9182201	1	4746	tags=22%, list=24%, signal=29%
HALLMARK_OXIDATIVE_PHOSPHORYLATION	200	-0.169291	-0.75653136	0.84375	0.97326046	1	6167	tags=29%, list=32%, signal=42%
HALLMARK_ALLOGRAFT_REJECTION	198	-0.18896207	-0.7560576	0.74605954	0.93655777	1	5885	tags=31%, list=30%, signal=44%
HALLMARK_APICAL_SURFACE	44	-0.19965178	-0.75042313	0.8518519	0.9105022	1	4526	tags=27%, list=23%, signal=35%
HALLMARK_PEROXISOME	104	-0.16306911	-0.7174592	0.92022264	0.92564195	1	5343	tags=25%, list=27%, signal=34%
HALLMARK_REACTIVE_OXYGEN_SPECIES_PATHWAY	49	-0.15868424	-0.5895435	0.9654545	0.9793496	1	7653	tags=39%, list=39%, signal=64%

Supplement Table 7-The STR authentications of (A) MDA-MB-231, (B) SK-BR3 and (C) MCF-7 cell lines

(A)

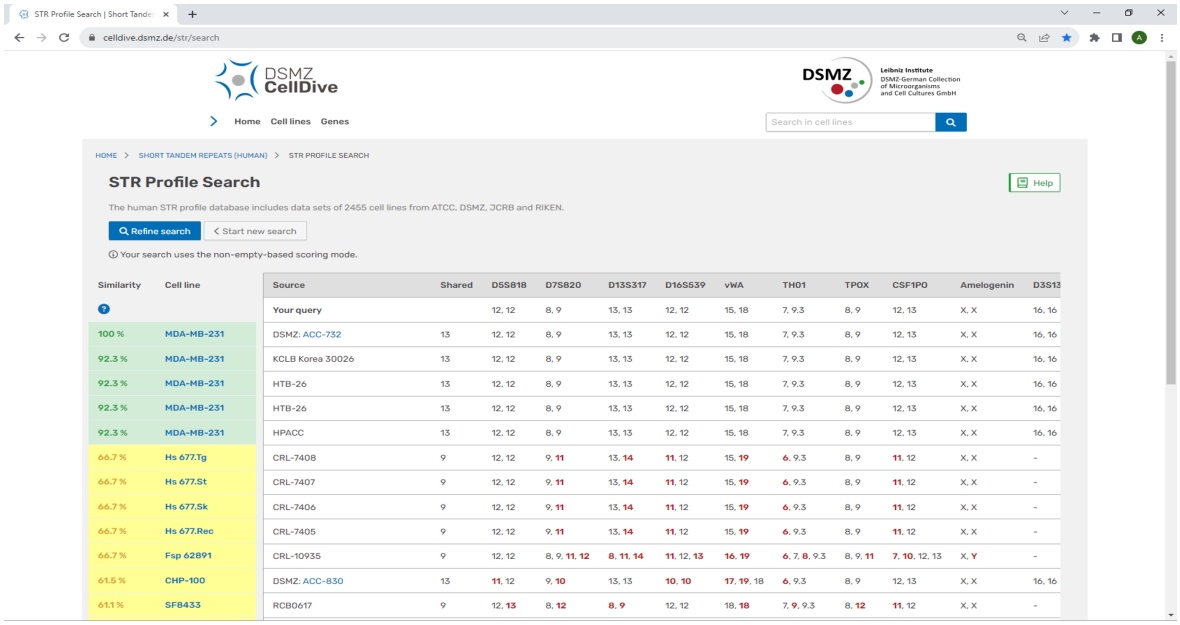

STR Profile Search | Short Tande

celldive.dsmz.de/str/search

DSMZ CellDive

Home Cell lines Genes

DSMZ Leibniz Institute DSMZ-German Collection of Microorganisms and Cell Cultures GmbH

Search in cell lines

HOME > SHORT TANDEM REPEATS (HUMAN) > STR PROFILE SEARCH

STR Profile Search

Help

The human STR profile database includes data sets of 2455 cell lines from ATCC, DSMZ, JCRB and RIKEN.

Refine search | Start new search

Your search uses the non-empty-based scoring mode.

Similarity	Cell line	Source	Shared	D5S818	D7S820	D13S317	D16S539	vWA	TH01	TPOX	CSF1PO	Amelogenin	D3S13
		Your query		12, 12	8, 9	13, 13	12, 12	15, 18	7, 9.3	8, 9	12, 13	X, X	16, 16
100 %	MDA-MB-231	DSMZ: ACC-732	13	12, 12	8, 9	13, 13	12, 12	15, 18	7, 9.3	8, 9	12, 13	X, X	16, 16
92.3 %	MDA-MB-231	KCLB Korea 30026	13	12, 12	8, 9	13, 13	12, 12	15, 18	7, 9.3	8, 9	12, 13	X, X	16, 16
92.3 %	MDA-MB-231	HTB-26	13	12, 12	8, 9	13, 13	12, 12	15, 18	7, 9.3	8, 9	12, 13	X, X	16, 16
92.3 %	MDA-MB-231	HTB-26	13	12, 12	8, 9	13, 13	12, 12	15, 18	7, 9.3	8, 9	12, 13	X, X	16, 16
92.3 %	MDA-MB-231	HPACC	13	12, 12	8, 9	13, 13	12, 12	15, 18	7, 9.3	8, 9	12, 13	X, X	16, 16
66.7 %	Hs 677.Tg	CRL-7408	9	12, 12	9, **11**	13, **14**	**11**, 12	15, **19**	**6**, 9.3	8, 9	**11**, 12	X, X	-
66.7 %	Hs 677.St	CRL-7407	9	12, 12	9, **11**	13, **14**	**11**, 12	15, **19**	**6**, 9.3	8, 9	**11**, 12	X, X	-
66.7 %	Hs 677.Sk	CRL-7406	9	12, 12	9, **11**	13, **14**	**11**, 12	15, **19**	**6**, 9.3	8, 9	**11**, 12	X, X	-
66.7 %	Hs 677.Rec	CRL-7405	9	12, 12	9, **11**	13, **14**	**11**, 12	15, **19**	**6**, 9.3	8, 9	**11**, 12	X, X	-
66.7 %	Fsp 62891	CRL-10935	9	12, 12	8, 9, **11, 12**	**8, 11, 14**	**11**, 12, **13**	**16, 19**	**6**, 7, **8**, 9.3	8, 9, **11**	**7, 10**, 12, 13	X, **Y**	-
61.5 %	CHP-100	DSMZ: ACC-830	13	**11**, 12	9, **10**	13, 13	**10, 10**	**17, 19**, 18	**6**, 9.3	8, 9	12, 13	X, X	16, 16
61.1 %	SF8433	RCB0617	9	12, **13**	8, **12**	**8, 9**	12, 12	18, **18**	7, **9**, 9.3	8, **12**	**11**, 12	X, X	-

(B)

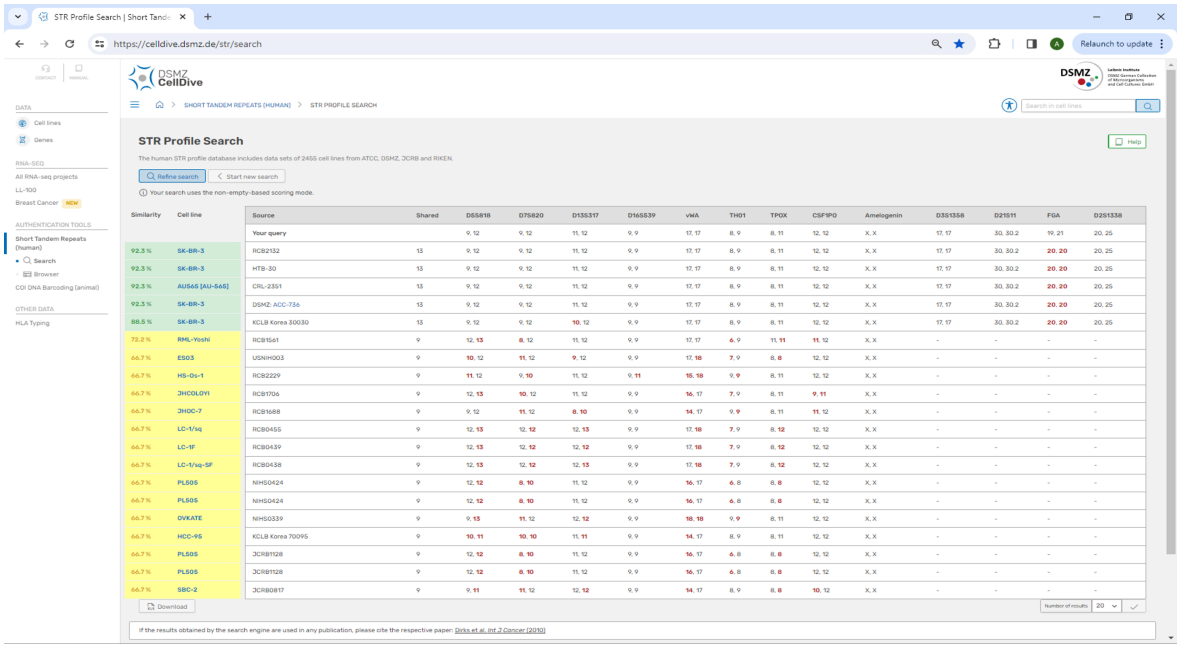

STR Profile Search | Short Tande

https://celldive.dsmz.de/str/search

Relaunch to update

DSMZ CellDive

DSMZ Leibniz Institute DSMZ-German Collection of Microorganisms and Cell Cultures GmbH

SHORT TANDEM REPEATS (HUMAN) > STR PROFILE SEARCH

STR Profile Search

Help

The human STR profile database includes data sets of 2455 cell lines from ATCC, DSMZ, JCRB and RIKEN.

Refine search | Start new search

Your search uses the non-empty-based scoring mode.

DATA
Cell lines
Genes
RNA-SEQ
All RNA-seq projects
LL-100
Breast Cancer NEW
AUTHENTICATION TOOLS
Short Tandem Repeats (human)
Search
Browser
COI DNA Barcoding (animal)
OTHER DATA
HLA Typing

Similarity	Cell line	Source	Shared	D5S818	D7S820	D13S317	D16S539	vWA	TH01	TPOX	CSF1PO	Amelogenin	D3S1358	D21S11	FGA	D2S1338
		Your query		9, 12	9, 12	11, 12	9, 9	17, 17	8, 9	8, 11	12, 12	X, X	17, 17	30, 30.2	19, 21	20, 25
92.3 %	SK-BR-3	RCB2132	13	9, 12	9, 12	11, 12	9, 9	17, 17	8, 9	8, 11	12, 12	X, X	17, 17	30, 30.2	**20, 20**	20, 25
92.3 %	SK-BR-3	HTB-30	13	9, 12	9, 12	11, 12	9, 9	17, 17	8, 9	8, 11	12, 12	X, X	17, 17	30, 30.2	**20, 20**	20, 25
92.3 %	AU565 [AU-565]	CRL-2351	13	9, 12	9, 12	11, 12	9, 9	17, 17	8, 9	8, 11	12, 12	X, X	17, 17	30, 30.2	**20, 20**	20, 25
92.3 %	SK-BR-3	DSMZ: ACC-736	13	9, 12	9, 12	11, 12	9, 9	17, 17	8, 9	8, 11	12, 12	X, X	17, 17	30, 30.2	**20, 20**	20, 25
88.5 %	SK-BR-3	KCLB Korea 30030	13	9, 12	9, 12	**10**, 12	9, 9	17, 17	8, 9	8, 11	12, 12	X, X	17, 17	30, 30.2	**20, 20**	20, 25
72.2 %	RML-Yoshi	RCB1561	9	12, **13**	**8**, 12	11, 12	9, 9	17, 17	**6**, 9	11, **11**	**11**, 12	X, X	-	-	-	-
66.7 %	ES03	USNIH003	9	**10**, 12	**11**, 12	9, 12	9, 9	17, **18**	7, 9	8, **8**	12, 12	X, X	-	-	-	-
66.7 %	HS-Os-1	RCB2229	9	**11**, 12	9, **10**	11, 12	9, **11**	**15, 18**	9, **9**	8, 11	12, 12	X, X	-	-	-	-
66.7 %	JHCOLOY1	RCB1706	9	12, **13**	**10**, 12	11, 12	9, 9	**16**, 17	7, 9	8, 11	9, **11**	X, X	-	-	-	-
66.7 %	JHOC-7	RCB1688	9	9, 12	**11**, 12	**8, 10**	9, 9	**14**, 17	9, **9**	8, 11	**11**, 12	X, X	-	-	-	-
66.7 %	LC-1/sq	RCB0455	9	12, **13**	12, **12**	12, **13**	9, 9	17, **18**	7, 9	8, **12**	12, 12	X, X	-	-	-	-
66.7 %	LC-1F	RCB0439	9	12, **13**	12, **12**	12, **12**	9, 9	17, **18**	7, 9	8, **12**	12, 12	X, X	-	-	-	-
66.7 %	LC-1/sq-SF	RCB0438	9	12, **13**	12, **12**	12, **13**	9, 9	17, **18**	7, 9	8, **12**	12, 12	X, X	-	-	-	-
66.7 %	PL505	NIHS0424	9	12, **12**	**8, 10**	11, 12	9, 9	**16**, 17	**6**, 8	8, **8**	12, 12	X, X	-	-	-	-
66.7 %	PL505	NIHS0424	9	12, **12**	**8, 10**	11, 12	9, 9	**16**, 17	**6**, 8	8, **8**	12, 12	X, X	-	-	-	-
66.7 %	OVKATE	NIHS0339	9	9, **13**	11, 12	12, **12**	9, 9	**18, 18**	9, **9**	8, 11	12, 12	X, X	-	-	-	-
66.7 %	HCC-95	KCLB Korea 70095	9	**10, 11**	**10, 10**	11, **11**	9, 9	**14**, 17	8, 9	8, 11	12, 12	X, X	-	-	-	-
66.7 %	PL505	JCRB1128	9	12, **12**	**8, 10**	11, 12	9, 9	**16**, 17	**6**, 8	8, **8**	12, 12	X, X	-	-	-	-
66.7 %	PL505	JCRB1128	9	12, **12**	**8, 10**	11, 12	9, 9	**16**, 17	**6**, 8	8, **8**	12, 12	X, X	-	-	-	-
66.7 %	SBC-2	JCRB0817	9	9, **11**	**11**, 12	12, **12**	9, 9	**14**, 17	8, 9	8, **8**	**10**, 12	X, X	-	-	-	-

Download

Number of results 20

If the results obtained by the search engine are used in any publication, please cite the respective paper: Dirks et al. Int J Cancer (2010)

(C)

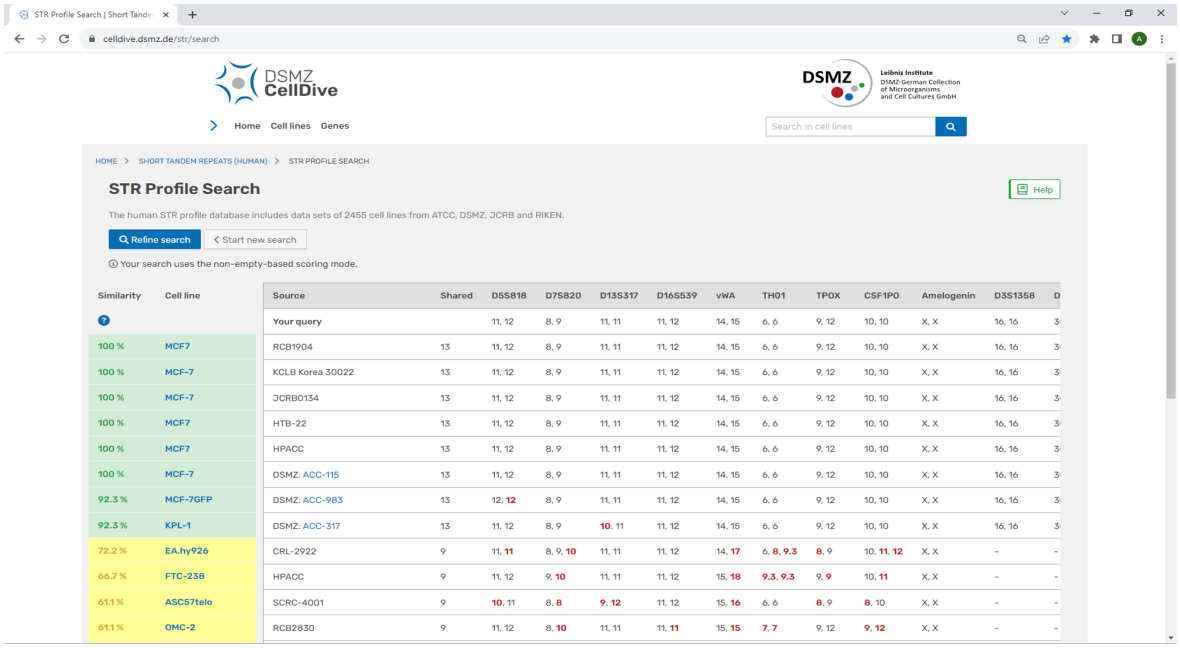

Similarity	Cell line	Source	Shared	D5S818	D7S820	D13S317	D16S539	vWA	TH01	TPOX	CSF1PO	Amelogenin	D3S1358	D
		Your query		11, 12	8, 9	11, 11	11, 12	14, 15	6, 6	9, 12	10, 10	X, X	16, 16	3
100 %	MCF7	RCB1904	13	11, 12	8, 9	11, 11	11, 12	14, 15	6, 6	9, 12	10, 10	X, X	16, 16	3
100 %	MCF-7	KCLB Korea 30022	13	11, 12	8, 9	11, 11	11, 12	14, 15	6, 6	9, 12	10, 10	X, X	16, 16	3
100 %	MCF-7	JCRB0134	13	11, 12	8, 9	11, 11	11, 12	14, 15	6, 6	9, 12	10, 10	X, X	16, 16	3
100 %	MCF7	HTB-22	13	11, 12	8, 9	11, 11	11, 12	14, 15	6, 6	9, 12	10, 10	X, X	16, 16	3
100 %	MCF7	HPACC	13	11, 12	8, 9	11, 11	11, 12	14, 15	6, 6	9, 12	10, 10	X, X	16, 16	3
100 %	MCF-7	DSMZ: ACC-115	13	11, 12	8, 9	11, 11	11, 12	14, 15	6, 6	9, 12	10, 10	X, X	16, 16	3
92.3 %	MCF-7GFP	DSMZ: ACC-983	13	12, **12**	8, 9	11, 11	11, 12	14, 15	6, 6	9, 12	10, 10	X, X	16, 16	3
92.3 %	KPL-1	DSMZ: ACC-317	13	11, 12	8, 9	**10**, 11	11, 12	14, 15	6, 6	9, 12	10, 10	X, X	16, 16	3
72.2 %	EA.hy926	CRL-2922	9	11, **11**	8, 9, **10**	11, 11	11, 12	14, **17**	6, **8**, **9.3**	**8**, 9	10, **11**, **12**	X, X	-	-
66.7 %	FTC-238	HPACC	9	11, 12	9, **10**	11, 11	11, 12	15, **18**	**9.3**, **9.3**	9, **9**	10, **11**	X, X	-	-
61.1 %	ASC57telo	SCRC-4001	9	**10**, 11	8, **8**	**9**, **12**	11, 12	15, **16**	6, 6	**8**, 9	**8**, 10	X, X	-	-
61.1 %	OMC-2	RCB2830	9	11, 12	8, **10**	11, 11	11, **11**	15, **15**	**7**, **7**	9, 12	**9**, **12**	X, X	-	-